RCA Victor Research Report 7-801-44

DURATION OF CYCLOTRON HARMONIC RESONANCES OBSERVED BY SATELLITES

I.P. Shkarofsky

JANUARY 1966

Fields and Plasma Branch

GODDARD SPACE FLIGHT CENTER

NATIONAL AERONAUTICS AND SPACE ADMINISTRATION

Greenbelt, Maryland

Prepared Under Contract No. NASw-957

with

NASA, Washington, D.C. 20546

RCA VICTOR COMPANY, LTD
RESEARCH LABORATORIES
MONTREAL, CANADA

RESEARCH LABORATORIES
RCA VICTOR COMPANY, LTD.
MONTREAL, CANADA

DURATION OF CYCLOTRON HARMONIC RESONANCES OBSERVED BY SATELLITES

Prepared By I.P. Shkarofsky
DR. I.P. SHKAROFSKY

Approved By F.J.F. Osborne
DR. F.J.F. OSBORNE
DIRECTOR, PLASMA AND SPACE PHYSICS

Approved By M.P. Bachynski
DR. M.P. BACHYNSKI
DIRECTOR OF RESEARCH

RCA VICTOR RESEARCH REPORT 7-801-44 JANUARY 1966

Prepared under Contract NASw-957 withthe National Aeronautics and Space Administration, Washington, D.C. 20546

- PREFACE -

This report contains the following:

Duration of Cyclotron Harmonic Resonances Observed by Satellite.

Appendix I : Dielectric Tensor in Vlasov Plasmas Near Cyclotron Harmonics.

Appendix II : Dispersion of Waves in Cyclotron Harmonic Resonance Regions in Plasmas.

Appendix III: List of Publications and Corrections to Previous Work.

DURATION OF CYCLOTRON HARMONIC RESONANCES
OBSERVED BY SATELLITES

I.P. Shkarofsky
RCA Victor Company, Ltd.
Research Laboratories
Montreal, Canada

- ABSTRACT -

Cyclotron harmonic waves which travel at a group velocity equal to the satellite velocity are investigated. The long duration of the resonances observed by satellites is associated with these matched conditions. Such a match can be accomplished for electrostatic waves when these waves are backward (frequency much less than the upper hybrid) but only for harmonics less than the fourth when these waves are forward (frequency above the upper hybrid). The relevant wavelengths are slightly greater than the free space wavelength parallel to magnetic field but much less than the free space wavelength perpendicular to magnetic field.

Wave matching can also be obtained near the Appleton-Hartree values when such waves can propagate. In this region we require a full electromagnetic plus relativistic analysis. The relevant wavelengths here are very large (of the order of an earth radius) parallel to magnetic field and slightly greater than the free space wavelength perpendicular to magnetic field.

The time response of these waves depends, of course, on the extent to which they are excited. Assuming that the Appleton-Hartree waves are excited with most of the input power (a plausible assumption) one finds the correct order of magnitude for the time response for these matching points. To obtain the correct dependence on harmonic number as well,

the above assumption is modified to include non-linear sheath effects and a model of the sheath field is deduced. With the same assumption (here probably incorrect, because of stronger sheath effects) for the electrostatic waves, a much longer time response is obtained. In general, where both matching points exist, one can expect both to be important.

Author

I INTRODUCTION

We find that the asymptotic time behaviour of the local plasma and magnetic-field-resonance phenomena observed by satellite topside sounders can be explained as follows. We consider the behaviour of the Vlsov plasma waves whose group velocities are equal or nearly equal to the satellite velocity. The physical concept is simply that only these waves stay with the satellite and account for the electric field long after excitation. The signal-amplitude decay is essentially due to wave-packet dispersion and varies typically as $t^{-\alpha}\exp(-i\omega_0 t)$, where α is a positive fraction, t is the time, and ω_0 the frequency for which the group-satellite velocity match is achieved.

Although the satellite velocity is much less than the electron thermal velocity, it is not correct to take the group velocity equal to zero because of important changes in the behaviour of the plasma dispersion equation. Also, while the ratio of the satellite velocity component perpendicular to the magnetic-field lines ($V_\perp$) to the electron thermal velocity (v_t) is small ($\sim 1/50$), it is still much larger than the ratio of the electron thermal velocity to the velocity of light (c). However, the velocity of light may not be taken always to be infinite as electrostatic treatments of the same problem do, since the relevant wave numbers in many cases are comparable to the free-space values, and the full electromagnetic equations must be used. This is in contrast to the resonances (e.g. cyclotron harmonics) actually observed in the laboratory which are associated with shorter wavelengths

and longitudinal waves.

In the satellite frame of reference (using a Galilean transformation), the matching of velocities emerges naturally from the "pinches" in the inversion of the Laplace-Fourier transformed Green's function. We shall discuss the application to electron-cyclotron harmonic resonances.

Matching points near free-space wavelengths, based on nonrelativistic calculations, yield a resonant frequency so near $[(\omega - n\omega_b)/n\omega_b < v_t^2/c^2]$ to the rest-mass cyclotron harmonic value, that the nonrelativistic theory is invalid. Relativistic theory must be used, which gives relative deviations up to 100 v_t^2/c^2. The various matching points are investigated and values for $\omega - n\omega_b$, $k_\parallel$ and time duration are calculated. The $k_\parallel$ values turn out to be so small that further work should be done to include magnetic field nonuniformities along field lines. The time duration agrees as far as order of magnitude with observations. We hypothesize that the excitation mechanism is due to sheath effects. With certain sheath models, we provide the necessary decrease of excitation level and the relative independence of signal duration as a function of harmonic number.

Matching points for electrostatic waves are obtained. The signal duration is deduced and compared with the results of other authors. The saddle point method is shown to be equivalent to the pinch method. Such matching points exist when the electrostatic waves are backward, but only for $n < 4$ when the electrostatic waves are forward.

The time duration of these waves is much longer than observed. This is attributed to the fact that the excitation level of these waves is not strong and that the sheath, larger than the wave packet, may inhibit these waves.

II SIMPLE CALCULATION OF THE SINGULAR TIME BEHAVIOUR FROM PINCHES

Let $\underset{\sim}{J}(\underset{\sim}{k},\omega)$ be the Fourier-Laplace transform of the source current and let $\underset{\sim}{E}(\underset{\sim}{k},\omega)$ be the corresponding electric field where, for example

$$\underset{\sim}{E}(\underset{\sim}{k},\omega) = \int d^3r \int dt\ e^{i(\omega t - \underset{\sim}{k}\cdot\underset{\sim}{r})} \underset{\sim}{E}(\underset{\sim}{r},t) \tag{1}$$

Here $\underset{\sim}{k}$ is wave-number, ω is angular frequency, $\underset{\sim}{r}$ is distance from source and t is the time. Suppose that the plasma medium has a dispersion relation given by the zeros of a dimensionless determinant D and let R_{ij} be the dimensionless minorsof D. Then using the summation convention on j

$$E_i(\underset{\sim}{k},\omega) = \frac{i\omega}{\varepsilon_o} \frac{R_{ij}}{\omega^2 D} J_j(\underset{\sim}{k},\omega) \tag{2}$$

and

$$E_i(\underset{\sim}{r},t) = \int dt' \int d^3r'\ G_{ij}(\underset{\sim}{r}-\underset{\sim}{r}')\ J_j(\underset{\sim}{r}',t') \tag{3}$$

where

$$G_{ij}(\underset{\sim}{r},t) = \frac{i}{(2\pi)^4 \varepsilon_o} \int \frac{d\omega}{\omega} e^{-i\omega t} \int d^3k\ e^{i\underset{\sim}{k}\cdot\underset{\sim}{r}} \frac{R_{ij}}{D} \tag{4}$$

is the Green's function. For an infinitessimal current dipole with moment IL,

$$\underset{\sim}{J}(\underset{\sim}{r}',t') = \underset{\sim}{I} L\ \delta(\underset{\sim}{r}')\ P(t') \tag{5}$$

where $\underset{\sim}{I}$ is the current vector in the direction of the dipole whose half-length is L. We then find,

$$E_i(\underset{\sim}{r},t) = \frac{i}{\varepsilon_o(2\pi)^4}\int\frac{d\omega}{\omega}\,P(\omega)\,e^{-i\omega t}\int d^3k\; e^{i\underset{\sim}{k}\cdot\underset{\sim}{r}}\frac{R_{ij}}{D}\,I_jL \qquad (6)$$

In the above $P(t')$ represents a pulse of frequency Ω, duration τ, so that

$$P(\omega) = \tau\left[\frac{e^{i(\omega-\Omega)\tau}-1}{i(\omega-\Omega)\tau}\right] \qquad (7)$$

The above integrals will be calculated in the neighbourhood of pinch points[1]. For a stationary observer, a pinch is a point satisfying $D = 0$ and $\partial\omega/\partial\underset{\sim}{k} = 0$, i.e. a zero velocity point on the dispersion curve. However, for an observer moving at a nonrelativistic velocity $\underset{\sim}{V}$, such as a satellite, pinches occur when the satellite velocity matches the group velocity, satisfying $D = 0$ and $\partial\omega/\partial\underset{\sim}{k} = \underset{\sim}{V}$. We let ω and $\underset{\sim}{k}$ be the angular frequency and wavenumber in the plasma frame of reference and ω' and $\underset{\sim}{k}'$ be the corresponding values in the moving satellite frame of reference. For nonrelativistic velocities

$$\omega' = \omega - \underset{\sim}{k}\cdot\underset{\sim}{V}, \quad \underset{\sim}{k}' \approx \underset{\sim}{k} - \omega\underset{\sim}{V}/c^2 \text{ so that } \omega = \omega' + \underset{\sim}{k}'\cdot\underset{\sim}{V} \text{ and } \underset{\sim}{k} = \underset{\sim}{k}' + \omega\underset{\sim}{V}/c^2 \qquad (8)$$

In the plasma frame of reference $D(\omega,\underset{\sim}{k}) = 0$. Assuming $\partial D/\partial\omega \neq 0$, we have

$$\frac{\partial D}{\partial\omega}\frac{\partial\omega}{\partial\underset{\sim}{k}} + \frac{\partial D}{\partial\underset{\sim}{k}} = 0 \qquad \text{or} \qquad \underset{\sim}{V}\frac{\partial D}{\partial\omega} + \frac{\partial D}{\partial\underset{\sim}{k}} = 0$$

if $\partial\omega/\partial\underset{\sim}{k} = \underset{\sim}{V}$. In the satellite frame of reference, use of the above result shows that

$$\frac{\partial D}{\partial\underset{\sim}{k}'} = \frac{\partial D}{\partial\omega}\frac{\partial(\omega' + \underset{\sim}{k}'\cdot\underset{\sim}{V})}{\partial\underset{\sim}{k}'} + \frac{\partial D}{\partial\underset{\sim}{k}} = (\underset{\sim}{V}-\underset{\sim}{V})\frac{\partial D}{\partial\omega}$$

vanishes. We, therefore, expand $D(\omega' + \underset{\sim}{k}'\cdot\underset{\sim}{V},\ \underset{\sim}{k}' + \omega\underset{\sim}{V}/c^2)$ to second order

in $\underset{\sim}{k}'$ near a pinch point, although for ω', we expand D only to first order. Thus in Cartesian coordinates

$$D = (\omega' - \omega_o')D_\omega + \tfrac{1}{2}(k_y' - k_{yo}')^2 D_{yy} + \tfrac{1}{2}(k_x' - k_{xo}')^2 D_{xx} + \tfrac{1}{2}(k_z' - k_{zo}')^2 D_{zz} \quad (9a)$$

$$\text{where } D_\omega = [\partial D/\partial\omega']_{\omega'=\omega_o'} \text{ and } D_{ii} = [\partial^2 D/\partial(k_i')^2]_{k_i'=k_{io}'} \quad (9b)$$

assuming D_ω and D_{ii} to be non zero. Here ω_o' and k_{io}' are the values of ω' and k_i' at the pinch point. We calculate only the response from $\omega' = \omega_o'$. Of course, a similar calculation can be done for $\omega' = -\omega_o'$, which will essentially change the $e^{-i\omega_o' t}$ expression in the final equation to a sine or cosine with a phase factor.

It is convenient to evaluate the integrals in the moving frame of reference with the satellite detecting the response. That is, we let $\underset{\sim}{r} = \underset{\sim}{V}t$. In Eq.(6), we can change $d\omega d^3k$ to $d\omega' d^3k'$. The factor in the exponential $-i(\omega t - \underset{\sim}{k}\cdot\underset{\sim}{r})$ becomes $-it(\omega - \underset{\sim}{k}\cdot\underset{\sim}{V}) = -i\omega' t$, since any additional factor such as $i\underset{\sim}{k}'\cdot\underset{\sim}{r}'$ is zero at $\underset{\sim}{r}' = 0$ where $\underset{\sim}{r}'$ is distance from the moving satellite. Near the pinch point, the most important variation in the relation for E occurs due to the zeros of D, assuming that R_{ij} is normalized to have no zeros. In fact, we then replace $R_{ij}(k_x, k_y, k_z)$ by $R_{ij}(k_{xo}, k_{yo}, k_{zo})$ and take it outside of the integrals* Similarly, $P(\omega)/\omega$ can be replaced by $P(\omega_o)/\omega_o$. The relation for E in Eq.(6) with the substitution from (9a) then becomes

$$E_i(t) = \frac{i\, R_{ij} I_j LP}{\varepsilon_o (2\pi)^4 \omega_o} \int_{ic-\infty}^{ic+\infty} e^{-i\omega' t} d\omega' \int_{-\infty}^{\infty} dk_y' \int_{-\infty}^{\infty} dk_x' \int_{-\infty}^{\infty} dk_z'$$

$$\times \frac{1}{(\omega' - \omega_o')D_\omega + \tfrac{1}{2}(k_y' - k_{yo}')^2 D_{yy} + \tfrac{1}{2}(k_x' - k_{xo}')^2 D_{xx} + \tfrac{1}{2}(k_z' - k_{zo}')^2 D_{zz}} \quad (10)$$

---

* A case when this is only approximate is given in Sec. IX(a).

where $c > 0$ is the usual constant in the inversion of the Laplace transform. The k_z' integral can be evaluated using $\int_{-\infty}^{\infty} dx/(x^2 + a^2) = \pi/a$ to give with $\varepsilon = (k_x' - k_{xo}')$

$$E_i(t) = \frac{iR_{ij}I_jLP}{8\pi^3\varepsilon_o\omega_o\sqrt{D_{zz}D_{xx}}} \int_{ic-\infty}^{ic+\infty} e^{-i\omega' t} d\omega' \int_{-\infty}^{\infty} dk_y' \int_{-\infty}^{\infty} d\varepsilon$$

$$\times \frac{1}{\left\{\left[\left(\omega' - \omega_o'\right) D_\omega + \frac{1}{2}\left(k_y' - k_{yo}'\right)^2 D_{yy}\right]\left(2/D_{xx}\right) + \varepsilon^2\right\}^{\frac{1}{2}}} \qquad (11)$$

Now only the singular part of the integral around $\varepsilon = 0$ is of interest so that we can replace the limits by $-\delta$ to δ and obtain the result $2\sinh^{-1}[\ ]$ or $2\cosh^{-1}[\ ]$, where $[\ ] = \delta(D_{xx}/2)^{\frac{1}{2}}[(\omega' - \omega_o')D_\omega + \frac{1}{2}(k_y' - k_{yo}')^2 D_{yy}]^{-\frac{1}{2}}$ depending on whether $[\ ]/\delta$ is greater or less than zero. In the vicinity of the pinch point ($\omega' = \omega_o'$ and $k_y' = k_{yo}'$), we can use the logarithmic approximation for $2\sinh^{-1}[\ ]$ or $2\cosh^{-1}[\ ]$ of large argument, viz. $2\ln[\ ]$, and keeping only the singular part, we write this simply as $-\ln[(k_y' - k_{yo}')^2 + (\omega' - \omega_o')2D_\omega/D_{yy}]$. Changing variables again to $x = (k_y' - k_{yo}')$ we find

$$E_i(t) = \frac{-iR_{ij}I_jLP}{8\pi^3\varepsilon_o\omega_o\sqrt{D_{zz}D_{xx}}} \int_{ic-\infty}^{ic+\infty} e^{-i\omega' t} d\omega' \int_{-\infty}^{\infty} dx\ \ln\left[x^2 + \frac{(\omega' - \omega_o')2D_\omega}{D_{yy}}\right] \qquad (12)$$

Now $\int \ln(x^2 + a^2)dx = x\ln(x^2 + a^2) - 2x + 2a\tan^{-1}(x/a)$. The most singular contribution arises from the region $x \approx 0$ but x/a large, i.e. from the $2a\tan^{-1}(x/a)$ term which gives $2\pi a$. Thus we are left to evaluate

$$E_i(t) = -\frac{i R_{ij} I_j LP}{4\pi^2 \varepsilon_o \omega_o \sqrt{D_{zz} D_{xx} D_{yy}/2D_\omega}} \int_{ic-\infty}^{ic+\infty} e^{-i\omega' t} (\omega' - \omega_o')^{\frac{1}{2}} d\omega' \qquad (13a)$$

The value of the integral is simply[2] $-e^{-i\omega_o' t}\sqrt{\pi}/t^{3/2}\sqrt{-i} = e^{-i\omega_o' t}\sqrt{-i\pi}/it^{3/2}$, so that

$$E_i(t) = -\frac{R_{ij} I_j LP\, e^{-i\omega_o' t}}{4\pi\varepsilon_o t^{3/2} \omega_o} \left[\frac{-2iD_\omega}{\pi D_{zz} D_{xx} D_{yy}}\right]^{\frac{1}{2}} \qquad (13b)$$

The same result can be obtained more directly by performing the ω integration before the k_x' and k_y' integrations in Eq.(11). That is we write

$$E_i(t) = \frac{iR_{ij} I_j LPe^{-i\omega_o' t}}{16\pi^3 \varepsilon_o \omega_o \sqrt{D_{zz} D_\omega/2}} \int_{-\infty}^{\infty} dk_y' \int_{-\infty}^{\infty} dk_x' \int_{ic-\infty}^{ic+\infty} e^{-i(\omega' - \omega_o')t}$$

$$\times \frac{d(\omega' - \omega_o')}{\left[(\omega' - \omega_o') + (k_y' - k_{yo}')^2 \frac{D_{yy}}{2D_\omega} + (k_x' - k_{xo}')^2 \frac{D_{xx}}{2D_\omega}\right]^{\frac{1}{2}}}$$

$$= \frac{i\sqrt{-i}\, R_{ij} I_j LPe^{-i\omega_o' t}}{8\pi^2 \varepsilon_o \omega_o \sqrt{\pi t\, D_{zz} D_\omega/2}} \int_{-\infty}^{\infty} dk_y' \exp\left[\frac{iD_{yy}}{2D_\omega}(k_y' - k_{yo}')^2 t\right]$$

$$\times \int_{-\infty}^{\infty} dk_x' \exp\left[\frac{iD_{xx}}{2D_\omega}(k_x' - k_{xo}')^2 t\right] \qquad (14a)$$

$$= -\frac{R_{ij} I_j LPe^{-i\omega_o' t}}{4\pi\varepsilon_o \omega_o t^{3/2}} \left[-\frac{2iD_\omega}{\pi D_{zz} D_{xx} D_{yy}}\right]^{\frac{1}{2}} \qquad (14b)$$

which is identical to Eq.(13b). In the above we have used the relations[2]

$$\int_{-\infty}^{\infty} dx\, \exp[i\alpha(x-x_0)^2] = \sqrt{i\pi/\alpha} \quad \text{and} \quad \int_{ic-\infty}^{ic+\infty} \frac{e^{-i\omega t}\, d\omega}{(\omega+\alpha)^{\frac{1}{2}}} = \frac{e^{i\alpha t}}{\sqrt{t}}\ 2\sqrt{-i\pi}$$

It is convenient to express D_{xx} and D_{yy} in terms of $D_\perp \equiv \left[\partial^2 D/\partial(k'_\perp)^2\right]_{k'_\perp = k'_{\perp o}}$. (We also denote $D_\parallel \equiv D_{zz}$.) To obtain this relationship, we now specify the direction of $\underset{\sim}{V}_\perp$ to be along the x-axis, and magnetic field to be along the z-axis. In general, if one changes from a Cartesian (k_x, k_y) to a cylindrical $(k_\perp, \phi)$ system, one has

$$\frac{\partial^2 D}{\partial k_x^2} = \cos^2\phi\, \frac{\partial^2 D}{\partial k_\perp^2} - \frac{2\cos\phi\, \sin\phi}{k_\perp}\, \frac{\partial^2 D}{\partial k_\perp \partial \phi} + \frac{\sin^2\phi}{k_\perp^2}\, \frac{\partial^2 D}{\partial \phi^2} + \frac{2\cos\phi\, \sin\phi}{k_\perp^2}\, \frac{\partial D}{\partial \phi} + \frac{\sin^2\phi}{k_\perp}\, \frac{\partial D}{\partial k_\perp} \qquad (15a)$$

and

$$\frac{\partial^2 D}{\partial k_y^2} = \sin^2\phi\, \frac{\partial^2 D}{\partial k_\perp^2} + \frac{2\cos\phi\, \sin\phi}{k_\perp}\, \frac{\partial^2 D}{\partial k_\perp \partial \phi} + \frac{\cos^2\phi}{k_\perp^2}\, \frac{\partial^2 D}{\partial \phi^2} - \frac{2\cos\phi\, \sin\phi}{k_\perp^2}\, \frac{\partial D}{\partial \phi} + \frac{\cos^2\phi}{k_\perp}\, \frac{\partial D}{\partial k_\perp} \qquad (15b)$$

We also find from $\partial D/\partial k'_{xo} = \partial D/\partial k'_{yo} = 0$ that $\partial D/\partial k'_{\perp o} = \partial D/\partial \phi_o = 0$. Since $\partial D/\partial \phi$ is propotional to $\partial(\omega' + \underset{\sim}{k}' \cdot \underset{\sim}{V})/\partial \phi$ (see below), we find that $\partial D/\partial \phi_o = 0$ when $\underset{\sim}{k}'_{\perp o}$ is parallel to $\underset{\sim}{V}_\perp$. Thus since we take $\underset{\sim}{V}_\perp$ along the x-axis, $\phi_o = 0$ and $\underset{\sim}{k}'_{\perp o}$ is also along the x-axis at a pinch point. We also note that $\partial D/\partial k'_{\perp o} = 0$ at the pinch point. Thus we obtain

$$D_{xx} = D_\perp \quad \text{and} \quad D_{yy} = \frac{1}{(k'_{\perp o})^2}\, \frac{\partial^2 D}{\partial \phi_o^2}$$

The angle ϕ occurs only in the $\omega' + \underset{\sim}{k}' \cdot \underset{\sim}{V} = \omega' + \underset{\sim}{k}'_\perp \cdot \underset{\sim}{V}_\perp + k_z V_z = \omega' + k'_\perp V_\perp \cos\phi + k_\parallel V_\parallel$

argument of D since everywhere else D is a function of $k_\parallel$ and $k_\perp$ rather than k_x or k_y separately. This means that we can write

$$\frac{\partial D}{\partial \phi} = \frac{\partial D}{\partial(\omega' + \underset{\sim}{k}' \cdot \underset{\sim}{V})} \frac{\partial(\omega' + \underset{\sim}{k}' \cdot \underset{\sim}{V})}{\partial \phi} = - \frac{\partial D}{\partial \omega} k_\perp' V_\perp \sin\phi$$

and

$$\frac{\partial^2 D}{\partial \phi^2} = \frac{\partial^2 D}{\partial \omega^2} (k_\perp' V_\perp \sin\phi)^2 - \frac{\partial D}{\partial \omega} k_\perp' V_\perp \cos\phi$$

Thus at the pinch point where $\phi = 0$, we obtain

$$\frac{\partial^2 D}{\partial \phi_o^2} = -D_\omega k_{\perp o}' V_\perp \quad \text{so that} \quad D_{xx} = D_\perp \quad \text{and} \quad D_{yy} = -D_\omega \frac{V_\perp}{k_{\perp o}'} \tag{16}$$

Substituting this in Eq.(13b) finally yields

$$E_i(t) = - \frac{R_{ij} I_j LP \, e^{-i\omega_o' t}}{4\pi\varepsilon_o t^{3/2} \omega_o} \left[\frac{2i \, k_{\perp o}'}{\pi D_\parallel D_\perp V_\perp}\right]^{\frac{1}{2}} = - \frac{\sqrt{i} \, R_{ij} I_j LP \, e^{-i\omega_o' t}}{4\pi\varepsilon_o t^{3/2} \, \omega_o T} \tag{17}$$

where $T \equiv [\pi D_\parallel D_\perp V_\perp / 2k_{\perp o}']^{\frac{1}{2}}$ (18)

R_{ij} can also be written in terms ϕ_o, $k_\perp$ and $k_\parallel$, with ϕ dependences such as 1, $\cos^2\phi$, $\sin^2\phi$, and $\cos\phi$, $\sin\phi$. Thus at the pinch point (see previous footnote)

$$R_{ij} = N_{ij}^{(1)} + \left[N_{ij}^{(2)} \cos^2\phi_o + N_{ij}^{(3)} \sin^2\phi_o + N_{ij}^{(4)} \cos\phi_o \sin\phi_o\right](k_{\perp o}^2 c^2/\omega_o^2)$$
$$= N_{ij}^{(1)} + N_{ij}^{(2)} k_{\perp o}^2 c^2/\omega_o^2 \tag{19}$$

The crucial parameter is T which is proportional to the product of the square roots of the curvatures of D with respect to $k_\perp$ and $k_\parallel$. As the dispersion curve becomes flatter, T becomes smaller and the time response for a given excitation level becomes longer.

The approach given above is, relatively speaking, simple-minded. A generalized and somewhat more rigorous approach is as follows. Let us include an $\exp[i\underset{\sim}{k}'\cdot\underset{\sim}{r}']$ factor in Eq.(10) where $\underset{\sim}{r}'$ is distance measured from the satellite. Also as indicated in the previous footnote, R_{ij} should, in general, be kept inside the integral. Similar to Eq.(19) we write

$$R_{ij} = N_{ij}^{(1)} + \left[N_{ij}^{(2)} k_x^2 + N_{ij}^{(3)} k_y^2 + N_{ij}^{(4)} k_x k_y \right] c^2/\omega_o^2 .$$

Also we define new variables (this notation will be used only in the rest of this section)

$$K_i \equiv (k_i' - k_{io}')(D_{ii}/2)^{\frac{1}{2}}, \quad R_i \equiv r_i'(2/D_{ii})^{\frac{1}{2}}, \quad \Omega \equiv (\omega' - \omega_o')D_\omega \text{ and } T \equiv t/D_\omega$$

Then

$$\underset{\sim}{k}'\cdot\underset{\sim}{r}' - \omega' t = \underset{\sim}{k_o}'\cdot\underset{\sim}{r}' - \omega_o' t + \underset{\sim}{K}\cdot\underset{\sim}{R} - \Omega T$$

$$R^2 = (r_x')^2(2/D_{xx}) + (r_y')^2(2/D_{yy}) + (r_z')^2(2/D_{zz})$$

and

$$d^3k'd\omega' = D_\omega^{-1}(D_{xx}D_{yy}D_{zz}/8)^{-\frac{1}{2}}\, d^3K d\Omega .$$

The modified Eq.(10) becomes

$$E_i(\underset{\sim}{R},t) = \frac{iLP\, \exp[i(\underset{\sim}{k_o}'\cdot\underset{\sim}{r}' - \omega_o' t)]}{\varepsilon_o (2\pi)^4 \omega_o D_\omega (D_{xx}D_{yy}D_{zz}/8)^{\frac{1}{2}}} [O_{ij}]_R\, I_j \int e^{-i\Omega T} d\Omega \int \frac{e^{i\underset{\sim}{K}\cdot\underset{\sim}{R}}\, d^3K}{\Omega + K^2}$$

where we have written $R_{ij} = [O_{ij}]_R$, to be explained. Any factor inside the integral such as

$$k_i'k_j' \equiv k_{io}'k_{jo}' + k_{io}'K_j(2/D_{jj})^{\frac{1}{2}} + k_{jo}'K_i(2/D_{ii})^{\frac{1}{2}} + K_iK_j(4/D_{ii}D_{jj})^{\frac{1}{2}}$$

can be changed into the following operator outside of the integrals

$$k'_{io}k'_{jo} - ik'_{io}(2/D_{jj})^{\frac{1}{2}}\partial/\partial R_j - ik'_{jo}(2/D_{ii})\partial/\partial R_i - (4/D_{ii}D_{jj})^{\frac{1}{2}}\partial^2/\partial R_i \partial R_j$$

Thus $[O_{ij}]_R$ is the differential operator with respect to R given by

$$[O_{ij}]_R = N_{ij}^{(1)} + \frac{N_{ij}^{(2)}c^2}{\omega_o^2}\left((k'_{xo})^2 - 2ik'_{xo}\left(\frac{2}{D_{xx}}\right)^{\frac{1}{2}}\frac{\partial}{\partial R_x} - \frac{2}{D_{xx}}\frac{\partial^2}{\partial R_x^2}\right)$$

$$+ N_{ij}^{(3)}\frac{c^2}{\omega_o^2}\left((k'_{yo})^2 - 2ik'_{yo}\left(\frac{2}{D_{yy}}\right)^{\frac{1}{2}}\frac{\partial}{\partial R_y} - \frac{2}{D_{yy}}\frac{\partial^2}{\partial R_y^2}\right)$$

$$+ N_{ij}^{(4)}\frac{c^2}{\omega_o^2}\left(k'_{xo}k'_{yo} - ik'_{xo}\left(\frac{2}{D_{yy}}\right)^{\frac{1}{2}}\frac{\partial}{\partial R_y} - ik'_{yo}\left(\frac{2}{D_{xx}}\right)^{\frac{1}{2}}\frac{\partial}{\partial R_x}\right.$$

$$\left. - \left(\frac{4}{D_{xx}D_{yy}}\right)^{\frac{1}{2}}\frac{\partial^2}{\partial R_x \partial R_y}\right)$$

We now apply the well-known exact result for the three-dimensional Fourier transform:

$$\int \frac{e^{i\underset{\sim}{K}\cdot\underset{\sim}{R}}\, d^3K}{\Omega + K^2} = 2\pi^2\,\frac{e^{-\sqrt{\Omega}\,R}}{R}$$

which shows immediately that the Laplace-transformed Green's function in space $G(\underset{\sim}{R},\Omega)$ varies as $e^{-\sqrt{\Omega}\,R}/R$. As a result, the electric field is

$$E(\underset{\sim}{R},t) = \frac{iLP\,\exp[i(\underset{\sim}{k}_o'\cdot\underset{\sim}{r}' - \omega_o' t)]}{4\pi^2\varepsilon_o\omega_o D_\omega (D_{xx}D_{yy}D_{zz}/2)^{\frac{1}{2}}}\,[O_{ij}]_R\, I_j \int_{ic-\infty}^{ic+\infty} e^{-i\Omega T}\,\frac{e^{-\sqrt{\Omega}\,R}}{R}\, d\Omega$$

It is easy to see by expanding the exponential $\exp(-\sqrt{\Omega}\,R)$ and taking the first singular term in $\Omega \equiv (\omega' - \omega_o')D_\omega$, that the above relation reduces to Eq.(13a) upon applying the previous simplication that $[O_{ij}] = R_{ij}$.

The final integral can also be evaluated exactly by using the Laplace transform identity[2]:

$$\int_{ic-\infty}^{ic+\infty} e^{-i\Omega T}\, e^{-\sqrt{\Omega}\,R}\, d\Omega = \left(\frac{i\pi}{T}\right)^{\frac{1}{2}} \frac{R}{T} \exp(-iR^2/4T)$$

With $T = t/D_\omega$, we obtain

$$E(\underset{\sim}{R},t) = \frac{LP}{4\pi\varepsilon_o\omega_o t^{3/2}} \exp[i(\underset{\sim}{k_d}\cdot\underset{\sim}{r}' - \omega_o' t)] \left(-\frac{2iD}{\pi D_{xx}D_{yy}D_{zz}}\right)^{\frac{1}{2}} [O_{ij}]_R \exp(-iR^2/4T)$$

which is identical to Eq.(13b) upon taking $\underset{\sim}{r}' = \underset{\sim}{R} = 0$ and simplifying $[O_{ij}]_R$ to R_{ij}. More generally, using the operator expression for $[O_{ij}]_R$, we find

$$[O_{ij}]_R = N_{ij}^{(1)} + \frac{N_{ij}^{(2)}c^2}{\omega_o^2}\left[\left(k_{xo}' - \frac{R_x}{T\sqrt{2D_{xx}}}\right)^2 + \frac{i}{D_{xx}T}\right]$$

$$+ \frac{N_{ij}^{(3)}c^2}{\omega_o^2}\left[\left(k_{yo}' - \frac{R_y}{T\sqrt{2D_{yy}}}\right)^2 \frac{i}{D_{yy}T}\right] + \frac{N_{ij}^{(4)}c^2}{\omega_o^2}\left(k_{xo}' - \frac{R_x}{T\sqrt{2D_{xx}}}\right)\left(k_{yo}' - \frac{R_y}{T\sqrt{2D_{yy}}}\right)$$

If we now take $\underset{\sim}{r}' = \underset{\sim}{R} = 0$, corresponding to satellite reception, and $k_{yo}' = 0$, corresponding to letting $\underset{\sim}{V_i}$ be along the x-axis, and using Eq.(16) yields

$$\left[O_{ij}\right]_R = N_{ij}^{(1)} + N_{ij}^{(2)} \left(\frac{k_{\perp o}' c}{\omega_o}\right)^2 \left(1 + \frac{iD_\omega}{(k_{\perp o}')^2 D_\perp t}\right) + N_{ij}^{(3)} \left(\frac{k_{\perp o}' c}{\omega_o}\right)^2 \frac{i}{k_{\perp o}' V_\perp t}$$

If we select only $N_{ij}^{(1)}$ and the first term in $N_{ij}^{(2)}$, our equation for E is identical with those obtained previously. The terms $N_{ij}^{(2)}$ and $N_{ij}^{(3)}$ are only important in one case, to be considered in Sec. IX(a). In fact, these terms are rederived there, starting from the simpler relation given in Eq.(14a).

The analysis given up till now is general and can be applied to the response due to any pinch point in a moving frame of reference. The following sections are concerned with the deduction of T near cyclotron harmonics. But first we give the formulas for the determinant and the minors in Sec. III.

III DETERMINANTS AND MINORS FOR CYCLOTRON HARMONICS

The determinant giving the dispersion equations in the plasma frame of reference can be written in the following form in terms of the "warm" dielectric elements $(\varepsilon_{11})_W$, $(\varepsilon_{13})_W$ and $(\varepsilon_{33})_W$ and with $k_x = k_\perp \cos\phi$, $k_y = k_\perp \sin\phi$

$$\begin{vmatrix} K_\perp - \frac{k_\parallel^2 c^2}{\omega^2} - \frac{k_\perp^2 c^2}{\omega^2}\sin^2\phi + (\varepsilon_{11})_W & i[K_x - (\varepsilon_{11})_W] + \frac{k_\perp^2 c^2}{\omega^2}\sin\phi\cos\phi & k_\perp k_\parallel \frac{c^2}{\omega^2}\cos\phi + (\varepsilon_{13})_W \\ -i[K_x - (\varepsilon_{11})_W] + \frac{k_\perp^2 c^2}{\omega^2}\sin\phi\cos\phi & K_\perp - \frac{k^2 c^2}{\omega^2} + \frac{k_\perp^2 c^2}{\omega^2}\sin^2\phi + (\varepsilon_{11})_W & i(\varepsilon_{13})_W + k_\perp k_\parallel \frac{c^2}{\omega^2}\sin\phi \\ k_\perp k_\parallel \frac{c^2}{\omega^2}\cos\phi + (\varepsilon_{13})_W & -i(\varepsilon_{13})_W + k_\perp k_\parallel \frac{c^2}{\omega^2}\sin\phi & K_\parallel - \frac{k_\perp^2 c^2}{\omega^2} + (\varepsilon_{33})_W \end{vmatrix}$$

$$= 0 \qquad (20)$$

where

$$K_\perp = 1 - \frac{\omega_p^2}{\omega^2 - \omega_b^2}, \quad K_\parallel = 1 - \frac{\omega_p^2}{\omega^2}, \quad K_x = \frac{\omega_p^2 \omega_b}{\omega(\omega^2 - \omega_b^2)} \qquad (21)$$

ω_p is the plasma frequency, ω_b is the electron cyclotron frequency and c is the velocity of light. We have considered only first order terms in $\lambda \equiv (k_\perp v_t/\omega_b)^2$ so that $i(\varepsilon_{12})_W = (\varepsilon_{11})_W = (\varepsilon_{22})_W$. Near the n^{th} cyclotron harmonic ($n \geq 2$) and to first order in $k_\parallel$, we have

$|(\varepsilon_{33})_W/(\varepsilon_{11})_W|$ of order λ and $|(\varepsilon_{13})_W/(\varepsilon_{11})_W| \ll 1$. To calculate the determinant, one can for simplicity set $\phi=0$ since the answer is independent of ϕ.

We first look for solutions having $(\varepsilon_{11})_W$ of order $(\varepsilon_{11})_c$ or of order K which will yield the extraordinary and plasma waves. In this case, one can neglect all $(\varepsilon_{13})_W$ terms. Denoting by D the determinant after dividing by the (33) element, one finds

$$D = \left(K_1 - \frac{k_\parallel^2 c^2}{\omega^2}\right)\left(K_r - \frac{k_\parallel^2 c^2}{\omega^2}\right) + \left(k_\perp k_\parallel \frac{c^2}{\omega^2}\right)^2 \left[1 - \frac{K_\perp - \frac{k^2 c^2}{\omega^2} + (\varepsilon_{11})_W}{K_\parallel - \frac{k_\perp^2 c^2}{\omega^2}}\right]$$

$$- \frac{k_\perp^2 c^2}{\omega^2} K_\perp + 2(\varepsilon_\parallel)_W \left[K_1 - \frac{k_\parallel^2 c^2}{\omega^2} - \frac{k_\perp^2 c^2}{2\omega^2}\right]$$

To first order in $k_\parallel/k_\perp$, one only has to keep the $k_\parallel$ dependence in $(\varepsilon_{11})_W$, so that

$$D \approx K_1 K_r - x\, K_\perp + (\varepsilon_{11})_W [2K_1 - x] \qquad (22a)$$

where

$$x = k_\perp^2 c^2/\omega^2 \quad \text{and} \quad K_{1,r} = 1 - \frac{\omega_p^2}{\omega(\omega \pm \omega_b)} \qquad (22b)$$

In order to evaluate the integrals in the previous section, one needs to know the minors of the determinant including the ϕ angular dependence. After division by the (33) element, one finds for these extraordinary-plasma waves

$$R_{11} = K_\perp - \frac{k_\parallel^2 c^2}{\omega^2} - \frac{k_\perp^2 c^2 \cos^2\phi}{\omega^2} + (\varepsilon_{11})_W - \frac{k_\perp^2 k_\parallel^2 c^4 \sin^2\phi}{\omega^4 [K_\parallel - k_\perp^2 c^2/\omega^2]} \approx K_\perp - x \cos^2\phi + (\varepsilon_{11})_W$$

(23a)

$$R_{12} = -R_{21} = -i[K_x-(\varepsilon_{11})_W] - \frac{k_\perp^2 c^2}{\omega^2}\sin\phi\cos\phi + \frac{k_\perp^2 k_\parallel^2 c^4}{\omega^4}\frac{\sin\phi\cos\phi}{[K_\parallel - k_\perp^2 c^2/\omega^2]}$$

$$\approx -i[K_x-(\varepsilon_{11})_W] - x\sin\phi\cos\phi \qquad (23b)$$

Similarly,

$$R_{22} \approx K_\perp - x\sin^2\phi + (\varepsilon_{11})_W \qquad (23c)$$

We next look for solutions having $(\varepsilon_{33})_W \sim (\varepsilon_{33})_c \sim K$ which will give the ordinary wave. After division by the product of elements $[(11)(22)-(12)(21)] \approx 2(\varepsilon_{11})_W [K_\perp - k_\parallel^2 c^2/\omega^2 - k_\perp^2 c^2/2\omega^2]$ and thereby normalizing R_{33} to one, we find that

$$D = K_\parallel - x + (\varepsilon_{33})_W + (\varepsilon_{13}^2)_W/(\varepsilon_{11})_W \qquad (24)$$

and even including the ϕ dependence we see that $R_{33} = 1$.

We finally seek solutions having $(\varepsilon_{22})_W \sim \lambda^{-2}(\varepsilon_{22})_c \sim \lambda^{-2}K$ to yield an extra wave which can exist. In this case, we have to include the small differences between $(\varepsilon_{22})_W$, $(\varepsilon_{11})_W$ and $(\varepsilon_{12})_W = -(\varepsilon_{21})_W$. Here $(\varepsilon_{13})_W$ and $(\varepsilon_{33})_W$ are both negligible and one obtains to first order in $k_\parallel$ after division by the (33) element multiplied by $(\varepsilon_{11})_W$, that

$$D = 2K_\perp - \frac{k_\perp^2 c^2}{\omega^2} - \frac{2k_\parallel^2 c^2}{\omega^2} + (\varepsilon_{22})_W - \frac{(\varepsilon_{12})_W(\varepsilon_{21})_W}{(\varepsilon_{11})_W} \approx 2K_\perp - x + (\varepsilon_{22})_W + \frac{(\varepsilon_{12}^2)_W}{(\varepsilon_{11})_W} \qquad (25a)$$

The warm elements cancel up to second order in λ. Since the warm elements are much larger than the cold elements, the minors after division by $(\varepsilon_{11})_W$ times the (33) element are

$$R_{11} = R_{22} = 1 \text{ and } R_{12} = -R_{21} = i \text{ so that } R_{11} + iR_{12} = 0,\ R_{11} - iR_{12} = 2. \qquad (25b)$$

In the following section, we investigate more fully the dispersion equations upon inserting the warm dielectric elements.

IV DISPERSION EQUATIONS

In this analysis, we assume ω to be complex and k to be real, since we are interested in a decaying signal after a pulse transmitter is shut off. We also assumed already that $\lambda \equiv (k_\perp v_t/\omega_b)^2 \ll 1$, that the frequency ($\omega$) of concern is very close to a cyclotron harmonic ($n\omega_b$) and that only first order terms in $k_\parallel$ are necessary to consider.

The dispersion equation for the extraordinary-plasma waves then has the form (see Eq.(22a) or Appendix II, Eq.(4) and Appendix I, Eq.(4)),

$$-\frac{x}{(\varepsilon_{11})_W} = \frac{1}{Pk_\perp^{2(n-2)}\mathcal{F}_{n+3/2}} = \frac{(2K_1 - x)x}{K_1K_r - K_\perp x} \tag{26a}$$

where

$$P = \frac{\omega_p^2}{\omega_b^2}\left(\frac{v_t}{\omega_b}\right)^{2(n-2)}\frac{n^2}{n!2^n} \tag{26b}$$

and $\mathcal{F}$ is a function of $k_\parallel c/\omega$ and of $n\omega_b/\omega$. If $k_\parallel$ is exceedingly small that a relativistic analysis is necessary (see Appendix I) then

$$\mathcal{F}_{n+3/2} = F_{n+3/2} + (k_\parallel^2 c^4/2v_t^2\omega^2)(F_{n+5/2} - 2F_{n+3/2} + F_{n+1/2}) \equiv F_{n+3/2} + k_\parallel^2\,\beta \tag{27a}$$

where the argument of the F functions is $\mu\delta$ with $\delta = (\omega - n\omega_b)/\omega$, $\mu = c^2/v_t^2$, $v_t = \sqrt{\kappa T/m}$ is the thermal velocity and Eq.(27a) defines β.

If $k_\parallel$ is somewhat larger that nonrelativistic analysis applies, then

$$\mathcal{F} = -(v_t\omega/\sqrt{2}\, k_\parallel c^2)\, Z(\zeta) \tag{27b}$$

where $\zeta = (\omega - n\omega_b)/\sqrt{2}\, k_\parallel v_t$ and Z is the plasma dispersion function of Fried and Conte[3].

The ordinary wave (for $n > 1$) shows appreciable dispersion effects only for very small $k_\parallel$ when relativistic analysis is necessary in which case its dispersion equation is (see Eq.(24) or Appendix II, Eq.(9) and Appendix I, Eq.(32)):

$$K_\parallel - x = -(\varepsilon_{33})_W + \frac{(\varepsilon_{13}^2)_W}{(\varepsilon_{11})_W}$$

$$= k_\perp^{2n} \frac{c^2}{\omega^2} P_n \left\{ F_{n+5/2} + \frac{k_\parallel^2 c^4}{2v_t^2\omega^2} \left[3(F_{n+7/2} - 2F_{n+5/2} + F_{n+3/2}) - \frac{2(F_{n+5/2} - F_{n+3/2})^2}{F_{n+3/2}} \right] \right\}$$

$$= k_\perp^{2n} \frac{c^2}{\omega^2} P_n \left\{ F_{n+5/2} + k_\parallel^2 \beta_{OR} \right\} \tag{28a}$$

where

$$P_n = \frac{\omega_p^2}{\omega_b^2} \left(\frac{v_t}{\omega_b} \right)^{2(n-1)} \frac{1}{n!\,2^n} \tag{28b}$$

and β_{OR} is defined from Eq.(28b).

Finally, the dispersion equation for the extra wave is (see Eq.(25a), or Appendix II, Sec. II(d)).

$$2K_1 - x = -(\varepsilon_{22})_W + \frac{(\varepsilon_{12})_W(\varepsilon_{21})_W}{(\varepsilon_{11})_W} \tag{29a}$$

where terms on the right hand side cancel up to the second order in λ. To first order in $k_\parallel$ (see Eq.(27a)), the relativistic analysis in Appendix II (Sec. II(d)) and Appendix I (Eq.(33)) yields,

$$2K_1 - x = \frac{x\lambda^2}{n^2} P k_\perp^{2(n-2)} \left[\frac{n+2}{n+1} \mathcal{F}_{n+7/2} - \frac{\mathcal{F}^2_{n+5/2}}{\mathcal{F}_{n+3/2}} \right]$$

$$\simeq \frac{c^2}{\omega^2} P_{ex} k_\perp^{2(n+1)} \left\{ \frac{n+2}{n+1} F_{n+7/2} - \frac{F^2_{n+5/2}}{F_{n+3/2}} \right.$$

$$+ \frac{c^4 k_\parallel^2}{2v_t^2\omega^2} \left[\frac{n+2}{n+1} (F_{n+9/2} - 2F_{n+7/2} + F_{n+5/2}) - \frac{2F_{n+5/2}}{F_{n+3/2}} (F_{n+7/2} - 2F_{n+5/2} + F_{n+3/2}) \right.$$

$$\left. \left. + \frac{F^2_{n+5/2}}{F^2_{n+3/2}} (F_{n+5/2} - 2F_{n+3/2} + F_{n+1/2}) \right] \right\}$$

$$= \frac{c^2}{\omega^2} P_{ex} k_\perp^{2(n+1)} \left\{ \frac{n+2}{n+1} F_{n+7/2} - \frac{F^2_{n+5/2}}{F_{n+3/2}} + k_\parallel^2 P_{ex} \right\} \tag{29b}$$

where

$$P_{ex} \equiv \frac{\omega_p^2}{\omega_b^2} \left(\frac{v_t}{\omega_b} \right)^{2n} \frac{1}{n! 2^n} \tag{29c}$$

and where β_{ex} is defined by the above relations.

In the following section, we use the relations deduced here to calculate the wave number for which matching between satellite and group velocity occurs in the direction parallel to the magnetic field.

V VALUES OF $k_\parallel$ AT THE PINCH POINT

Let us first match satellite velocity to group velocity in the direction parallel to the magnetic field. An examination of the dispersion equations reveals that the most rapid variations of ω_r (the real part of ω) and $k_\parallel$ arise from changes in the $\mathcal{F}$ functions, rather than from the K functions.

When $k_\parallel$ is minute, Eq.(27a) applies. The $k_\parallel^2$ second term is assumed to be smaller than the dominant first term. We note that all functions except $\mathcal{F}$ are more or less real with $\omega \approx \omega_r$ since $\omega_i << \omega_r$. Hence, it is necessary to make $\mathcal{F}$ real as well in order to satisfy the dispersion equations. This can be accomplished to first order by making real the first term, e.g. $F_{n+3/2}$, in Eq.(27a). In fact, we say that the imaginary contributions in the $k_\parallel^2$ factor are cancelled by the small imaginary terms elsewhere in the dispersion equation. As a result, we are dealing with a function, such as

$$\mathrm{Re}\,\mathcal{F}_{n+3/2} = F_{n+3/2} + (k_\parallel^2 c^4/2v_t^2\omega^2{}_r)\ \mathrm{Re}\,[F_{n+1/2} - 2F_{n+3/2} + F_{n+5/2}] \qquad (30)$$

where $F_{n+3/2}$ is taken, with complex argument, along its real track and where Re[ ] is the real part of the indicated combination of functions along this same track.

In order to match satellite to group velocity, we differentiate Eq.(30) and set $\partial\omega_r/\partial k_\parallel = V_\parallel$. Defining $\delta_r = (\omega_r - n\omega_b)/n\omega_b$, we find to first order that we can match the extraordinary-plasma waves with

$$k_{\parallel} = -\frac{n\omega_b V_{\parallel}}{c^2} \frac{\partial F_{n+3/2}/\partial(\mu\delta_r)}{\mathrm{Re}\left[F_{n+1/2} - 2F_{n+3/2} + F_{n+5/2}\right]} = -\frac{\mu V_{\parallel} \partial F_{n+3/2}/\partial(\mu\delta_r)}{2n\omega_b \, \mathrm{Re}\beta} \qquad (31)$$

where β is given by Eq.(27c).

For the ordinary wave, we have a different factor (see Eq.(28a)) multiplying $k_{\parallel}^2$ in the dispersion relation with $F_{n+5/2}$ as the dominant part. Using similar arguments to the above, a match is obtained for

$$k_{\parallel} = \frac{-n\omega_b V_{\parallel}}{c^2} \frac{\partial F_{n+5/2}/\partial(\mu\delta_r)}{\mathrm{Re}\left[3F_{n+7/2} - 2F_{n+5/2} + F_{n+3/2} - \frac{2\left(F_{n+5/2} - F_{n+3/2}\right)^2}{F_{n+3/2}}\right]} = \frac{-\mu V_{\parallel} \partial F_{n+5/2}/\partial(\mu\delta_r)}{2n\omega_b \mathrm{Re}\beta_{OR}} \qquad (32)$$

where $F_{n+5/2}$ is taken along its real track and $\mathrm{Re}\beta_{\parallel}$ is the real part of the indicated combination of functions in Eq.(28a) along this same path.

For the extra wave, we note that we require very large values of F to satisfy the dispersion Eq.(29b). Using the relations in Appendix I, Eq.(28), for large F, we note that

$$\frac{n+2}{n+1} F_{n+7/2} - \frac{F_{n+5/2}^2}{F_{n+3/2}} \approx \frac{F_{n+7/2}}{(n+1)(2n+3)} \qquad (33)$$

Similar considerations to the above show that a match occurs for

$$k_{\parallel} = -\frac{\mu V_{\parallel} \, \partial F_{n+7/2}/\partial(\mu\delta_r)}{(n+1)(2n+3)2n\omega_b \mathrm{Re}\beta_{ex}} \qquad (34)$$

where $F_{n+7/2}$ is taken along its real track and $\mathrm{Re}\beta_{ex}$ is the real part of the indicated combination of functions in Eq.(29b) along this same path.

Plots of the functions $F_{n+3/2}$ and $F_{n+3/2}/[\partial F_{n+3/2}/\partial(\mu\delta_r)]$ $\equiv F/F'$ for $n = 1$ to 7 are shown in Figs. 1 and 2 in the region where F is large and negative. One notes that the ratio F/F' is always of order one in this region.

Let us now investigate whether one can match with slightly larger $k_\parallel$ values where the Z-function is valid and where one can use nonrelativistic theory. We still assume $\lambda < 1$. Note that for $\lambda \ll 1$, we use large values of Z, thereby requiring the analytic continuation of Z (see Appendix II, Sec. IV). To satisfy the dispersion relation (Eq.(26a) with (27b)) for the extraordinary-plasma wave, the Z-function has to be real. The most rapid variations result from the ω and $k_\parallel$ dependences of $Z/k_\parallel$. Whether or not we need the analytic continuation of Z, provided it is real, it can be written as a function of $\zeta_r = (\omega_r - n\omega_b)/\sqrt{2}\, k_\parallel v_t$. The matching condition then gives the following result.

$$\frac{\partial(Z/k_\parallel)}{\partial k_\parallel} + V_\parallel \frac{\partial(Z/k_\parallel)}{\partial \omega_r} = 0 \quad \text{or} \quad \frac{V_\parallel}{\sqrt{2}\, v_t} - \zeta_r = \frac{Z}{\partial Z/\partial \zeta_r} \tag{35}$$

When $\lambda \ll 1$ or more accurately $(n^2\lambda^{n-1}/2^n n!) < (\omega v_t/\omega_p c)^2 K_\perp$, the analytic continuation is used to provide large values of Z, given by (see Appendix I, Eq.(29)) $Z \simeq \pm 2\pi \exp[(\pi/4\zeta_r)^2]$ and Z increases as $\zeta_r \to 0$. Thus $Z/(\partial Z/\partial \zeta_r) = 8\zeta_r^3/\pi^2$ which is small compared to $-\zeta_r$. As a result we have from Eq.(35):

$$\zeta_r = V_\parallel/v_t\sqrt{2} \tag{36a}$$

This fixes the value of Z as well. However, in the $\lambda \ll 1$ region,

we want Z to attain huge values which vary as ω_r varies, even though assigning a value to $k_{\parallel}$. The value in Eq.(36a) is useless since Z cannot become too large once the argument of the exponential is fixed.

When λ is larger $(n^2\lambda^{n-1}/2^n n! > (\omega v_t/\omega_p c)^2 K_\perp)$, we do not need the analytic continuation of Z. As a result, for $\zeta >> 1$, $Z \approx -\zeta^{-1}[1+(2\zeta^2)^{-1}]$. We can also neglect the imaginary part of ω and take ζ to be real. Thus $Z/Z' = -\zeta(1-\zeta^{-2})$ and Eq.(35) becomes

$$\zeta = \sqrt{2}\ v_t/V_{\parallel} \qquad \text{or} \qquad \mu\delta = 2k_{\parallel}c^2/\omega V_{\parallel} \tag{36b}$$

which is consistent with the preassumption that $\zeta > 1$. In order for the asymptotic expansion of Z to be valid, we also require $\mu\delta >> 1$, which is obeyed provided $k_{\parallel}c/\omega >> V_{\parallel}/2c$. (See the discussion in Appendix I, end of Sec. III.) The largest value that $\omega v_t Z/\sqrt{2}\ c^2 k_{\parallel}$ can attain is $(\mu\delta)^{-1}$ of order one. The electrostatic dispersion equation for this case can be obtained from Eqs.(26a,b) and (27b) for $\lambda < 1$, $x >> 1$ and with $\mathcal{F} \approx (v_t\omega/\sqrt{2}\ k_{\parallel}c^2)$ $\cdot\zeta^{-1}(1 + 1/2\zeta^2) = \mu\delta(1 + 1/2\zeta^2)$, viz.

$$\frac{\omega - n\omega_b}{\omega} = \frac{\omega_p^2}{\omega^2}\,\frac{n^2\lambda^{n-1}}{2^n n! K_\perp}\left(1 + \frac{k_{\parallel}^2\ v_t^2}{(\omega - n\omega_b)^2}\right) \tag{37}$$

Near the matching point, the term in the parenthesis is of order $[1 + (V_{\parallel}/2v_t)^2] \simeq 1$. Because of the limitation that $\mu\delta > 1$, we can allow the rest of the right-hand side to be as small as v_t^2/c^2 before the large inverse argument approximation for Z becomes invalid. This means that $(n^2\lambda^{n-1}/2^n n!) > (\omega v_t/\omega_p c)^2 K_\perp$ which is the inequality

we stated at the start.

We conclude that we can match $k_{\parallel}$ for $\lambda \ll 1$ (that is near electromagnetic modes) when relativistic F function applies but not when the Z function applies. For larger λ when the waves become electrostatic, we can match with a larger $k_{\parallel}$ value using the nonrelativistic Z-function.

In the following section, we perform the analysis for matching perpendicular to magnetic field.

VI VALUES OF $k_{\perp}$ AT PINCH POINTS FOR LARGE REFRACTIVE INDEX

The next task is to match satellite and group velocities perpendicular to the magnetic field direction. Since the $k_{\parallel}$ term is very small, we shall neglect it in the following discussion.

First, we show that for $n > 4$ and $\omega > \omega_T$ where $\omega_T^2 \equiv \omega_b^2 + \omega_p^2$, we require unrealistically small values of $V_{\perp}$ to obtain a match using the Bernstein electrostatic mode. For $\omega \gg \omega_T$ (or $K_{\perp} \simeq 1$), the matching points (if they exist) would not be far displaced in frequency from the n^{th} harmonic. Hence only the n^{th} term in the well-known I_n expansion is necessary and then the electrostatic mode is given by

$$\omega - n\omega_b = \omega_p^2 \, nI_n e^{-\lambda}/\omega_b \lambda K_{\perp} \qquad (38)$$

This equation is the extension for larger λ of Eq.(37). Note that here, $(\omega - n\omega_b)/\omega$ is sufficiently large that the $(-\zeta^{-1})$ limit applies for Z and one does not need the analytic continuation of Z.

For matching, we differentiate Eq.(38) with respect to k_x and k_y (in the two directions perpendicular to magnetic field) and we equate $\partial\omega/\partial k_x = V_x$ and $\partial\omega/\partial k_y = V_y$. The derivative of $K_\perp$ gives a negligible contribution. Combining the x and y- expressions gives

$$V_x/V_y = k_x/k_y \text{ and hence } V_\perp/k_\perp = V_x/k_x = V_y/k_y \text{ or } \underset{\sim}{k}_\perp \cdot \underset{\sim}{V}_\perp = k_\perp V_\perp \quad (39a)$$

Using this, we find that the matching condition is

$$V_\perp \left(\frac{\omega_b^2}{v_t \omega_p^2}\right) \frac{\omega}{n\omega_b} K_\perp = \frac{2n}{\lambda^{3/2}} I_n \, e^{-\lambda}\left[-\lambda\left(1 - \frac{I_{n+1}}{I_n}\right) + n - 1\right] \quad (39b)$$

Since $V_\perp/v_t$ can be as large as 1/16 and ω_p^2/ω_b^2 varies between 1/4 and 100 for satellite altitudes between 500 and 30,000km (see Fig.3), we note that the maximum value of the left-hand side is $4/16 = 0.25$. Even assuming $V_\perp/V \simeq 1/10$, we require, for $K_\perp \simeq 1$, the right-hand side to attain a value of 0.025. In Fig. 4, we present plots of the right-hand side for $n = 2$ to 5, and we find large enough values for $n \leq 4$ only and not for larger n. The maximum group velocity points are also tabulated in Table 1. Thus using the Bernstein electrostatic mode, we cannot match perpendicular to the magnetic field for $n > 4$ and $\omega > \omega_T$.

The lack of this matching capability is equivalent to the lack of a stationary point in the integration over $k_\perp$ to obtain the time response. The stationary phase method has been used by Deering and Fejer[4]. In order to evaluate the $k_\perp$ integration, they look for points where $ak_\perp^{2n-2} \pm k_\perp r_\perp$ is stationary where in our notation $ak_\perp^{2(n-1)}$

is simply the small λ limit of $(\omega_p^2 n\, I_n e^{-\lambda}/\omega_b \lambda K_\perp)t$. The stationary point is more accurately obtained by solving

$$\frac{\partial}{\partial k_\perp}\left[\frac{\omega_p^2\, n I_n e^{-\lambda} t}{\omega_b \lambda K_\perp} \pm k_\perp r_\perp\right] = 0 \quad \left(\text{rather than } \frac{\partial}{\partial k_\perp}[a k_\perp^{2(n-1)} \pm k_\perp r_\perp] = 0\right)$$

which yields exactly Eq.(39) with $r_\perp/t$ replacing $V_\perp$. Thus by adopting properly the I_n function rather than its expansion when $\lambda \sim 1$, we do not find any stationary points for satellite reception ($r_\perp = V_\perp t$) when $n > 4$ and $K_\perp \sim 1$. Deering and Fejer remark that the Shkarofsky and Johnston's requirement that a matching point exist, is not necessary for electrostatic waves. This argument is self-defeating since they require an identical condition to calculate their time response in the satellite by the stationary phase method.

When $\omega \ll \omega_T$ or $(n\omega_b)^2 \ll \omega_p^2$ or $K_\perp \approx -\omega_p^2/\omega_b^2(n^2-1)$, the electrostatic waves are backward and matching in the perpendicular direction is much easier to accomplish. In this limit, we have an extra (n^2-1) factor coming from $K_\perp$ which helps the matching to such a degree as to make it far more often possible. Equation(39) can be written as

$$-\frac{V_\perp}{v_t} = \frac{2(n^2-1)n\, I_n e^{-\lambda}}{\lambda^{3/2}}\left[-\lambda\left(1 - \frac{I_{n+1}}{I_n}\right) + n - 1\right] \qquad (40)$$

In Table 2, the maximum of the right-hand side is given. These values are only an indication since they are based on the approximation using a single I_n, which is especially bad for backward waves. Nonetheless, we conjure from the values $(\partial\omega/v_t\partial k$ values greater than

TABLE 1

Maximum Group Velocity for the Bernstein Electrostatic Mode When $\omega_p^2 << (n\omega_b)^2$

n	λ	$\left(\frac{\partial\omega}{\partial k}\right)_{max} \frac{\omega_b^2}{v_t \omega_p^2} K_1$	$(\omega - n\omega_b)\frac{\omega_b}{\omega_p^2} K_1$
2	0.2	0.1475	0.041
3	1	0.055	0.0245
4	2	0.0269	0.0137
5	3	0.0151	0.00757

TABLE 2

Approximate Maximum Group Velocity Values for the Bernstein Electrostatic Mode when $\omega_p^2 >> (n\omega_b^2)$

n	λ	$\left(\frac{\partial\omega}{\partial k}\right)_{max} \frac{1}{v_t}$	$(n\omega_b - \omega)/n\omega_b$
2	0.2	0.4425	0.061
3	1	0.440	0.0653
4	2	0.401	0.0513
5	3	0.378	0.0363

0.25) given in the Table, that a match is possible up to quite large n values.

When matching occurs for backward or forward electrostatic waves with $\lambda < 1$, we use the small argument approximation I_n in Eq.(39) and find

$$\lambda = \left[- \frac{V_\perp \, 2^n n!}{v_t 2n(n-1)(n^2-1)} \left(1 - \frac{\omega_b^2 (n^2-1)}{\omega_p^2} \right) \right]^{2/[2n-3]} \tag{41}$$

(We note that the small λ approximation breaks down for large n since Eq.(41) indicates that $\lambda \to 1$ for large n.) Equation(37) yields

$$\frac{\omega - n\omega_b}{n\omega_b} = \frac{V_\perp}{2n(n-1)v_t} \left[- \frac{V_\perp \, 2^n n!}{v_t 2n(n-1)(n^2-1)} \left(1 - \frac{\omega_b^2 (n^2-1)}{\omega_p^2} \right) \right]^{1/[2n-3]}$$

$$= V_\perp k_\perp / [2(n-1) n\omega_b] \tag{42}$$

In order to satisfy the requirement that $|(n\omega_b - \omega)/n\omega_b| > (v_t/c)^2$, we need

$$\left| \left(\frac{V_\perp c^2}{v_t^3} \right)^n \frac{v_t^4}{V_\perp c^3} \right| > [2n(n-1)]^{n-1} \left[\frac{n^2-1}{2^n n! \left(1 - \frac{\omega_b^2 (n^2-1)}{\omega_p^2} \right)} \right]^{\frac{1}{2}} \tag{43}$$

For example when $n = 2$ we need $|V_\perp c / v_t^2| > [6/|1 - 3\omega_b^2/\omega_p^2|\,]^{\frac{1}{2}}$ and when $n = 3$ we need $|V_\perp^2 c^3 / v_t^5| > 24\,[6/|1 - 8\omega_b^2/\omega_p^2|\,]^{\frac{1}{2}}$ which are easily satisfied for satellite parameters. For larger n, the inequality in Eq.(43) becomes even easier to realize.

Substituting Eq.(42) into Eq.(36b) yields the magnitude

of $k_{\parallel}c/\omega$, namely: $k_{\parallel}/k_{\perp} = V_{\perp}V_{\parallel}/\,[4v_t^2(n-1)]$ and

$$\frac{k_{\parallel}c}{\omega} = \frac{V_{\parallel}V_{\perp}c}{v_t^3 4n(n-1)}\left[-\frac{V_{\perp}\,2^n n!}{v_t^{2n}(n-1)(n^2-1)}\left(1-\frac{\omega_b^2(n^2-1)}{\omega_p^2}\right)\right]^{1/[2n-3]} \qquad (44)$$

For typical values $k_{\parallel}c/\omega$ is somewhat less than one. (The condition that $k_{\parallel}c/\omega$ be greater than $V_{\parallel}/2c$ is the same as requiring $|\mu\delta| > 1$). We see from Eq.(44) that the pinch point for electrostatic waves parallel to magnetic field occurs for wavelengths somewhat greater than the free space value. Perpendicular to magnetic field, the wavelength given by Eq.(41) is very much less than the free space value.

The frequency measured by the satellite is $\omega' = \omega - \underset{\sim}{k}\cdot\underset{\sim}{V} \approx \omega - k_{\perp}\cdot V_{\perp}$. The Doppler shift $\Delta\omega$ associated with the electrostatic matching point is

$$-\frac{\Delta\omega}{n\omega_b} = \frac{k_{\perp}V_{\perp}}{n\omega_b} = \frac{\sqrt{\lambda}\;V_{\perp}}{nv_t}$$

so that

$$-\frac{\Delta\omega}{\omega - n\omega_b} = 2(n-1) \qquad (45)$$

The Doppler shift is larger than the deviation from the harmonic due to matching.

It remains to be shown that in spite of the relatively large value of $k_{\parallel}$ in Eq.(44), no other terms in the electrostatic dispersion equation are as important as those used. In general, the electrostatic dispersion equation for all $k_{\parallel}$ has the form[5]

$$k_\perp^2 [(\varepsilon_{11})_c + (\varepsilon_{11})_w] + k_\parallel^2 [(\varepsilon_{33})_c + (\varepsilon_{33})_w] + 2k_\perp k_\parallel (\varepsilon_{13})_w = 0$$

Substituting the cold and warm dielectric elements in terms of the Z function given in Appendix I, Eq. (31), yields

$$k_\perp^2 K_\perp + k_\parallel^2 K_\parallel + \frac{\omega_p^2 n^2 \lambda^{n-1}}{\omega k_\parallel v_t \sqrt{2}\, 2^n n!} \left[k_\perp^2 Z - \frac{\lambda k_\parallel^2}{n^2} \zeta Z' - k_\perp k_\parallel \sqrt{2\lambda}\, Z' \right] = 0$$

Using $Z = -\zeta^{-1}[1 + (2\zeta^2)^{-1}]$ and $\zeta Z' = \zeta^{-1}$ gives

$$K_\perp + \frac{k_\parallel^2 K_\parallel}{k_\perp^2} - \frac{\omega_p^2 n^2 \lambda^{n-1}}{\omega 2^n n! (\omega - n\omega_b)} \left[1 + \frac{k_\parallel^2 v_t^2}{(\omega - n\omega_b)^2} + \frac{\sqrt{2}\, v_t^3 k_\parallel^3}{\omega(\omega - n\omega_b)} + \frac{2\sqrt{2}\, v_t^3 k_\parallel^3}{\omega(\omega - n\omega_b)^2} \right] = 0$$

The latter two terms in the brackets are small near the pinch values of $k_\parallel$ and $\omega - n\omega_b$. Use of Eqs.(44), (42) and (41) shows that the second term in the brackets is larger than the third and fourth by order $(\omega/k_\parallel V_\parallel)^2$ and $\omega/k_\parallel V_\parallel$ respectively, and is also larger than the $k_\parallel^2 K_\parallel / k_\perp^2$ term by order $(v_t/V_\perp)^2$. Hence the dispersion equation we have used previously in Eq.(37) is correct in the neighbourhood of pinch values having $\lambda < 1$.

Deering and Fejer[4] use Eq.(37) without the $k_\parallel^2$ additional term. To obtain the time response, instead of integrating over $k_\parallel^2$ as one should, they estimate the value of this integral based on Landau damping considerations. This approximation inherently introduces an error which indeed leads to the wrong time dependence. They obtain a t^{-1} decrease, whereas we find in Sec.VIII at $t^{-3/2}$ decrease. The correct approach should be based on the $k_\parallel$ pinch value using Eq.(37) which, as proven above, contains the most important terms.

We conclude that one can match satellite to group velocity for $n \leq 4$ with electrostatic Bernstein waves both in the perpendicular direction with a wavelength much less than the free space wavelength and in the parallel direction with a wavelength somewhat larger than the free space value. For $n > 4$, one can only match when $\omega_p^2 >> (n\omega_b)^2$, i.e. where the Bernstein waves are backward. Figure 3 shows that this can occur below 800km or above 15,000km. Since Alouette 1 travels at 1,000km, these backward waves are infrequently observed. Alouette 2 should satisfy the conditions for backward waves at lower altitudes. When $(n\omega_b)^2 >> \omega_p^2$ which very often occurs for Alouette 1, it is very difficult to obtain a match for harmonics greater than the fourth. The reason for this is that the dispersion relation for the electrostatic mode is very "flat" i.e. varies over a very large range of k_1 for a slight change in ω, so that the group velocity is small and the satellite travels faster than the wave. (Parenthetically, the extra wave mentioned in Sec. IV is even "flatter" when $x >> 1$ by about v_t^2/c^2 and hence no matching point can be expected for this additional wave for large reflective index values.)

There is, however, the distinct possibility that the matching condition in the perpendicular direction may not be required for electrostatic waves because of finite antenna length. The reason for this has been recently implied by Calvert and Van Zandt[6]. Suppose we are dealing with excited wave packets having very small group velocities, but spread out throughout the original region of

excitation, which is about an antenna length. Since in the time that the cyclotron resonances last, the satellite travels about an antenna length, the satellite, in this picture, is essentially moving through and sampling in distance the more or less stationary blobs or wave packets in the excited region. However, an analysis including finite antenna size is too complex and will not be done here.

VII VALUES OF $k_\perp$ AT PINCH POINTS FOR REFRACTIVE INDEX NEAR OR LESS THAN ONE

Let us now attempt to obtain a match for lower $k_\perp$ values near or less than the free-space values. As shown in Sec. V, $k_\parallel$ can only be matched in this region if the relativistic analysis is used. We therefore restrict the following analysis for matching $k_\perp$ also to the relativistic analysis.

Case(i): Consider first the extraordinary wave given in Eqs.(26a) to (27a) with $k_\parallel = 0$, viz.

$$\frac{1}{Pk_\perp^{2(n-2)}F_{n+3/2}} = \frac{(2K_1 - x)x}{K_1K_r - K_\perp x} \tag{46}$$

Denote $F' \equiv \partial F_{n+3/2}/\partial(\mu\delta_r)$ with the derivative taken along the track of real $F_{n+3/2}$. Differentiate respectively with respect to k_x and k_y and equate $\partial\omega_r/\partial k_x = V_x$ and $\partial\omega_r/\partial k_y = V_y$. The terms involving derivatives of the K- and x- functions with respect to ω_r are negligible since $\omega_r >> k_\perp V_\perp$. Omitting, for simplicity, the $n+3/2$ subscript

on F and F', one has

$$-\frac{F'\mu}{Pk_\perp^{2(n-2)}F^2}\frac{k_xV_x}{n\omega_b}-\frac{2(n-2)k_x^2}{Pk_\perp^{2(n-2)}Fk_\perp^2}\simeq\frac{2xk_x^2}{k_\perp^2(K_1K_r-K_\perp x)}\left[2(K_1-x)+\frac{(2K_1-x)K_\perp x}{K_1K_r-K_\perp x}\right]$$

Subtracting the x- and y- derivative expressions gives

$V_x/V_y = k_x/k_y$. Hence $V_\perp/k_\perp = V_x/k_x = V_y/k_y$ or $\underset{\sim}{k}_\perp \cdot \underset{\sim}{V}_\perp = k_\perp V_\perp$

Adding the x- and y- expressions then yields

$$-\frac{F'\mu}{Pk_\perp^{2(n-2)}F^2}\frac{k_\perp V_\perp}{n\omega_b}-\frac{2(n-2)}{Pk_\perp^{2(n-2)}F}=\frac{2x}{(K_1K_r-K_\perp x)}\left[2(K_1-x)+\frac{(2K_1-x)K_\perp x}{K_1K_r-K_\perp x}\right] \tag{47a}$$

Substitute Eq.(46) into (47a) for F or F^2 and obtain

$$(n-1)2K_1-nx+\frac{(2K_1-x)K_\perp x}{K_1K_r-K_\perp x}=-\left(\frac{K_1K_r-K_\perp x}{2x}\right)\left(\frac{F'\mu}{Pk_\perp^{2(n-2)}F^2}\frac{k_\perp V_\perp}{\omega}\right) \tag{47b}$$

$$=-\left(\frac{2K_1-x}{2}\right)\left(\frac{F'\mu}{F}\frac{k_\perp V_\perp}{\omega}\right)=-\left(\frac{x(2K_1-x)^2}{2(K_1K_r-K_\perp x)}\right)\left(Pk_\perp^{2(n-2)}F'\mu\frac{k_\perp V_\perp}{\omega}\right) \tag{47c,d}$$

There are three regions where one can satisfy the above equations, namely near (i) the Appleton-Hartree solution, $x \approx K_1K_r/K_\perp$ (ii) near $x \approx 2K_1$ and (iii) for $x \ll 1$. Let us consider these separately.

CASE (i): When $x \approx K_1K_r/K_\perp > 0$ we find from Eqs.(46) and (47c)

$$x - \frac{K_\perp K_r}{K_\perp} \approx - \frac{K_\perp^3 K_r}{K_\perp^3} k_\perp^{2(n-2)} PF = \frac{2K_\perp K_r}{K_\perp} \frac{F\omega}{F'\mu k_\perp V_\perp} \tag{48a}$$

where $K_\perp = (K_\perp + K_r)/2$. Also from Eq.(42d), we note that

$$2\left(\frac{K_\perp}{K_\perp}\right)^2 = -Pk_\perp^{2(n-2)}\mu \frac{F'k_\perp V_\perp}{\omega} \tag{48b}$$

which shows that $(V_\perp k_\perp F'/\omega) < 0$. Hence from Eq.(48a), we can have $x \gtrless K_\perp K_r/K_\perp$ depending on whether $F \lessgtr 0$. This is consistent with the signs of F used in Appendix II, Figs. 3(a) and 3(b), near the electromagnetic solution. Since $\pm k_\perp = \omega\sqrt{x}/c$, Eq.(48a) gives a very small deviation of x from $K_\perp K_r/K_\perp$, of the order of $v_t^2/cV_\perp$.

$$\left| x - \frac{K_\perp K_r}{K_\perp} \right| = 2\sqrt{\frac{K_\perp K_r}{K_\perp}} \frac{F}{F'} \frac{v_t^2}{cV_\perp} \tag{48c}$$

Equation (48b) cannot be satisfied for n = 1 since the right-hand side is much larger than the left-hand side. This is again consistent with the results in Appendix II. For n = 2, Eqs.(48a-c) can be satisfied for values of F of order one. In fact for $x < K_\perp K_r/K_\perp$, we can use the region where $F > 0$ and both ω and $k_\perp$ are real. As is shown in Appendix II, Section III(a), $\partial\omega/\partial k_\perp$ is of order v_t^2/c at $\omega = n\omega_b$ and increases to about c as ω tends towards the Appleton-Hartree solution. At some intermediate point, the slope must equal $V_\perp$. Thus a match is readily obtained for n = 2 and $\omega > n\omega_b$ on the $F > 0$ branch with real ω and real $k_\perp$. Of course, one can also match for $x > K_\perp K_r/K_\perp$ and n = 2 on the $F < 0$ branch with complex ω, using the analytic continuation of F where

both F and F' are very large (see Figs. 1 and 2). Since two matching points exist differing relativistically in ω and by deviations from $K_1K_r/K_\perp$ of $v_t^2/cV_\perp$, beating between these pinch points occurs, but after a time duration much longer than the interference times on the second harmonic resonance observed[6] by Explorer XX. (We shall show later that multiple pinch points also exist for all harmonics near $x = 2K_1$ when $K_1 > 0$, but again this cannot explain the interference effects observed[6] even for high harmonics.) In References 4 and 6, the interference is associated with beating between electrostatic wave packets.

For $n \geq 3$, we can only match both $k_\parallel$ and $k_\perp$ near $x \approx K_1K_r/K_\perp$ using the $F < 0$ branch, with the values in Figs. 1 and 2. If we attempt to use the $F > 0$ branch, we have to recall the behaviour of F shown in Appendix I, Figs. 3 and 4. Since $n \geq 3$, $\partial\omega/\partial k_\perp$ at $\omega = n\omega_b$ is of order c and lower group velocities only occur in the region $\omega_r < n\omega_b$ (not shown in Fig. 4 of Appendix I) where the F curve turns around. In fact, F is not large here but F' goes to ∞ at the turn around point. In order to satisfy Eq.(48b), we have to go quite close to $F' = \infty$. This, however, upsets the $k_\parallel$ matching point in Eq.(31), since upon substituting Eq.(48b) into Eq.(31) we find that $k_\parallel$ becomes too large. As a result for $n \geq 3$, we can only use the $x > K_1K_r/K_\perp$ matching points and the calculations given below were actually done only for $F < 0$.

We note that the above matching points are present only when there exists an Appleton-Hartree solution, i.e. when $K_1K_r/K_\perp > 0$. When K_1, K_r and $K_\perp$ are all greater than zero, the Appleton-Hartree wave is called the X-wave, and when $K_1 > 0$ but $K_r < 0$ and $K_\perp < 0$, it

is known as the Z-wave. Equation (48c) shows that x (the square of the refractive index perpendicular to magnetic field where the wave group velocity equals the satellite velocity) is composed of the Appleton-Hartree part plus a correction term. These two parts are plotted separately in Fig. 5 versus ω_p^2/ω_b^2 for n = 1 to 7 and for the $x > K_l K_r/K_\perp$ matching point. The X and Z-wave values are both illustrated, the Z-wave curves being the more vertical ones. In Fig. 6, the corresponding values of $c^2(\omega_r - n\omega_b)/n\omega_b v_t^2$ are given which provide an indication of the deviation from the exact cyclotron harmonic value in the plasma medium. The deviation recorded by the satellite is the above value with the Doppler shift $k_\perp V_\perp$ subtracted. The calculations were performed by solving Eq.(48b) as a function of ω_p^2/ω_b^2 to yield F', taking $v_t^2/cV_\perp = 0.03$ and $c^2/v_t^2 = 3 \times 10^6$. Then Figs. 1 and 2 for $F \ll 0$ were used to give F and $(\omega_r - n\omega_b)/n\omega_b$. With these values, one can also calculate from Eq.(31) the magnitude of $k_n c^2/\omega V_n$, the normalized wave number in the medium where the group velocity matches the satellite velocity in the parallel direction. Plots are shown in Fig. 7.

The results in Figs. 5 to 7 indicate the following:

$\underline{(k_\perp c/\omega)^2}$: The theory is only valid if the deviation from $K_l K_r/K_\perp$ is small. Figure 5 shows that $K_l K_r/K_\perp$ varies from about 5 to 0.02 in which range the deviation is between 5% and 30%. For the lower values where K_l or K_r approaches zero, or less than 1% near a cut-off, the approximations begin to fail. Over most of the range of ω_p^2/ω_b^2, one can conclude that the

wavelength perpendicular to magnetic field is several times larger than the free-space wavelength. The analysis may have to include both finite antenna length and possibly sheath effects for the Z-wave values giving smaller wavelengths or $(k_\perp c/\omega)^2 > 1$.

$\underline{(\omega - n\omega_b)c^2/n\omega_b v_t^2}$: In all cases to within 0.6% of a resonance or a cut-off, this parameter is less than 100. Usually it is greater than 10 for the X-wave and $n > 3$. The Doppler shift correction, $k_\perp V_\perp/\omega = \sqrt{K_l K_r/K_\perp}\, V_\perp/c$ is also of the same order of magnitude. This theory therefore indicates very small deviations from the harmonic.

$\underline{k_\parallel c^2/\omega V_\parallel}$: This parameter is generally about 0.25 for the third harmonic decreasing to 0.15 for the seventh. Since $c^2/\omega V_\parallel$ is of the order of 0.25 earth radii, such small values of the $k_\parallel$ indicate characteristic lengths ($\sim 1/k_\parallel$) of one earth radius This length is larger than the nonuniformities in the magnetic field which one can expect to be present over distances greater than 0.1 earth radius. However, the energy, travelling at the light velocity, has not arrived yet in the times of concern to these large distances given by $1/k_\parallel$. All that the analysis is attempting to say is that the satellite travels in a uniform static excitation field spread over huge distances in the parallel direction. Nonuniformities in magnetic field may produce some effect on the signal amplitude. The question of whether one can have $k_\parallel \to 0$ in magnetic field systems with nonuniformities

at the ends depends on boundary conditions, and will not be theorized upon here. One can suggest looking for possible correlations of variations in signal strength with non-uniformities along magnetic field lines.

CASE (ii): When $x \approx 2K_1 > 0$, we can also get, from Eqs.(46) and (47), two matching points on each side of $x \gtrless 2K_1$ with $F \gtrless 0$ respectively. To see this, expanding around $x \approx 2K_1$, we find from Eq.(47b)

$$-\frac{F^2}{F'} = \frac{c^2 V_\perp}{8Pk_\perp^{2n-5} v_t^2 \omega} \tag{49}$$

so that $F'k_\perp V_\perp/\omega < 0$ and from Eq.(47a,c) we obtain

$$x - 2K_1 = \frac{K_1}{2Pk_\perp^{2(n-2)}F} = -\frac{4K_1}{\mu}\frac{F}{F'}\frac{\omega}{k_\perp V_\perp} \text{ or } |x - 2K_1| = 2\sqrt{2K_1}\frac{F}{F'}\frac{v_t^2}{cV_\perp} \tag{50}$$

Our basic Eq.(50) is still valid very close to $x \approx 2K_1$ although in this region, the $F > 0$ and $F < 0$ branches couple (see Appendix II). To prove this, we note that the coupling occurs for a value of $FPk_\perp^{2(n-2)} \sim \lambda^{-1} \sim c^2/v_t^2$ whereas Eq.(50) only requires a value of $FPk^{2(n-2)} \sim cV_\perp/v_t^2$ which is much smaller. Supposedly there are two other matching points, even closer to $x \approx 2K_1$ in the coupling region of the $F > 0$ and $F < 0$ branches, near the point of zero group velocity for this particular dispersion curve. Similarly, the extra wave (to be investigated later on) has four matching points near $x = 2K_1$, two sufficiently far away from the coupling region and two within the coupling region (see Figs. 3(a),(c),(d),(e)

in Appendix II). The points within the coupling region will not be considered due to the complexity of the analysis. We only calculated the two points for the above extraordinary wave and the two for the extra wave where matching can occur near but outside of the coupling regions. The interference effects due to these matching points would only be observable after a time of the order of $\frac{v_t^2}{c^2}\left(\frac{n\omega_b}{\omega_1' - \omega_2'}\right)$ which is of the order of 0.1 - 2 sec.

In Figures 8a, b, we show values of the two parts in Eq.(50) versus ω_p^2/ω_b^2 based on the $x \approx 2K_1$ matching points for positive and negative F respectively. Corresponding values of $(\omega_r - n\omega_b)/n\omega_b$ and of $k_\parallel c^2/\omega V_\parallel$ are given in Figures 9a, b and 10a, b.

CASE (iii): We now consider the matching point for $x \ll 1$. This point is a direct consequence of the relativistic analysis which shows that ω rises rapidly above $n\omega_b$ as $k_\perp$ tends to zero. Because of the rapid use, the slope $\partial\omega/\partial k_\perp$ becomes large enough to effect a match with $V_\perp$. For $x \ll 1$, Eqs.(46) and (47) reduce to

$$k_\perp = -\frac{2(n-1)v_t^2\omega}{c^2 V_\perp}\,\frac{F}{\bar{F}}, \tag{51}$$

For $n = 1$, we obtain no matching point.

(b) ORDINARY WAVE

A similar analysis can be performed using the ordinary wave dispersion relation given in Eq.(28b) with $k_\parallel = 0$, viz.

$$\frac{1}{P_{\parallel}k_{\perp}^{2(n-1)}F_{n+5/2}} = \frac{x}{K_{\parallel} - x} \tag{52}$$

Equating $\partial\omega_r/\partial k_\perp = V_\perp$ and letting $\omega >> k_\perp V_\perp$ we find

$$n(K_{\parallel} - x) + x = -\frac{(K_{\parallel} - x)^2}{2xP_{\parallel}k_{\perp}^{2(n-1)}} \frac{F'_{n+5/2}}{F^2_{n+5/2}} \frac{\mu k_\perp V_\perp}{\omega} = -k_\perp(K_{\parallel} - x) \frac{F'_{n+5/2}}{2F_{n+5/2}} \frac{\mu V_\perp}{\omega} \tag{53}$$

As $x \to 0$, we obtain a matching point when

$$k_\perp = -2nv_t^2\omega F_{n+5/2}/c^2V_\perp F'_{n+5/2} \tag{54}$$

(Compare with Eq.51). The values for matching on each side of $x = K_{\parallel}$ are given by

$$x - K_{\parallel} = \frac{2K_{\parallel}F_{n+5/2}}{F'_{n+5/2}} \frac{\omega}{\mu k_\perp V_\perp} \quad \text{or} \quad |x - K_{\parallel}| = 2\sqrt{K_{\parallel}} \frac{F_{n+5/2}}{F'_{n+5/2}} \frac{v_t^2}{cV_\perp} \tag{55a}$$

and

$$F'_{n+5/2} = -2\, v_t^2/[cV_\perp\sqrt{K_{\parallel}}\, P_{\parallel}k_{\perp}^{2(n-1)}] \tag{55b}$$

In particular, for $n = 1$ and $x \lesssim K_{\parallel}$, there is a matching point for real $k_\perp$, ω and $F_{7/2}$ (see discussion in Appendix II after Eq.(17)).

In Fig. 11, we provide plots of $K_{\parallel}$ and the additional correction term in Eq.(55a) for the ordinary wave matching point giving $x \gtrsim K_{\parallel}$. (The $x \lesssim K_{\parallel}$ matching point suffers when $n > 1$ from the same difficulty as the extraordinary point $x \lesssim K_l K_r/K_\perp$. Namely, one requires huge values of F' and this jeopardizes the $k_{\parallel}$ matching point in Eq.(32).) In Figs. 12 and 13, the values of $(\omega_r - n\omega_b)/n\omega_b$ and $k_{\parallel}c^2/\omega V_{\parallel}$ are also

given. The conclusions to be drawn here are similar to those for the X-wave given above.

The advantages of the matching points near these coupling points are the negligible difference $(\omega_r - n\omega_b)/n\omega_b$, the negligible imaginary part of ω, the negligible Doppler shift, that it may be easier to excite a wavelength of the order of the free space wavelength and that the n = 1 case can be included for the ordinary wave.

(c) EXTRA WAVE

As pointed out above, two matching points occur for the extra wave given in Eq.(29b) near $x \approx 2K_1$ but sufficiently outside of the $F > 0$ and $F < 0$ coupling region. When $k_n = 0$, Eq.(29b) combined with Eq.(33) is

$$\frac{(n+1)(2n+3)}{P_{ex}k_\perp^{2n}F_{n+7/2}} = \frac{x}{2K_1 - x} \tag{56}$$

Equating $\partial\omega_r/\partial k_\perp = V_\perp$ and letting $\omega >> k_\perp V_\perp$, we find

$$(2K_1 - x)(n+1)+x = -\frac{(2K_1-x)^2(n+1)(2n+3)}{2xP_{ex}k_\perp^{2n}}\frac{F'_{n+7/2}}{F^2_{n+7/2}}\frac{\mu k_\perp V_\perp}{\omega} = -\frac{(2K_1-x)F'_{n+7/2}}{2F_{n+7/2}}\frac{\mu k_\perp V_\perp}{\omega} \tag{57}$$

The matching point as $x \to 0$, is

$$k_\perp = -2(n+1)v_t^2\omega\, F_{n+7/2}/c^2V_\perp F'_{n+7/2} \tag{58}$$

We are mainly concerned with the points near $x \approx 2K_1$, which are given by

$$x - 2K_1 = 4K_1 \frac{F_{n+7/2}}{F'_{n+7/2}} \frac{\omega}{\mu k_\perp V_\perp} \quad \text{or} \quad |x - 2K_1| = 2\sqrt{2K_1} \frac{F_{n+7/2}}{F'_{n+7/2}} \frac{v_t^2}{cV_\perp} \tag{59a}$$

and

$$F'_{n+7/2} = -2(n+1)(2n+3)v_t^2/[cV_\perp\sqrt{2K_1}\, P_{ex} k_\perp^{2n}] \tag{59b}$$

In Fig.14a, b, we give plots of the two parts in Eq.(59a) for negative and positive F respectively. Figures 15a, b and 16a, b give the corresponding values of $(\omega_r - n\omega_b)/n\omega_b$ and $k_\parallel c^2/\omega V_\parallel$.

Having investigated quite carefully the pinch values, we now proceed to use the analysis in Section II to determine the time response for the various waves.

VIII TIME DECAY OF CYCLOTRON HARMONICS FOR ELECTROSTATIC WAVES

All calculations are done in the satellite frame of reference (ω', k') where from Eq.(8)

$$\omega = \omega' + \underset{\sim}{k}' \cdot \underset{\sim}{V} \quad \text{and} \quad \underset{\sim}{k} = \underset{\sim}{k}' + \omega' \underset{\sim}{V}/c^2 \tag{60}$$

From Eqs.(22a), (23a, b) and (37), we can redefine D, R_{11} and R_{12} by dividing through by -x to give

$$D = K_\perp + \varepsilon_{11} = K_\perp - \frac{\omega_p^2}{\omega_b} \frac{n\lambda^{n-1}}{2^n n!(\omega' + \underset{\sim}{k}'_\perp \cdot \underset{\sim}{V}_\perp + k'_\parallel V_\parallel - n\omega_b)} \left[1 + \frac{(k'_\parallel + \omega' V_\parallel/c^2)^2 v_t^2}{(\omega' + \underset{\sim}{k}'_\perp \cdot \underset{\sim}{V}_\perp + k'_\parallel V_\parallel - n\omega_b)^2}\right] \tag{61}$$

and

$$R_{11}(\phi_o) \tilde{=} \cos^2\phi_o = 1, \quad R_{12}(\phi_o) = -R_{21}(\phi_o) \tilde{=} \sin\phi_o \cos\phi_o = 0 \text{ and}$$
$$R_{22}(\phi_o) = \sin^2\phi_o = 0 \tag{62}$$

We take $V_\perp$ and $k'_{\perp o}$ along the x axis, since near the pinch point we have from Eq.(39a), $k'_{\perp o} || V_\perp$. We can also neglect, if we wish, the small differences of ω in the $K_\perp$ and λ quantities.

According to the analysis in Sec. II, we have to calculate $D_\perp = \partial^2 D/\partial(k'_\perp)^2$ and $D_n = \partial^2 D/\partial(k'_n)^2$ at the pinch points.

One can readily show from Eq.(61) that $\partial D/\partial k'_n = 0$ when

$$(k'_{no} - \omega_o' V_n/c^2) \simeq (V_n/2v_t^2)(\omega_o' - \underset{\sim}{k}_o' \cdot \underset{\sim}{V} - n\omega_b) \tag{63}$$

which is identical to Eq.(36b) using Eq.(60). Taking the second derivative, one obtains

$$D_n = -\frac{\omega_p^2 n \lambda_o^{n-1}(2v_t^2 - 4V_n^2)}{\omega_b 2^n n!(\omega_o' + \underset{\sim}{k}_o' \cdot \underset{\sim}{V} - n\omega_b)^3} \simeq -\frac{2K_\perp v_t^2}{(\omega_o' + \underset{\sim}{k}_o' \cdot \underset{\sim}{V} - n\omega_b)^2} \tag{64}$$

Similarly $\partial D/\partial k'_\perp = 0$ at

$$(k'_{\perp o} + \omega_o' V_\perp/c^2)V_\perp = 2(n-1)(\omega_o' + \underset{\sim}{k}_o' \cdot \underset{\sim}{V} - n\omega_b) \tag{65a}$$

which agrees again with Eq.(42). Note that the correction $\omega_o' V_\perp/c^2$ to $k'_{\perp o}$ is negligible. In fact, solving Eqs.(65a) and (61) obtains

$$(k'_{\perp o} v_t/\omega_b)^{2n-3} = K_\perp \omega_b^2 2^n n! V_\perp/[v_t \omega_p^2 2n(n-1)] \tag{65b}$$

which is identical to Eq.(41). The second derivative of D yields

$$D_\perp \simeq -2(n-1)(2n-3)K_\perp/(k'_{\perp o})^2$$

Evaluating the quantity T in Eq.(18), namely $T = [\pi D_n D_\perp V_\perp/2k'_{\perp o}]^{\frac{1}{2}}$, and using Eq.(65a, b), give the following result:

$$T = \frac{2K_\perp v_t (n-1)^{3/2}}{(k'_{\perp o})^{3/2}} \left(\frac{2\pi(2n-3)}{V_\perp}\right)^{\frac{1}{2}}$$

$$= 2K_\perp v_t \left(\frac{v_t}{\omega_b}\right)^{3/2} (n-1)^{3/2} \left(\frac{2\pi(2n-3)}{V_\perp}\right)^{\frac{1}{2}} \left[\frac{v_t \omega_p^2 2n(n-1)}{V_\perp \omega_b^2 2^n n! K_\perp}\right]^{s/[4n-6]} \qquad (66)$$

The expression for the electric field response as a function of time follows from Eq.(17):

$$E_x(t) = \frac{-\sqrt{i}\, I_x LP(n\omega_b)}{4\pi\varepsilon_o (n\omega_b t)^{3/2}} \exp\left\{-it\left[n\omega_b - \frac{(2n-3)}{2(n-1)} k_{\perp o} V_\perp\right]\right\}$$

$$\times \left[\frac{\omega_p^3}{K_\perp v_t}\left(\frac{V_\perp n}{\pi(2n-3)v_t}\right)^{\frac{1}{2}} \frac{1}{[2(n-1)]^{3/2}}\right]\left[\frac{V_\perp \omega_b^2 2^n n! K_\perp}{v_t \omega_p^2 2n(n-1)}\right]^{s/[4n-6]} \qquad (67)$$

where from Eqs.(42) and (45), we have applied

$$\omega_o' \simeq \omega_o - n\omega_b - k_{\perp o} V_\perp + n\omega_b = -k_{\perp o} V_\perp \left(1 - \frac{1}{2(n-1)}\right) + n\omega_b = n\omega_b - \frac{(2n-3)}{2(n-1)} k_{\perp o} V_\perp$$

(68)

It is instructive to prove that we obtain the identical result by using the stationary phase method of Deering and Fejer[4] and working in the plasma rather than satellite frame of reference. We shall redo their analysis with the proper k_n^2 dependence given in Eq.(37). We start with their Eqs.(84-86) for the potential Φ which in our notation reads

$$\Phi(\underset{\sim}{r}, t, \phi_o = 0) = \iint d\omega d^3k \left(-\frac{iI_x LP\cos\phi}{(2\pi)^4 \varepsilon_o k_\perp K_\perp \omega}\right)\left[\frac{(\omega - n\omega_b)\exp[-i(\omega t - \underset{\sim}{k}\cdot\underset{\sim}{r})]}{\omega - n\omega_b - \frac{\omega_p^2 n\lambda^{n-1}}{\omega_b 2^n n! K_\perp}\left(1 + \frac{k_n^2 v_t^2}{(\omega - n\omega_b)^2}\right)}\right]$$

where we consider only the $\omega = n\omega_b$ resonance and as before we take $r_\perp$ parallel to the x-axis ($\phi_o = 0$). (The $\omega = -n\omega_b$ resonance can similarly be calculated.) Also $\underset{\sim}{E}(\underset{\sim}{r},t) = -\underset{\sim}{\nabla}_r \Phi(\underset{\sim}{r},t)$.

Using $2\pi i\, J_1(k_\perp r_\perp) = \int_0^{2\pi} d\phi e^{ik_\perp r_\perp \cos\phi}\cos\phi$, we can immediately perform the ϕ integration to yield

$$\Phi(\underset{\sim}{r},t) = -\int_{ic-\infty}^{ic+\infty} d\omega e^{-i\omega t} \int_0^\infty k_\perp dk_\perp J_1(k_\perp r_\perp)\left(\frac{I_x LP}{8\pi^3 \varepsilon_o k_\perp K_\perp \omega}\right)\frac{(\omega - n\omega_b)^3 \omega_b 2^n n! K_\perp}{\omega_p^2 n\lambda^{n-1} v_t^2}$$

$$\times \int_{-\infty}^{\infty} \frac{dk_\parallel e^{ik_\parallel r_\parallel}}{k_\parallel^2 + \left[\frac{(\omega - n\omega_b)^2}{v_t^2} - \frac{(\omega - n\omega_b)^3 \omega_b 2^n n! K_\perp}{\omega_p^2 n\lambda^{n-1} v_t^2}\right]}$$

Using the Fourier transform identity $\int_{-\infty}^{\infty} e^{ixy} dx/(x^2+\alpha^2) = \pi e^{-\alpha|y|}/\alpha \approx \pi/\alpha$, where the approximation applies near $\alpha = 0$, we find

$$\Phi(r_\perp,t) = -\int_0^\infty dk_\perp J_1(k_\perp r_\perp)\left[\frac{I_x LP}{8\pi^2 \varepsilon_o K_\perp v_t n\omega_b}\right]\left[-\frac{\omega_b 2^n n! K_\perp}{\omega_p^2 n\lambda^{n-1}}\right]^{\frac{1}{2}}$$

$$\times \int_{ic-\infty}^{ic+\infty} \frac{d\omega e^{-i\omega t}(\omega - n\omega_b)^2}{\left[(\omega - n\omega_b) - \frac{\omega_p^2 n\lambda^{n-1}}{\omega_b 2^n n! K_\perp}\right]^{\frac{1}{2}}}$$

The ω Laplace transform can be evaluated next, using

$$\int \frac{d\omega e^{-i\omega t}\omega^2}{[\omega - \alpha]^{\frac{1}{2}}} = \frac{e^{-i\alpha t}\alpha^2}{\sqrt{t}}\, 2\sqrt{-i\pi}$$

Using this value, we obtain $E = -\partial\phi/\partial r_\perp = -k_\perp \partial\phi/\partial(k_\perp r_\perp)$:

$$E(r_\perp,t) = \sqrt{i/\pi}\,\frac{e^{-in\omega_b t} I_x LP\, a^{3/2}}{K_\perp v_t 4\pi\varepsilon_0 n\omega_b t^2}\int_0^\infty k_\perp^{3n-2}\, J_1'(k_\perp r_\perp)\exp(-iak_\perp^{2(n-1)})dk_\perp$$

$$\text{where } a = \left(\frac{v_t}{\omega_b}\right)^{2(n-1)}\frac{\omega_p^2 nt}{\omega_b 2^n n! K_\perp}$$

To evaluate the $k_\perp$ integral, we note that for electrostatic waves and for reception near the satellite during the time of interest, $k_\perp r_\perp \sim k_\perp V_\perp t >> 1$, so that we can apply the large argument expansion of $J_1'(k_\perp r_\perp)$:

$$J_1'(k_\perp r_\perp) = -\left(\frac{1}{2\pi k_\perp r_\perp}\right)^{\frac{1}{2}}\frac{1}{i}\left[e^{i(k_\perp r_\perp - \frac{3\pi}{4})} - \text{c.c.}\right] \sim -\left(-\frac{i}{2\pi k_\perp r_\perp}\right)^{\frac{1}{2}} e^{ik_\perp r_\perp}$$

where c.c. means "complex conjugate", which we shall omit in the following for simplicity. (Including it changes the final exponentials into sines or cosines.) Thus

$$E(r_\perp,t) = -\frac{e^{-in\omega_b t} I_x LP\, a^{3/2}}{K_\perp v_t\sqrt{2r_\perp}\,\pi 4\pi\varepsilon_0 n\omega_b t^2}\int_0^\infty k_\perp^{3n-5/2}\exp[i(k_\perp r_\perp - ak_\perp^{2(n-1)})]$$

Similar to the analysis in Deering and Fejer, we look for stationary points for the exponential (see Section VI above). That is, denoting

$$f(k) = k_\perp r_\perp - ak_\perp^{2(n-1)}$$

the stationary point occurs at $\partial f/\partial k_{\perp 0} = 0$ and the value[7] of the integral is approximately

$$\int = k_{\perp 0}^{3n-5/2}\left(-\frac{2\pi}{i\partial^2 f/\partial k_{\perp 0}^2}\right)^{\frac{1}{2}}\exp[if(k_{\perp 0})]$$

We obtain immediately

$$k_{\perp o} = \left[\frac{r_\perp}{2a(n-1)}\right]^{1/[2n-3]}, \quad f(k_{\perp o}) = k_{\perp o}(r_\perp - a k_{\perp o}^{2n-3}) = \left(k_{\perp o} r_\perp\right)\frac{(2n-3)}{2(n-1)}$$

and $\partial^2 f/\partial k_{\perp o}^2 = 2a(n-1)(2n-3)k_{\perp o}^{2(n-2)}$

Thus

$$E(r_\perp,t) = -\frac{\sqrt{i}\, I_x LPa[2(n-1)(2n-3)\pi r_\perp]^{-\frac{1}{2}}}{4\pi\varepsilon_0 n\omega_b K_\perp v_t t^2}\left[\frac{r_\perp}{2a(n-1)}\right]^{(4n-1)/(4n-6)}$$

$$\times \exp\left\{-i\left(n\omega_b t - \left(k_{\perp o} r_\perp\right)\frac{(2n-3)}{2(n-1)}\right)\right\}$$

$$= -\frac{\sqrt{i}\, I_x LP}{4\pi\varepsilon_0 (n\omega_b)^{3/2}}\frac{(r_\perp)^{(n+1)/(2n-3)}}{t^{(8n-7)/(4n-6)}}\exp\left\{-i\left(n\omega_b - \left(k_{\perp o} r_\perp\right)\frac{(2n-3)}{2(n-1)}\right)\right\}$$

$$\times\left[\frac{\omega_b^3}{K_\perp v_t^3 V_\perp^{5/(4n-6)}}\left(\frac{n}{\pi(2n-3)v_t}\right)^{\frac{1}{2}}\frac{1}{[2(n-1)]^{3/2}}\right]\left[\frac{V_\perp\omega_b^2 2^n n! K_\perp}{v_t\omega_p^2 2n(n-1)}\right]^{8/[4n-6]}$$

This expression reduces immediately to Eq.(67) when $r_\perp = V_\perp t$ and is the proper result that Deering and Fejer would obtain had they started with the correct $k_\parallel$ dependence.

The above more complex calculation essentially substantiates the simpler analysis in Section II and indeed emphasizes the importance of the pinch points as discussed in Section VI.

IX TIME DECAY OF CYCLOTRON HARMONICS FOR THE OTHER WAVES

(a) EXTRAORDINARY WAVE

From Eqs.(27a) and (26a) we obtain the following formula for D.

$$D = K_1K_r - xK_\perp - Pk_\perp^{2(n-2)}x(2K_1 - x)F_{n+3/2}$$

$$-\left(k_n' + \frac{\omega V_n}{c^2}\right)^2 Pk_\perp^{2(n-2)}x(2K_1 - x)\frac{c^4}{2(n\omega_b)^2 v_t^2}\,\mathrm{Re}\left[F_{n+5/2} - 2F_{n+3/2} + F_{n+1/2}\right] \tag{69}$$

where the argument of F is $[(\omega' - n\omega_b + \underset{\sim}{k_\perp'}\cdot\underset{\sim}{V_\perp} + k_n'V_n)/n\omega_b]$. Let F' denote the derivative of F with respect to this argument. Setting $\partial D/\partial(k_n') = 0$ yields the same relation as in Eq.(31), viz.

$$k_n' + \frac{\omega V_n}{c^2} = -\frac{n\omega_b V_n}{c^2}\,\frac{F'_{n+3/2}}{\mathrm{Re}\left[F_{n+5/2} - 2F_{n+3/2} + F_{n+1/2}\right]} \tag{70}$$

We next calculate the second derivative

$$D_n \simeq -Pk_\perp^{2(n-2)}x(2K_1 - x)\frac{c^4}{(n\omega_b v_t)^2}\,\mathrm{Re}\left[F_{n+5/2} - 2F_{n+3/2} + F_{n+1/2}\right]$$

$$\simeq -(K_1K_r - xK_\perp)\,\frac{c^4}{(n\omega_b v_t)^2}\,\frac{\mathrm{Re}\left[F_{n+5/2} - 2F_{n+3/2} + F_{n+1/2}\right]}{F_{n+3/2}} \tag{71}$$

since the k_n^2 term in Eq.(69) is small.

Since $k_\perp' \simeq k_\perp$ with a negligible correction, one finds

$$\frac{\partial A}{\partial k_\perp'} = -2K_\perp\frac{c^2}{\omega^2}k_\perp - 2(n-1)Pk_\perp^{2n-3}\frac{c^2}{\omega^2}F_{n+3/2}2K_1 - Pk_\perp^{2(n-1)}\frac{c^2}{\omega^2}\frac{V_\perp c^2}{\omega v_t^2}F'_{n+3/2}2K_1$$

$$+ 2n\,Pk_\perp^{2n-1}\frac{c^4}{\omega^2}F_{n+3/2} + Pk_\perp^{2n}\frac{c^4}{\omega^4}\frac{V_\perp c^2}{\omega v_t^2}F'_{n+3/2} \tag{72}$$

and solving $\partial A/\partial k_\perp' = 0$ with Eq.(69) yields exactly the same result as in Eq.(47b-d). Differentiate again Eq.(72) and substitute into the answer the value of $2K_\perp c^2/\omega^2$ obtainedby equating Eq.(72) to zero. The result is

$$D_\perp = \frac{8(K_\parallel K_r - xK_\perp)}{(2K_\parallel - x)k_{\perp o}^2}\left\{\left[\frac{n(n-1)x}{2} - K_\parallel(n-1)(n-2)\right] + \left(\frac{\mu V_\perp k_{\perp o}}{n\omega_b}\right)\left[\frac{(4n-1)}{8}x + K_\parallel\frac{(5-4n)}{4}\right]\frac{F'_{n+3/2}}{F_{n+3/2}}\right.$$

$$\left. + \left(\frac{\mu V_\perp k_{\perp o}}{n\omega_b}\right)^2 \frac{(x-2K_\parallel)}{8}\,\frac{F''_{n+3/2}}{F_{n+3/2}}\right\} \qquad (73)$$

Let us first consider the $x \ll 1$ matching point (for $n \geq 2$) given in Eq.(51), viz.

$$k_{\perp o} \approx k'_{\perp o} = -2(n-1)\,\frac{v_t^2 n\omega_b}{c^2 V_\perp}\,\frac{F_{n+3/2}}{F'_{n+3/2}} \qquad (74)$$

(Note that even here, $k'_{\perp o} >> \omega' V_\parallel/c^2$ by order $v_t^2/V_\perp V_\parallel$.) In this limit, all three parts in the braces in Eq.(73) are equally important and using Eq.(74), we find

$$D_\perp = \frac{2K_\parallel K_r}{k_{\perp o}^2}\left[(n-1)(2n-1) - 2(n-1)^2\,\frac{F''_{n+3/2}\,F_{n+3/2}}{(F'_{n+3/2})^2}\right] \qquad (75)$$

From Eqs. (71), (74) and (75), one obtains for T in Eq.(18):

$$\frac{T}{(n\omega_b)^{\frac{1}{2}}} = K_\parallel K_r\,\frac{c^5 V_\perp^2\sqrt{\pi}}{v_t^4(n\omega_b)^3 2(n-1)^{3/2}}\left(\frac{F'_{n+3/2}}{F_{n+3/2}}\right)^{3/2}$$

$$\times\left\{\frac{\mathrm{Re}(F_{n+5/2} - 2F_{n+3/2} + F_{n+1/2})}{2F_{n+3/2}}\left[(n-1)(2n-1) - 2(n-1)^2\,\frac{F''_{n+3/2}F_{n+3/2}}{(F'_{n+3/2})^2}\right]\right\}^{\frac{1}{2}} \qquad (76)$$

The minors R_{ij} when $x \ll 1$ and $\phi_o = 0$ are obtainable from Eqs.(23a-c):

$$R_{11} = R_{22} \approx K_\perp + (\varepsilon_{11})_w = K_\perp - Pk_\perp^{2(n-2)} x\, F_{n+3/2} \approx K_\perp - K_l K_r/2K_l = K_l/2$$

$$R_{12} = -R_{21} = -i(K_x - (\varepsilon_{11})_w) = -i(K_x + K_r/2) = -iK_l/2$$

since $K_{\perp,x} = (K_l \pm K_r)/2$. Defining

$$E_{l,r} = E_x \pm iE_y \quad , \quad I_{l,r} = I_x \pm iI_y \tag{77}$$

and since $E_x \propto (R_{11}I_x - R_{12}I_y)$ and $E_y \propto (R_{12}I_x + R_{22}I_y)$, one finds from Eq.(17) that $E_r = 0$ and

$$E_l = -\frac{\sqrt{i}\, I_l}{K_r} \frac{LP(\omega_o')e^{-i\omega_o' t}}{4\pi\varepsilon_o (n\omega_b t)^{3/2}} \left[\frac{(n\omega_b)^3 v_t^4\, 2(n-1)^{3/2}}{c^5 V_\perp^2 \sqrt{\pi}} \left(\frac{F_{n+3/2}}{F'_{n+3/2}} \right)^{3/2} \right] \{\ \}^{-\frac{1}{2}} \tag{78}$$

where $\{\ \}$ is the quantity within the braces in Eq.(76).

Next we consider the matching point near the Appleton-Hartree extraordinary wave, given in Eq.(48c):

$$x - \frac{K_l K_r}{K_\perp} = 2\left(\frac{K_l K_r}{K_\perp} \right)^{\frac{1}{2}} \frac{F_{n+3/2}}{F'_{n+3/2}} \frac{v_t^2}{cV_\perp} \tag{79}$$

This time, the last term in Eq.(73) is the largest since $c^2 V_\perp k_\perp / v_t^2 n\omega_b$ is much greater than one. Using $x - 2K_l \approx -K_l^2/K_\perp$ here, we obtain

$$D_\perp = -(K_l K_r - xK_\perp) \frac{c^4 V_\perp^2}{v_t^4 (n\omega_b)^2} \frac{F''_{n+3/2}}{F_{n+3/2}} \tag{80}$$

Combining the various expressions with Eq.(79) readily yields T:

$$\frac{T}{(n\omega_b)^{\frac{1}{2}}} = \left(\frac{2\pi V_\perp}{c}\right)^{\frac{1}{2}} \frac{c^4 K_\perp}{v_t (n\omega_b)^3} \left(\frac{K_\parallel K_r}{K_\perp}\right)^{\frac{1}{4}} \left[\frac{F''_{n+3/2}}{(F'_{n+3/2})^2} \mathrm{Re}\left(F_{n+5/2} - 2F_{n+3/2} + F_{n+1/2}\right)\right]^{\frac{1}{2}} \quad (81)$$

The minors in Eq.(23) are more complex in this case since the $\sin^2\phi$ and $\cos^2\phi$ parts have to be included in the integrals. We can most readily do this in Eq.(14) where neglecting the contribution at ∞ from the integrals, we can write

$$\int_{-\infty}^{\infty} \exp(i\alpha y^{2q}) y^p dy = \exp\left[\frac{i\pi}{4q}\left(p+1\right)\right] \Gamma\left(\frac{p+1}{2q}\right) \Big/ q\alpha^{(p+1)/2q}$$

assuming $(p+1)/q$ is an odd integer. If $(n+1)/q$ is an even integer, the integral is equal to zero.

For the $\sin^2\phi$ or $\cos^2\phi$ terms we find

$$\int_{-\infty}^{\infty} k^2 e^{i\alpha(k-k_o)^2} dk = \sqrt{i\pi/\alpha}\left(k_o^2 + \frac{i}{2\alpha}\right)$$

where $k_o = 0$ for the $\sin^2\phi$ term since we take $\phi_o = 0$ and $k_{yo} = k_\perp \sin\phi_o = 0$. The $\sqrt{i\pi/\alpha}$ has already been included in T; the additional factor shown needs to be inserted. Also, since $\varepsilon_{11} \approx (K_\parallel K_r - xK_\perp)/(2K_\parallel + x)$ is much less than $K_\perp$ or K_x, we find

$$R_{11} = K_\perp - x\left[1 + \frac{i\, D_\omega}{k_{xo}^2 D_{xx} t}\right] = \frac{(K_\parallel - K_r)^2}{4K_\perp} - \frac{ic^2 D_\omega}{\omega^2 D_\perp t} = \frac{(K_\parallel - K_r)^2}{4K_\perp} - \frac{i}{\omega t}\left(\frac{v_t}{V_\perp}\right)^2 \frac{F'_{n+3/2}}{F''_{n+3/2}}$$

using $D_\omega = -(K_\parallel K_r - xK_\perp)c^2 F'_{n+3/2} \Big/ v_t^2\, \omega F_{n+3/2}$ and Eq.(80). The additional term in R_{11} is usually small. We can also obtain R_{22} using Eq.(16):

$$R_{22} = K_\perp - \frac{ic^2 D_\omega}{\omega^2 D_{yy} t} = K_\perp + \frac{ic}{\omega t V_\perp}\left(\frac{K_\parallel K_r}{K_\perp}\right)^{\frac{1}{2}}$$

$$R_{12} = -R_{21} \approx -iK_x = -i(K_1 - K_r)/2$$

One finds as a result of combining all the above parts that

$$E_{x,y} = -\frac{\sqrt{i}\, e^{-i\omega_0' t}}{4\pi\varepsilon_0 (n\omega_b t)^{3/2} K_\perp} \left(\frac{c}{2\pi V_\perp}\right)^{\frac{1}{2}} v_t \frac{(n\omega_b)^3}{c^4} \left(\frac{K_\perp}{K_1 K_r}\right)^{\frac{1}{4}} \left[\frac{(F'_{n+3/2})^2}{F''_{n+3/2}\, \mathrm{Re}[F_{n+5/2} - 2F_{n+3/2} + F_{n+1/2}]}\right]^{\frac{1}{2}}$$

$$\cdot \left\{ \left[\frac{(K_1 - K_r)^2}{4K_\perp} - \frac{i}{n\omega_b t}\left(\frac{v_t}{V_\perp}\right)^2 \frac{F'_{n+3/2}}{F''_{n+3/2}}\right] I_x L + \frac{i(K_1 - K_r)}{2} I_y L \right\} \text{ for } E_x$$

or

$$\cdot \left\{ \left[K_\perp + \frac{ic}{n\omega_b t V_\perp}\left(\frac{K_1 K_r}{K_\perp}\right)^{\frac{1}{2}}\right] I_y L - \frac{i(K_1 - K_r)}{2} I_x L \right\} \text{ for } E_y \qquad (82)$$

Actually, one should investigate fully the applicability of the above results when $k_0^2 \alpha$ such as $k_{\perp 0}^2 D_\perp t/D_\omega$ is of order one, since the expansion method in Section II may only be valid for $k_0^2\, \alpha >> 1$. In any case, the additional $k_0^2\, \alpha$ terms, being of order one, do not introduce a major error.

Comparison of the results on the response in Eq.(82) with that in Eq.(78) shows that the pinch point for small $x << 1$ gives a smaller contribution by order $(v_t^3/cV_\perp^2)(V_\perp/c)^{\frac{1}{2}}$. Hence we can neglect this contribution. Because of the complex nature of Eq.(82), we do not plot any response results for this particular matching point.

We finally calculate for the extraordinary wave the contribution from the pinches at $x \approx 2K_1$. Although the above values for $D_\perp$ and $D_\parallel$ can be used, it is more rigorous to redo the calculation, by defining a new D and new R_{ij} quantities equal to the previous ones, divided by $-\varepsilon_{11} = Pk_\perp^{2(n-2)} x\, F_{n+3/2}$. In this manner, the magnitudes of R_{ij}

do not become large. From Eq.(69)

$$D = x - 2K_1 + (K_1K_r - xK_\perp)/[Pk_\perp^{2(n-1)}(c^2/\omega^2)F_{n+3/2}]$$

$$- \left(k_\parallel' + \frac{\omega V_\parallel}{c^2}\right)^2 (2K_1 - x)\, \frac{c^4}{2(n\omega_b v_t)^2}\, \frac{Re[F_{n+5/2} - 2F_{n+3/2} + F_{n+1/2}]}{F_{n+3/2}} \qquad (83)$$

Since in this case, ε_{11} is much larger than $K_\perp$, K_x or x, we find from Eq.(23) (after renormalizing by dividing by $-\varepsilon_{11}$) that

$$R_{11} = R_{22} = -1, \quad R_{12} = -R_{21} = -i.$$

From Eq.(83), one can readily show that

$$D_\parallel = \frac{c^4(x - 2K_1)}{(n\omega_b v_t)^2 F_{n+3/2}} Re[\ \ ] = \frac{c^4}{v_t^2}\, \frac{K_1^2\, Re[\ \ ]}{Pk_{\perp o}^{2(n-1)} c^2 F_{n+3/2}^2}$$

where Re[ ] is the quantity in Eq.(83). Also using

$$x - 2K_1 \approx -\frac{4K_1}{\mu}\, \frac{F_{n+3/2}}{F'_{n+3/2}}\, \frac{\omega}{k_{\perp o} V_\perp} \approx \frac{K_1^2}{Pk_\perp^{2(n-1)}(c^2/\omega^2)F_{n+3/2}}$$

one finds near $x \approx 2K_1$

$$D_\perp = (V_\perp \mu)^2 \frac{K_1^2}{Pk_{\perp o}^{2(n-1)} c^2 F_{n+3/2}} \left[\frac{F''_{n+3/2}}{F_{n+3/2}} - 2\left(\frac{F'_{n+3/2}}{F_{n+3/2}}\right)^2\right]$$

Thus

$$\frac{T}{(n\omega_b)^{\frac{1}{2}}} = \frac{i(2K_1)^{\frac{1}{4}} c^4}{\omega^3 v_t} \left(\frac{2\pi V_\perp}{c}\right)^{\frac{1}{2}} \left[\left(\frac{2F'_{n+3/2}}{F_{n+3/2}} - \frac{F''_{n+3/2}}{F'_{n+3/2}}\right) \frac{Re(F_{n+5/2} - 2F_{n+3/2} + F_{n+1/2})}{F'_{n+3/2}}\right]^{\frac{1}{2}} \qquad (84)$$

Finally $E_1 = 0$ and

$$E_r = \frac{I_r LP(\omega_o')e^{-i\omega_o' t}}{\sqrt{i}\,4\pi\varepsilon_o (n\omega_b t)^{3/2}} \frac{2(n\omega_b)^3 v_t}{(2K_1)^{\frac{1}{4}} c^4} \left(\frac{c}{2\pi V_\perp}\right)^{\frac{1}{2}}$$

$$\times \left[\left(\frac{2F'_{n+3/2}}{F_{n+3/2}} - \frac{F''_{n+3/2}}{F'_{n+3/2}}\right) \frac{\mathrm{Re}\left[F_{n+5/2} - 2F_{n+3/2} + F_{n+1/2}\right]}{F'_{n+3/2}}\right]^{-\frac{1}{2}} \qquad (85)$$

The time response $n\omega_b t$ can be seen to be proportional to

$$A = \left[\left(\frac{2F'_{n+3/2}}{F_{n+3/2}} - \frac{F''_{n+3/2}}{F'_{n+3/2}}\right) \frac{\mathrm{Re}\left[F_{n+5/2} - 2F_{n+3/2} + F_{n+1/2}\right]}{F'_{n+3/2}}\right]^{-1/3} \frac{1}{(2K_1)^{1/6}} \qquad (86)$$

This quantity is plotted versus (ω_p^2/ω_b^2) in Figures 17 and 18 for $x \gtrsim 2K_1$ (positive F) and $x \lesssim 2K_1$ (negative F). Note that

$$n\omega_b t = n^2 A \left[\left|\frac{2I_r LP\omega_b^3 v_t}{E_r 4\pi\varepsilon_o c^4}\left(\frac{c}{2\pi V_\perp}\right)^{\frac{1}{2}}\right|\right]^{2/3} \qquad (87)$$

We now proceed to consider the pinches for the ordinary wave.

(b) ORDINARY WAVE

The dispersion relationship for the ordinary wave is given in Eq.(28b) and can be written as follows in the satellite frame of reference

$$D = K_n - x - P_n k_\perp^{2n} \frac{c^2}{(n\omega_b)^2} F_{n+5/2} - \left(k_n' + \frac{\omega V_n}{c^2}\right)^2 P_n k_\perp^{2n} \frac{c^2}{(n\omega_b)^2} \mathrm{Re}(\beta_{OR}) \qquad (88)$$

Using the same procedure as for Eq.(69), we find

$$D_n = -2P_n k_\perp^{2n} \frac{c^2}{(n\omega_b)^2} \mathrm{Re}(\beta_{OR}) = -(K_n - x) \frac{2}{F_{n+5/2}} \mathrm{Re}(\beta_{OR}) \qquad (89)$$

$\partial D/\partial k_\perp' = 0$ gives Eq.(53), and $D_\perp \equiv \partial^2 D/\partial(k_{\perp o}')^2$ becomes

$$D_\perp = \frac{(K_\parallel - x)}{(k_{\perp o}')^2}\left\{4n(1-n) + \frac{F'_{n+5/2}}{F_{n+5/2}}\frac{\mu V k_{\perp o}'}{\omega}(1-4n) - \left(\frac{\mu V k_{\perp o}'}{\omega}\right)^2 \frac{F''_{n+5/2}}{F_{n+5/2}}\right\} \qquad (90)$$

We recall that there exist matching points for $x \ll 1$ and for $x \approx K_\parallel$. First consider the $x \ll 1$ pinch point. We obtain

$D_\parallel \approx -2K_\parallel \mathrm{Re}\beta_{OR}/F_{n+5/2}$

$k_{\perp o} \approx -2n\frac{v_t^2}{c^2}\frac{\omega}{V_\perp}\frac{F_{n+5/2}}{F'_{n+5/2}}$ (Eq.(54)) and all three terms in D are important.

$$D_\perp \approx \frac{2nK_\parallel}{(k_{\perp o}')^2}\left[(2n+1) - 2n\frac{F''_{n+5/2}F_{n+5/2}}{(F'_{n+5/2})^2}\right].$$

We therefore find that

$$\frac{T}{(n\omega_b)^{\frac{1}{2}}} \equiv \left(\frac{\pi D_\parallel D_\perp V_\perp}{2k_{\perp o}' n\omega_b}\right)^{\frac{1}{2}} = \frac{K_\parallel c^5 V_\perp^2}{v_t^4 (n\omega_b)^3 2n}\left(\frac{\pi}{2}\right)^{\frac{1}{2}}\left(\frac{F'_{n+5/2}}{F_{n+5/2}}\right)^{3/2}\left\{\frac{\mathrm{Re}\left[\beta_{OR}/(c^4/2v_t^2\omega^2)\right]}{F_{n+5/2}} \times \left[(2n+1) - \frac{2nF''_{n+5/2}F_{n+5/2}}{(F'_{n+5/2})^2}\right]\right\}^{\frac{1}{2}}$$

and using $R_{33} = 1$ (see Eq.(24))

$$E_\parallel = -\frac{\sqrt{i}\, I_\parallel LP(\omega_o')e^{-i\omega_o' t}}{4\pi\varepsilon_o (n\omega_b t)^{3/2}}\left[\frac{(n\omega_b)^3 v_t^4 2n}{c^5 V_\perp^2 K_\parallel}\left(\frac{2}{\pi}\right)^{\frac{1}{2}}\left(\frac{F_{n+5/2}}{F'_{n+5/2}}\right)^{3/2}\right]\left[(2n+1) - \frac{2n\,F''_{n+5/2}F_{n+5/2}}{(F'_{n+5/2})^2}\right]^{-\frac{1}{2}}$$

$$\times\, \mathrm{Re}\left[\frac{3(F_{n+7/2} - 2F_{n+5/2} + F_{n+3/2})}{F_{n+5/2}} - \frac{2(F_{n+5/2} - F_{n+3/2})^2}{F_{n+3/2}F_{n+5/2}}\right]^{-\frac{1}{2}} \qquad (91)$$

We next consider the $x \approx K_\parallel$ pinch point which gives a larger

response. Here the last term in $D_\perp$ is most important. Also since

$$x - K_\parallel \approx 2K_\parallel \frac{F_{n+5/2}}{F'_{n+5/2}} \frac{\omega}{\mu k'_{\perp o} V_\perp}$$

we obtain

$$D_\parallel = \frac{4\mathrm{Re}(\beta_{OR})}{F'_{n+5/2}} \frac{K_\parallel \omega}{\mu k'_{\perp o} V_\perp} \quad , \quad D_\perp = \frac{2K_\parallel}{(k'_{\perp o})^2} \frac{F''_{n+5/2}}{F'_{n+5/2}} \frac{\mu k_{\perp o} V_\perp}{\omega} \tag{92a,b}$$

Hence,

$$\frac{T}{(n\omega_b)^{\frac{1}{2}}} = \left(\frac{2\pi V_\perp}{c}\right)^{\frac{1}{2}} \frac{c^4 (K_\parallel)^{\frac{1}{4}}}{v_t (n\omega_b)^3} \left\{\frac{F''_{n+5/2}}{(F'_{n+5/2})^2} \mathrm{Re}\left[\frac{\beta_{OR}}{c^4/2v_t^2\omega^2}\right]\right\}^{\frac{1}{2}}$$

and

$$E_\parallel = -\frac{\sqrt{i}\, I_\parallel L P(\omega_o') e^{-i\omega_o' t} (n\omega_b)^3 v_t}{4\pi\varepsilon_o (n\omega_b t)^{3/2} (K_\parallel)^{\frac{1}{4}} c^4} \left(\frac{c}{2\pi V_\perp}\right)^{\frac{1}{2}}$$
$$\times \left\{\frac{F''_{n+5/2}}{(F'_{n+5/2})^2} \mathrm{Re}\left[3(F_{n+7/2} - 2F_{n+5/2} + F_{n+3/2}) - \frac{2(F_{n+5/2} - F_{n+3/2})^2}{F_{n+3/2}}\right]\right\}^{-\frac{1}{2}} \tag{93}$$

The time response is proportional to

$$A_\parallel = \left\{\quad\right\}^{-1/3} \frac{1}{(K_\parallel)^{1/6}} \tag{94a}$$

so that

$$n\omega_b t = n^2 A_\parallel \left[\left| \frac{I_\parallel L P \omega_b^3 v_t}{E_\parallel 4\pi\varepsilon_o c^4} \left(\frac{c}{2\pi V_\perp}\right)^{\frac{1}{2}} \right|\right]^{2/3} \tag{94b}$$

where $\{\ \}$ is the quantity in the braces in Eq.(93). The normalized time parameter A_n is plotted in Fig. 19 versus ω_p^2/ω_b^2 for $n \geq 2$. (The case n = 1 requires not too large F values, and is slightly more difficult to calculate. Two pinch points exist. Values have not been calculated.)

We next provide similar results for the extra wave.

(c) EXTRA WAVE

The formulae for this wave are obtainable from Eqs.(29b), (33) and (25b), namely $R_{11} = R_{22} = 1$, $R_{12} = -R_{21} = -i$ and

$$D = 2K_1 - x - P_{ex}\, k_\perp^{2(n+1)} \frac{c^2}{\omega^2} \frac{F_{n+7/2}}{(n+1)(2n+3)} - \left(k_\parallel' + \frac{\omega V_\parallel''}{c^2}\right)^2 P_{ex} k_\perp^{2(n+1)} \frac{c^2}{\omega^2} \mathrm{Re}(\beta_{ex}) \tag{95}$$

One readily finds (see also Eqs.(57), (58) and (59a))

$$D_\parallel = (x - 2K_1)2\mathrm{Re}\beta_{ex}(n+1)(2n+3)/F_{n+7/2} \tag{96}$$

$$D_\perp = \frac{(x - 2K_1)}{(k_{\perp o}')^2} \left\{ 4n(n+1) + (4n+3) \frac{F'_{n+7/2}}{F_{n+7/2}} \frac{\mu V_\perp k_{\perp o}'}{\omega} + \left(\frac{\mu V_\perp k_{\perp o}'}{\omega}\right)^2 \frac{F''_{n+7/2}}{F_{n+7/2}} \right\} \tag{97}$$

Matching at $x \ll 1$, i.e. at $k_{\perp o} \approx -2(n+1)v_t^2 \omega F_{n+7/2} \Big/ c^2 V_\perp F'_{n+7/2}$, yields

$$D_\parallel = -4K_1 \mathrm{Re}\beta_{ex}(n+1)(2n+3)/F_{n+7/2}$$

$$D_\perp = \frac{4K_1(n+1)}{(k_{\perp o}')^2} \left[(2n+3) - 2(n+1) \frac{F''_{n+7/2} F_{n+7/2}}{(F'_{n+7/2})^2} \right]$$

$$\frac{T}{(n\omega_b)^{\frac{1}{2}}} = \frac{K_1 c^5 V_\perp^2}{v_t^4 (n\omega_b)^3} \left[\frac{\pi(2n+3)}{2(n+1)}\right]^{\frac{1}{2}} \left(\frac{F'_{n+7/2}}{F_{n+7/2}}\right)^{3/2} \left\{\frac{\mathrm{Re}\left[\beta_{ex}/(c^4/2v_t^2\omega^2)\right]}{F_{n+7/2}} \times \left[(2n+3) - 2(n+1)\,\frac{F''_{n+7/2} F_{n+7/2}}{(F'_{n+7/2})^2}\right]\right\}^{\frac{1}{2}} \quad (98)$$

$E_1 = 0$ and

$$E_r = -\frac{\sqrt{i}\, I_r LP(\omega_0') e^{-i\omega_0 t}}{K_1 4\pi\varepsilon_0 (n\omega_b t)^{3/2}} \left[\frac{2(n\omega_b)^3 v_t^4}{c^5 V_\perp^2} \left(\frac{2(n+1)}{\pi(2n+3)}\right)^{\frac{1}{2}} \left(\frac{F_{n+7/2}}{F'_{n+7/2}}\right)^{3/2}\right] \{\ \}^{-\frac{1}{2}} \quad (99)$$

where $\{\ \}$ is the quantity within the braces in Eq.(98) and the real part of $\beta_{ex}/(c^4/2v_t^2\omega^2)$ is given in Eq.(29b).

Finally, the two pinch points for positive and negative F at

$$x = 2K_1 + \frac{4K_1 F_{n+7/2}}{F'_{n+7/2}} \frac{\omega}{\mu k'_{\perp o} V_\perp}$$

give

$$D_{\parallel} = \frac{8\mathrm{Re}\beta_{ex}}{F'_{n+7/2}} K_1 (n+1)(2n+3) \frac{\omega}{\mu k'_{\perp o} V_\perp}$$

$$D_\perp = \frac{4K_1}{(k'_{\perp o})^2} \frac{F''_{n+7/2}}{F'_{n+7/2}} \frac{\mu k'_{\perp o} V_\perp}{\omega}$$

$$\frac{T}{(n\omega_b)^{\frac{1}{2}}} = \left(\frac{2\pi V_\perp}{c}\right)^{\frac{1}{2}} \frac{c^4 (2K_1)^{\frac{1}{4}}}{v_t (n\omega_b)^3} \left\{\frac{F''_{n+7/2}}{(F'_{n+5/2})^2} \mathrm{Re}\left[\frac{\beta_{ex}}{c^4/2v_t^2\omega^2}\right]\right\}^{\frac{1}{2}} \left[(n+1)(2n+3)\right]^{\frac{1}{2}} \quad (100)$$

and

$$E_r = - \frac{\sqrt{i}\, I_r LP(\omega_o') e^{-i\omega_o' t}}{4\pi\varepsilon_o (n\omega_b t)^{3/2} (2K_1)^{1/4}} \frac{2(n\omega_b)^3 v_t}{c^4} \left(\frac{c}{2\pi V_\perp}\right)^{\frac{1}{2}}$$

$$\times \left\{ \frac{(n+1)(2n+3)F''_{n+7/2}}{(F'_{n+5/2})^2} \mathrm{Re}\left[\frac{n+2}{n+1} (F_{n+9/2} - 2F_{n+7/2} + F_{n+5/2}) \right.\right.$$

$$\left.\left. - \frac{2F_{n+5/2}}{F_{n+3/2}} (F_{n+7/2} - 2F_{n+5/2} + F_{n+3/2}) + \frac{F^2_{n+5/2}}{F^2_{n+3/2}} (F_{n+5/2} - 2F_{n+3/2} + F_{n+1/2}) \right] \right\}^{-\frac{1}{2}} \tag{101}$$

The time response can be normalized with respect to

$$A_{ex} = \left\{ \quad \right\}^{-1/3} \frac{1}{(2K_1)^{1/6}} \tag{102a}$$

so that

$$n\omega_b t = n^2 A_{ex} \left[\left| \frac{2I_r LP\omega_b^3 v_t}{E_r 4\pi\varepsilon_o c^4} \left(\frac{c}{2\pi V_\perp}\right)^{\frac{1}{2}} \right| \right]^{2/3} \tag{102b}$$

where $\left\{ \quad \right\}$ is the quantity within the braces in Eq.(101). The parameter A_{ex} is plotted versus ω_p^2/ω_b^2 in Fig. 20 for $x \gtrsim 2K_1$ (negative F) and in Fig. 21 for $x \lesssim 2K_1$ (positive F).

The above completes the analysis on the time response. The time results near $x \approx 2K_1$ or K_n have been plotted in Figs. 17 to 21. In the following, we discuss these results and show how the experimental harmonic dependence when compared with theory can provide a gross picture of the sheath around the satellite.

X DISCUSSION ON TIME DECAY, EXCITATION OF HARMONICS AND SHEATH EFFECTS

The time response given by theory for the electrostatic pinch points is much longer than observed experimentally. As an example let us consider Eq.(68) for $n=2$, $\omega_p = 2\omega_b = 2\pi Mc$, so that $|K_\perp| = \frac{1}{3}$ and $n\omega_b t = \left|\frac{ILP\omega_b^3}{E4\pi\varepsilon_0}\frac{1}{24\sqrt{6\pi}}\right|^{2/3}\left(\frac{V_\perp}{v_t^2}\right)^2$. Let us assume the experimental values applicable to Alouette 1 data. The receiver sensitivity is 10^2 above κTB, which at $10^7{}^\circ K$ (galactic noise temperature) and 2×10^4 cps bandwidth is 2.76×10^{-10} watts. With a matched load of 400Ω, the antenna voltage at the terminals is 3.32×10^{-4} volts, and an antenna length of 47 m gives a minimum field sensitivity of 7×10^{-6} V/m. The transmitter dipole moment, using the output of 100 W into 400Ω, is 23A-m. We also take (see Eq.(7)), $P(\omega) \sim \tau \sim 10^{-4}$ sec, corresponding to the centre of the pulse train. Other representative values are as follows: $v_t = 1.7\times10^5$ m/s and $V_\perp = 3.3\times10^3$ m/s. We thus obtain

$$2\omega_b t = 1.2\times10^6 \qquad \text{or} \qquad t = 0.19 \text{ sec.}$$

which is about two orders of magnitude too large. Higher order harmonics have even a much longer response because of the extra factors of $v_t/V_\perp$ that appear in Eq.(68). To explain the observed smaller time response when pinch points exist for electrostatic waves, we say that it is difficult to excite, with the dipole antenna and its associated surrounding sheaths, wavelengths in the perpendicular direction which are much smaller than the free-space or antenna length. Thus the electromagnetic pinch points are much easier to excite and are not affected as much by sheaths since their wavelengths are of the order of that in free-space. The minute electrostatic wavelengths probably

cannot be sustained in the sheath for the length of time that the above theory based on homogeneity predicts. This does not say that they are not important. In general, when electromagnetic and electrostatic matching points exist, one can expect both to be important.

We now discuss the time decay of the electromagnetic pinch points. Because of the complexity of Eq.(87a) for the extraordinary wave near $x \approx K_l K_r / K_\perp$, we calculate only results for the $x \approx 2K_l$ and $x \approx K_\parallel$ matching points. In all these cases, we have a formula such as

$$n\omega_b t = n^2 A \left| \frac{ILP\omega_b^3 v_t}{E 4\pi\varepsilon_0 c^4} \left(\frac{c}{2\pi V_\perp} \right)^{\frac{1}{2}} \right|^{2/3} \tag{103}$$

where I denotes either $I_\parallel$ or $2I_r$. Let us assume again the experimental date for Alouette 1 given above. We also adopt a typical value for $\omega_b = 1.2\pi$ Mc/s (or frequency = 0.6 Mc/s), and obtain from Eq.(103)

$$n\omega_b t \approx n^2 A \times 5.5 \times 10^3 \text{cycles} \tag{104}$$

The parameter A varies between 0.6 and 1.5 and is given for various pinch points in Figs. 17 to 21.

The experimental data on $n\omega_b t$ as given by Fejer and Calvert[8] is given in Fig. 22. We see that the cyclotron harmonic ringing lasts typically for 10^3 to 10^4 cycles which agrees as far as order of magnitude with Eq.(104). There do not seem to be any pronounced effects for $n \geq 2$ on ω_p/ω_b which again agrees with the relative insensitivity (within a factor of 3) of the parameter A, even very close to cut-offs, in Figs. 17 to 21. The experimental deviations[9] from

cyclotron harmonic values are within 1% as predicted by this theory in Figs. 6, 9, 12 and 15. (Note that the theoretical deviations measured by a moving body are the values plotted in the Figures with the Doppler shift subtracted.) Lockwood[10] states that the favoured orientation for cyclotron harmonic resonance is when the antenna is oriented along the magnetic field. Theoretically, this indicates the importance of the ordinary wave contribution, given in Fig. 19. Calvert and Van Zandt[6] also find increases in signal exactly perpendicular to magnetic field which can be attributed to the other waves.

The only apparent disagreement of this theory and experiment seems to arise from the n^2 factor in Eq.(104). (We note that the electrostatic theory in Section VIII suffers as well from such a serious discrepancy.) The n^2 factor says that higher harmonics last for a longer time. Physically this is a result of Eqs.(17) and (18) where it is shown that the response is larger when the curvature of the dispersion curve is less, and this theory predicts "shallower" dispersion curves for higher harmonics. If higher harmonics last longer, why do the experimental ringing durations decrease slightly with harmonic number as shown in Fig. 22? This contradiction is only an apparent one, since we have assumed in Eq.(104) that all harmonics are excited to the same degree with the same field amplitude. Obviously, the excitation mechanism favours the lower harmonics. That is we hypothesize that the higher harmonics are excited to a lesser intensity than the lower ones but, once excited, last for a longer time. In effect, we want the two effects to balance out in order to reproduce

the more-or-less independence or slight decrease with harmonic number shown in Fig. 22. The slight changes in the A factor with harmonic number are sufficient to account for the net decrease in response.

In order to include the excitation effect, we have to adapt a physical method for higher cyclotron harmonic excitation. The picture adopted below is identical to that postulated by Johnston and Nuttall[11], and essentially rests on the non-linear variation of the electric field within the sheath. We assume that the very strong antenna field acts on the electrons in the antenna sheath whose motions are influenced by the steady nonuniform electric field of the sheath and the ambient magnetic field. Johnston and Nuttall (Eq.(5)) show that the perturbed exciting electric current density varies with harmonic number n as $b_n n$, where b_n is defined below. Thus in order for all the harmonics to last the same time, we require, according to Eq.(103) with $I \propto b_n n$, that $b_n \propto n^{-4}$. In the model of Johnston and Nuttall, the magnetic field is along the z-axis, the electric field in the sheath is along the x-axis and varies with x. An electron in the sheath oscillates according to the solution of the equation:

$$\ddot{x} + \omega_b^2 x + (e/m)[E(x) - V] = 0 \qquad (105)$$

where V is constant and a dot signifies $\partial/\partial t$. The coefficients b_n are defined by the solution of Eq.(105), viz.

$$x(t)/x_0 - c = \sum_1^{\infty} b_n(\cos n\omega_b t + \beta_n) \qquad (106)$$

where x_o and c are constants. Let us work backwards to calculate $E(x)$, assuming that $b_n \propto n^{-4}$. With $\beta_n = \pi$ for simplicity, we assume a solution of the form

$$x(t)/x_o - c = -\sum_1^\infty (\cos n\omega_b t)/n^4 \tag{107}$$

Let $\cos(n\omega_b t) = \cos\theta$ where $0 \leq \theta < 2\pi$, $\theta = \omega t - 2m\pi$ with m an integer. Then we can use the following identities[12]:

$$-\frac{x}{x_o} + c = \sum_1^\infty \frac{\cos n\theta}{n^4} = \frac{\pi^4}{90} - \frac{\pi^2\theta^2}{12} + \frac{\pi\theta^3}{12} - \frac{\theta^4}{48} = \frac{\pi^2}{6}\left(\frac{\theta^2}{4} - \frac{\pi\theta}{2} + \frac{\pi^2}{8}\right) - \frac{(\theta-\pi)^4}{48} + \frac{\pi^4}{90} \tag{108}$$

$$\frac{\ddot{x}}{x_o\omega_b^2} = \sum_1^\infty \frac{\cos n\theta}{n^2} = \frac{\pi^2}{6} - \frac{\pi\theta}{2} + \frac{\theta^2}{4} \tag{109}$$

since $\partial/\partial t = \omega_b \partial/\partial\theta$. For $x = x_o$ at $t = 0$, we let $c = \pi^4/90$. If we solve Eq.(109) for θ in terms of $\ddot{x}$, we obtain

$$\theta = \pi \pm \left[\frac{\pi^2}{3} + \frac{4\ddot{x}}{\omega_b^2 x_o}\right]^{\frac{1}{2}} \tag{110}$$

Substitution of Eqs.(110) and (109) into (108) yields with $c = \pi^4/90$

$$\frac{x}{x_o} = -\frac{\pi^2}{6\omega_b^2}\frac{\ddot{x}}{x_o} + \frac{\pi^4}{144} + \frac{1}{48}\left(\frac{\pi^2}{3} + \frac{4\ddot{x}}{\omega_b^2 x_o}\right)^2$$

or

$$\left(\frac{\ddot{x}}{x_o}\right)^2 - \frac{\pi^2}{3}\omega_b^2\left(\frac{\ddot{x}}{x_o}\right) + \left(\frac{\pi^4}{36} - \frac{3x}{x_o}\right)\omega_b^4 = 0$$

Solving for $\ddot{x}$ yields

$$\frac{\ddot{x}}{x_o\omega_b^2} = \frac{\pi^2}{6} \pm \left(\frac{3x}{x_o}\right)^{\frac{1}{2}} \tag{111}$$

Finally, substituting this into Eq.(105) and choosing the constant $V = E_o + x_o\omega_b^2\pi^2 m/6e$, where $E = E_o$ at $x = x_o$, results in

$$-\frac{e}{m\omega_b^2 x_o}(E - E_o) = \frac{x}{x_o} \pm \left(\frac{3x}{x_o}\right)^{\frac{1}{2}} \qquad (112)$$

We have succeeded in deriving two possible gross variations of the electric field in the sheath which can provide the proper apparent independence of the resonance duration on harmonic number. Figure 23 illustrates these two variations. For sufficiently large x/x_o, E has to tend to zero, but this is not accounted for in the simple-minded theory presented above.

We have also shown that the excitation mechanism favours lower harmonics whereas the resonance relaxation after the pulse is shut-off favours the higher harmonics. The long relaxation times have been associated with points on the dispersion curve where the wave group velocity matches satellite velocity.

For electrostatic waves, such matching perpendicular to magnetic field can be accomplished when the waves are backward, but only for the lower harmonics when the waves are forward. Matching with electrostatic waves may, however, not be necessary due to finite antenna size where the whole volume surrounding the antenna is excited with the satellite moving faster and thereby sampling the wave packets. This analysis including finite antenna size has not been done here and should be considered in any future work. Furthermore, sheath effects have to be included since the sheaths are larger than the electrostatic perpendicular wavelengths. Sheath effects may explain why the electrostatic

resonances do not last as long as theory predicts.

For electromagnetic waves, matching points of importance are those near $x \approx K_l K_r / K_\perp$, $x \approx K_\parallel$ and $x \approx 2K_l$, the first two having one such point and the latter having at least four such points. The resonance duration predicted by these points, modified by the excitation effect on harmonic number, is in agreement with observations. The theory requires further analysis on the effect of magnetic field inhomogeneity in the parallel direction. Also one should check the applicability of the analysis in Section II for $k_\perp^2 D_\perp t / 2D_\omega \approx k_\perp V_\perp t$ of order one rather than much greater than one. We do not expect a more extensive development to produce significant changes. Finally, for all this theory based on pinch points, one should investigate the time that one has to wait before the asymptotic time behaviour becomes valid. Here again we believe that, even though $k_\perp V_\perp t$ may be small, the theory is correct to first order, as is indicative from the generalized approach also given in Section II.

Appendix III provides a list of publications and a discussion on previous work[13] and the modifications that have been found necessary. In Appendix I and II, we give the material corrected and condensed from Parts I and II respectively in a previous report[13]. The nonrelativistic analysis has been elaborated upon and its regime of applicability is illustrated. Both of these reports are scheduled to be published in the February 1966 issue of Physics of Fluids.

ACKNOWLEDGEMENTS

The author appreciates the helpful suggestions of Dr. T.W. Johnston and the continuous encouragement of Dr. F.J.F. Osborne during the course of this work. The author is also thankful to Mr. D. Jassby for all the computational work and to Mrs. M. Gore for her fine typing of the manuscript.

This research was supported by the National Aeronautics and Space Administration, Goddard Space Flight Center, Fields and Plasma Branch, Greenbelt, Maryland, under Contract NASw-957.

REFERENCES

1. J. Nuttall, Phys. Fluids 8, 286 (1965); J. Geophys. Res. 70, 1119 (1965).

2. W. Magnus and F. Oberhettinger "Formulas and Theorems for the Special Functions of Mathematical Physics", Chelsea Publ. Co. (1949), p.127, 129.

3. B.D. Fried and S.D. Conte, "The Plasma Dispersion Function", Academic Press Inc., N.Y. (1961).

4. W.D. Deering and J.A. Fejer, Phys. Fluids 8, 2066 (1965); (see also P.A. Sturrock, ibid 8, 88 (1965)).

5. T.H. Stix, "The Theory of Plasma Waves", McGraw-Hill Book Co., Inc. (1962), p.224.

6. W. Calvert and T.E. Van Zandt, "Fixed-Frequency Observations of Plasma Resonances in the Topside Ionosphere", ESSA, Boulder Colorado, October 10, 1965. (To be published.) (See also Science 146, 391 (1964).)

7. P.M. Morse and H. Feshbach, "Methods of Theoretical Physics", McGraw-Hill Book Co., Inc. Part 1 (1953), p.441.

8. J.A. Fejer and W. Calvert, J. Geophys. Res. 69, 5049 (1964); (see also W. Calvert and G.B. Goe, ibid 68, 6113 (1963).)

9. R.E. Barrington and L. Herzberg, "Frequency Variation in Ionospheric Cyclotron Harmonic Series Obtained by the Alouette 1 Satellite", DRTE, Ottawa, Ontario (to be published).

10. G.E.K. Lockwood, Can. J. Phys. 43, 291 (1965). (see also 41, 190 (1963).)

11. T.W. Johnston and J. Nuttall, J. Geophys. Res. 69, 2305 (1964).

12. I.M. Ryshik and I.S. Gradstein, "Tables of Series, Products and Integrals", Deutscher Verlag der Wissenschaften, Berlin (1957), p.38.

13 I.P. Shkarofsky and T.W. Johnston, Phys. Rev. Letters 15, 51 (1965); "Satellite Cyclotron Harmonic Resonances", RCA Victor Research Report 7-801-35 (1965).

CAPTIONS FOR FIGURES

Figure 1 — Calculated plots of the $F_{n+3/2}$ functions for $n = 1,2 \ldots 7$ in the region where the function are large and negative. The real part of ω is denoted as ω_r.

Figure 2 — Calculated plots of $F'_{n+3/2}/F_{n+3/2}$, the derivative taken with respect to the abscissa $c^2(\omega_r - n\omega_b)/n\omega_b v_t^2$, for $n = 1,2 \ldots 7$ in the region where $F_{n+3/2}$ is large and negative.

Figure 3 — Ratio of plasma to cyclotron frequency (or Larmor radius to Debye length) versus altitude with an assumed model of electron density and magnetic field at the equator for daytime and sunspot minimum conditions.

Figure 4 — Plot of the normalized group velocity versus $\lambda = k_\perp^2 v_t^2/\omega_b^2$ for the Bernstein electrostatic mode, when $\omega^2 >> \omega_p^2 + \omega_b^2$, for $n = 2$, 3, 4 and 5.

Figure 5 — The values of $(k_\perp c/\omega)^2 \approx K_1 K_r/K_\perp$ versus $(\omega_p/\omega_b)^2$ for the extraordinary X or Z-wave and the additive deviation $\Delta(k_\perp c/\omega)^2$ where the matching occurs for $n = 2$ to 7. The more vertical curves correspond to the Z-wave and the flatter ones to the X-wave.

Figure 6 — The values of $(\omega_r - n\omega_b)c^2/n\omega_b v_t^2$ where matching occurs for the X and Z-waves near $(k_\perp c/\omega)^2 \approx K_1 K_r/K_\perp$.

Figure 7 The values of $k_{\parallel}c^2/n\omega_b V_{\parallel}$ where matching occurs for the X and Z-waves near $(k_{\perp}c/\omega)^2 \approx K_1K_r/K_{\perp}$.

Figure 8(a,b,c) The values of $(k_{\perp}c/\omega)^2 \approx 2K_1$ versus $(\omega_p/\omega_b)^2$ for the extraordinary wave (Fig. 8a) and the deviation $\Delta(k_{\perp}c/\omega)^2$ either additive (Fig. 8b, curve ---- $(k_{\perp}c/\omega)^2 > 2K_1$) or subtractive (Fig. 8c, curve ——— $(k_{\perp}c/\omega)^2 < 2K_1$) where matching occurs. Differences in Figs. 8b, c are negligible for $n \geq 6$.

Figure 9(a,b) The values of $(\omega_r - n\omega_b)c^2/n\omega_b v_t^2$ for the cases in Figs. 8b, c. For curve ---- $(k_{\perp}c/\omega)^2 > 2K_1$ and for curve —— $(k_{\perp}c/\omega)^2 < 2K_1$. Differences are negligible for $n \geq 6$.

Figure 10(a,b) The values of $k_{\parallel}c^2/n\omega_b V_{\parallel}$ for the cases in Figs. 8b, c. Separate plots are not shown since the differences between values for $(k_{\perp}c/\omega)^2$ greater and less than $2K_1$ are negligible when $n > 2$. For $n = 2$, some values are shown for $(k_{\perp}c/\omega)^2 > 2K_1$.

Figure 11 The values of $(k_{\perp}c/\omega)^2 \approx K_{\parallel}$ versus $(\omega_p/\omega_b)^2$ for the ordinary wave and the additive deviation $\Delta(k_{\perp}c/\omega)^2$ where matching occurs.

Figure 12 The values of $(\omega_r - n\omega_b)c^2/n\omega_b v_t$ for the case in Fig. 11.

Figure 13 The values of $k_{\parallel}c^2/n\omega_b V_{\parallel}$ for the cases in Fig. 11.

Figure 14(a,b,c) The values of $(k_{\perp}c/\omega)^2 \approx 2K_1$ versus $(\omega_p/\omega_b)^2$ for the extra wave (Fig. 14a) and the deviation $\Delta(k_{\perp}c/\omega)^2$, either additive (Fig. 14b, curve ---- $(k_{\perp}c/\omega)^2 > 2K_1$) or subtractive (Fig. 14c, curve —— $(k_{\perp}c/\omega)^2 < 2K_1$) where matching occurs. Single curves are shown when the differences in the magnitudes of the deviations are negligible.

Figure 15(a,b) The values of $(\omega_r - n\omega_b)c^2/n\omega_b v_t^2$ for the cases in Figs. 14b,c. For curve ---- $(k_{\perp}c/\omega)^2 > 2K_1$ and for curve —— $(k_{\perp}c/\omega)^2 < 2K_1$. Differences are negligible for larger n.

Figure 16(a,b) The values of $k_{\parallel}c^2/n\omega_b V_{\parallel}$ for the cases in Figs. 14b,c. Single curves are shown for larger n.

Figure 17 Plot of the normalized duration response parameter given in Eq.(86), corresponding to the cases in Figs. 8b, 9a and 10a.

Figure 18 — Same as Fig. 17 corresponding to the cases in Figs. 8c, 9b and 10b.

Figure 19 — Plot of the normalized duration response parameter given in Eq.(94a) corresponding to the cases in Figs. 11, 12 and 13.

Figure 20 — Plot of the normalized duration response parameter given in Eq.(102a) corresponding to the cases in Figs. 14b, 15a and 16a.

Figure 21 — Same as Fig. 20 corresponding to the cases in Figs. 14c, 15b and 16b.

Figure 22 — These cyclotron harmonic observational results are from Fejer and Calvert (1964) Fig. 4. Their theoretical curves have been removed and relevant frequency conditions - $n\omega_b$ equals ω_R, ω_T, ω_p, ω_L - have been indicated by R, T, P and L respectively. (ω_R, ω_T, ω_p and ω_L are the values of ω for which K_r, $K_\perp$, $K_\parallel$ and K_l go to zero respectively.) In their notation f_H and f_N are the cyclotron and plasma frequencies $\omega_b/2\pi$ and $\omega_p/2\pi$. According to Fejer and Calvert the data points represent the results of averaging one to three dozen observations.

Figure 23 — Models of the electric field variation in the sheath near the antennas which can explain the independence of the time duration on harmonic number.

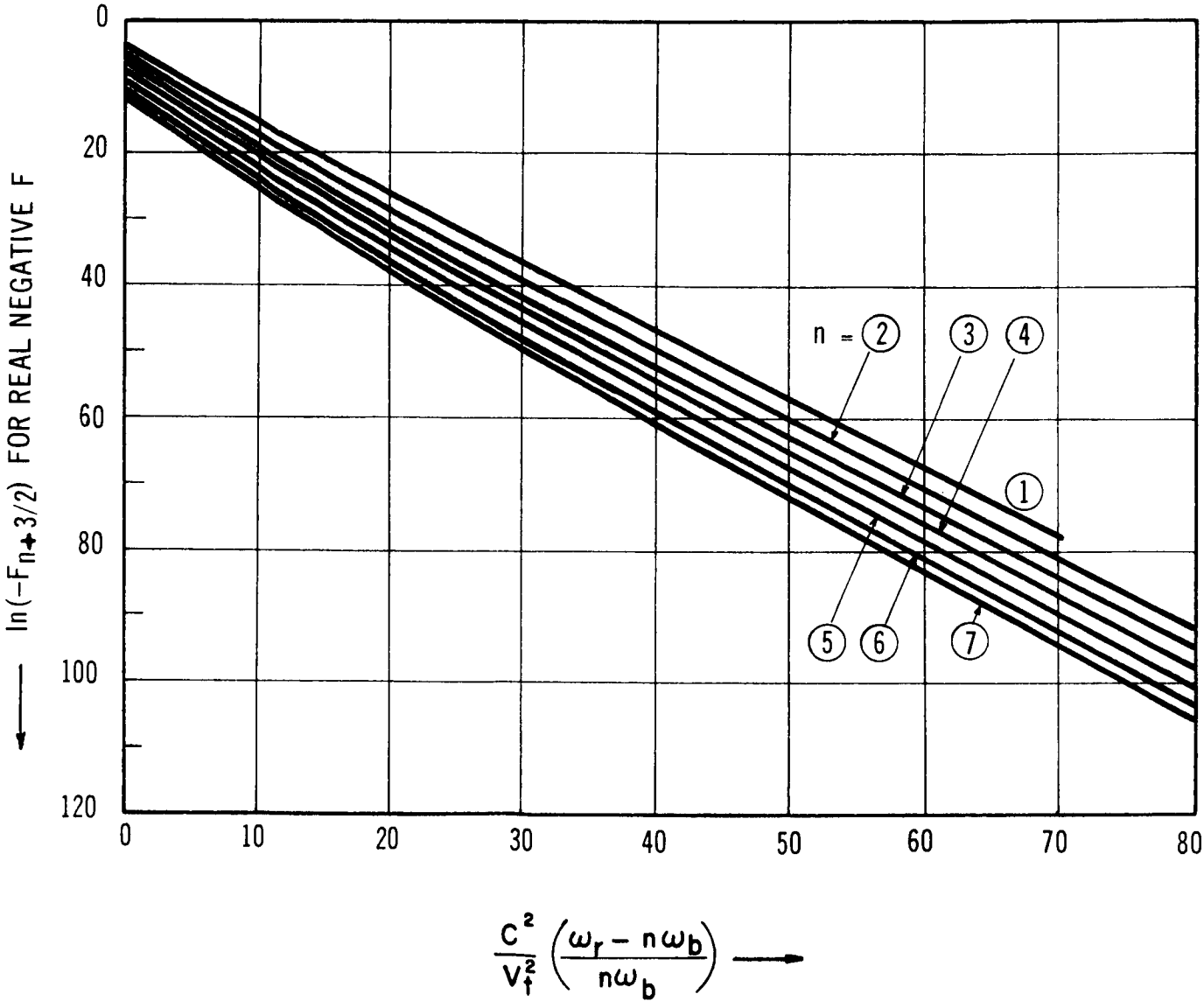
0
20
40
60
80
100
120
0
10
20
30
40
50
60
70
80
n = 2
3
4
1
5
6
7
$\ln(-F_{n+3/2})$ FOR REAL NEGATIVE F
$\frac{C^2}{V_t^2}\left(\frac{\omega_r - n\omega_b}{n\omega_b}\right)$

FIGURE 1

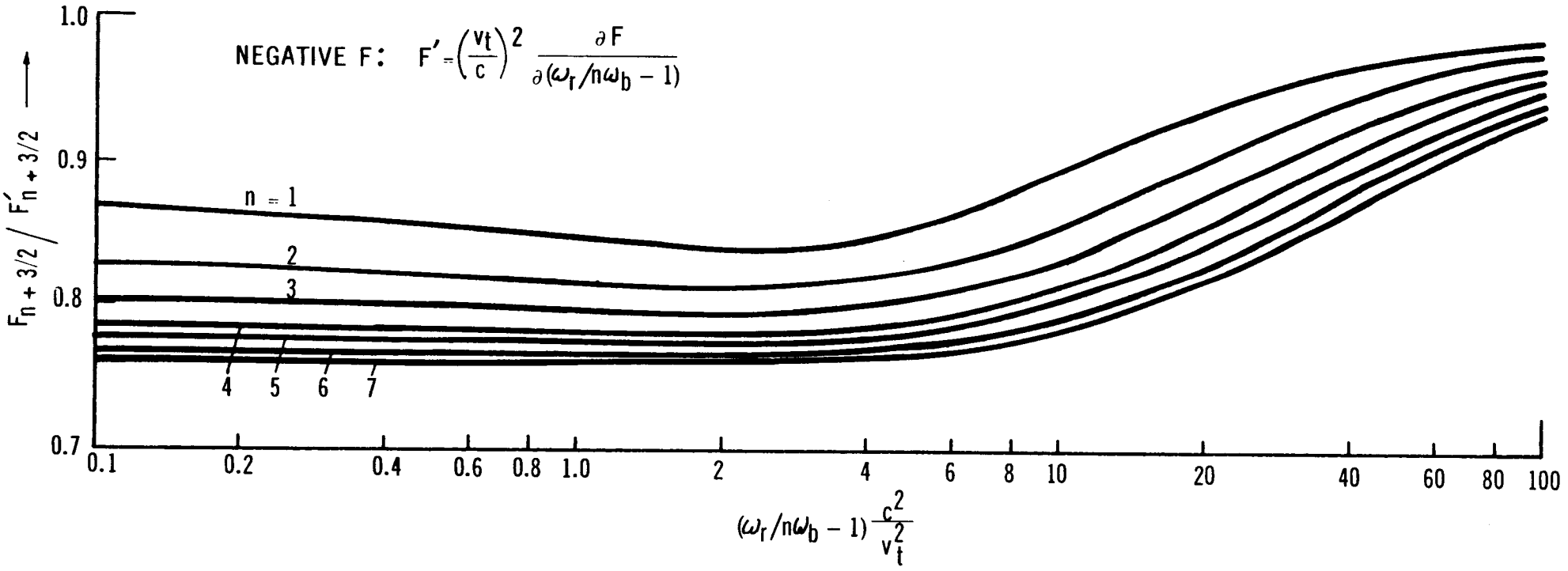
NEGATIVE F: $F' = \left(\frac{v_t}{c}\right)^2 \frac{\partial F}{\partial(\omega_r/n\omega_b - 1)}$
$F_{n+3/2} / F'_{n+3/2}$
1.0
0.9
0.8
0.7
n = 1
2
3
4
5
6
7
0.1
0.2
0.4
0.6
0.8
1.0
2
4
6
8
10
20
40
60
80
100
$(\omega_r/n\omega_b - 1)\frac{c^2}{v_t^2}$

FIGURE 2

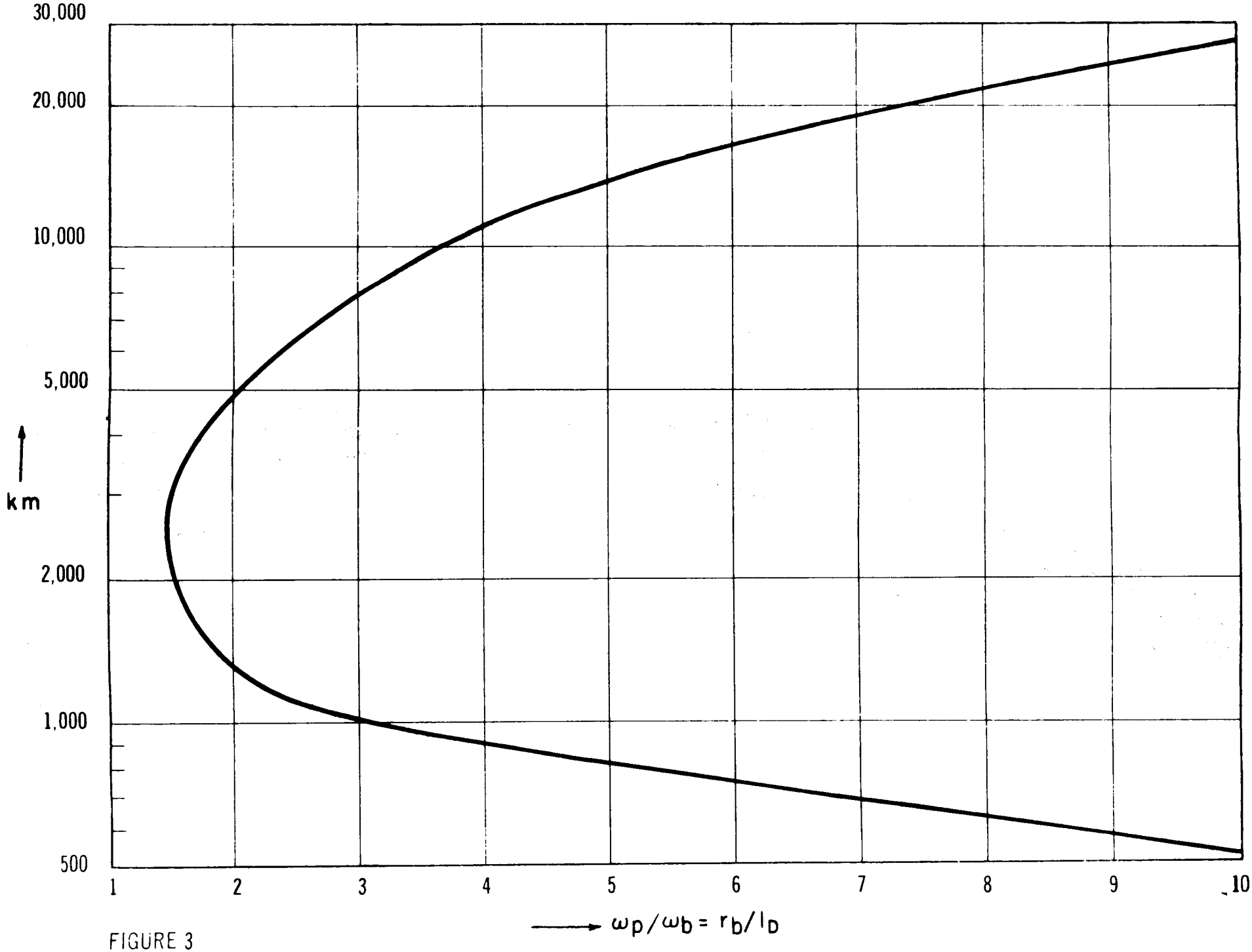
30,000
20,000
10,000
5,000
2,000
1,000
500
km
1
2
3
4
5
6
7
8
9
10
ωp/ωb = rb/lD

FIGURE 3

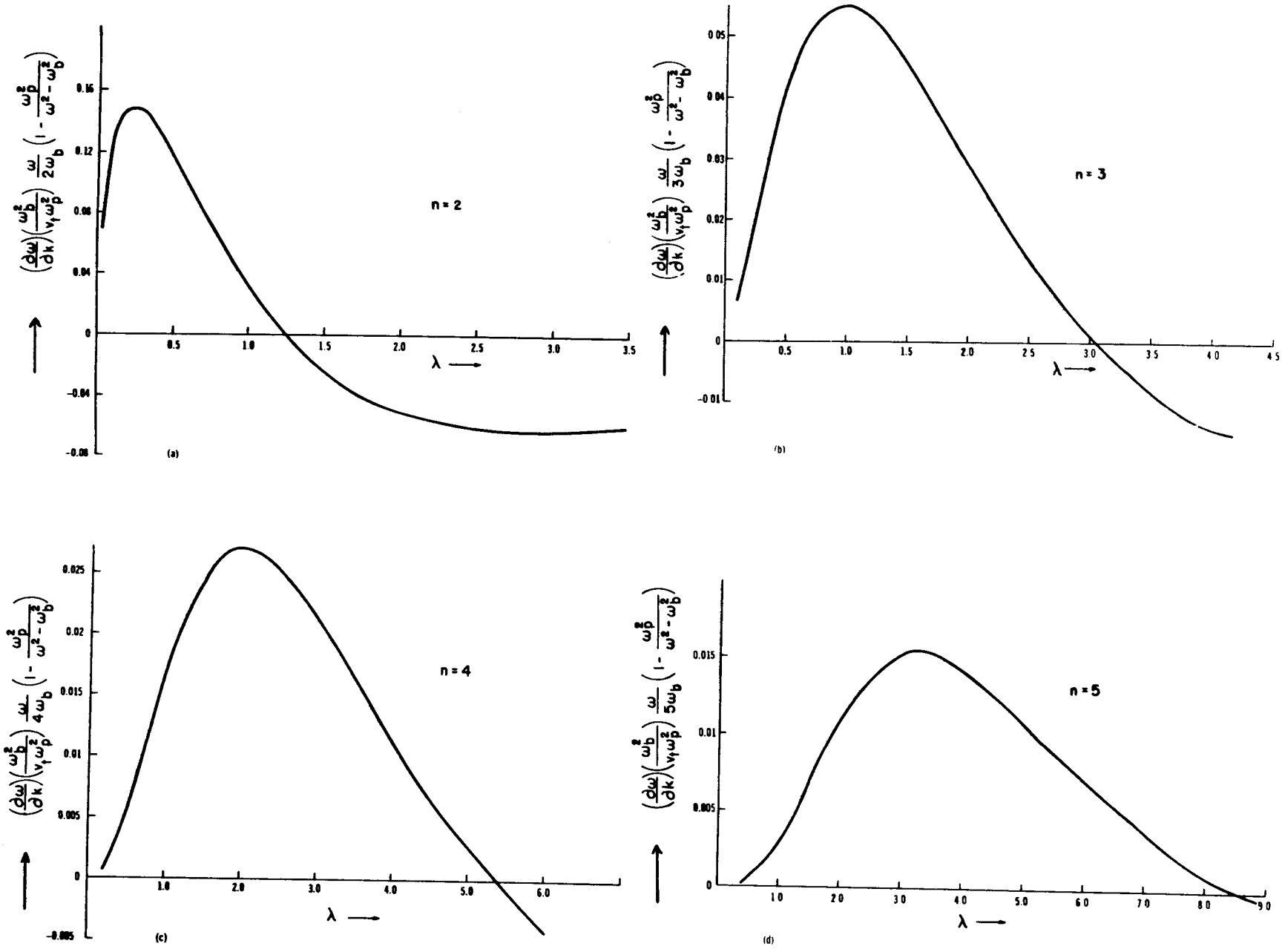

FIGURE 4

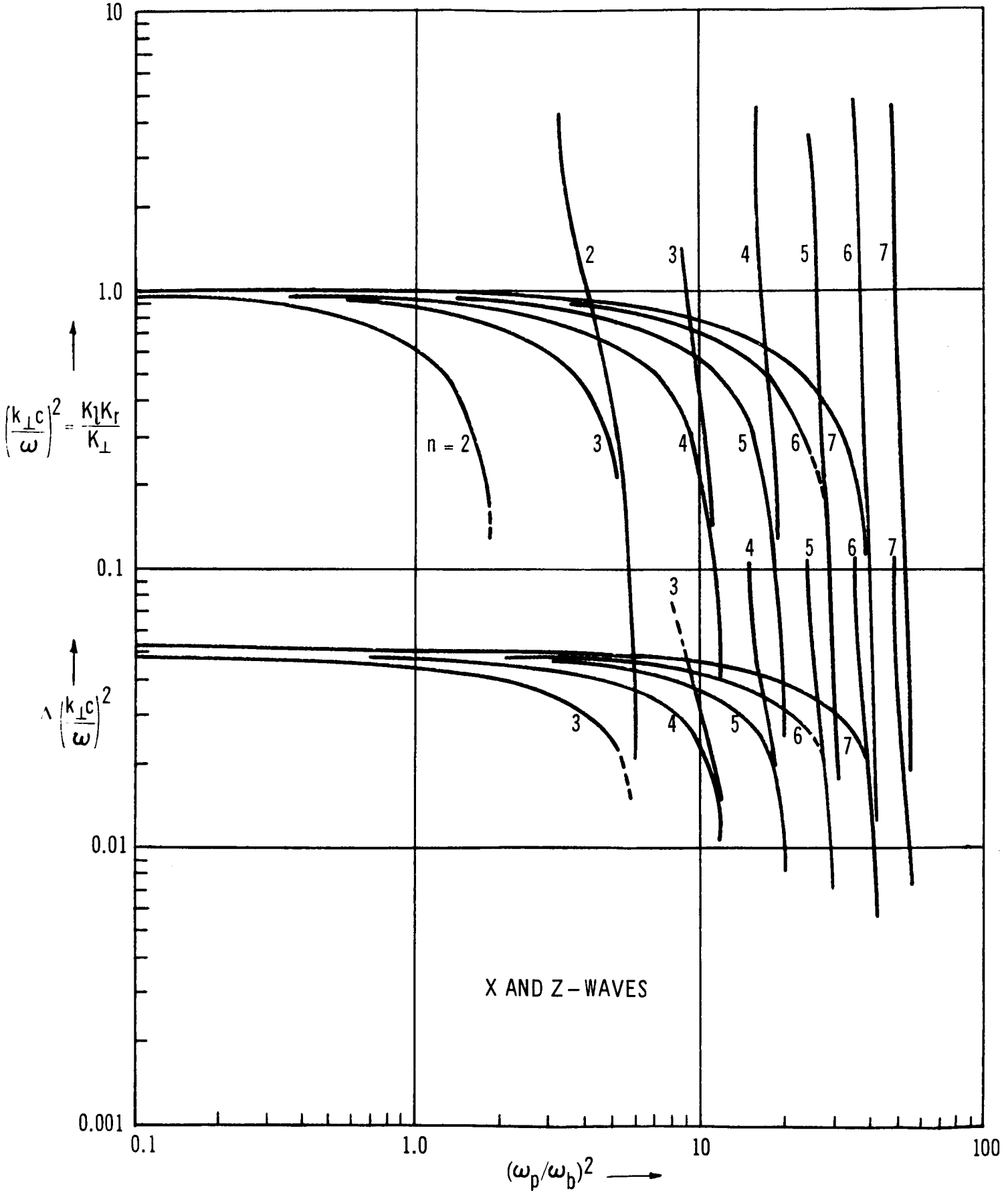
10
1.0
0.1
0.01
0.001
0.1
1.0
10
100
$\left(\frac{k_\perp c}{\omega}\right)^2 = \frac{K_l K_r}{K_\perp}$
$\Lambda \left(\frac{k_\perp c}{\omega}\right)^2$
$(\omega_p/\omega_b)^2 \longrightarrow$
n = 2
2
3
4
5
6
7
X AND Z – WAVES

FIGURE 5

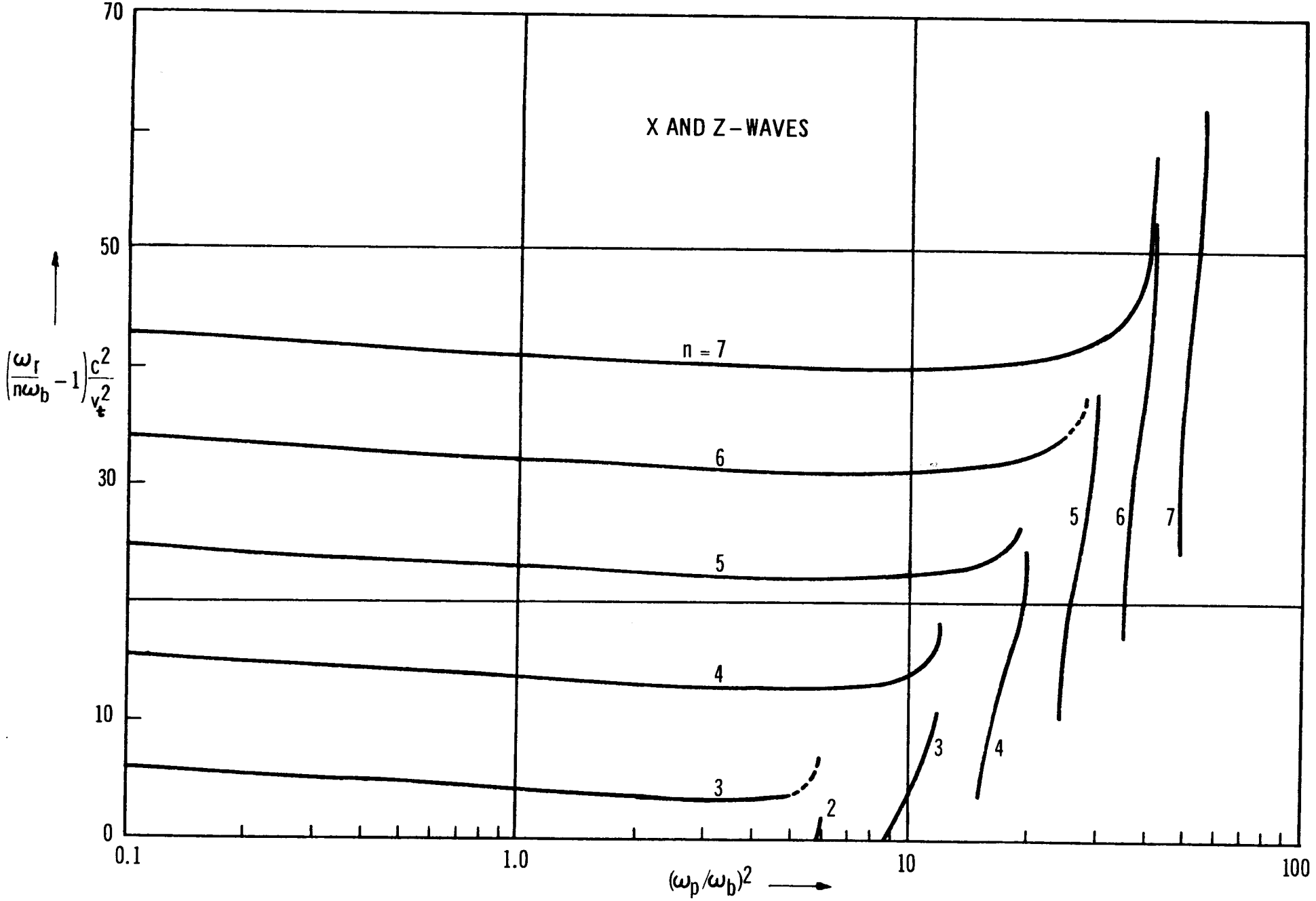
X AND Z – WAVES
70
50
30
10
0
0.1
1.0
10
100
$\left(\frac{\omega_r}{n\omega_b} - 1\right)\frac{c^2}{v_t^2}$
$(\omega_p/\omega_b)^2$
n = 7
6
5
4
3
2
3
4
5
6
7

FIGURE 6

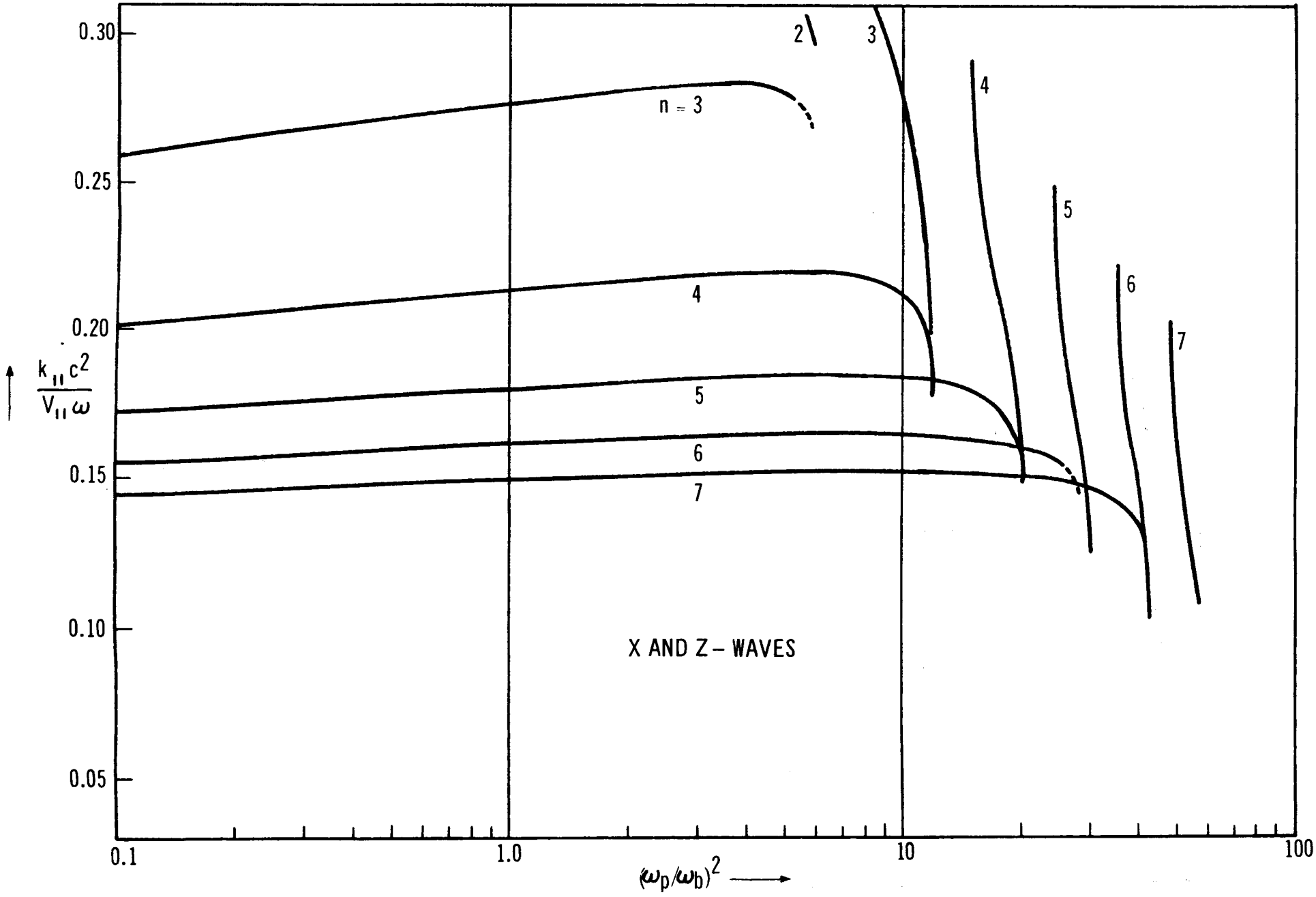
0.30
0.25
0.20
0.15
0.10
0.05
$\frac{k_{11}c^2}{V_{11}\omega}$
n = 3
4
5
6
7
2
3
4
5
6
7
X AND Z – WAVES
0.1
1.0
10
100
$(\omega_p/\omega_b)^2$

FIGURE 7

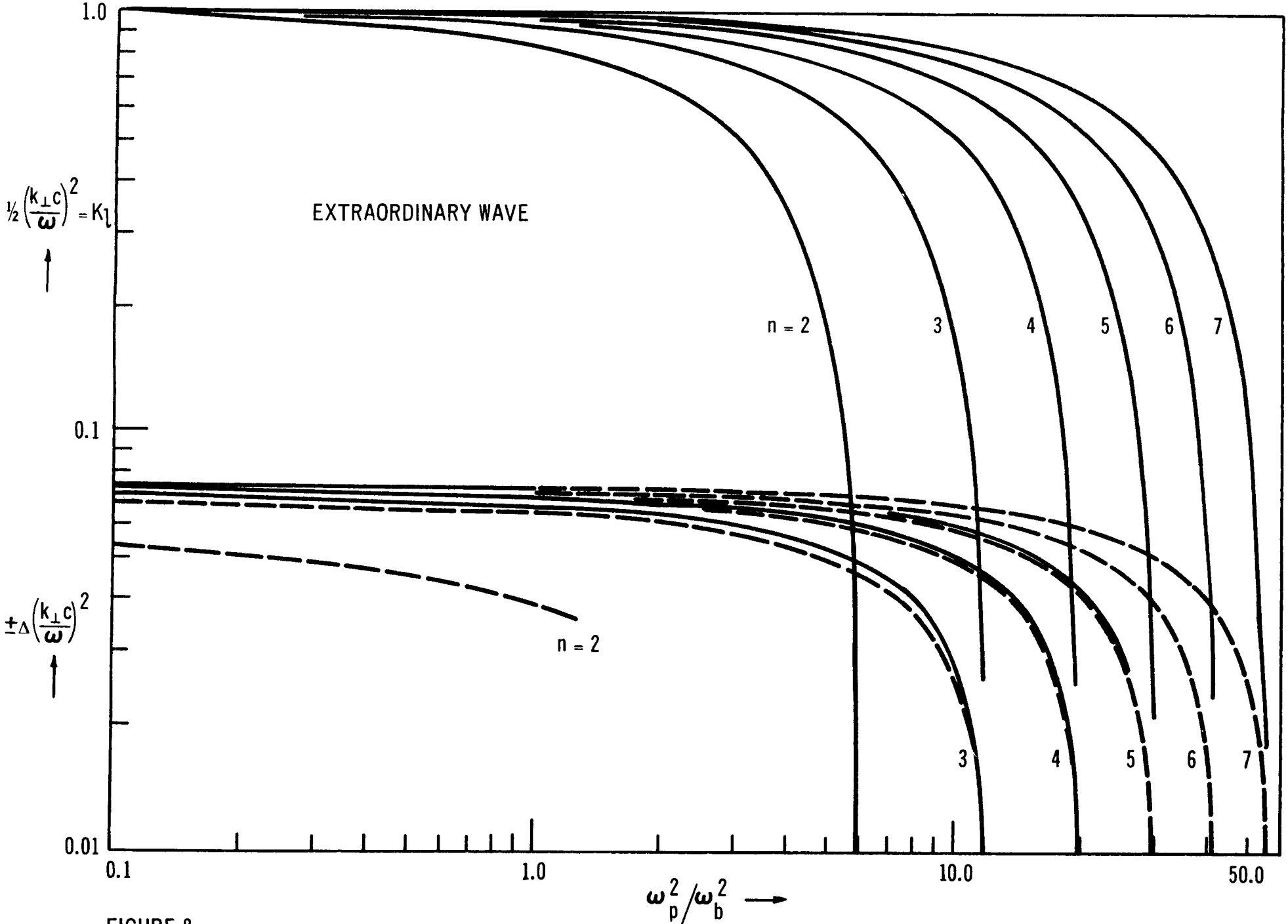
1.0
0.1
0.01
$\frac{1}{2}\left(\frac{k_\perp c}{\omega}\right)^2 = K_1$
EXTRAORDINARY WAVE
n = 2
3
4
5
6
7
$\pm\Delta\left(\frac{k_\perp c}{\omega}\right)^2$
n = 2
3
4
5
6
7
0.1
1.0
10.0
50.0
ω_p^2/ω_b^2 →

FIGURE 8

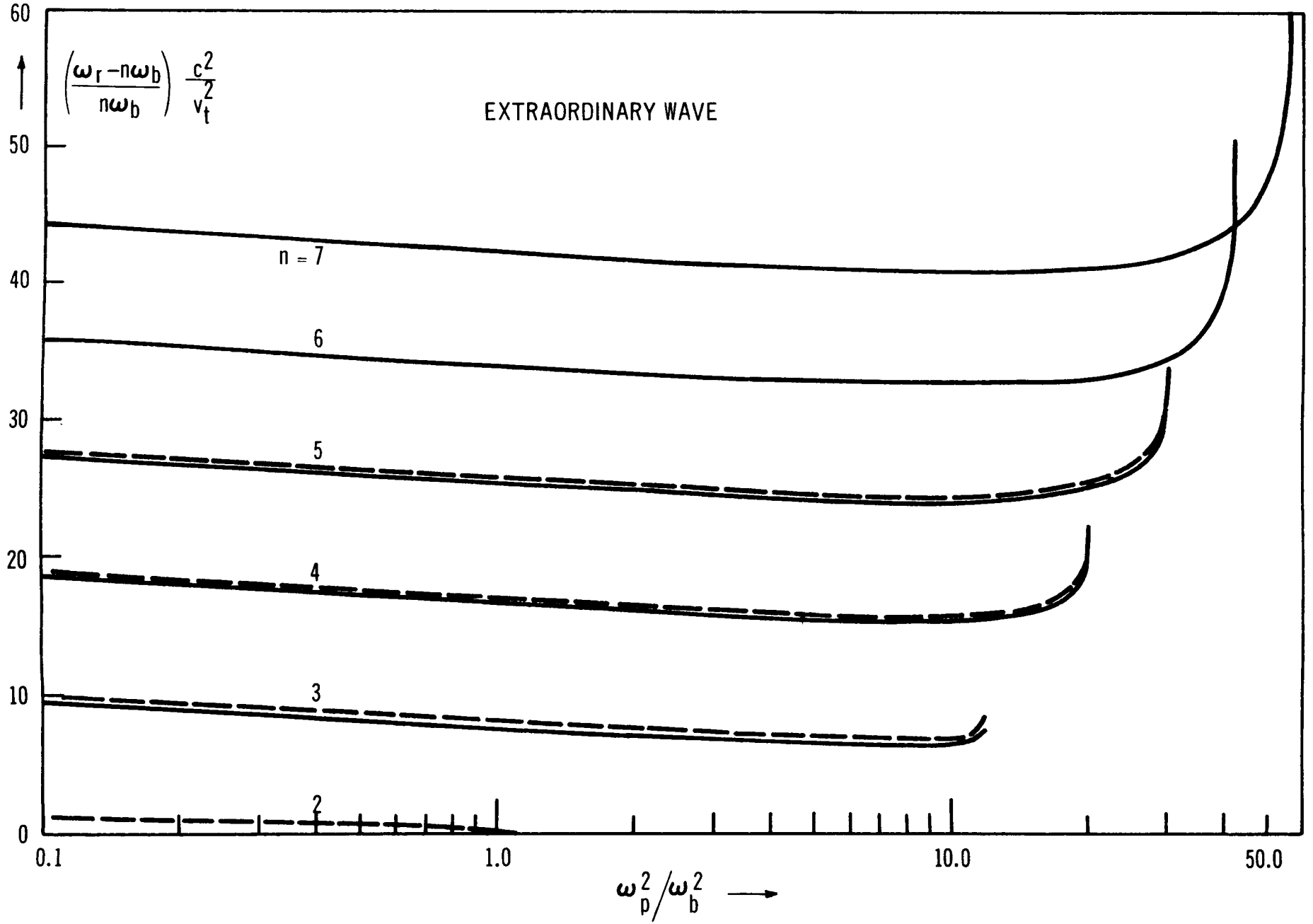
60
50
40
30
20
10
0
$\left(\frac{\omega_r - n\omega_b}{n\omega_b}\right)\frac{c^2}{v_t^2}$
EXTRAORDINARY WAVE
n = 7
6
5
4
3
2
0.1
1.0
10.0
50.0
ω_p^2/ω_b^2

FIGURE 9

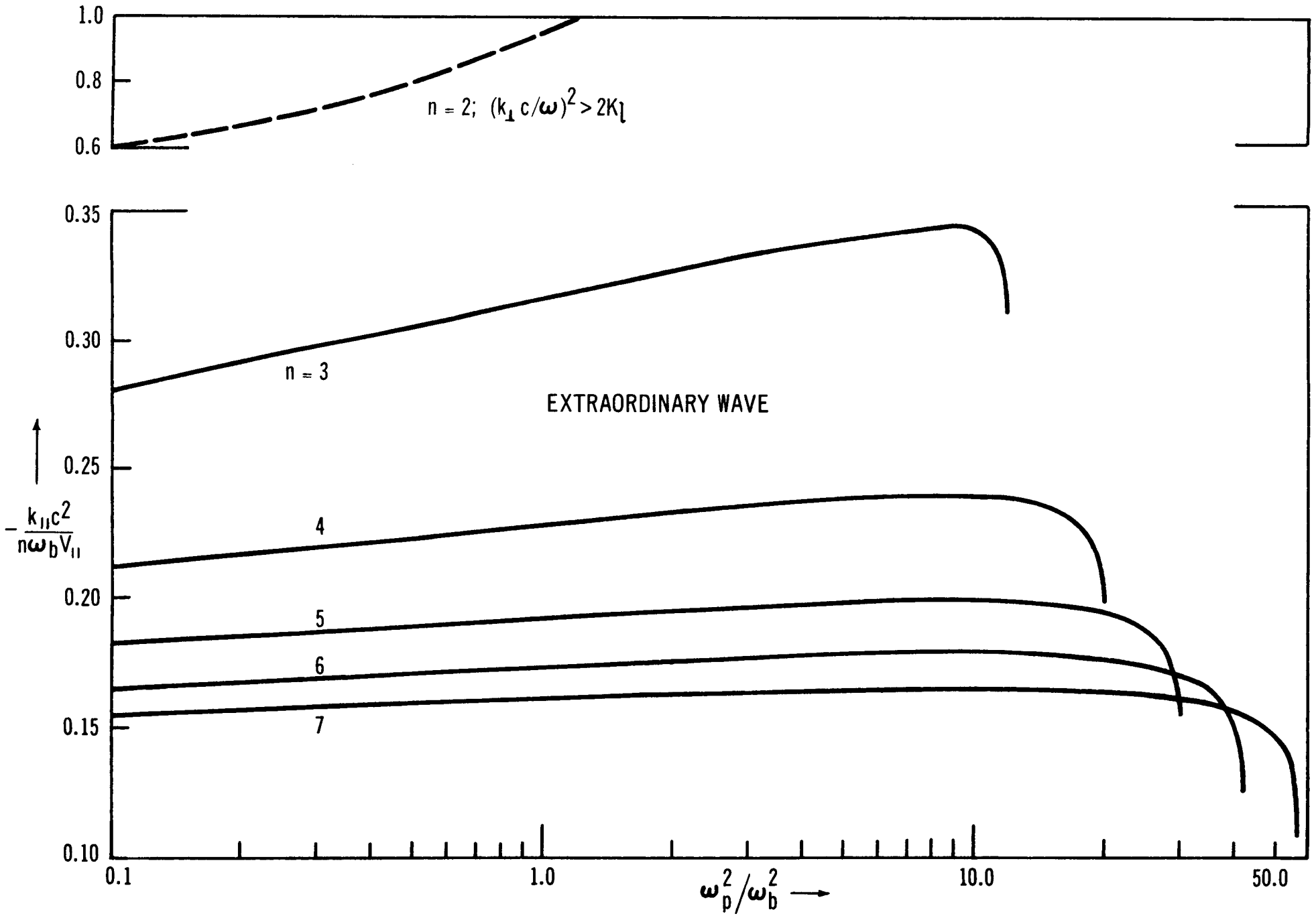
1.0
0.8
0.6
n = 2; $(k_\perp c/\omega)^2 > 2K_\parallel$
0.35
0.30
0.25
0.20
0.15
0.10
n = 3
EXTRAORDINARY WAVE
4
5
6
7
$-\frac{k_{\parallel}c^2}{n\omega_b V_{\parallel}}$
0.1
1.0
10.0
50.0
ω_p^2/ω_b^2 →

FIGURE 10

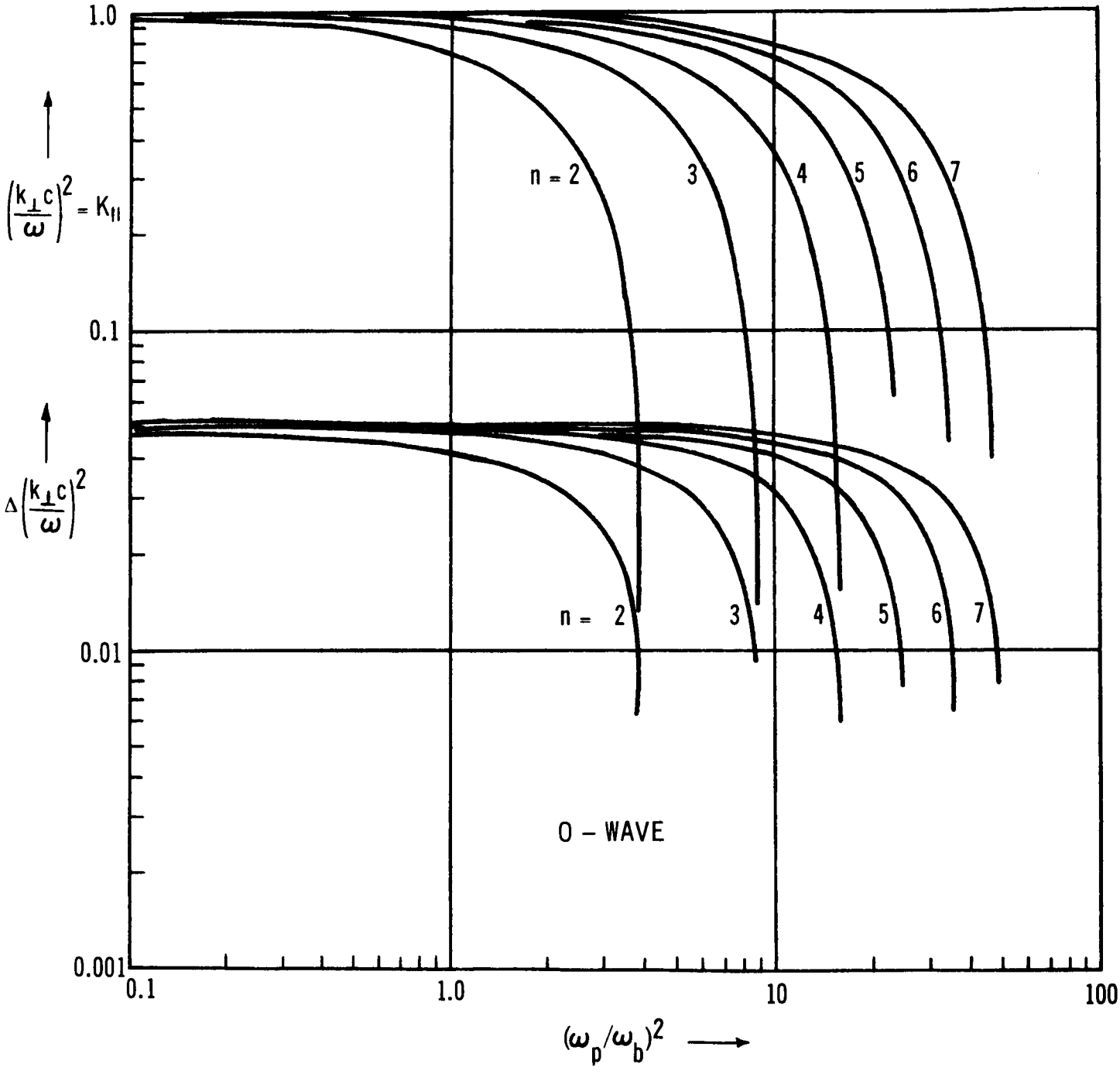
1.0
0.1
0.01
0.001
$\left(\frac{k_\perp c}{\omega}\right)^2 = K_{11}$
$\Delta\left(\frac{k_\perp c}{\omega}\right)^2$
n = 2
3
4
5
6
7
n = 2
3
4
5
6
7
O – WAVE
0.1
1.0
10
100
$(\omega_p/\omega_b)^2$ ⟶

FIGURE 11

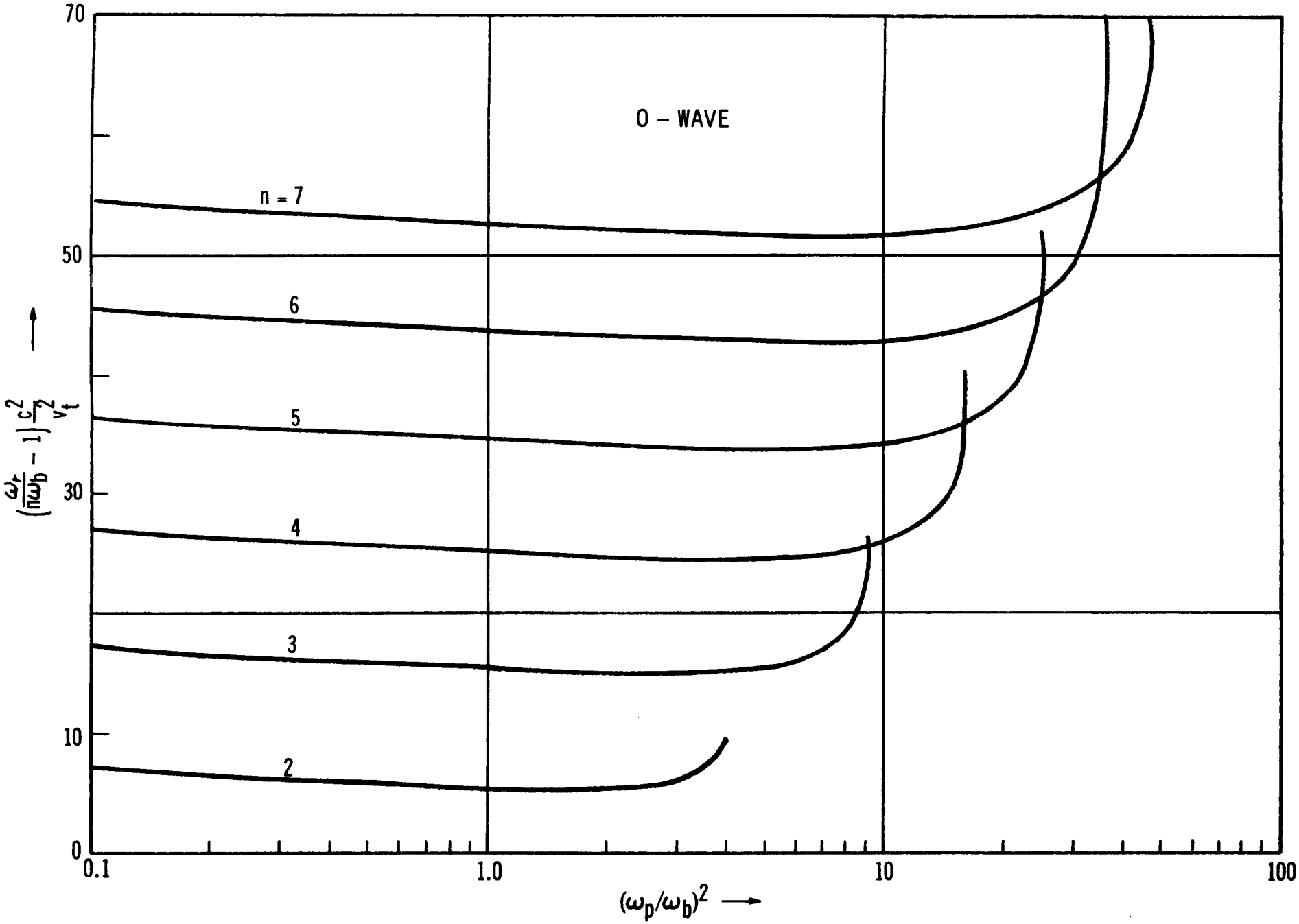
70
50
30
10
0
0.1
1.0
10
100
O – WAVE
n = 7
6
5
4
3
2
$\left(\frac{\omega_r}{n\omega_b} - 1\right)\frac{c^2}{v_t^2}$ ⟶
$(\omega_p/\omega_b)^2$ ⟶

FIGURE 12

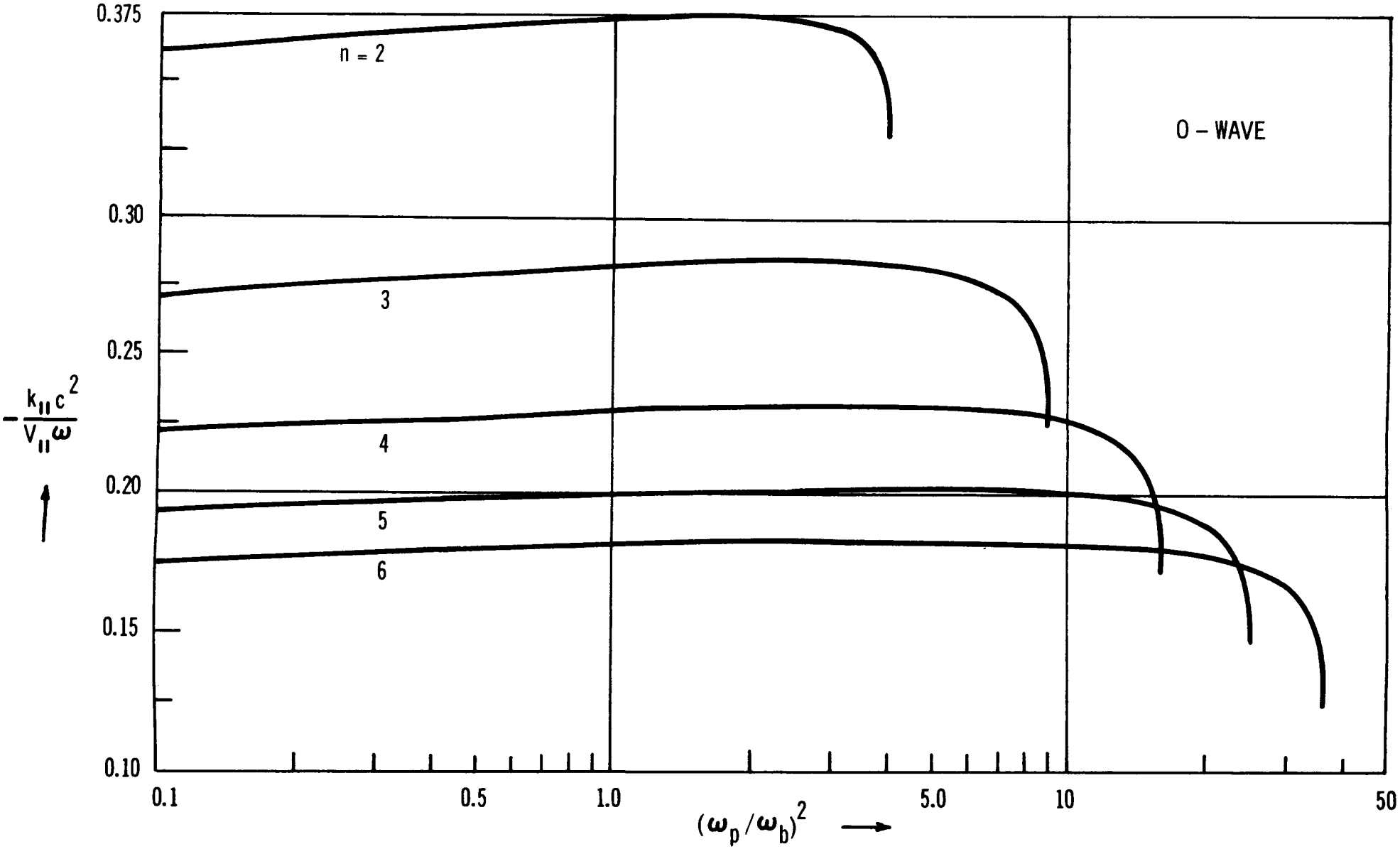
0.375
0.30
0.25
0.20
0.15
0.10
n = 2
3
4
5
6
O – WAVE
$-\frac{k_{\parallel} c^2}{V_{\parallel} \omega}$
0.1
0.5
1.0
5.0
10
50
$(\omega_p / \omega_b)^2$

FIGURE 13

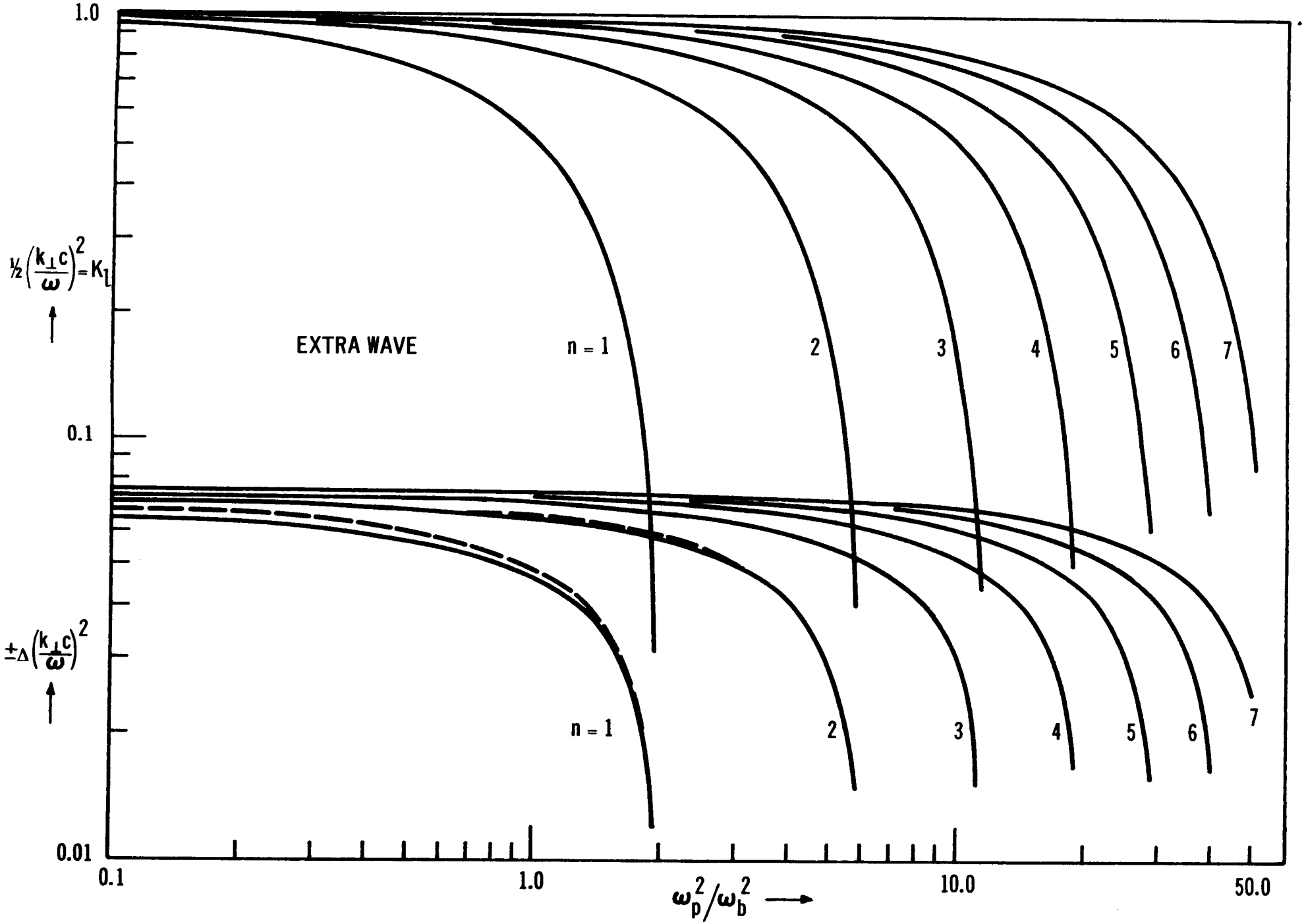
1.0
$\frac{1}{2}\left(\frac{k_\perp c}{\omega}\right)^2 = K_\parallel$
EXTRA WAVE
n = 1
2
3
4
5
6
7
0.1
$\pm\Delta\left(\frac{k_\perp c}{\omega}\right)^2$
n = 1
2
3
4
5
6
7
0.01
0.1
1.0
10.0
50.0
ω_p^2/ω_b^2 ⟶

FIGURE 14

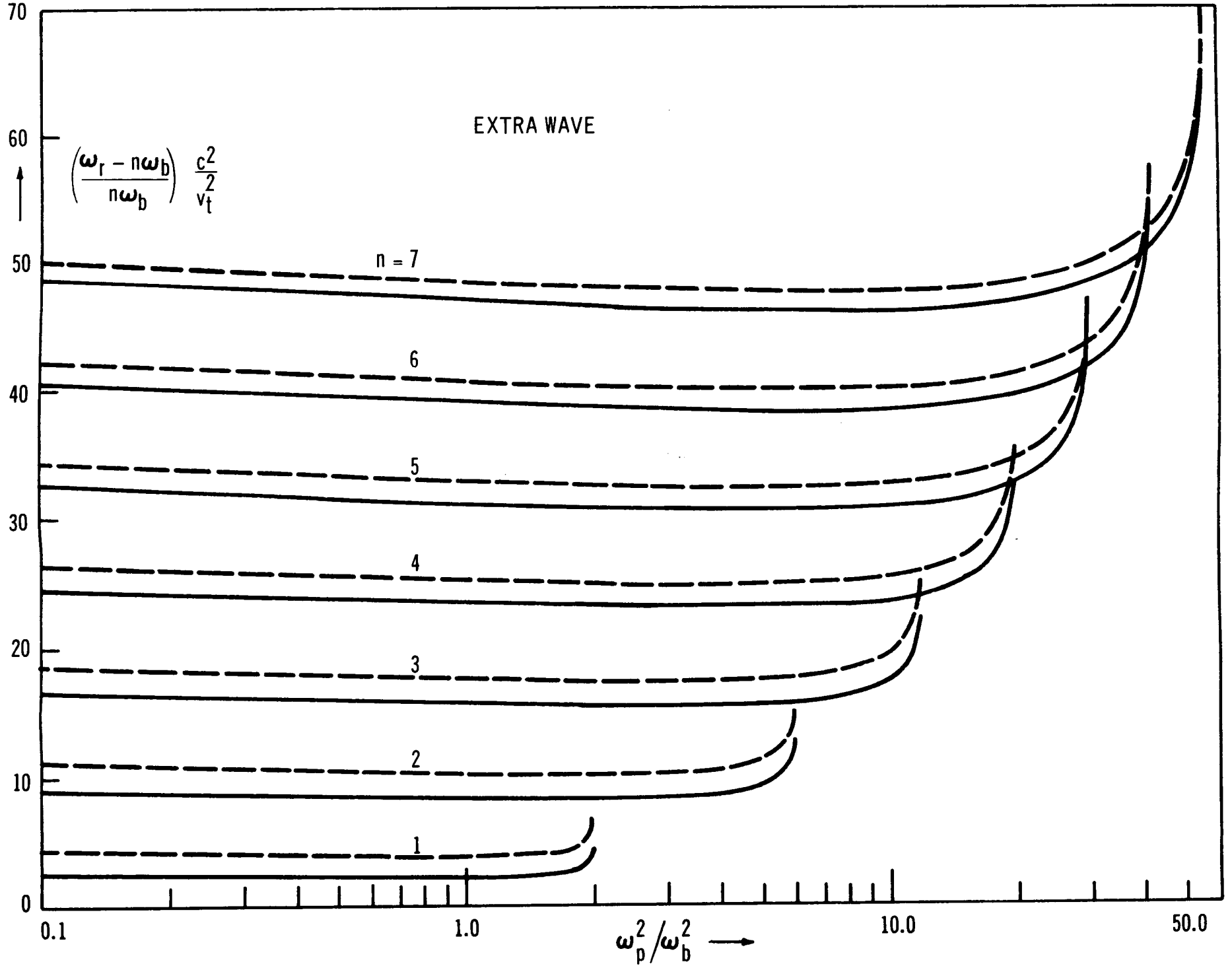
EXTRA WAVE
$\left(\frac{\omega_r - n\omega_b}{n\omega_b}\right) \frac{c^2}{v_t^2}$
n = 7
6
5
4
3
2
1
70
60
50
40
30
20
10
0
0.1
1.0
10.0
50.0
ω_p^2/ω_b^2

FIGURE 15

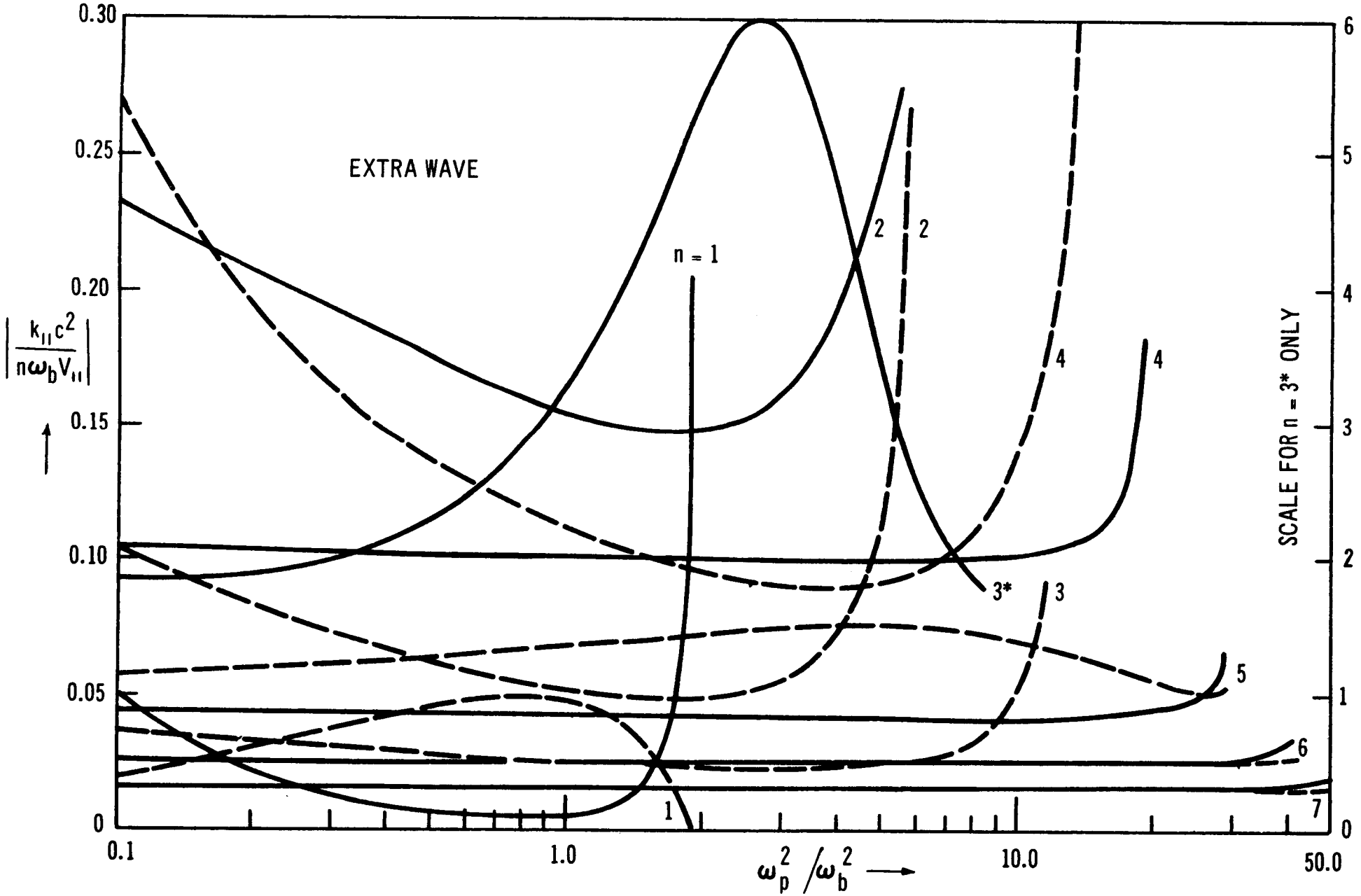
0.30
0.25
0.20
0.15
0.10
0.05
0
$\left|\frac{k_{\parallel}c^2}{n\omega_b V_{\parallel}}\right|$
EXTRA WAVE
n = 1
2
2
4
4
3*
3
5
6
1
7
SCALE FOR n = 3* ONLY
6
5
4
3
2
1
0
0.1
1.0
10.0
50.0
ω_p^2/ω_b^2 ⟶

FIGURE 16

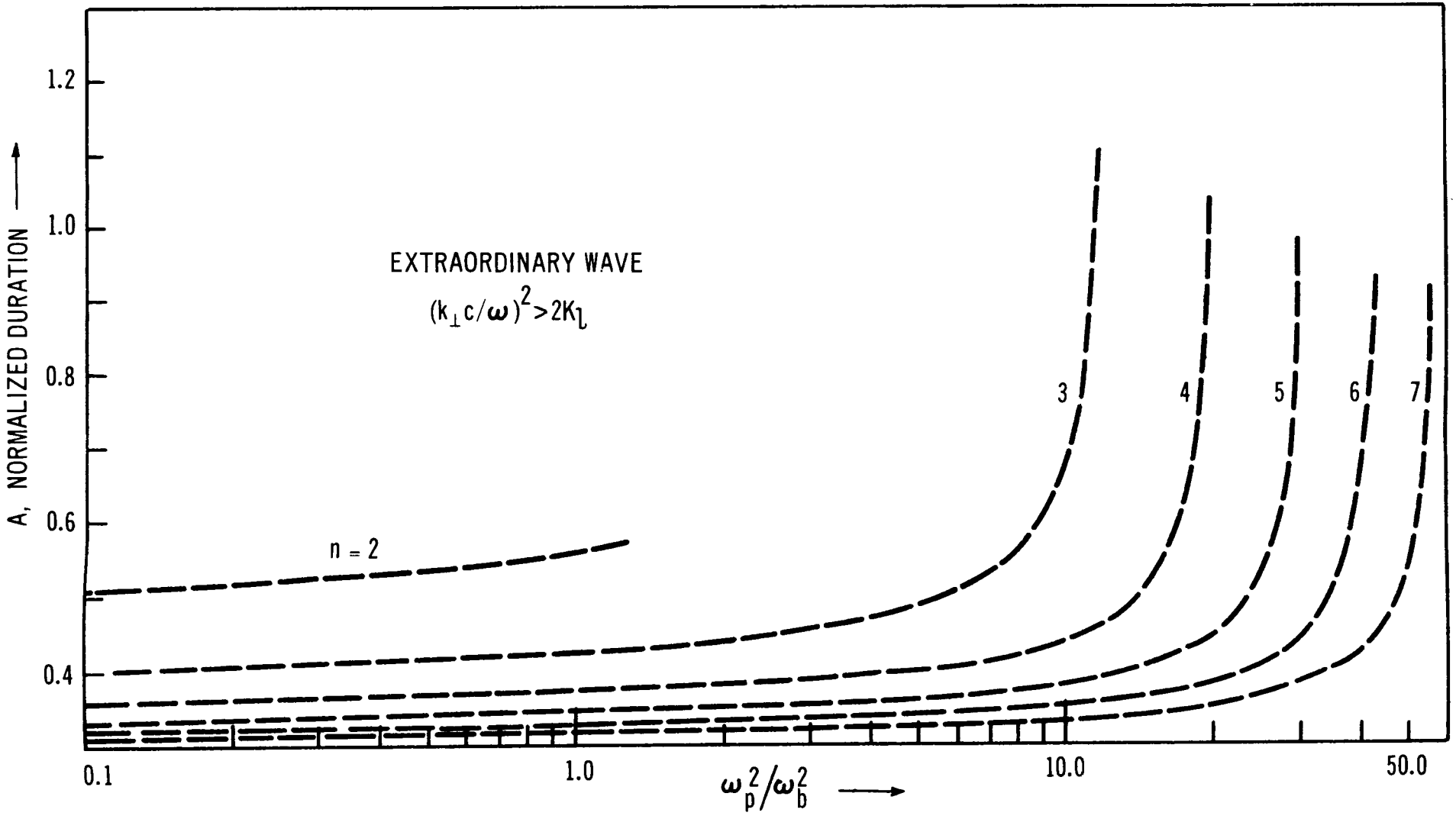
A, NORMALIZED DURATION
1.2
1.0
0.8
0.6
0.4
EXTRAORDINARY WAVE
$(k_\perp c/\omega)^2 > 2K_l$
n = 2
3
4
5
6
7
0.1
1.0
10.0
50.0
ω_p^2/ω_b^2

FIGURE 17

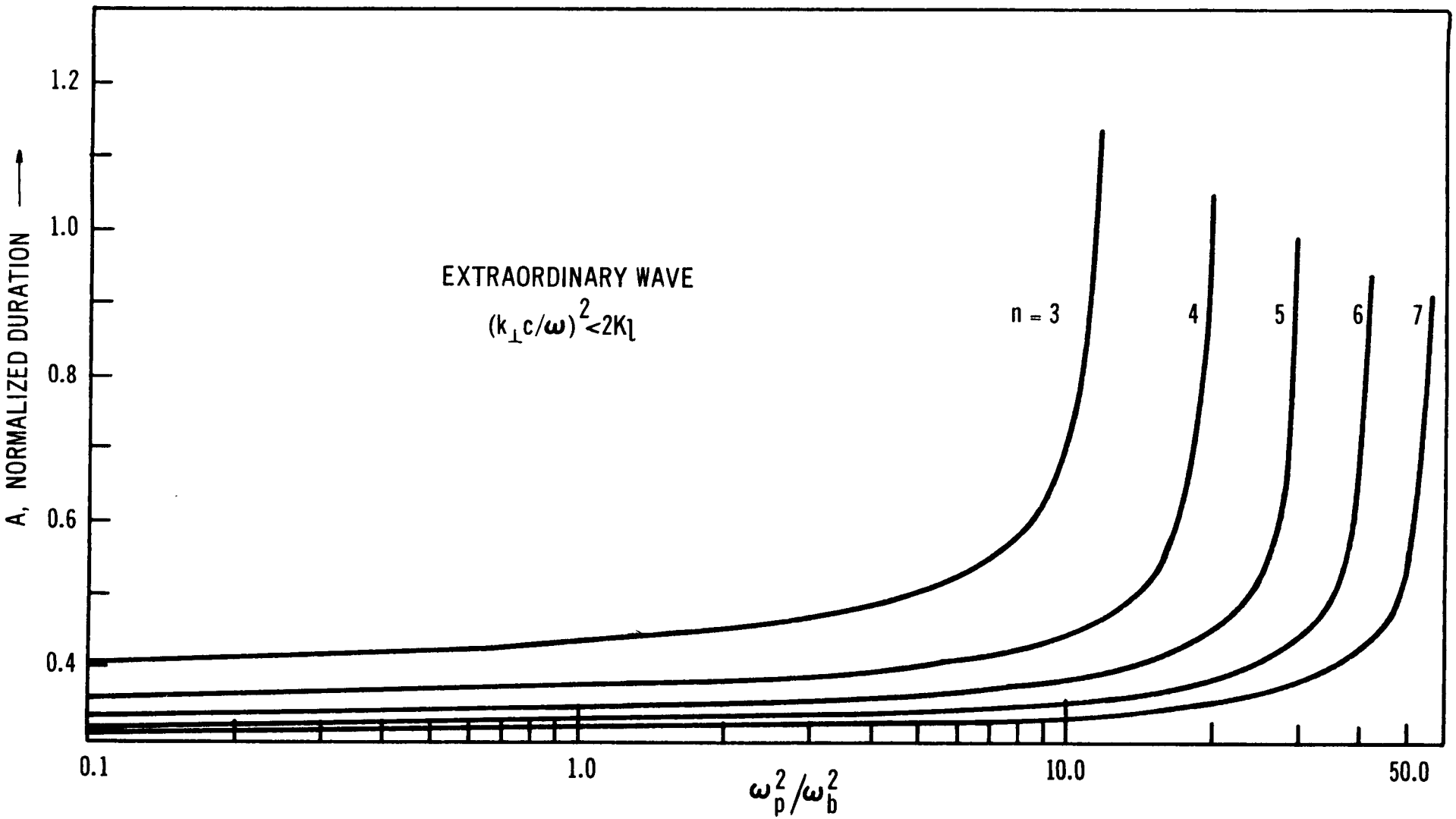
A, NORMALIZED DURATION
1.2
1.0
0.8
0.6
0.4
EXTRAORDINARY WAVE
$(k_\perp c/\omega)^2 < 2K_l$
n = 3
4
5
6
7
0.1
1.0
10.0
50.0
ω_p^2/ω_b^2

FIGURE 18

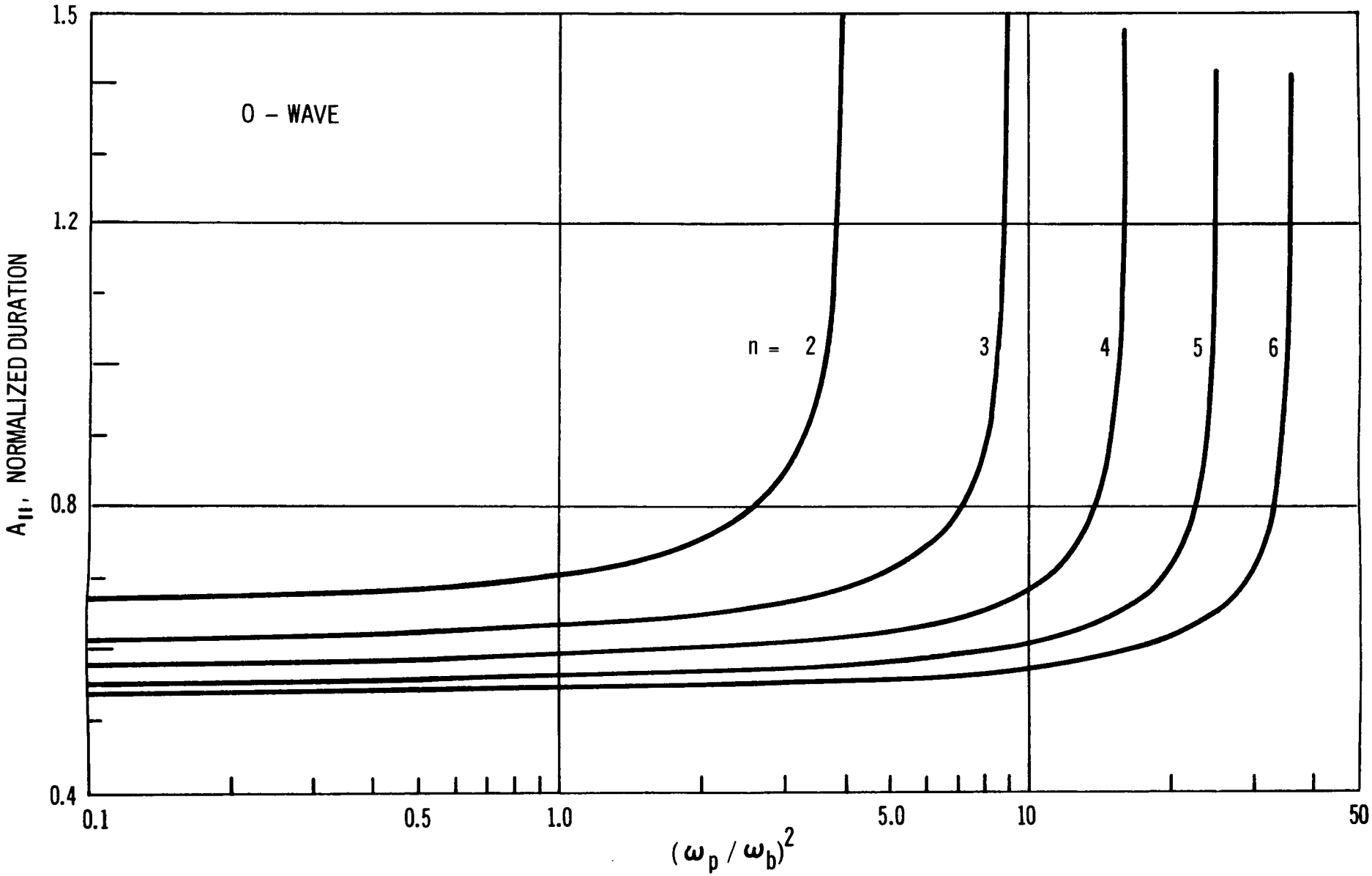
1.5
1.2
0.8
0.4
O – WAVE
n = 2
3
4
5
6
A_{II}, NORMALIZED DURATION
0.1
0.5
1.0
5.0
10
50
$(\omega_p / \omega_b)^2$

FIGURE 19

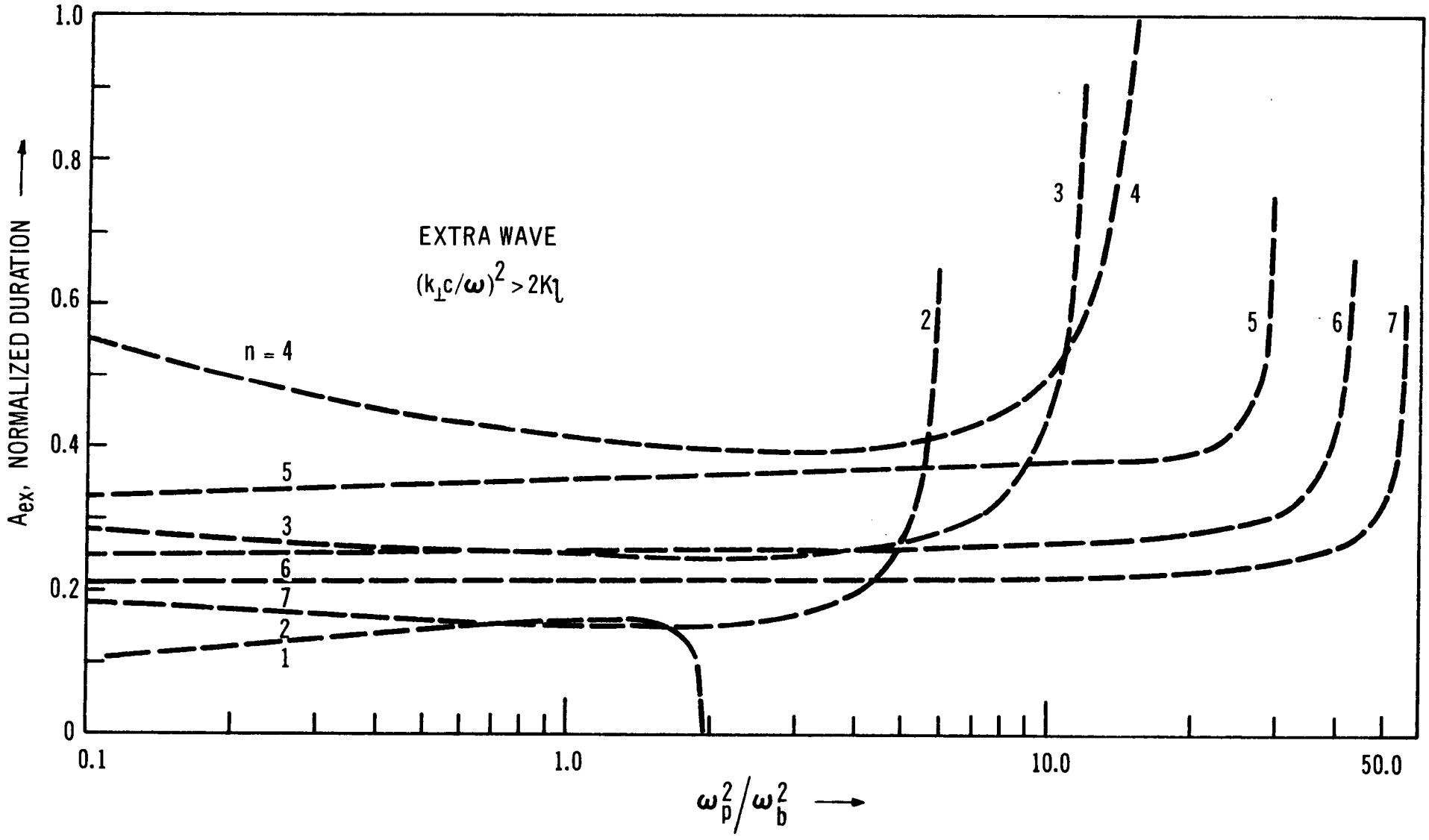
1.0
0.8
0.6
0.4
0.2
0
A_{ex}, NORMALIZED DURATION
EXTRA WAVE
$(k_\perp c/\omega)^2 > 2K\ell$
n = 4
1
2
3
4
5
6
7
0.1
1.0
10.0
50.0
ω_p^2/ω_b^2

FIGURE 20

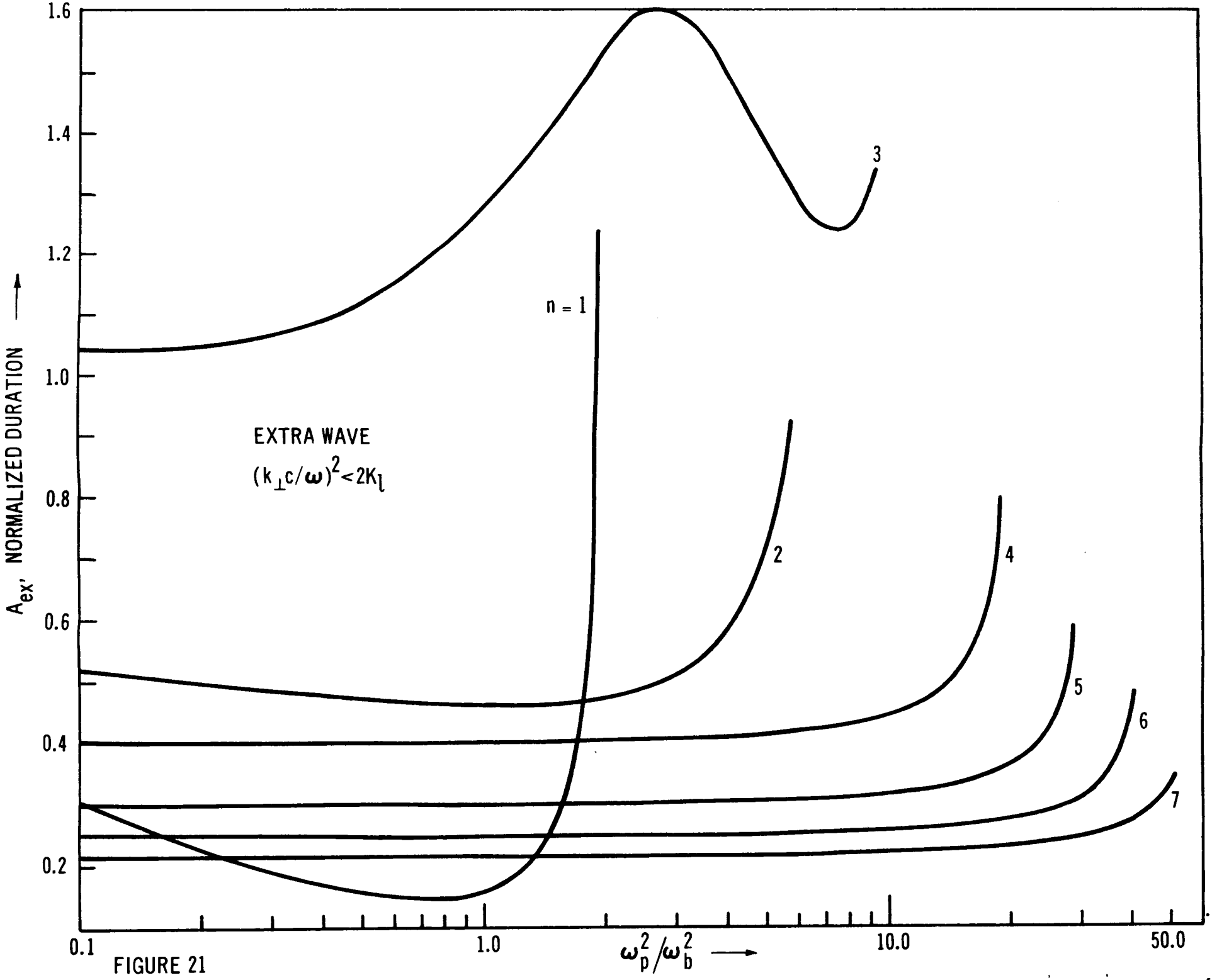
1.6
1.4
1.2
1.0
0.8
0.6
0.4
0.2
A_{ex}, NORMALIZED DURATION
EXTRA WAVE
$(k_\perp c/\omega)^2 < 2K_l$
n = 1
2
3
4
5
6
7
0.1
1.0
10.0
50.0
ω_p^2/ω_b^2

FIGURE 21

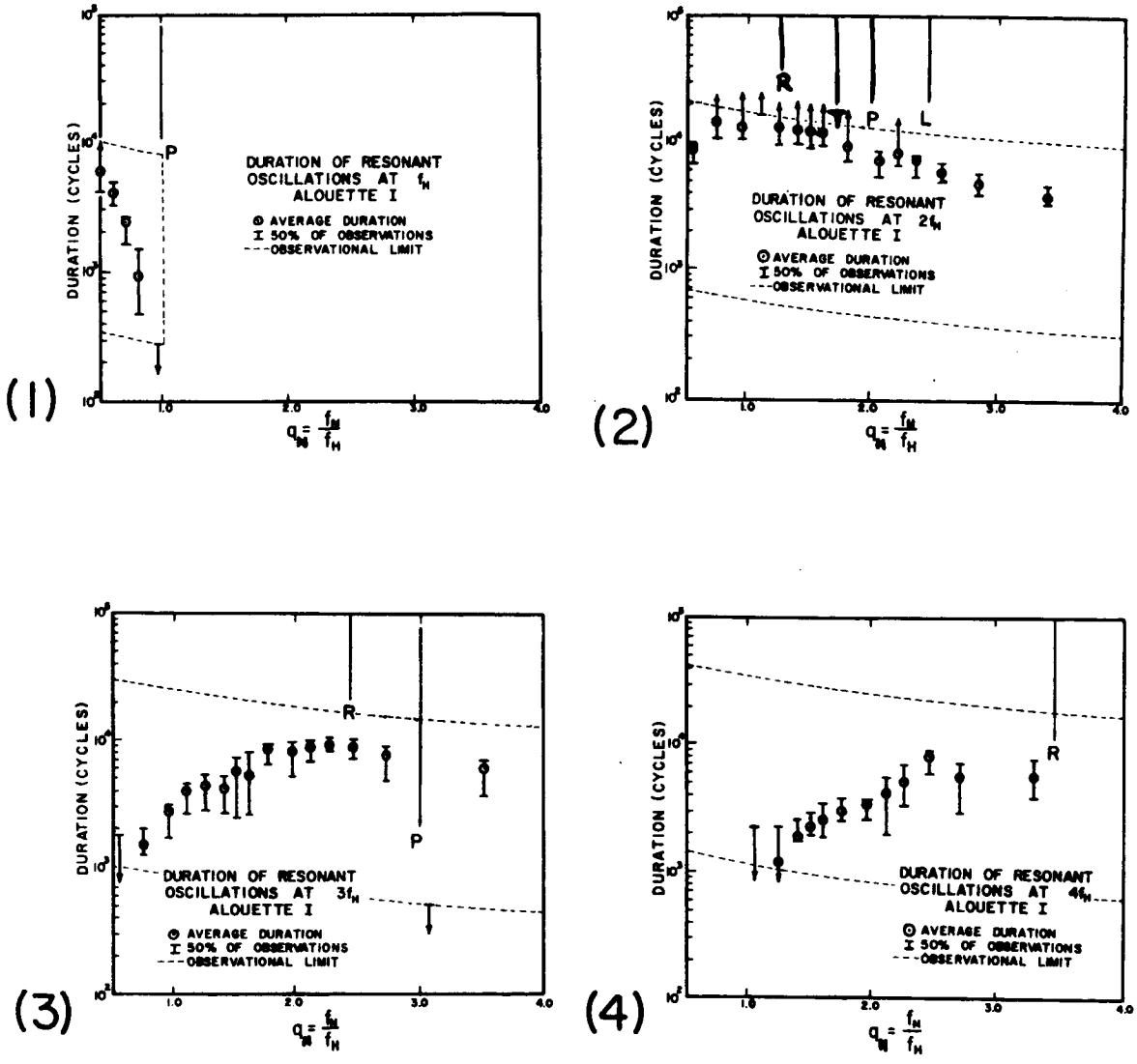
(1)
DURATION (CYCLES)
DURATION OF RESONANT OSCILLATIONS AT f_H ALOUETTE I
⊙ AVERAGE DURATION
I 50% OF OBSERVATIONS
---OBSERVATIONAL LIMIT
P
$q = \frac{f_M}{f_H}$
(2)
DURATION (CYCLES)
DURATION OF RESONANT OSCILLATIONS AT $2f_H$ ALOUETTE I
⊙ AVERAGE DURATION
I 50% OF OBSERVATIONS
---OBSERVATIONAL LIMIT
R
P
L
$q = \frac{f_M}{f_H}$
(3)
DURATION (CYCLES)
DURATION OF RESONANT OSCILLATIONS AT $3f_H$ ALOUETTE I
⊙ AVERAGE DURATION
I 50% OF OBSERVATIONS
---OBSERVATIONAL LIMIT
R
P
$q = \frac{f_M}{f_H}$
(4)
DURATION (CYCLES)
DURATION OF RESONANT OSCILLATIONS AT $4f_H$ ALOUETTE I
⊙ AVERAGE DURATION
I 50% OF OBSERVATIONS
---OBSERVATIONAL LIMIT
R
$q = \frac{f_M}{f_H}$

FIGURE 22

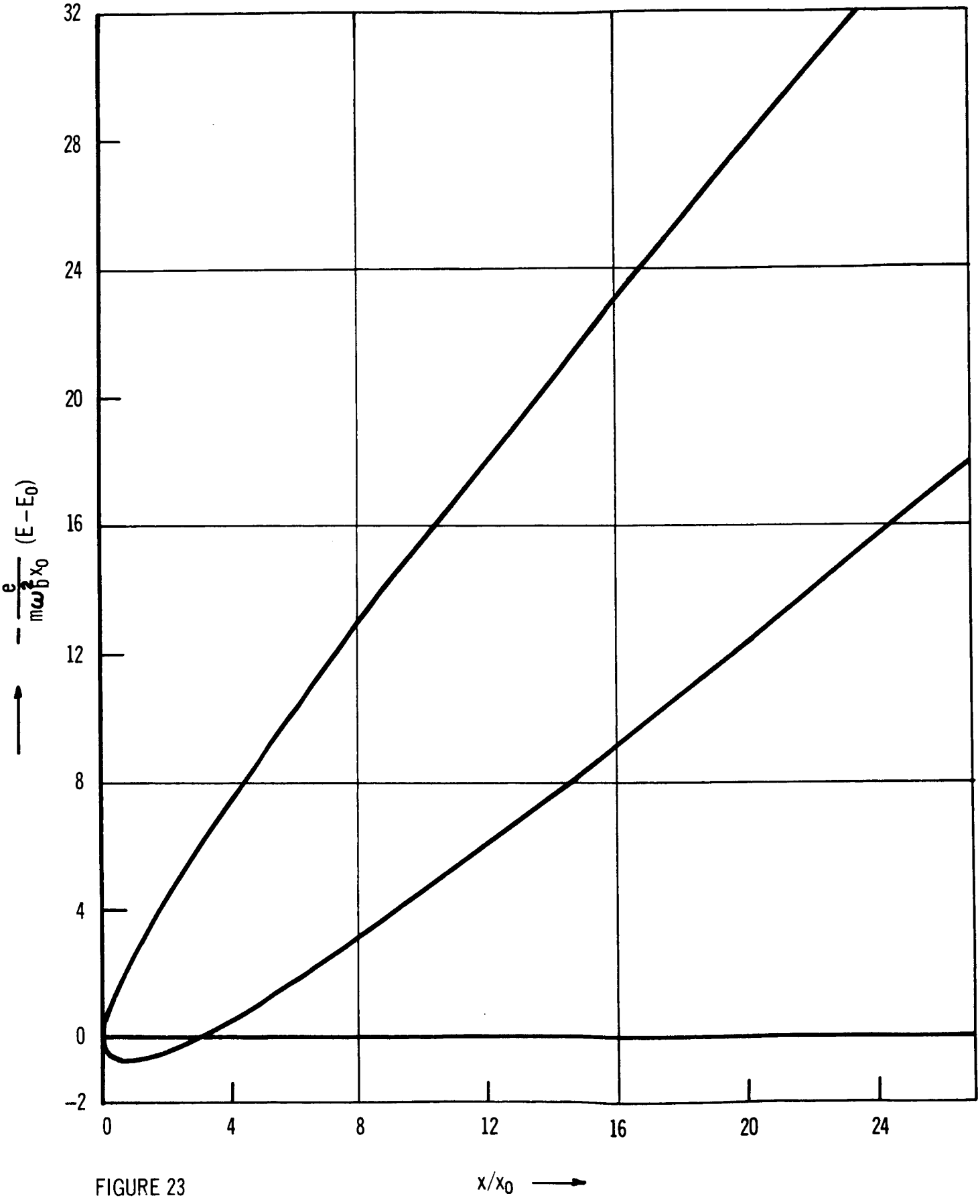

FIGURE 23

APPENDIX I

DIELECTRIC TENSOR IN VLASOV PLASMAS NEAR CYCLOTRON HARMONICS

I.P. Shkarofsky

RCA Victor Company, Ltd.
Research Laboratories
Montreal, Canada

- ABSTRACT -

The relativistic expression for the dielectric tensor obtained by Trubnikov is simplified in the very weakly relativistic limit at and near electron cyclotron harmonics. Wave numbers parallel to magnetic field are included, leading to relativistic damping when this wave number is minute and to cyclotron damping when it is sufficiently large. The transition to the nonrelativistic Z-function is shown and the regions of validity of the various functions are indicated. Collisional damping is neglected. The dielectric elements given here are also applicable to cases of complex ω and real k. An example of such a situation arises in Alouette cyclotron harmonic reception when one is concerned with an initial time value problem. For this application, we provide the analytic continuation of a complicated function and investigate the tracks where it is real for complex ω.

I. INTRODUCTION

In this paper, we discuss and simplify the dielectric tensor of a plasma near electron cyclotron harmonics. A relativistic approach has to be used since the difference $\omega - n\omega_b$ (between angular frequency and cyclotron harmonic frequency) is of order $\omega v_t^2/c^2$ in many wave number regions of interest. We restrict ourselves to small transverse wave numbers i.e. we take $\lambda \equiv k_\perp^2 v_t^2/\omega_b^2$ less than one. At first we consider general values for $k_\parallel$ (wave number parallel to magnetic field) but later we consider only the region $k_\parallel c^2/v_t\omega < 1$.

A relativistic expression for the dielectric tensor $\underset{\sim}{\varepsilon}$ of a plasma was obtained by Trubnikov[1] which will not be rederived here. This expression is exceedingly complicated and simplification is necessary for further analysis of dispersion equations. For $k_\parallel = 0$, Dnestrovskii et al[2] have obtained such a simplification. Original contributions in this report are the inclusion of $k_\parallel$ in the analysis and the derivation of the dielectric tensor elements for complex ω and real k rather than vice versa. The latter extension requires the analytic continuation of a complicated function.

Application[3] of the analysis is aimed towards explanation of cyclotron harmonic resonances in the local ionosphere observed by the Alouette 1 satellite. The Alouette emits a pulse of energy and observes long lasting time returns exactly at the cyclotron resonances. Since we are dealing with a time decaying signal or an initial value problem, we have to consider complex ω rather than real ω. The uniformity in space is sufficient that we can consider very small values for $k_\parallel$. In the laboratory, this would require unrealistically large

---

1. B.A. Trubnikov - Collection - Plasma Physics and the Problem of Controlled Thermonuclear Reactions, Editor, M.A. Leontovich, Pergamon Press, N.Y. (1959), Vol. III, p.122. See also the derivation in W.E. Drummond & M.N. Rosenbluth Phys. Fluids 6, 276 (1961), eqs. (19-21).
2. Yu.N. Dnestrovskii, D.P. Kostomarov, & N.V. Skrydlov, Sov.Phys.- Tech.Phys. 8, 691 (1964).
3. I.P. Shkarofsky and T.W. Johnston, Phys.Rev. Letters 15, 51 (1965).

plasma containers so that the very long wavelength disturbances considered here may be difficult to simulate in the laboratory. This in in contrast to the cyclotron resonances actually observed in the laboratory[4], which are associated with shorter wavelengths and are somewhat shifted from the exact cyclotron harmonic values.

In the analysis, we neglect collisional damping since it is negligible for the times of interest during which harmonics effects are measured on the Alouette.

II. DIELECTRIC CONSTANT FOR GENERAL VALUES OF $k_{\parallel}$

Trubnikov's equation[1] for the elements $\varepsilon_{\alpha\beta}$ of the tensor $\underset{\sim}{\varepsilon}$ for a (relativistic) Maxwellian velocity distribution function is

$$\varepsilon_{\alpha\beta} - \delta_{\alpha\beta} = \frac{i\omega_p^2}{\omega\omega_b} \frac{c^4}{v_t^4 K_2\left(\frac{c^2}{v_t^2}\right)} \int_0^\infty d\xi \left\{ \frac{K_2(\sqrt{R})}{R} T_{\alpha\beta}^{(1)} - \frac{K_3(\sqrt{R})}{R^{3/2}} T_{\alpha\beta}^{(2)} \right\} \qquad (1)$$

where

$$T_{\alpha\beta}^{(1)} = \begin{pmatrix} \cos\xi & -\sin\xi & 0 \\ \sin\xi & \cos\xi & 0 \\ 0 & 0 & 1 \end{pmatrix}$$

$$T_{\alpha\beta}^{(2)} = \frac{c^2}{\omega_b^2} \begin{pmatrix} k_\perp^2 \sin^2\xi & -k_\perp^2 \sin\xi(1-\cos\xi) & k_\perp k_\parallel \xi \sin\xi \\ k_\perp^2 \sin\xi(1-\cos\xi) & -k_\perp^2 (1-\cos\xi)^2 & k_\perp k_\parallel \xi(1-\cos\xi) \\ k_\perp k_\parallel \xi \sin\xi & -k_\perp k_\parallel \xi(1-\cos\xi) & k_\parallel^2 \xi^2 \end{pmatrix}$$

K_ν is a MacDonald function of order ν.

$$R = \left(\frac{c^2}{v_t^2} - i\xi\frac{\omega}{\omega_b}\right)^2 + 2\left(\frac{k_\perp c}{\omega_b}\right)^2 \left(1-\cos\xi\right) + \frac{k_\parallel^2 c^2 \xi^2}{\omega_b^2}$$

---

4. F.W. Crawford, G.S. Kino, H.H. Weiss, Phys.Rev.Letters 13, 229 (1964).

$\omega_p = \sqrt{n_e e^2/\varepsilon_0 m}$ is the plasma frequency, $\omega_b = eB/m$ is the angular cyclotron frequency, $v_t = \sqrt{\kappa T/m}$ is the thermal velocity and i, n_e, e, ε_0, m, B, c, κ, T and ω have their usual significance. The wave numbers perpendicular and parallel to the magnetic field are denoted as $k_\perp$ and $k_\parallel$ and taken along the x and z directions respectively. In the following, we denote by $\mu = c^2/v_t^2$, the square of the ratio of light to thermal velocity and let this be very large.

In the very weakly relativistic case ($\mu >> 1$), the asymptotic expression, $K_\nu(x) = e^{-x}\sqrt{\pi/2x}$ for large argument, applies.

We also simplify the expression for R by assuming $(k_\perp v_t/\omega_b)^2 < 1$, so that

$$\sqrt{R} = \mu\left[\left(1 - \frac{i\xi\omega}{\mu\omega_b}\right)^2 + \frac{k_\parallel^2 v_t^2}{\mu\omega_b^2}\xi^2\right]^{\frac{1}{2}} + \Lambda(1 - \cos\xi)$$

where

$$\Lambda \equiv \frac{k_\perp^2 v_t^2}{\omega_b^2}\left[\left(1 - \frac{i\xi\omega}{\mu\omega_b}\right)^2 + \frac{k_\parallel^2 v_t^2 \xi^2}{\mu\omega_b^2}\right]^{-\frac{1}{2}}$$

The above expression for $\sqrt{R}$ has to be used in the exponent. However, in the $T_{\alpha\beta}$ matrices and in the R factors, we can omit the $\Lambda(1 - \cos\xi)$ part of $\sqrt{R}$. Thus we see that $k_\perp^2 c^2/\omega_b^2\sqrt{R} \approx \Lambda$. At this stage we can introduce the familiar modified Bessel function (I_n) expansion, $\exp(\Lambda\cos\xi) = \sum_{-\infty}^{\infty} I_n(\Lambda)\exp(-in\xi)$. Using this expansion, we can express all the sin ξ and cos ξ combinations in series form. For example, denoting $I_n' = dI_n/d\Lambda$ we note that $\cos\xi\exp(\Lambda\cos\xi) = \sum I_n' e^{-in\xi}$. Further observation shows that $\xi^2 k_\parallel^2 c^2/\omega_b\sqrt{R} \approx k_\parallel \partial e^{-\sqrt{R}}/\partial k_\parallel$ and changing variables to $t = \xi\omega/\mu\omega_b$, we find that

$t = i\partial \exp(-in\mu \frac{\omega_b}{\omega} t)/\partial(n\mu \frac{\omega_b}{\omega})$. Hence the form for $\varepsilon_{\alpha\beta}$ becomes

$$\varepsilon_{\alpha\beta} - \delta_{\alpha\beta} = i \frac{\omega_p^2}{\omega^2}\mu \sum_{n=-\infty}^{\infty} \int_0^{\infty} \frac{dt e^{-\Lambda} T_{\alpha\beta}^{(3)} \exp\left\{\mu - \mu\left[(1-it)^2 + \frac{k_\parallel^2 c^2 t^2}{\omega^2}\right]^{\frac{1}{2}} - in\mu \frac{\omega_b}{\omega} t\right\}}{\left[(1-it)^2 + \frac{k_\parallel^2 c^2 t^2}{\omega^2}\right]^{7/4}} \tag{2}$$

with

$$T_{\alpha\beta}^{(3)} = \left[(1-it)^2 + \frac{k_\parallel^2 c^2 t^2}{\omega^2}\right]^{\frac{1}{2}} \begin{pmatrix} \frac{n^2 I_n}{\Lambda} & -in(I_n' - I_n) & 0 \\ in(I_n' - I_n) & \frac{n^2 I_n}{\Lambda} + 2\Lambda(I_n - I_n') & 0 \\ 0 & 0 & I_n\left(1 + k_\parallel \frac{\partial}{\partial k_\parallel}\right) \end{pmatrix}$$

$$+ \frac{k_\perp k_\parallel c^2}{\omega \omega_b} \begin{pmatrix} 0 & 0 & \frac{nI_n}{\Lambda} \\ 0 & 0 & i\left(I_n' - I_n\right) \\ \frac{nI_n}{\Lambda} & -i\left(I_n' - I_n\right) & 0 \end{pmatrix} \frac{\partial}{\partial\left(n\mu \frac{\omega_b}{\omega}\right)}$$

and

$$\Lambda = \lambda\left[(1-it)^2 + \frac{k_\parallel^2 c^2 t^2}{\omega^2}\right]^{-\frac{1}{2}}, \quad \lambda \equiv \frac{k_\perp^2 v_t^2}{\omega_b^2}$$

Let us now restrict ourselves to $\Lambda << 1$ rather than $\Lambda \sim 1$, so that $I_n \approx \Lambda^n / 2^n n!$

It is also proper to change the sum over n to start from 0. Note that $I_{-n} = I_n$. Define furthermore a function $\mathcal{J}_q$ dependent on two dimensionless parameters $\mu\omega_b n/\omega$ and $k_\parallel c/\omega$ besides q.

$$\mathcal{J}_q\left(\frac{\mu n\omega_b}{\omega}, \frac{k_\parallel c}{\omega}\right) \equiv -i\int_0^\infty \frac{dt \exp\left\{\mu - \mu\left[(1-it)^2 + \frac{k_\parallel^2 t^2 c^2}{\omega^2}\right]^{\frac{1}{2}} - in\mu\frac{\omega_b}{\omega}t\right\}}{\left[(1-it)^2 + \frac{k_\parallel^2 c^2 t^2}{\omega^2}\right]^{q/2}} \qquad (3)$$

As a result writing $\mathcal{J}_q\binom{a}{b} = \mathcal{J}_q\left(\mu\frac{n\omega_b}{\omega}, \frac{k_\parallel c}{\omega}\right) \pm \mathcal{J}_q\left(-\mu\frac{n\omega_b}{\omega}, \frac{k_\parallel c}{\omega}\right)$ we have for $\Lambda \ll 1$:

$$\left.\begin{array}{l}\varepsilon_{11} - 1 = \varepsilon_{22} - 1 \text{ (combination a)} \\ i\varepsilon_{12} = -i\varepsilon_{21} \text{ (combination b)}\end{array}\right\} = -\frac{\omega_p^2}{\omega^2}\mu \sum_0^\infty \frac{n^2\lambda^{n-1}}{2^n n!} \mathcal{J}^{\binom{a}{b}}_{n+3/2} \qquad (4a)$$

$$\varepsilon_{33} - 1 = -\frac{\omega_p^2}{\omega}\mu\left\{\frac{\partial}{\partial k_\parallel}\left[k_\parallel \mathcal{J}_{5/2}(0, \frac{k_\parallel c}{\omega})\right] + \sum_1^\infty \frac{\lambda^n}{2^n n!}\frac{\partial}{\partial k_\parallel}\left(k_\parallel \mathcal{J}^{(a)}_{n+5/2}\right)\right\} \qquad (4b)$$

$$\left.\begin{array}{l}\varepsilon_{13} = \varepsilon_{31} \text{ (combination a)} \\ -i\varepsilon_{23} = i\varepsilon_{32} \text{ (combination b)}\end{array}\right\} = -\frac{\omega_p^2}{\omega^2}\mu\frac{k_\perp k_\parallel c^2}{\omega\omega_b}\sum_0^\infty \frac{n\lambda^{n-1}}{2^n n!}\frac{\partial}{\partial(n\mu\omega_b/\omega)} \mathcal{J}^{\binom{a}{b}}_{n+5/2} \qquad (4c)$$

III. APPROXIMATIONS FOR THE $\mathcal{J}$ - FUNCTION

(a) The case of $k_\parallel = 0$ and the F-function

Exactly perpendicular to the magnetic field, the $\mathcal{J}_q$ function reduces to the F_q function:

$$F_q(\mu\delta) \equiv -i\int_0^\infty \frac{dt}{(1-it)^q} e^{i\mu\delta t}, \quad \delta \equiv \frac{\omega - n\omega_b}{\omega} \qquad (5)$$

first given by Dnestrovskii et al[2,5] who also plot the real and imaginary parts of the function for real ω and $n = 1,2,3$ (see their Figs. 1,2).

Starting from Eq.(5) with q a half integer and assuming $\mathrm{Im}(z) > 0$ for complex $z \equiv \mu\delta$, we can integrate by parts a sufficient number of times until the power q is reduced to $\frac{1}{2}$. We obtain

$$F_q(z) = \sum_{p=0}^{q-3/2} (-z)^p \frac{\Gamma(q-1-p)}{\Gamma(q)} + \frac{i(-1)^{q-3/2}}{\Gamma(q)} \sqrt{\pi}\, z^{q-\frac{1}{2}} \int_0^\infty \frac{e^{izt}\,dt}{(1-it)^{\frac{1}{2}}} \qquad (6)$$

This reduces to the following expression for real ω and $\omega \leq n\omega_b$, given[5] by Dnestrovskii et al.

$$F_q(\mu\delta < 0) = \sum_{p=0}^{q-3/2} |\mu\delta|^p \frac{\Gamma(q-1-p)}{\Gamma(q)} - \frac{|\mu\delta|^{q-\frac{1}{2}}\sqrt{\pi}}{\Gamma(q)} \int_0^1 \frac{e^{-|\mu\delta|\,t}}{(1-it)^{\frac{1}{2}}}\,dt$$

$$- \frac{i\pi}{\Gamma(q)} |\mu\delta|^{q-1}\, e^{-|\mu\delta|} \qquad (7)$$

The imaginary contribution in (7) arises from the region around $it \approx 1$ as shown by Dnestrovskii et al who rotate the contour through 90°. Note also that for real z, F_q has an imaginary contribution only for $z < 0$ since q is a half-integer. Note that

$$\int_0^\infty \frac{e^{izt}\,dt}{(1-it)^{\frac{1}{2}}} = i\sqrt{\frac{\pi}{z}}\, e^z \left[1 - \Phi(\sqrt{z})\right] = \frac{1}{\sqrt{z}}\, Z(i\sqrt{z}).$$

Thus the more general expression in (6) valid for complex ω can also be expressed in terms of the error function Φ or in terms of the Z function[6] which is already tabulated and usually defined by

$$Z(x) \equiv 2ie^{-x^2} \int_{-\infty}^{ix} e^{-y^2}\,dy \qquad (8)$$

---

5. There is an error in Dnestrovskii et al[2]. The sign of the last term is negative as given here and not positive as given in their Eq. VIII and Fig.2.
6. B.D. Fried & S.D. Conte, The Plasma Dispersion Function, Academic Press, N.Y.(1961)

Thus

$$F_q = \sum_{p=0}^{q-3/2} (-z)^p \frac{\Gamma(q-1-p)}{\Gamma(q)} + \frac{\sqrt{\pi}}{\Gamma(q)} (-z)^{q-3/2} \left[i\sqrt{z}\, Z(i\sqrt{z}) \right] \tag{9}$$

To be of greater use, the $F_q(z)$ function defined above only for $\mathrm{Im}z > 0$ has to be analytically continued for $\mathrm{Im}z < 0$. Fortunately, we have succeeded in expressing F in terms of Z, a function whose analytic continuation has been considerably investigated (see Fried and Conte[6]). Thus we can allow Eq.(9) to be valid everywhere in the complex z plane using the proper continuation for Z.

The following expansions of $Z(\zeta)$ are valid throughout the complex ζ plane[6].

$$Z(\zeta) = i\sqrt{\pi}\, e^{-\zeta^2} - \zeta \sum_{l=0}^{\infty} (-\zeta^2)^l \sqrt{\pi}/\Gamma(l+3/2) \tag{10}$$

$$\text{For } |\zeta| >> 1, \quad Z(\zeta) \simeq i\sqrt{\pi}\sigma\, e^{-\zeta^2} - \sum_{l=0}^{\infty} \zeta^{-(2l+1)}\, \Gamma(l+\tfrac{1}{2})/\sqrt{\pi} \tag{11}$$

where $\sigma = 0,1,2$ for $\mathrm{Im}\,\zeta > 0$, $\mathrm{Im}\,\zeta = 0$, $\mathrm{Im}\,\zeta < 0$ respectively.

Let us now substitute Eq.(10) into (9). We obtain, using the formula $\Gamma(\frac{1}{2}+n)\Gamma(\frac{1}{2}-n) = \pi/\cos\pi n$:

$$\Gamma(n+3/2)F_{n+3/2}(z) = \sum_{p=0}^{\infty} (-z)^p\, \Gamma(n-p+\tfrac{1}{2}) - \pi(-z)^n \sqrt{z}\, e^z \tag{12}$$

For large arguments, $|z| >> 1$, it is convenient to substitute Eq.(11) into (9). Using again $q = n+3/2$, we find

$$\Gamma(n+3/2)F_{n+3/2}(z) = -\pi\sigma(-z)^n \sqrt{z}\, e^z - \sum_{p=0}^{\infty} \frac{\Gamma(p+n+3/2)}{(-z)^{p+1}} \tag{13}$$

where $\sigma = 0,1,2$ for Im $i\sqrt{z}$ greater, equal or less than zero respectively.

(b) The case of small $k_{\parallel}$

We investigate first order $k_{\parallel}$ values satisfying

$$|y^2| \ll \mu^{-1} \quad \text{and} \quad |\mu y(2\delta - y^2)| \ll 1 \tag{14}$$

where $y \equiv k_{\parallel}c/\omega$. Subject to these conditions, Eq.(3) reduces to

$$\mathcal{J}_q(\mu\delta) = -i \int_0^\infty \frac{dt}{(1-it)^q} \exp\left[i\mu\delta t - \frac{\mu y^2}{2} \frac{t^2}{(1-it)}\right] \tag{15}$$

We can further expand to first order the t^2 exponential part, and using $-t^2 = (1-it)^2 - 2(1-it) + 1$, we relate $\mathcal{J}_q$ to the F_q function in Eq.(5).

$$\mathcal{J}_q(\mu n\omega_b/\omega, y) = F_q + (y^2\mu/2)(F_{q-1} - 2F_q + F_{q+1}) \tag{16}$$

The same relation holds for $\mathcal{J}_q(-\mu n\omega_b/\omega, y)$ if we substitute $\mu(\omega + n\omega_b)/\omega$ for the argument of F_q. We note that Eqs.(4) now apply with the following substitutions.

$$\frac{\partial}{\partial k_{\parallel}}\left(k_{\parallel}\mathcal{J}_q^{(a)}\right) = F_q^{(a)} + \frac{3y^2\mu}{2}\left(F_{q-1}^{(a)} - 2F_q^{(a)} + F_{q+1}^{(a)}\right) \quad \text{and} \quad \frac{\partial \mathcal{J}_q^{(a)}}{\partial(n\mu\omega_b/\omega)} = F_{q-1}^{(a)} - F_q^{(a)} \tag{17a,b}$$

where

$$F_q^{(a)} = F_q\left[\mu(\omega - n\omega_b)/\omega\right] \pm F_q\left[\mu(\omega + n\omega_b)/\omega\right] \tag{17c}$$

For larger $k_{\parallel}$ values limited by $|y^2| < |\delta|$, we can still use Eq.(15), but expanded to higher order. We write

$-\mu t^2y^2/2(1-it) = -it\mu y^2/2 + \mu y^2/2(1-it) - \mu y^2/2$ and expand in a power series the resulting $\exp(\mu y^2/2(1-it))$ term in Eq.(15) to yield

$$\mathcal{J}_q = e^{-\mu y^2/2} \sum_p \left(\frac{\mu y^2}{2}\right)^p \frac{1}{\Gamma(p+1)} F_{q+p}\left[\frac{\mu}{2}(2\delta - y^2)\right]$$

We now show that the exponential part of F (see Eq.12) can be summed. Denote this part of $\mathcal{J}_q$ by $\mathcal{J}_q^{(1)}$. Then, since $z = \mu(2\delta - y^2)/2$ here, we obtain

$$\mathcal{J}_q^{(1)} = \pi \exp\left[\mu(\delta - y^2)\right] \sum_p \frac{(-1)^{p+q-\frac{1}{2}}}{\Gamma(p+q)\,\Gamma(p+1)} \left(\mu\delta - \frac{\mu y^2}{2}\right)^{p+q-1} \left(\frac{\mu y^2}{2}\right)^p$$

$$= (-1)^{q-\frac{1}{2}} \pi \exp\left[\mu(\delta - y^2)\right] (2\delta/y^2 - 1)^{(q-1)/2} J_{q-1}\left[\mu y(2\delta - y^2)^{\frac{1}{2}}\right] \quad (18a)$$

$$= -i\pi \exp\left[\mu(\delta - y^2)\right] (1 - 2\delta/y^2)^{(q-1)/2} I_{q-1}\left[\mu y(y^2 - 2\delta)^{\frac{1}{2}}\right] \quad (18b)$$

where J and I are Bessel functions. Since q is a half-integer, we note that for real y and δ, $\mathcal{F}_q^{(1)}$ and the total $\mathcal{J}_q$ are real only for $2\delta \geq y^2$. (In particular for $y = 0$ and real ω, we have seen that F_q is complex only for $\delta < 0$.) An indication of the $y^2 = 2\delta$ boundary, equivalent to $k_\parallel{}^2c^2 = \omega^2 - n^2\omega_b{}^2$, has already been given by Rukhadze and Silin[7].

The small argument expansion of (18) yields (16) in conjunction with (12), justifying the second restriction in (14). These approximations and limits are illustrated in Fig. 1. We also indicate in the figure an "intermediate" region where $|2\delta| \gg |y^2|$ and $|\mu y(2\delta - y^2)^{\frac{1}{2}}| \gg 1$ from which

7. A.A. Rukhadze and V.P. Silin, Sov.Phys. - Tech.Phys. 7, 307 (1962), Eq.V.

it follows that $|\mu\delta| >> 1$. Here we can use $\mathcal{J}_q = [2/\mu(2\delta - y^2)] + \sigma\, \mathcal{J}_q^{(1)}$ where $\mathcal{J}_q^{(1)}$ is given by Eq.(18a) and $\sigma = 0,1,2$ depending on whether $\mathrm{Im}\,[i\sqrt{2\delta - y^2}] = \mathrm{Im}[-\sqrt{y^2 - 2\delta}]$ is greater, equal or less than zero.

(c) Large values of $k_\parallel$ where nonrelativistic analysis is applicable

We can obtain the nonrelativistic expression under the conditions (see Fig. 1)

$$|y|^2 >> |2\delta|, \quad |y| >> \mu^{-\frac{1}{2}} \quad \text{and} \quad |y^2(y^2 - 2\delta)| >> \mu^{-2} \tag{19}$$

In this case the main contribution from the integral in (3) arises from $t << 1$, so that $[(1 - it)^2 + y^2 t^2]^{\frac{1}{2}} \approx 1 - it + y^2 t^2/2$. The integral we are left to evaluate is

$$\mathcal{J}_q = -i \int_0^\infty dt \exp\left\{ i\mu t\left(1 - \frac{n\omega_b}{\omega}\right) - \frac{\mu y^2 t^2}{2} \right\} = -ie^{-\zeta^2} \int_{-\infty}^{i\zeta} e^{-x^2} dx \left(\frac{v_t \omega \sqrt{2}}{k_\parallel c^2} \right)$$

$$= -\frac{v_t \omega}{k_\parallel c^2 \sqrt{2}}\, Z(\zeta) \tag{20}$$

where Z is the plasma dispersion function[6] defined in Eq.(8) and

$$\zeta \equiv (\omega - n\omega_b)/v_t k_\parallel \sqrt{2} = \delta\sqrt{\mu}/y\sqrt{2} \tag{21}$$

Substituting these results into (2) we obtain in terms of the Z- function, the well known expressions[6] for $\varepsilon_{\alpha\beta}$, which need not be rewritten here. In particular for large arguments $|\zeta| >> 1$,

$$Z(\zeta) = i\sqrt{\pi}\, \sigma e^{-\zeta^2} - \zeta^{-1} \quad \text{and} \quad \mathcal{J}_q = -i\sqrt{\pi}\, \sigma v_t \omega e^{-\zeta^2}/k_\parallel c^2 \sqrt{2} + (\mu\delta)^{-1} \tag{22}$$

where $\sigma = 0,1,2$ depending on whether $\mathrm{Im}\,\zeta = -\mathrm{Im}\,y$ is greater, equal or less than zero. Note that in using the relativistic analysis for small $k_\parallel$ values, we are not faced with the "problem" of which is smaller $k_\parallel v_t \sqrt{2}$ or

$\omega - n\omega_b$ in the ζ argument of the less exact Z-function. Combining $|\zeta| \gg 1$ together with (19), we see that (22) is valid provided

$$|\mu^2\delta^2| \gg |2\mu\gamma^2| \gg |4\mu\delta| \gg 1 \tag{23}$$

To prove the assertions in (19) on how large $k_\parallel$ has to be before nonrelativistic analysis becomes applicable, we will show the transition from (18b) to (20) for the exponential part of $\mathcal{J}_q$. We use the original definition in (3) and make the transformation

$$it = \frac{1}{1-\gamma^2}\left[1 - \frac{\gamma(1-\delta)}{(\gamma^2+\delta^2-2\delta)^{\frac{1}{2}}}\right] + i\varepsilon$$

The motivation for the above transformation is that first order ε terms cancel in the expansion of the exponential factor in $\mathcal{J}_q$ and only terms of order ε^2 or higher survive. We find

$$\mathcal{J}_q^{(1)} = -i\,\frac{(\gamma^2+\delta^2-2\delta)^{q/2}}{\gamma^q}\,\exp\left[\frac{\mu(\delta-\gamma^2)+\mu\gamma(\gamma^2+\delta^2-2\delta)^{\frac{1}{2}}}{1-\gamma^2}\right]\int_0^\infty d\varepsilon\,\exp\left[-\frac{\mu\varepsilon^2}{2\gamma}\left(\gamma^2+\delta^2-2\delta\right)^{3/2}\right]$$

$$= -i\sqrt{\frac{\pi}{2\mu}}\,\frac{(\gamma^2+\delta^2-2\delta)^{q/2-3/4}}{\gamma^{q-\frac{1}{2}}}\,\exp\left[\frac{\mu(\delta-\gamma^2)+\mu\gamma(\gamma^2+\delta^2-2\delta)^{\frac{1}{2}}}{1-\gamma^2}\right] \tag{24}$$

This relation applies for $|\mu\gamma(\gamma^2-2\delta)^{\frac{1}{2}}| \gg 1$, since then Eq.(18b) yields the same result as Eq.(24) for $|\gamma| \ll 1$ and $|\delta^2| \ll |\delta| \ll 1$, namely

$$\mathcal{J}_q^{(1)} = -i\sqrt{\frac{\pi}{2\mu}}\,\frac{1}{\gamma}\left(1-\frac{2\delta}{\gamma^2}\right)^{q/2-3/4}\,\exp\left\{-\frac{\mu}{2}\left[\sqrt{\gamma^2-2\delta}-\gamma\right]^2\right\} \tag{25}$$

In the limiting situation of $|\gamma^2| \gg |\delta|$, we find from (24) that

$$\mathcal{J}_q^{(1)} = -\frac{i}{\gamma}\sqrt{\frac{\pi}{2\mu}}\left[1-\frac{\delta}{\gamma^2}\,(q-3/2)\right]\exp\left[-\zeta^2\left(1+\frac{\delta}{\gamma^2}\right)\right] \approx -\frac{i\sqrt{\pi}\,e^{-\zeta^2}}{(\sqrt{2}k_\parallel c^2/\omega v_t)} \tag{26}$$

Since $i\sqrt{\pi}\,e^{-\zeta^2}$ is one of the parts of the Z function (see Eq.(10)) and recalling Eq.(20), we see that the transition of the $\mathcal{J}_q$ function to the

Z function has been demonstrated at least for part of these functions. That is as $k_\parallel$ ranges from 0 to above ω/v_t, the exponential part of $\mathcal{F}_q$ changes from Eq. (12) i.e. $(-1)^{q-\frac{1}{2}} \pi(\mu\delta)^{q-1} e^{\mu\delta}/\Gamma(q)$ to $- i\sqrt{\pi}\, e^{-\zeta^2}(v_t\omega/k_\parallel c^2\sqrt{2})$, the latter corresponding to part of the Z(q) function. From (26) we note that the Z function becomes valid only for $k_\parallel$ large enough that $|\gamma^2| >> |\delta|$, which is the first condition in (19).

We have shown that different functions are required for cyclotron harmonic effects in various ranges of γ and δ. For sufficiently large $|\gamma|$ given in (19), one can use the nonrelativistic $Z(\zeta)$ function whereas for sufficiently small $|\gamma|$, given in (14), one requires the $F(\mu\delta)$ function derived from relativistic theory. In the intermediate region, one can use one of the forms in (18), (24) and (25) for the non-principal part.

Of particular interest in the large argument expansions are the situations for validity of just the inverse argument part (e.g. $-\zeta^{-1}$ part in the Z function), and of the exponential part alone. When $|\mu\delta| >> 1$, the first part of $\mathcal{F}_q$ seems to be equal to $(\mu\delta)^{-1}$ for all γ except $\gamma \approx 2\delta$, since in the intermediate region we obtained $2/\mu[2\delta - \gamma^2] \approx [\mu\delta]^{-1}$, with similar results in the region of validity of the F and Z functions (see Eqs. 13 and 22). The $(-\zeta^{-1})$ expansion can thus be used even outside of the region of validity of the Z-function itself, provided we do not need the analytic continuation (or exponential part) of Z. The only restrictions are $|\zeta| >> 1$ and $|\mu\delta| >> 1$. However Z has an additional exponential contribution either for situations where ω and $k_\parallel$ are both real, with $k_\perp$ taken to be complex (and then $\sigma = 1$) or if $\mathrm{Im}\omega < 0$ with real $k_\parallel$ and $k_\perp$ as for time-decaying waves (and then $\sigma = 2$). The exponential part is small compared to ζ^{-1} only if $\mathrm{Re}\,\zeta >> \mathrm{Im}\,\zeta$ in which case $|Z| < 1$. Since by (23), $\sqrt{\mu}|\gamma| >> 1$, we see that $|\omega v_t Z/c^2 k_\parallel| < 1$. When $\mathrm{Im}\,\zeta >> \mathrm{Re}\,\zeta$, the exponential part gives the main contribution to Z and then $|Z| >> 1$. Thus we must be cautious of analyses on cyclotron harmonics which

use $Z = -\zeta^{-1}$ rather than its exponential part in the region where large values of $|\omega v_t Z/c^2 k_\parallel|$ are required. Actually, large values are needed to counteract the small $I_n(\lambda)$ function in all regions of $\lambda << 1$ for $n > 2$ except for the Bernstein electrostatic modes and very close to the Appleton-Hartree modes. The coupling region between the two and the region of $k_\perp$ values much less than the Appleton-Hartree values, need a very large $|\omega v_t Z/c^2 k_\parallel|$ magnitude. These regions exist only for $Im\omega < 0$ since only then can the exponential part of the functions attain huge real values as demonstrated in the next section.

IV. THE TRACKS OF REAL F_q and ReZ

We are interested in the frequency track of real F_q i.e. in finding the values of real and imaginary ω for real F_q. Strictly speaking, we should actually be concerned with the function $\mathcal{F}_q$ rather than F_q. However, the previous section indicated the great difficulty in a complete analysis or expansion of $\mathcal{F}_q$. We restrict the analysis to small $k_\parallel$ values for which we get a substantial component of group velocity propagation perpendicular to the magnetic field lines, and then the damping of the wave (viz $\mathcal{F}_q^{(1)}$ in Sec. III) is small. We are mainly concerned at first with $k_\parallel^2 < v_t^2\omega^2/c^4$ in which case Eq.(16) applies to a first approximation and $\mathcal{F}_q \approx F_q$ to zero approximation. Hence the track of real F_q very nearly follows the track of real $\mathcal{F}_q$ for very small $k_\parallel$.

In a nonrelativistic treatment, $\omega/[\mu(\omega - n\omega_b)]$ is the real function that replaces F_q in the analysis. Thus nonrelativistically, the function goes to $\pm\infty$ as $\omega \to n\omega_b$. Relativistically, we note that F_q remains real for real $\omega \geq n\omega_b$. For real $\omega < n\omega_b$, F_q is complex and bounded[2]. The track of real F_q to be found below is identical for $\omega \geq n\omega_b$ and ω is also real here.

Beyond this $\omega = n\omega_b$ point on the track, we can expect the track for complex ω to yield larger and larger values of F_q as $|\mu\delta|$ increases and eventually F_q goes to $+\infty$. There is also a distinctly separate track for negative F_q for which F_q goes to $-\infty$. These tracks in some sense imitate the non-relativistic behaviour.

The mathematical statement of the above is simple. We recall Eq.(13) valid for large $|\mu\delta|$. The positive F_q track which follows the curve of Dnestrovskii et al[2] up to $\omega = n\omega_b$ is obtained by taking Im $i\sqrt{\mu\delta} > 0$ which is satisfied since $\mu\delta$ is real and positive here. Hence $\sigma = 0$ and for $\mu\delta >> 1$, F_q is a decreasing function behaving as $(\mu\delta)^{-1}$. However, beyond the $\omega = n\omega_b$ point, we change to the lower sheet for which Im $\omega < 0$ or Im $i\sqrt{\mu\delta} < 0$. Although the real part of ω initial dips below $n\omega_b$, it soon rises again above $n\omega_b$, so that the real part of $\mu\delta$ is positive and steadily increasing. Since $\sigma = 2$ in this case, F_q goes to infinity as $2\pi|\mu\delta|^{q-1}e^{|\mu\delta|}/\Gamma(q)$. Of course we cannot believe our analysis if δ is not small, but even for $\delta = 0.1$, $e^{\mu\delta}$ is an enormous number.

The negative F_q track is also readily understood. The track always lies in the lower half plane. The initial part of the track follows at first $(\mu\delta)^{-1}$. Although for this track Im $i\sqrt{\mu\delta} < 0$ always, and $\sigma = 2$, we note that the real part of $z \equiv \mu\delta$ is negative and consequently, the exponential part in Eq. (13) decays as $e^{-|z|}$ and F decreases as z^{-1} for large negative z. However, as ω_{real} increases, the real part of z becomes positive. Keeping ω_{imag} negative ($\sigma = 2$), F_q goes to minus infinity as $-2\pi|\mu\delta|^{q-1}e^{|\mu\delta|}/\Gamma(q)$. Note that the singularity of $F_q(z)$ is located at Im $i\sqrt{z} = -\infty$ or $z = \infty$ on the lower sheet. The tracks one must take in either the z or $i\sqrt{z}$ planes to make F_q real are shown in Fig. 2. (If one follows the indicated ω points, one gets the tracks for real ω and complex F_q corresponding to the results of

Dnestrovskii et al[2].)

A schematic plot of the real function F_q versus the real part of ω is shown in Fig. 3. The enclosed region refers to $\delta < 1$ and is the region where our analysis applies. Figure 4 provides accurate plots of the F functions in those parts of the enclosed regions where they are large in magnitude. Also shown are the corresponding values of ω_i versus ω_r.

It can easily be shown how F is made real for large $|z|$ values. In this case we use Eq.(13) with $\sigma = 2$: $F_{n+3/2}(z) \approx 1/z - 2\pi(-z)^n\sqrt{z}\, e^z/\Gamma(n+3/2)$. Writing $z = |z| e^{i\theta}$ we see that

$$F_{n+3/2}(z) \approx \frac{(\cos\theta - i\sin\theta)}{|z|} + \frac{2\pi|z|^{n+\frac{1}{2}}}{\Gamma(n+3/2)} e^{|z|\cos\theta}\, e^{-i\pi(n+1)} e^{i(n+\frac{1}{2})\theta} e^{i|z|\sin\theta}$$

When $2\pi > \theta > 3\pi/2$ for which $\cos\theta > 0$, we require the argument of the sine function part of the exponential to be very near zero for large real positive F and very near $-\pi$ for large real negative F.

$$|z|\sin\theta + (n+\tfrac{1}{2})\theta - \pi(n+1) = 0 \quad \text{or} \quad = -\pi \tag{27}$$

In this case and provided $|z| < \mu$, we have respectively

$$F_{n+3/2}(z) \approx \pm \frac{2\pi|z|^{n+\frac{1}{2}} e^{|z|\cos\theta}}{\Gamma(n+3/2)} \tag{28}$$

Also $(c^2/v_t^2)(\omega_r - n\omega_b)/n\omega_b \approx z\cos\theta$ and $c^2\omega_i/v_t^2 n\omega_b \approx |z|\sin\theta$.

A similar analysis can be performed in the region of applicability of the Z-function. Here the variation is simpler, since the exponential part goes to $\pm\infty$ at $\omega = n\omega_b$ similar to the ζ^{-1} part. To find the track of real Z for large $|Z| \gg 1$ and $|\zeta| \gg 1$, we write $\zeta \equiv x + iy$, $y < 0$, so that $Z \approx 2i\sqrt{\pi}\, e^{-\zeta^2} = 2\sqrt{\pi}\, e^{y^2 - x^2}(\sin 2xy - i\cos 2xy)$. Thus the positive and negative tracks of interest are given respectively by

$$Z = \pm 2\pi e^{y^2} \quad \text{and} \quad 2xy = \pm \pi/2 \tag{29}$$

We note that in this region where Z is large, the imaginary part of ζ or ω can be considerable indicating that the wave is damped in time. Note also that Eqs.(27) and (29) are the least damped solutions of many other tracks and are the only ones which connect up with opposite limits having more or less real arguments.

V. THE DIELECTRIC TENSOR ELEMENTS

Near the nth cyclotron harmonic ($n \neq 1$ - see end of this section), $\pm \omega \approx n\omega_b$. Besides the n = 0 and n = 1 terms, we need to keep only the nth harmonic term. Then we can write cold (c) and warm (w) elements for $\underset{\sim}{\varepsilon} = \underset{\sim}{\varepsilon}_c + \underset{\sim}{\varepsilon}_w$ where the $(\mu\delta)^{-1}$ approximations apply for $\underset{\sim}{\varepsilon}_c$, viz. $\mathcal{J}_{3/2} = v_t^2/c^2$ for n = 0 and $\mathcal{J}_{5/2} = v_t^2(\omega \pm \omega_b)/\omega c^2$ for $n = \pm 1$. Thus (4) becomes

$$(\varepsilon_c)_{11,22} = 1 - \omega_p^2/(\omega^2 - \omega_b^2) \quad ; \quad (\varepsilon_c)_{33} = 1 - \omega_p^2/\omega^2 \tag{30a,b}$$

$$\text{and} \quad -i(\varepsilon_c)_{12} = i(\varepsilon_c)_{21} = \omega_p^2\,\omega_b/\omega(\omega^2 - \omega_b^2) \tag{30c}$$

For the warm terms, it is convenient to consider positive ω near $n\omega_b$ independently from negative ω near $n\omega_b$. When $\omega \approx n\omega_b$, the contribution from $-\omega$ is negligible of course and vice versa. For this reason we restrict ourselves in the following to positive ω, bearing in mind that negative ω can be treated in a similar manner. Thus in the Z-function we consider only the argument $\zeta = (\omega - n\omega_b)/k_n v_t\sqrt{2}$ and in the F function we consider the argument $\mu\delta = \mu(\omega - n\omega_b)/\omega$.

For the nonrelativistic case subject to (19), the approximation $\mathcal{J} = -v_t\omega Z/k_n c^2\sqrt{2}$ yields the following warm elements when $\lambda << 1$.

$$(\varepsilon_w)_{11,22} = i(\varepsilon_w)_{12} = -i(\varepsilon_w)_{21} = \frac{\omega_p^2}{\omega k_n v_t\sqrt{2}} \quad \frac{n^2\lambda^{n-1}}{2^n n!} \quad Z(\zeta) \tag{31a}$$

$$(\varepsilon_w)_{33} = -\frac{\omega_p^2}{\omega k_n v_t\sqrt{2}} \quad \frac{\lambda^n}{2^n n!}\,\zeta\, Z'(\zeta) \tag{31b}$$

$$(\varepsilon_w)_{13,31} = -i(\varepsilon_w)_{23} = i(\varepsilon_w)_{32} = -\frac{\omega_p^2}{\omega k_n v_t} \frac{n\lambda^{n-\frac{1}{2}}}{2^{n+1}n!} Z'(\zeta) \tag{31c}$$

where $Z'(\zeta) = \partial Z/\partial\zeta$. (The approximation $Z = -\zeta^{-1}$ for large ζ is invalid in certain regions, see Sec.III.)

From relativistic analysis subject to (14), we find using the equations in (4) and (17)

$$(\varepsilon_w)_{11,22} = i(\varepsilon_w)_{12} = -i(\varepsilon_w)_{21}$$

$$= -\frac{\omega_p^2}{\omega^2} \mu \frac{n^2\lambda^{n-1}}{2^n n!} \left[F_{n+3/2} + \frac{k_n^2 c^4}{2v_t^2\omega^2} (F_{n+5/2} - 2F_{n+3/2} + F_{n+1/2}) \right] \tag{32a}$$

$$(\varepsilon_w)_{33} = -\frac{\omega_p^2}{\omega^2} \mu \frac{\lambda^n}{2^n n!} \left[F_{n+5/2} + \frac{3k_n^2 c^4}{2v_t^2\omega^2} (F_{n+7/2} - 2F_{n+5/2} + F_{n+3/2}) \right] \tag{32b}$$

$$(\varepsilon_w)_{13,31} = -i(\varepsilon_w)_{23} = i(\varepsilon_w)_{32} = \frac{\omega_p^2}{\omega^2} \mu \frac{k_\perp k_n c^2}{\omega\omega_b} \frac{n\lambda^{n-1}}{2^n n!} \left[F_{n+5/2} - F_{n+3/2} \right] \tag{32c}$$

In certain cases[8] we require higher order λ terms to the dielectric tensor elements. These terms will now be derived for $k_n = 0$ using Eq.(2) and expanding $e^{-\Lambda} I_n(\Lambda)$ to two higher order terms. In the manipulations yielding Eq.(4) from (2), we note that every extra power of Λ raises the order of q in $\mathcal{F}_q$ (or F_q for $k_n = 0$) by one. Thus we obtain, using the series expansion of $e^{-\Lambda} I_n(\Lambda)$:

$$(\varepsilon_{11})_w = -\mu \frac{\omega_p^2}{\omega^2} \frac{n^2}{2^n n!} \lambda^{n-1} \left[F_{n+3/2} - \lambda F_{n+5/2} + \lambda^2 F_{n+7/2} \left(\frac{1}{4(n+1)} + \frac{1}{2} \right) \right] \tag{33a}$$

$$(\varepsilon_{33})_w = -\mu \frac{\omega_p^2}{\omega} \frac{\lambda^n}{2^n n!} \left[F_{n+5/2} - \lambda F_{n+7/2} + \lambda^2 F_{n+9/2} \left(\frac{1}{4(n+1)} + \frac{1}{2} \right) \right] \tag{33b}$$

---

8. I.P. Shkarofsky, "Dispersion of Waves in Cyclotron Harmonic Resonance Regions in Plasmas", submitted for publication.

$$(-i\varepsilon_{21})_w = (i\varepsilon_{12})_w = -\mu \frac{\omega_p^2}{\omega^2} \frac{n^2}{2^n n!} \lambda^{n-1} \left[F_{n+3/2} - \frac{\lambda(1+n)}{n} F_{n+5/2} + \frac{\lambda^2}{n} \left(\frac{n+2}{4(n+1)} + 1 + \frac{n}{2} \right) F_{n+7/2} \right] \quad (33c)$$

$$(\varepsilon_{22})_w = -\mu \frac{\omega_p^2}{\omega^2} \frac{n^2}{2^n n!} \lambda^{n-1} \left[F_{n+3/2} - \lambda \frac{(2+n)}{n} F_{n+5/2} + \frac{\lambda^2}{n^2} \left(2 + 2n + \frac{n^2}{4(n+1)} + \frac{n^2}{2} \right) F_{n+7/2} \right] \quad (33d)$$

When the Z-function applies, the above equations can be used with all F's replaced by $-v_t \omega Z / k_\parallel c^2 \sqrt{2}$. The additional terms provide correction terms in the dispersion relations and give rise to a completely new wave as is shown in Ref. 8.

For the fundamental frequency, the "cold terms" in Eq.(30) are incorrect except for ε_{33}. For the "cold terms", we allow only $n = -1$ in ε_{11} and ε_{12} keeping $n = 1$ for the "warm terms". Thus

$$1 - (\varepsilon_c)_{11} = 1 - (\varepsilon_c)_{22} = -i(\varepsilon_c)_{12} = i(\varepsilon_c)_{21} = \omega_p^2 / [2\omega(\omega + \omega_b)] \quad (34)$$

To order λ^2, the warm terms are given by Eqs. (33a-d) for $k_\parallel = 0$. If we wish to include $k_\parallel$ to first order we can use Eqs.(32a,b,c) with $n = 1$.

IV. RELATION TO OTHER WORK

Trubnikov[9], Drummond and Rosenbluth[10], Beard[11], Beard and Baker[12], Oster[13] and Bekefi et al[14] have all considered cyclotron radiation from a

9. B.A. Trubnikov, Phys. Fluids, 4, 195 (1961)
10. W.E. Drummond & M.N. Rosenbluth, Phys. Fluids 3, 45 (1960); 3, 491 (1960); 6, 276 (1961)
11. D.B. Beard, Phys. Fluids 2, 379 (1959)
12. D.B. Beard & J.C. Baker, Phys Fluids 4, 278, 611 (1961); 5, 1113 (1962)
13. L. Oster, Phys.Rev. 116, 474 (1959); 119, 1444 (1960); 121, 961 (1961)
14. G. Bekefi, J.L. Hirshfield & S.C. Brown, Phys.Rev. 122, 1037 (1961)

hot plasma. Their basis is either the individual particle approach with perhaps some account for the distribution function or otherwise the full relativistic approach (Eq.1) without applying the expansion in terms of Bessel functions. The values for the dielectric matrix elements are integrated either using a computer or applying a saddle point method as first indicated by Trubnikov. They also provide results as $k_{\parallel}$ varies away from zero or for sufficiently large $k_{\parallel}$. However, one basic assumption of these workers is that $k^2c^2/\omega^2 = 1$ and $\omega >> \omega_p$ which simplifies the analysis exceedingly. Essentially, they consider only the electromagnetic extraordinary and ordinary waves near the light line rather than investigating wave dispersion for the whole range of k values with $\lambda \lesssim 1$ as we do in Ref.8. The saddle point method is useful when v_t/c is not too small and cyclotron harmonic lines can overlap. In the very slightly relativistic limit when the lines are distinct, the Bessel function expansion is more appropriate. Some work when $\omega \approx \omega_p$ for the strongly relativistic case is given by Beard[15], who also provides an excellent summary of the above papers.

Demidov and Frank-Kamenetskii[16] have treated less rigorously the same problem as Dnestrovskii et al[2]. Their results disagree and it seems that Demidov's final function, equivalent to our F function, is in error. On the other hand, the works of Rukhadze and Silin[7] and Gershman[17] conform in principle with our and Dnestrovskii et al's results.

Many authors have treated the line shape and absorption effects near cyclotron harmonics using nonrelativistic theory. (See for example, Silin and Rukhadze[18], Gershman[19].) If $k_{\parallel}$ is sufficiently large that the conditions in

---

15. D.B. Beard, Radiation and Waves in Plasmas, Editor - M. Mitchner, Stanford Un. Press, Stanford (1961) p.66; Phys.Fluids 3, 324 (1960)
16. V.P. Demidov & D.A. Frank-Kamenetskii, Sov.Phys. - Tech.Phys. 8, 686 (1964)
17. B.N. Gershman, Sov.Phys. Doklady 6, 314 (1961)
18. V.P. Silin & A.A. Rukhadze, Electromagnetic Properties of Plasma and Plasma-Like Media , Glavatomizdat, Moscow (1961), pp. 144-7 (in Russian)
19. B.N. Gershman, Sov.Phys. JETP 11, 657 (1960)

(19) are satisfied, these analyses are valid and the concept of "cyclotron" absorption" is meaningful. Our development here and in Ref.8 covers the range of lower $k_{\parallel}$ values, after the transition from "cyclotron absorption" to "relativistic absorption" has occurred.

We complete this report having shown that the relativistic analysis is necessary in certain regions. The transition to the nonrelativistic case has been clearly illustrated and its region of applicability has been indicated. The necessary dielectric tensor elements have been derived with which we can investigate the dispersion of waves near cyclotron harmonics.

ACKNOWLEDGEMENTS

The author acknowledges very stimulating discussions with Dr. T.W. Johnston and his many useful leads. This work was supported by the Fields and Plasma Branch of the Goddard Space Flight Center, National Aeronautics and Space Administration, Greenbelt, Maryland under Contract NASw-957.

CAPTIONS FOR FIGURES

Figure 1 Regions of applicability of cyclotron harmonic dispersion functions when $\mu = 10^6$ shown here for real y and δ. In this case, the functions are real below $y^2 = 2\delta$ and complex above. The F-function is valid in the lower region and $\mu\delta = 1$ separates the regions where the small and large argument expansions apply. The Z-function is valid in the upper region and has a similar division at $\zeta = 1$ or $\mu\delta^2 = 2y^2$.

Figure 2a The two tracks of real F in the complex z plane. The positive F track runs from $\omega = -0$ through $\omega = n\omega_b$ and then turns to the lower sheet. The negative F track runs from $\omega = 0$ on the lower sheet. Both tend towards the singularity of the F function.

2b The same tracks in the complex $i\sqrt{z}$ plane.

Figure 3 Schematic plot of the values of F versus real part of ω for complex ω and real F. The rectangular cut indicates the region where the analysis is valid.

Figure 4 Calculated plots of the $F_{n+3/2}$ functions for $n = 1,2...7$ in those parts of the rectangular cut where the functions are large. Also shown are the values of the imaginary part versus the real part of ω. The equations used for the calculations are (27) and (28). Also $z = \mu\delta$. In (a) is plotted the tracks of lnF for positive real F and of ln(-F) for negative real F. In (b) and (c) are shown the values of $-\omega_i c^2/n\omega_b v_t^2$ for the respective positive and negative real F curves.

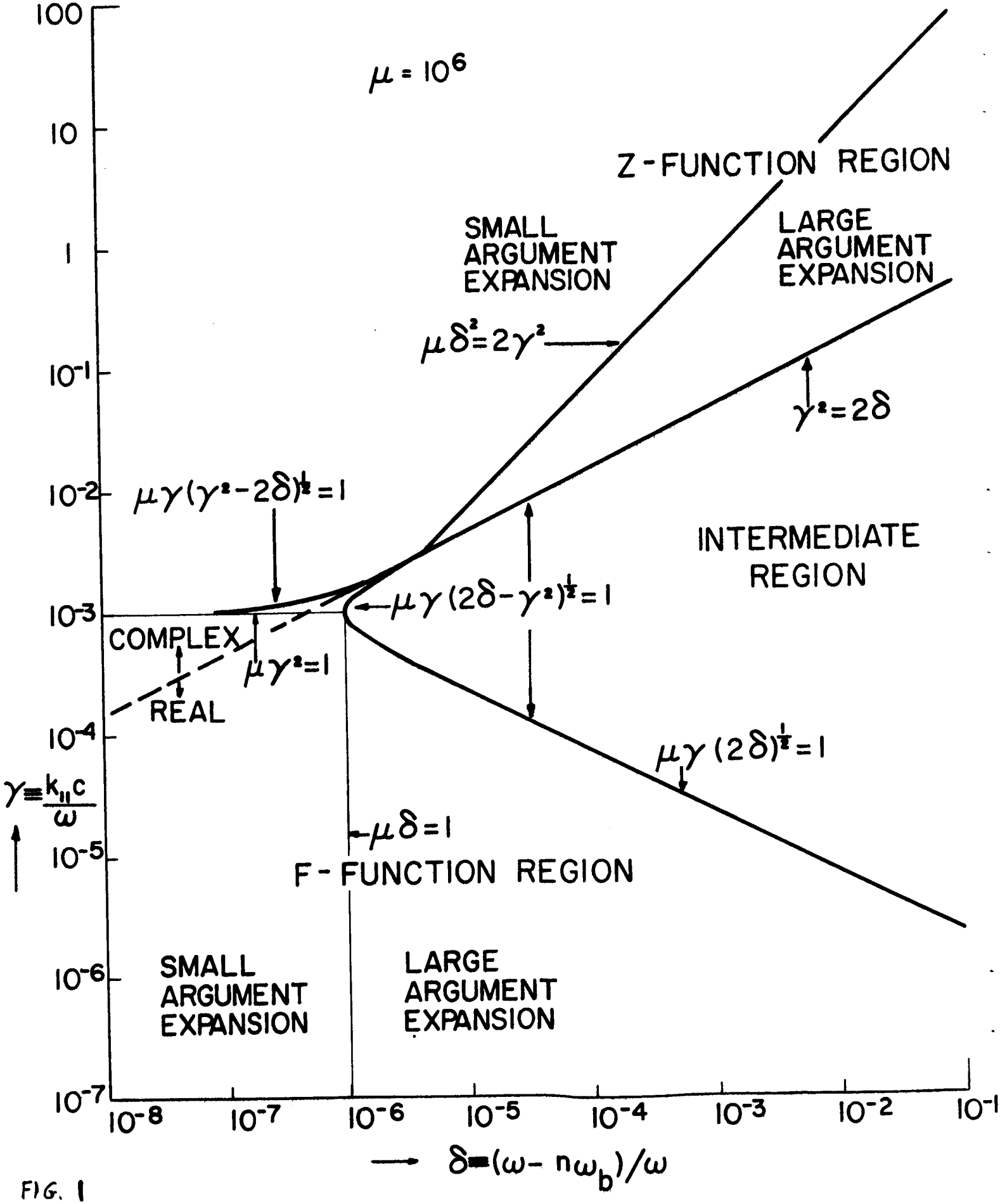
100
10
1
10^{-1}
10^{-2}
10^{-3}
10^{-4}
10^{-5}
10^{-6}
10^{-7}
$\mu = 10^6$
Z-FUNCTION REGION
SMALL ARGUMENT EXPANSION
LARGE ARGUMENT EXPANSION
$\mu\delta^2 = 2\gamma^2$
$\gamma^2 = 2\delta$
$\mu\gamma(\gamma^2 - 2\delta)^{\frac{1}{2}} = 1$
INTERMEDIATE REGION
$\mu\gamma(2\delta - \gamma^2)^{\frac{1}{2}} = 1$
COMPLEX
REAL
$\mu\gamma^2 = 1$
$\mu\gamma(2\delta)^{\frac{1}{2}} = 1$
$\gamma \equiv \frac{k_{\parallel} c}{\omega}$
$\mu\delta = 1$
F-FUNCTION REGION
SMALL ARGUMENT EXPANSION
LARGE ARGUMENT EXPANSION
10^{-8}
10^{-7}
10^{-6}
10^{-5}
10^{-4}
10^{-3}
10^{-2}
10^{-1}
$\delta \equiv (\omega - n\omega_b)/\omega$

FIG. 1

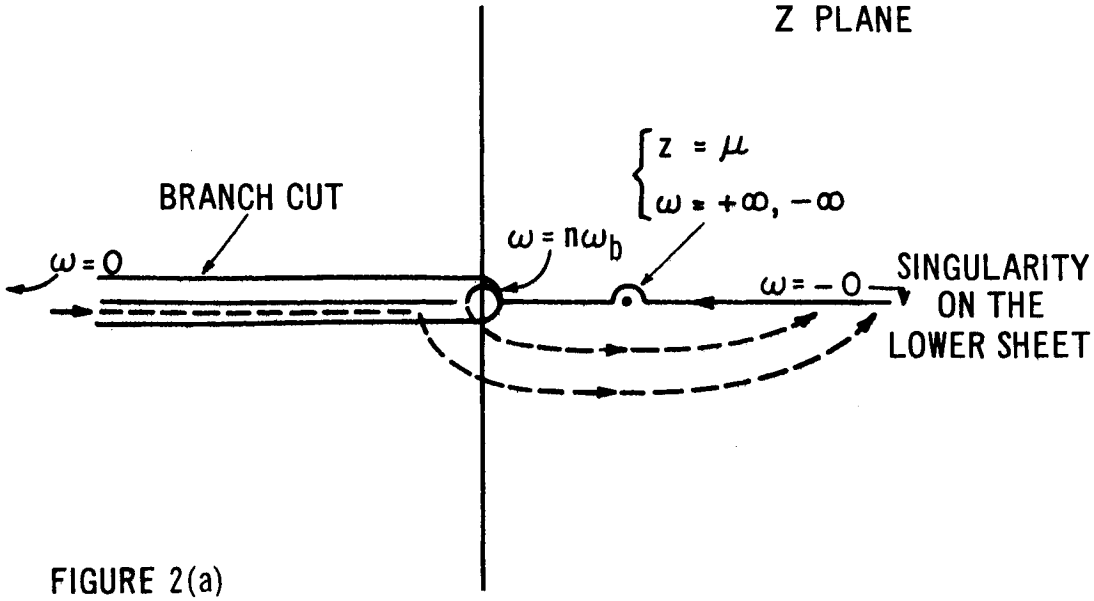

FIGURE 2(a)

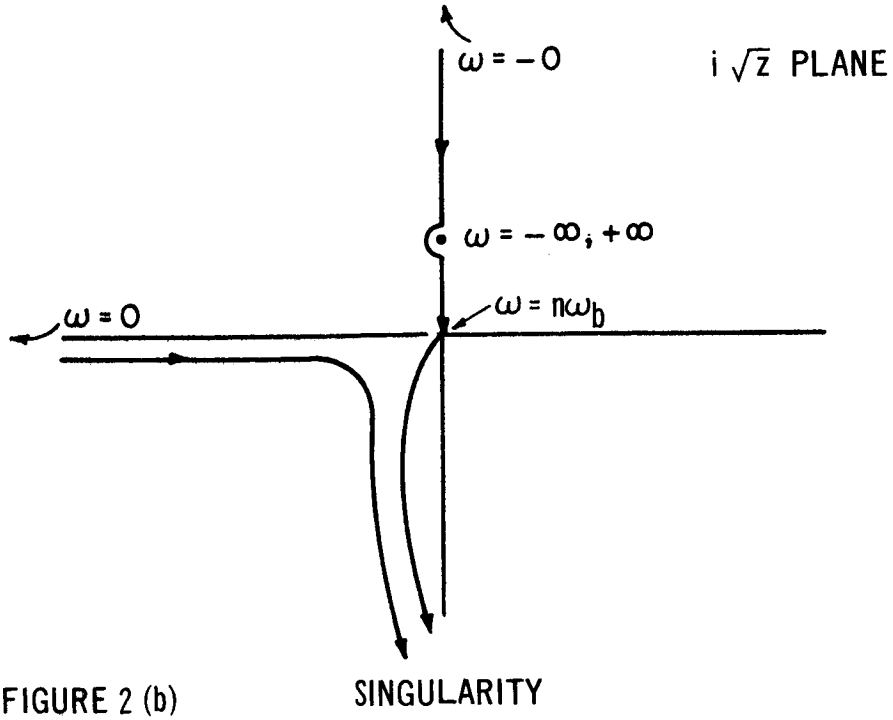

FIGURE 2 (b)

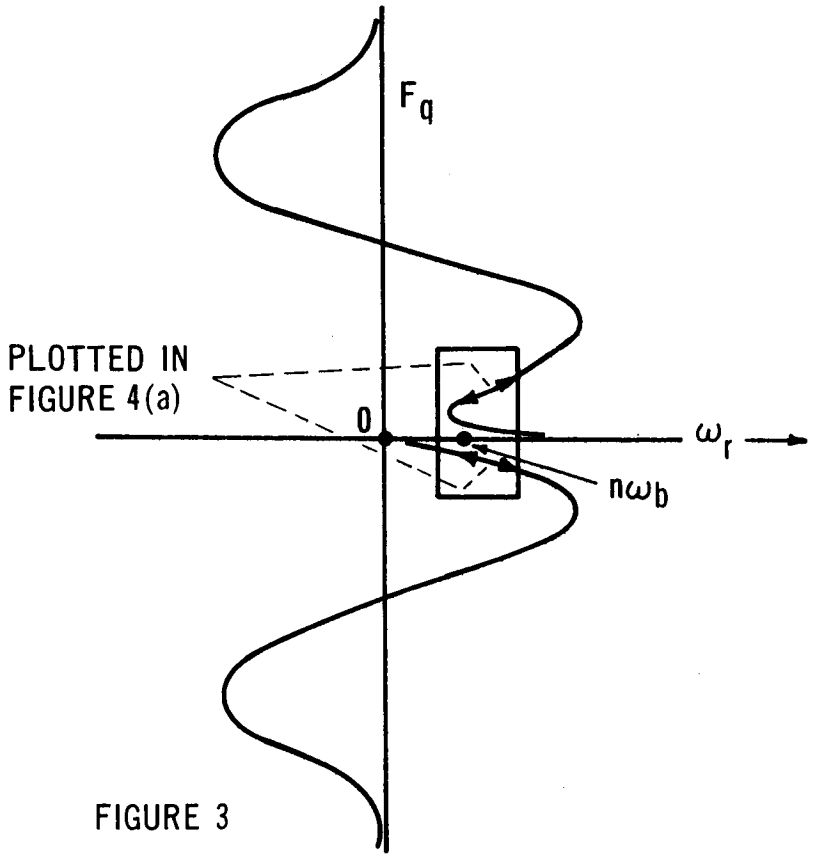

FIGURE 3

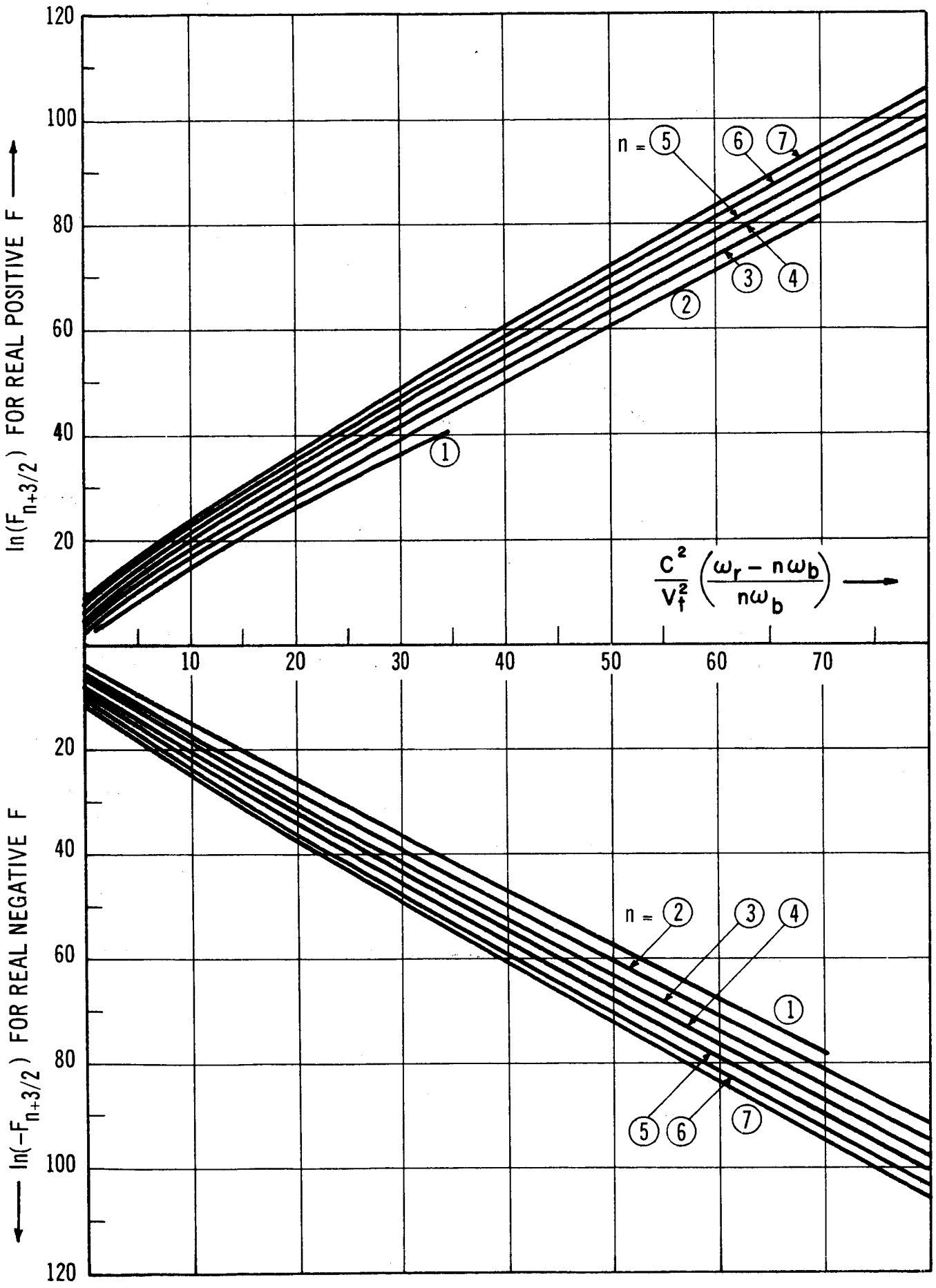
120
100
80
60
40
20
$\ln(F_{n+3/2})$ FOR REAL POSITIVE F
n = 5 6 7
3 4
2
1
$\frac{C^2}{V_f^2}\left(\frac{\omega_r - n\omega_b}{n\omega_b}\right)$
10 20 30 40 50 60 70
20
40
60
80
100
120
$\ln(-F_{n+3/2})$ FOR REAL NEGATIVE F
n = 2 3 4
1
5 6 7

Fig. 4(a)

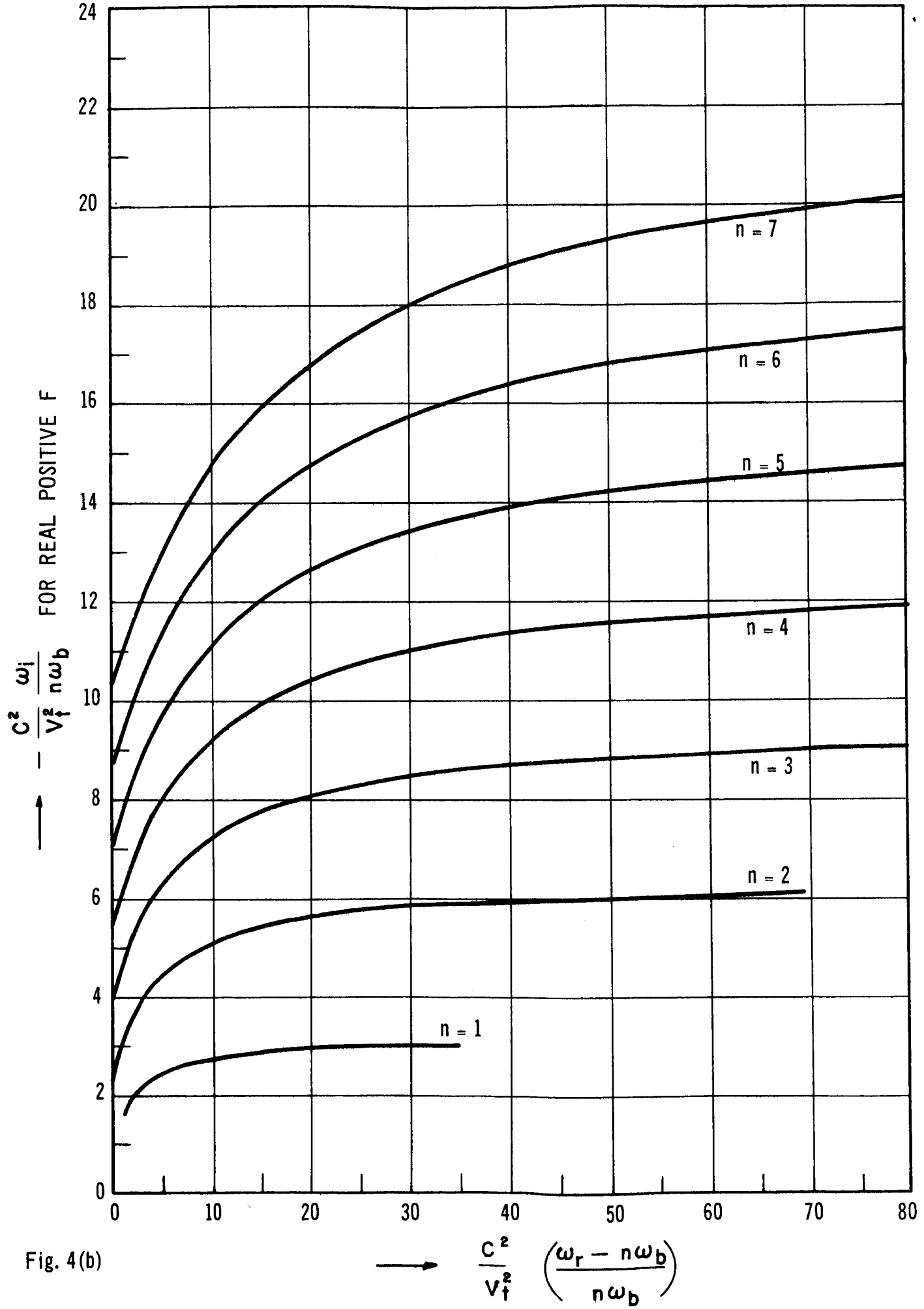
24
22
20
18
16
14
12
10
8
6
4
2
0
0
10
20
30
40
50
60
70
80
n = 7
n = 6
n = 5
n = 4
n = 3
n = 2
n = 1
$-\frac{C^2}{V_f^2}\frac{\omega_i}{n\omega_b}$ FOR REAL POSITIVE F
$\frac{C^2}{V_f^2}\left(\frac{\omega_r - n\omega_b}{n\omega_b}\right)$

Fig. 4(b)

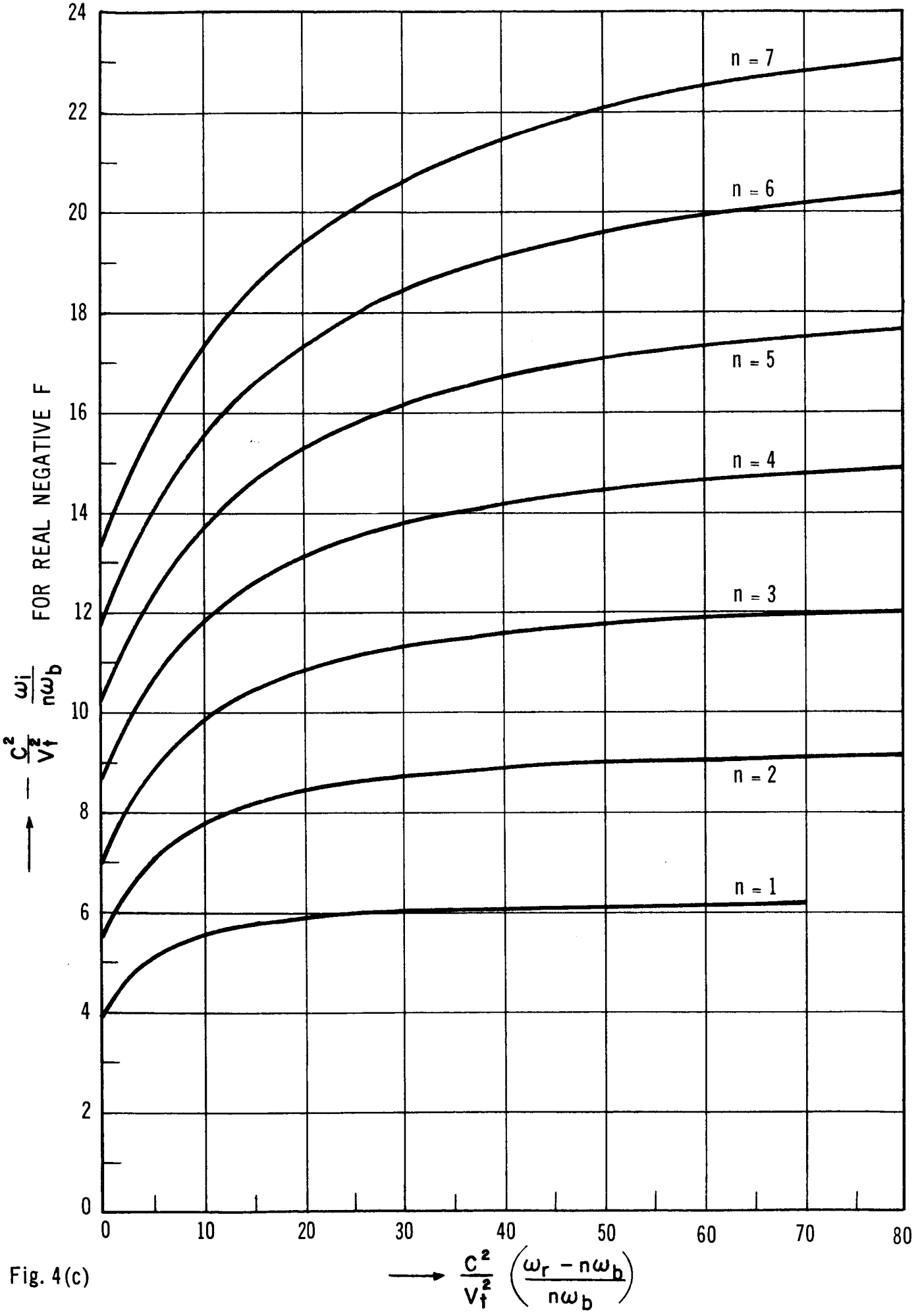
n = 7
n = 6
n = 5
n = 4
n = 3
n = 2
n = 1
$\frac{C^2}{V_f^2} \frac{\omega_i}{n\omega_b}$ FOR REAL NEGATIVE F
$\frac{C^2}{V_f^2} \left(\frac{\omega_r - n\omega_b}{n\omega_b} \right)$
0
2
4
6
8
10
12
14
16
18
20
22
24
0
10
20
30
40
50
60
70
80

Fig. 4(c)

DISPERSION OF WAVES IN CYCLOTRON HARMONIC RESONANCE REGIONS IN PLASMAS

I.P. Shkarofsky

RCA Victor Company, Ltd.
Research Laboratories
Montreal, Canada

- ABSTRACT -

The dispersion of waves near electron cyclotron harmonics is investigated including to first order, wave numbers parallel to the magnetic field. The proper relativistic form for the dielectric tensor elements is applied. The relativistic formulation is compared with the nonrelativistic one applicable for larger wavenumbers parallel to magnetic field and the differences are noted. In either analysis, different behaviours result depending on whether the wave number or frequency is taken to be complex. In the former case, the waves near the Appleton-Hartree values are localized and a gap exists between them and the higher order cyclotron harmonic plasma waves. In the latter case, this gap does not occur but the relativistic analysis shows a rapid rise in frequency above the harmonic as one tends to zero wave number perpendicular to magnetic field. We also show that the large argument expansion in terms of inverse argument of the non-relativistic Z-function produces incorrect dispersion results in certain regions.

I. INTRODUCTION

In this paper, we investigate the dispersion of plasma waves near cyclotron harmonics when $\lambda \equiv k_\perp^2 v_t^2/\omega_b^2 < 1$, applying relativistic analysis[1] and comparing the results with those found from nonrelativistic analysis. The former approach is valid for very small and zero $k_\parallel$ whereas the latter has to be used for sufficiently large $k_\parallel$ given in Ref.1. In either analysis, we have to take either ω or $k_\perp$ to be complex in certain regions and we find totally different dispersion curves very near $n\omega_b$ depending on these two situations. For complex $k_\perp$ and real ω, the case of a steady r-f signal decaying in space, it will be shown that we get the extraordinary, ordinary and plasma waves but with gaps in the $k_\perp$ spectrum except possibly for the second harmonic. That is, regions exist where one cannot obtain a real ω for a given complex $k_\perp$ and these gaps effectively separate the Appleton-Hartree and Bernstein electrostatic plasma waves. On the other hand, for complex ω and real $k_\perp$, the case of a time-decaying r-f pulse, we can cover the complete $\lambda < 1$ spectrum except for a tiny region near $k_\perp = 0$, where relativistic analysis indicates a rapid rise in frequency above the harmonic, but in nonrelativistic analysis ω approaches the harmonic with very strong damping. The existence of an extra wave in addition to the ordinary and coupled extraordinary-plasma wave is also indicated. These results are in essence, the original contributions here on the subject of dispersion of cyclotron harmonics.

Dnestrovskii and Kostomarov[2] and other authors have, for $k_\parallel = 0$, used the inverse argument approximation of the nonrelativistic Z-dispersion function. As shown in Ref.1, the applicability of this for $\lambda << 1$ is limited to the Bernstein modes and very close to the Appleton-Hartree modes. This incorrect

---

1. I.P. Shkarofsky - "Dielectric Tensor in Vlasov Plasmas Near Cyclotron Harmonics", submitted for publication.
2. Yu.N. Dnestrovskii and D.A. Kostomarov - Sov.Phys. JETP 13, 986 (1961); 14, 1089 (1962).

use of nonrelativistic theory predicts for minute $k_{\parallel}$, three waves with both real ω and real $k_{\perp}$ near each cyclotron harmonic, and no gaps exist in the $k_{\perp}$ spectrum. In Ref.2, dispersion curves are computed based on this analysis. Some of the analytical results will be presented here with remarks on their limited regions of applicability.

II. THE DISPERSION EQUATION FOR $\lambda \equiv k_{\perp}^2 v_t^2/\omega_b^2 < 1$ AND $k_{\parallel}^2 c^4/v_t^2\omega^2 < 1$

(a) Basic Relations

We shall derive the dispersion relation for the above values of very small $k_{\parallel}$ and moderately small $k_{\perp}$ where $k_{\perp}$, $k_{\parallel}$ are wave numbers perpendicular and parallel to magnetic field lines, $\omega_b = |eB/m|$, $v_t^2 = \kappa T/m$, and e, m, B, c, ω, κ and T have their usual significance. The analysis will use the relativistic dielectric tensor elements expanded to first order in λ and $k_{\parallel}^2$. We shall point out in Secs. III and IV the corresponding nonrelativistic results and the substitutions required to obtain them.

The dispersion relation for waves in a plasma is

$$D = \left| -\frac{k^2c^2}{\omega^2}\delta_{\alpha\beta} + \frac{c^2}{\omega^2}k_\alpha k_\beta + \varepsilon_{\alpha\beta} \right| = 0 \qquad (1)$$

We write $\varepsilon_{\alpha\beta} = (\varepsilon_{\alpha\beta})_c + (\varepsilon_{\alpha\beta})_w$, which are respectively the "cold" Appleton-Hartree dielectric tensor elements and the "warm" elements associated with a particular cyclotron harmonic.

We now insert the dielectric tensor elements given by Eqs.(30) and (32) of Shkarofsky[1]. With $k_{\perp}$ along the x axis and $k_{\parallel}$ and B along the z axis, the elements of determinent D to be evaluated are given by

$$D_{11} + k_{\parallel}^2\frac{c^2}{\omega^2} - K_{\perp} = D_{22} + k^2\frac{c^2}{\omega^2} - K_{\perp} = iD_{12} + K_{\times} = -iD_{21} + K_{\times}$$
$$= -k_{\perp}^{2(n-1)}\frac{c^2}{\omega^2}P(\rho + \beta k_{\parallel}^2)$$

$$D_{13} - k_\perp k_\parallel c^2/\omega^2 = D_{31} - k_\perp k_\parallel c^2/\omega^2 = -iD_{23} = iD_{32} = -k_\perp k_\parallel (c^4/\omega^4) Q k_\perp^{2(n-1)} \eta$$

$$D_{33} = K_\parallel - \frac{k_\perp^2 c^2}{\omega^2} - k_\perp^{2n} \frac{c^2}{\omega^2} P_\parallel (\rho_\parallel + \beta_\parallel k_\parallel^2) \qquad (2)$$

where $K_\perp = 1 - \frac{\omega_p^2}{(\omega^2 - \omega_b^2)}$; $K_\parallel = 1 - \frac{\omega_p^2}{\omega^2}$; $K_\times = \frac{\omega}{\omega_b}\left(K_\parallel - K_\perp\right) = \frac{\omega_p^2 \omega_b}{\omega(\omega^2 - \omega_b^2)}$ (3a,b,c)

$$P = \frac{\omega_p^2}{v_t^2}\left(\frac{v_t}{\omega_b}\right)^{2(n-1)} \frac{n^2}{n!2^n} \; ; \quad Q = \frac{\omega_p^2 \omega}{n\omega_b v_t^2}\left(\frac{v_t}{\omega_b}\right)^{2(n-1)} \frac{n^2}{n!2^n} \; ; \quad P_\parallel = \frac{\omega_p^2}{v_t^2}\left(\frac{v_t}{\omega_b}\right)^{2n} \frac{1}{n!2^n}$$

(3d,e,f)

$$\rho = F_{n+3/2}(\mu\delta); \quad \beta = \frac{c^4}{2v_t^2\omega^2}\left(F_{n+1/2} - 2F_{n+3/2} + F_{n+5/2}\right); \quad \eta = F_{n+3/2} - F_{n+5/2} \qquad (3g,h,i)$$

$$\rho_\parallel = F_{n+5/2} \; ; \; \beta_\parallel = \frac{3c^4}{2v_t^2\omega^2}\left(F_{n+3/2} - 2F_{n+5/2} + F_{n+7/2}\right) \qquad (3j,k)$$

Also $\omega_p = \sqrt{n_e e^2/\varepsilon_0 m}$ is the plasma frequency, $k^2 = k_\perp^2 + k_\parallel^2$, n_e is electron density and n is the order of the cyclotron harmonic ($n \neq 1$). The function F_q is defined by $F_q(\mu\delta) \equiv -i\int_0^\infty dt e^{i\mu\delta t}/(1-it)^q$ where $\mu = c^2/v_t^2$ and $\delta = (\omega - n\omega_b)/\omega$ and was investigated at length in Ref.1.

(b) The Extraordinary and Plasma Modes

Let us restrict ourselves at present to the extraordinary and plasma waves; later we consider the ordinary wave. Since the ordinary wave is associated with the 33 element of the determinant, for the other waves the warm part of this element is of higher order in λ and can be neglected. That is we approximate the 33 element by $(K_\parallel - k_\perp^2 c^2/\omega^2)$. Now one can expand the determinant by using the subdeterminants of the 33, 32 and 31 elements and dividing the result by the 33 element.

An order of magnitude comparison of the terms involving Q with the product term $P\beta k_\parallel^2$ shows that all the Q terms are negligible for the ranges of

$k_\parallel$ and $k_\perp$ of interest. Thus the determinant simplifies to the following expression:

$$-x\left[K_\perp - \frac{k_\parallel^2 c^2}{\omega^2}\left(1 - \frac{K_\perp - \frac{k^2c^2}{\omega^2}}{K_\parallel - \frac{k_\perp^2 c^2}{\omega^2}}\right) + 2\left(K_1 - \frac{k_\parallel^2 c^2}{\omega^2}\right) Pk_\perp^{2(n-2)}(\rho + \beta k_\parallel^2)\right]$$

$$+ x^2\left[Pk_\perp^{2(n-2)}(\rho + \beta k_\parallel^2)\right] + \left(K_1 - \frac{k_\parallel^2 c^2}{\omega^2}\right)\left(K_r - \frac{k_\parallel^2 c^2}{\omega^2}\right) = 0 \qquad (4)$$

where

$$K_1 = K_\perp + K_\times = 1 - \frac{\omega_p^2}{\omega(\omega + \omega_b)}\ ; \quad K_r = K_\perp - K_\times = 1 - \frac{\omega_p^2}{\omega(\omega - \omega_b)} \qquad (5a,b)$$

$$K_\perp = (K_1 + K_r)/2 = 1 - \frac{\omega_p^2}{(\omega^2 - \omega_b^2)} \qquad \text{and} \quad x = \frac{k_\perp^2 c^2}{\omega^2} \qquad (5c,d)$$

The quadratic equation (4) in x can be solved when $\left|Pk_\perp^{2(n-2)}(\rho + \beta k_\parallel^2)\right| << 1$. The smaller x solution is

$$x = \left(K_1 - \frac{k_\parallel^2 c^2}{\omega^2}\right)\left(K_r - \frac{k_\parallel^2 c^2}{\omega^2}\right) \Bigg/ \left[K_\perp - \frac{k_\parallel^2 c^2}{\omega^2}\left(1 - \frac{K_\perp - \frac{k^2c^2}{\omega^2}}{K_\parallel - \frac{k_\perp^2 c^2}{\omega^2}}\right)\right] \qquad (6a)$$

which is the extraordinary electromagnetic mode. The larger x solution is

$$x = \left[K_\perp - \frac{k_\parallel^2 c^2}{\omega^2}\left(1 - \frac{K_\perp - \frac{k^2c^2}{\omega^2}}{K_\parallel - \frac{k_\perp^2 c^2}{\omega^2}}\right)\right] \Bigg/ \left[k_\perp^{2(n-2)} P(\rho + \beta k_\parallel^2)\right] \qquad (6b)$$

which is the mode for large wave numbers. If we consider real ω and complex $k_\perp$ or x, then $|\rho|$ lies within bounds of order one near the harmonics. Since $\left|Pk_\perp^{2(n-2)}\right|$ is always less than one for $\lambda \lesssim 1$, we see that the above condition on $\left|Pk_\perp^{2(n-2)}\rho\right| << 1$ is satisfied. As a result the solution of Eq.(4) can never deviate much from the cold em mode or large wave number mode. One cannot

propagate a wave for $k_\perp$ values between these two modes. These arguments do not apply to n = 2, which is reconsidered in Sec.III.

The situation for real $k_\perp$ or x and complex ω is different. As shown in Ref.1, the F function or ρ can be continued into the lower half plane and can attain huge real values. In fact the product $Pk_\perp^{2(n-2)}\rho$ can easily become of order one. Under these conditions one can obtain solutions of Eq.(4) for any non-zero value of x.

We note that for $n \geq 2$, $K_\parallel$, K_r and $K_\perp$ are given in Eq.(5) whereas for n = 1, we use Eq.(34) of Ref.1 to find equivalently that $K_\perp = K_\times + 1 = 1 - \omega_p^2/2\omega(\omega + \omega_b)$ so that

$$K_\parallel = 1 - \omega_p^2/\omega(\omega + \omega_b), \quad K_r = 1 \quad \text{and } K_\perp = (K_\parallel + 1)/2 \qquad (7)$$

Dispersion effects based on this will be discussed in Sec.III.

(c) <u>The Ordinary Wave</u>

Besides the extraordinary-plasma wave mode, there is another wave associated with the Eq.(2), namely the ordinary wave. To obtain the dispersion relation for this ordinary wave including first order k_n terms, we expand D and divide this time by X, where X denotes the following combination of elements [(11)(22) - (12)(21)], viz,

$$X = \left[K_\parallel - \frac{k_n^2c^2}{\omega^2} - \frac{k_\perp^2c^2}{2\omega^2}\right]\left[K_r - \frac{k_n^2c^2}{\omega^2} - \frac{k_\perp^2c^2}{2\omega^2} - 2k_\perp^{2(n-1)}\ \frac{c^2}{\omega^2}P(\rho + \beta k_n^2)\right] - \frac{k_\perp^4c^4}{4\omega^4}$$

To obtain any noticeable deviation for n > 1 from the "cold ordinary wave" $K_n - k_\perp^2c^2/\omega^2 = 0$, we require $k_\perp^{2n}c^2P_n\rho_n/\omega^2$ to be of order one. In this case we note that the $k_\perp^{2(n-1)}\frac{c^2}{\omega^2}Pp$ terms are much greater than one by order λ^{-1}, so that in X, we can neglect K_r, k^2c^2/ω^2, etc with respect to the warm term.

$$X \approx -2k_\perp^{2(n-1)} \frac{c^2}{\omega^2} P\rho \left[K_1 - \frac{k_\parallel^2 c^2}{\omega^2} - \frac{k_\perp^2 c^2}{2\omega^2} \right] \tag{8}$$

Similarly in evaluating D, we keep only products of warm tones, viz. PQ, Q^2 and PQ^2. The PQ^2 and PQ terms cancel. The determinant thus becomes the following, after division by X and then inserting Eq.(8).

$$K_\parallel - \frac{k_\perp^2 c^2}{\omega^2} - k_\perp^{2n} \frac{c^2}{\omega^2} P_\parallel (\rho_\parallel + \beta_{OR} k_\parallel^2) = 0 \tag{9}$$

where from Eqs.(3d-g,i,k) we have

$$P_\parallel \beta_{OR} \equiv P_\parallel \beta_\parallel - \frac{Q^2 \eta^2 c^4}{P\rho\omega^4} \quad \text{and} \quad \beta_{OR} = \frac{c^4}{2v_t^2\omega^2} \left\{ 3F_{n+7/2} - 2F_{n+5/2} + F_{n+3/2} - 2F_{n+3/2}^2 \Big/ F_{n+3/2} \right\}$$

(d) The Extra Wave

By restricting ourselves to $k_\parallel = 0$, we can investigate more fully the higher powers of λ neglected previously. Using the proper relativistic approach, we find the additional terms negligible for the two waves given above, except when $2K_\perp = x$. An extra wave exists if one investigates the dispersion relations using two higher orders in the λ expansion. This wave is decoupled from the other two in this limit of $k_\parallel = 0$. For larger $k_\parallel$ where the nonrelativistic Z-function is applicable[1], a third wave also results, coupled to the extraordinary wave. A coupled third wave has also appeared in calculations of cyclotron harmonics upon the ad hoc incorrect application of the $-\zeta^{-1}$ expansion of the Z-function in nonrelativistic analysis (e.g. Dnestrovskii and Kostomarov[2] — see Sec.IV for a full discussion).

For $k_\parallel = 0$, the dispersion equation (1) for the extraordinary and plasma waves reduces to $\varepsilon_{11}(\varepsilon_{22} - x) - \varepsilon_{12}\varepsilon_{21} = 0$ with $x = k^2c^2/\omega^2$, $k = k_\perp$ Inserting the cold elements given in Eq.(3b) and the warm elements given in Eq.(33) of Ref.1, we find

$$K_1K_r - xK_\perp - 2xK_1k^{2(n-2)}P\left[F_{n+3/2} - \frac{\lambda}{n}F_{n+5/2}(1+n) + \frac{\lambda^2}{n}F_{n+7/2}\left(\frac{n+2}{4(n+1)} + 1 + \frac{n}{2}\right)\right]$$

$$- k^{2(n-2)}Px\lambda^2K_\perp\frac{(2+n)}{n^2(n+1)}F_{n+7/2} + x^2k^{2(n-2)}P\left[F_{n+3/2} - \lambda F_{n+5/2} + \lambda^2F_{n+7/2}\left(\frac{1}{4(n+1)} + \frac{1}{2}\right)\right]$$

$$+ k^{4(n-2)}\frac{P^2x^2\lambda^2}{n^2}\left[F_{n+3/2}F_{n+7/2}\left(\frac{n+2}{n+1}\right) - F^2_{n+5/2}\right] = 0 \qquad (10)$$

where K_1, K_r, $K_\perp$ and P are defined in Eqs.(3) and (5) and $\lambda \equiv k^2c^2/\omega_b{}^2$.

If higher powers in λ are neglected in (10), we simply obtain

$$\left[\frac{1}{k^{2(n-2)}P}\right]\frac{1}{F_{n+3/2}} \equiv \left[\frac{\omega_b{}^2 2^n n!}{\omega_p{}^2\lambda^{n-2}n^2}\right]\frac{1}{F_{n+3/2}} = \frac{(2K_1 - x)x}{K_1K_r - K_\perp x} \qquad (11)$$

Since $k^{2(n-2)}P$ is extremely small, $F_{n+3/2}$ has to be large for x to deviate away from the electromagnetic mode ($K_1K_r \approx K_\perp x$) or the electrostatic mode ($x >> 1$). For large F, all x values are possible except when $x \to 2K_1$ for which we might seem to require $F \to \infty$. This, however, is not necessary since we then include the higher powers of λ given in Eq.(10). In fact, when $x \approx 2K_1$, Eq.(10) shows that a higher order of magnitude of F is required of order $(\lambda k^{2(n-2)}P)^{-1}$ instead of $(k^{2(n-2)}P)^{-1}$. Equation (10) also shows that the only case we need these higher λ values for $\lambda < 1$ is near $x \approx 2K_1$.

A new wave appears if one looks for solutions having even larger values of F of order $(\lambda^2k^{2(n-2)}P)^{-1}$. One can readily deduce the dispersion equation in this case to be

$$\left[\frac{\omega_b{}^2 2^n n!}{\omega_p{}^2\lambda^{n-2}n^2}\right]\left[\frac{(n+2)F_{n+7/2}}{n+1} - \frac{F^2_{n+5/2}}{F_{n+3/2}}\right]^{-1} = \frac{x\lambda^2}{n^2[2K_1 - x]} \qquad (12)$$

This wave is decoupled from the coupled extraordinary-plasma wave. Near $x \approx 2K_1$ each of the two combine with extra terms of order $(\lambda k^{2(n-2)}P)^{-1} \sim F$

and smoothly pass through this transition. This wave exists only if ω is complex and k real in which case F can become very large[1], When ω is real and k complex we would not expect this wave to exist.

III. DISPERSION CURVES BASED ON RELATIVISTIC ANALYSIS

(a) Real ω, Complex k Curves

We can now plot ω - k dispersion curves for zero $k_{\parallel}$ based on the above analysis. First we consider the case of real ω, complex F_q and hence complex k. Then we investigate the case of greater interest to us, namely real F_q, real k and complex ω.

When ω is real, the complex function F_q is plotted in Figs.1 and 2 of Dnestrovskii et al[3]. We note that both the real and imaginary parts of F_q lie within bounds of order one near the harmonic. As a result $k^{2(n-2)}{}_P F_q$ is an extremely small number for $n > 2$. Noting that $K_\perp = (K_l + K_r)/2$, we can readily solve the quadratic equation (11) to yield under these conditions:

$$x = \frac{K_l K_r}{K_\perp}\left(1 - k^{2(n-2)}{}_P F_{n+3/2} \frac{K_l^2}{K_\perp^2}\right) \tag{13a}$$

and

$$x = \frac{K_\perp}{k^{2(n-2)}{}_P F_{n+3/2}} + 2K_l - \frac{K_l K_r}{K_\perp} \approx \frac{K_\perp}{k^{2(n-2)}{}_P F_{n+3/2}} \tag{13b}$$

These represent respectively, the electromagnetic and electrostatic solutions. When $n > 2$, a schematic drawing is given in Fig.1a to 1d for the four possible situations, namely

---

3. Yu.N. Dnestrovskii, D.P. Kostomarov and N.V. Skrydlov, Sov.Phys. Tech.Phys. 8 691 (1964). The sign of the imaginary part of F is incorrectly given as positive. It should be negative as discussed in Ref.1.

(i) $K_{1,r,\perp} > 0$ (ii) $K_{1,r,\perp} < 0$ (iii) $K_{1,\perp} > 0$, $K_r < 0$ (iv) $K_1 > 0$, $K_{r,\perp} < 0$ (14)

or

(i) $\omega_L < \omega_T < \omega_R < n\omega_b$ (ii) $n\omega_b < \omega_L < \omega_T < \omega_R$ (iii) $\omega_L < \omega_T < n\omega_b < \omega_R$

(iv) $\omega_L < n\omega_b < \omega_T < \omega_R$, where $\omega_{L,R,T}$ are the ω values for which $K_{1,r,\perp} = 0$ respectively:

$$\omega_{L,R} = (\mp \omega_b/2) + (\omega_b^2/4 + \omega_p^2)^{\frac{1}{2}} \quad \text{and} \quad \omega_T = (\omega_p^2 + \omega_b^2)^{\frac{1}{2}}$$

The first solution in Eq.(13a) only exists if $K_1 K_r/K_\perp$ is positive and then it represents the Appleton-Hartree equation (extraordinary mode) $k^2c^2/\omega^2 = x = K_1 K_r/K_\perp$ with a small correction term (for $n > 2$). One notes from Eq.(13a) that for $\omega \geq n\omega_b$, $x < K_1 K_r/K_\perp$ since $F > 0$ whereas for $\omega << n\omega_b$, F is more or less real and negative so that $x > K_1 K_r/K_\perp$ (see Fig.1 of Ref.3). Hence the dispersion curves have a very small "wiggle" around $n\omega_b$ for $n > 2$ as illustrated in the left-hand parts of Figs. 1a and 1d. The slope $\partial\omega/\partial k$ at $\omega = n\omega_b$ is altered negligibly by the warm terms for $n > 3$.

When $n = 2$, the change in dispersion is significant. The "warm" term gives the dominant contribution to the slope at $\omega = n\omega_b$ since it is larger than the "cold" part by c^2/v_t^2. Using $dF_{7/2}/d(\mu\delta) = -4/15$, we have $(\partial\omega/\partial k)/(\omega/k) = 15(K_\perp v_t \omega_b/K_1 c\omega_p)^2$ at $\omega = 2\omega_b$. Hence the slope is very minute at this point, changing greatly as ω recedes from $2\omega_b$ towards the Appleton-Hartree values. The behaviour as the real part (k_r) of k goes to zero is more difficult to sort out and more investigation is required. When K_r is negative, we conjure that $\omega \to 2\omega_b$ as $k_r \to 0$ and the imaginary (k_i) of k remains finite and is given by the solution of Eq.(11) with $F_{7/2} = 2/5$ and $x = -k_i^2$.

Upon substituting Eq.(7) into Eq.(11), we obtain the dispersion equation for $n = 1$, namely

$$2K_1 - x = \left[2K_1 - (K_1 + 1)x \right] \omega^2 v_t^2/\omega_p^2 c^2 F_{5/2} \qquad (15)$$

Since $|F_{5/2}|$ is of order one in the region of $\omega = \omega_b$, x is localized around $2K_1$, viz. $x \approx 2K_1 + K_1^2 2\omega^2 v_t^2/\omega_p^2 c^2 F_{5/2}$. The warm term provides a negligible correction of the opposite sign to that in Eq.(13a). This solution exists only if $K_1 > 0$.

We now investigate the other branch of the dispersion curve associated with the solution in Eq.(13b). This solution occurs for large values of x when $n > 2$. When $n = 1$, Eq.(15) shows that no extra solutions exist for $x >> 1 >> \lambda$ so that this electrostatic mode does not exist. Using Eq.(3d) for P, Eq.(13b) can be written as

$$k^{2(n-1)} = \frac{v_t^2}{c^2}\left(\frac{\omega_b^2}{v_t^2}\right)^{n-1}\left(\frac{\omega}{n\omega_b}\right)^2\left[\frac{\omega_b^2}{\omega_p^2} - \frac{\omega_b^2}{\omega^2 - \omega_b^2}\right]\frac{2^n n!}{F_{n+3/2}} \qquad (16)$$

We thus see that $k \propto F^{-1/[2(n-1)]}$. Using the plot[3] of complex F versus $\mu\delta$, we present here in Figs. 2a and 2b, polar plots of F^{-1} and $F^{-1/[2(n-1)]}$. The latter can be used to give the variation of k_r versus $\mu\delta$ when $K_\perp > 0$ or $\omega > \omega_T$. In the opposite situation when $K_\perp < 0$ or $\omega < \omega_T$, we present in these figures, plots involving $(-F)^{-1}$ and $(-F)^{-1/[2(n-1)]}$, taking the root in the sector which gives positive k_i and negligible dampling for large $-k_r$. The dispersion curves are shown on the right-hand sides of Figs. 1a-d. The dashed portions of the curve are the regions where k is quite complex. Figs. 1a-d show a minimum value for the real part of k or λ below which the dispersion relation cannot be satisfied for $n \geq 3$. This minimum value is much larger than the k_r values associated with the extraordinary em mode. Note that for $n = 2$, the angle $\pi/2(n-1) = \pi/2$, and Fig.2b indicate that no such minimum exists. If $K_\perp < 0$ one can obtain very low values of k_r with non-infinite damping. A detailed analysis is necessary to see if the em and es waves can join, but this will not be done here.

Let us now evaluate the group velocity of the es mode when $K_\perp > 0$ at the point $\omega = n\omega_b$. Write k equal to $F^{-1/[2(n-1)]}$ times a factor which is more or less constant with respect to ω. That is, we assume that the crucial variation in ω is due to F. We find using $\partial k/\partial\omega = 1/(\partial\omega/\partial k)$ that

$(\partial\omega/\partial k)/(\omega/k) = 2(n-1)(n-\frac{1}{2})\ v_t^2/c^2$ at $\omega = n\omega_b$. Also since $\partial^2 k/\partial\omega^2 = -(\partial^2\omega/\partial k^2)/(\partial\omega/\partial k)^3$ and $d^2F_{n+3/2}\Big/d(\mu\delta)^2 = 2(n^2-\frac{1}{4})^{-1}(n-3/2)^{-1}$ at $\omega = n\omega_b$, we can evaluate the next derivative to obtain $(\partial^2\omega/\partial k^2)/(\omega/k^2) = 4(n-1)(n-\frac{1}{2})^3 v_t^2/(n-3/2)c^2$. These relations indicate that the slope and curvature of the es mode are very small. The slope only becomes large in the immediate vicinity of the turn around point where k is quite complex.

We also look at the nonrelativistic limit for F of the form $(\mu\delta)^{-1}$, i.e. $F = \omega v_t^2/[c^2(\omega - n\omega_b)] = 2\omega^2 v_t^2/[c^2(\omega^2 - n^2\omega_b^2)]$. The latter expression includes $-\omega$ values as well, and applies outside of the relativistic range at both ends of the em solution, but only when $\mu^{-1} << |\delta| << 1$ for the es-solution. In the latter case, one can write using Eq.(16)

$$\frac{\omega^2 - n^2\omega^2}{2\omega^2} = \left(\frac{v_t k}{\omega_b}\right)^{2(n-1)} \left(\frac{n\omega_b}{\omega}\right)^2 \frac{1}{2^n n!} \left[\frac{\omega_b^2}{\omega_p^2} - \frac{\omega_b^2}{\omega^2 - \omega_b^2}\right]^{-1}$$

which is the usual relation quoted for the Bernstein[4] es mode when $\lambda << 1$.

Besides the extraordinary wave, we have the ordinary wave. When $k_\parallel = 0$, its dispersion relation is simply

$$\varepsilon_{33} = 0 \quad \text{or} \quad \frac{\omega_b^2}{\omega_p^2} \frac{2^n n!}{\lambda^{n-1} F_{n+3/2}} = \frac{x}{\left(1 - \frac{\omega_p^2}{\omega^2}\right) - x} \tag{17}$$

where $\lambda = k^2 v_t^2/\omega_b^2$ and $x = k^2c^2/\omega^2$. Because of the bound character of $|F|$ for real ω near $n\omega_b$, a solution exists for $n > 1$ (including $n = 2$) only when $\omega^2 \geq \omega_p^2$, i.e. when the denominator on the right-hand side is near zero. One can readily show that a wiggle occurs in the dispersion curve similar to that for the extraordinary wave and that the deviation of k from the $x = 1 - \omega_p^2/\omega^2$ curve is very small.

The obvious conclusion from Fig.1 is that no direct coupling when $\lambda << 1$

4. I.B. Bernstein, Phys.Rev. 109, 10 (1958).

exists between em and es waves at cyclotron harmonics for real ω. The only coupling point occurs at ω_T, which we have not considered. Here no gap exists and the em wave converts to an es wave as k increases.

When n = 1, the Appleton-Hartree solution experiences a large "wiggle" around ω_b. Neglecting higher order λ terms (viz. $\lambda F_{9/2} << 1$), Eq.(17) is valid for n = 1 also and we obtain $x = [1 - \omega_p^2/\omega_b^2] \; / \; [1 + \omega_p^2 \, F_{7/2}/2\omega_b^2]$. At $\omega = \omega_b$, $F_{7/2} = {}^2/_5$. This equation has previously been derived by Dnestrovskii et al[3] and Gershman[5].

(b) Real k, Complex ω Dispersion Curves

In contrast to the real ω situation, a slightly complex frequency permits dispersion for all k values except a tiny region near k = 0. The reason for this is that F becomes very large for complex ω (see Fig.4 of Ref.1) and the k variation in Eqs.(11), (16) and (17) can become large. We neglect the imaginary part (ω_i) of ω in $K_\perp$, K_l, K_r etc. The importance of ω_i arises only in the argument of the F function where it may become comparable to $\omega_r - n\omega_b$, whereas in the K functions it need only be negligible compared to ω_r, the real part of ω. Thus, provided F is made real, k will also be practically real.

Let us consider the four possible situations given in Eq.(14) for the dispersion curves. These are illustrated in Figs. 3a to 3d.

For the high-frequency case in Fig. 3a, K_l, K_r and $K_\perp$ are positive and $K_l > K_r$ or $n\omega_b > \omega_R > \omega_T > \omega_L$. The solution for the combined extraordinary-plasma wave is that given in Eq.(11) with the correction from Eq.(10) when $x \approx 2K_l$. We also require the plot of F versus ω_r given in Figs. 3 and 4 of Ref.1. We can follow the Bernstein

---

5. B.N. Gershman, Sov.Phys. - Doklady 6, 314 (1961)

es mode from large to small λ up to $\omega = n\omega_b$ using real ω, real k and the real positive branch of F. As k further decreases, we continue using Eq.(16) along this positive branch, passing through a minimum $\omega_r < n\omega_b$ value when $\partial k/\partial\omega_r = \infty$ or $\partial F/\partial\omega_r = \infty$ in Fig.3 of Ref.1. Then the curve passes again through $\omega_r = n\omega_b$. The frequency rises steadily above $n\omega_b$ as k decreases and $x \to 2K_1$ since F appears to be infinite at this point according to Eq.(11). However, Eq.(10) limits the maximum values that F and ω attain. Essentially around $x = 2K_1$, coupling occurs between the $F > 0$ and $F < 0$ branches which accounts for the awkward behaviour. For values of $x < 2K_1$, we therefore shift to the $F < 0$ track and the dispersion curve connects with the em wave when $\omega \ll n\omega_b$. On the opposite side of the Appleton-Hartree solution, we again use the $F > 0$ track. We follow the same behaviour as for the es mode, with ω decreasing slightly below $n\omega_b$ and rising again. A remarkable result is that near $k = 0$, F becomes larger and larger resulting in ω increasing more and more above $n\omega_b$ rather than tending to $n\omega_b$. As ω increases above $n\omega_b$ by an appreciable fraction of $n\omega_b$, our analysis which restricts ω to be near $n\omega_b$ fails. A full investigation of what actually happens then, is beyond the scope of this work and is actually not necessary for further analysis.

The low-frequency case, shown in Fig.3b, is for $K_1 < 0$, $K_r < 0$, $K_\perp < 0$ and $|K_r| > |K_1|$ or $n\omega_b < \omega_L < \omega_T < \omega_R$. For large k values, we must choose the $F < 0$ track and, since no Appleton-Hartree solution exists, we follow this track for all lower k values as shown in Fig.3b.

The high-intermediate-frequency situation in Fig.3c is for $K_1 > 0$, $K_r < 0$, $K_\perp > 0$ with $K_1 > |K_r|$ or $\omega_L < \omega_T < n\omega_b < \omega_R$. For large k, we must use the $F > 0$ track which can be followed for lower k values up to $x \approx 2K_1$. At $x = 2K_1$, we apply the correction in Eq.(10). For $x < 2K_1$, we change to the $F < 0$ track and continue for all lower k values.

When $K_1 > 0$, $K_r < 0$, $K_\perp < 0$ with $|K_r| > K_1$ or $\omega_L < n\omega_b < \omega_T < \omega_R$ (the low-intermediate-frequency situation), the Appleton-Hartree solution $x = K_1 K_r / K_\perp$ occurs at a higher x value than $x = 2K_1$. This case is illustrated in Fig.3d. For large k values we require the $F < 0$ track which connects to the Appleton-Hartree solution as shown in Fig.3d. Between $x = K_1 K_r / K_\perp$ and $x = 2K_1$, we use the $F > 0$ track and for $x < 2K_1$ we use the $F < 0$ track.

In all four cases, the large-k portions of the curve make a smooth transition to the appropriate well known electrostatic cyclotron harmonic mode (sometimes called a Bernstein mode[4]).

The above formulation applies to $n = 2$ as well except that the excursion from the Appleton-Hartree solution occurs for larger values of $\omega - n\omega_b$ and it connects up sooner with the es mode.

For $n = 1$, ω_b has a negligible effect. Equation (15) shows that for a large excursion from the Appleton-Hartree solution, $F_{5/2}$ must become exceedingly small (rather than large as for $n > 1$). Since F cannot go to zero before going to ∞ (see Fig.3 of Ref.1), the dispersion curve for complex ω is about the same as for real ω, viz. $x = 2K_1$ and only exists if $K_1 > 0$ (See Fig.4).

In Figs.3e and 3f, we show the additional wave given by Eq.(12) which has different behaviours depending on K_1 greater or less than zero. When $K_1 < 0$, one requires negative F values, and when $K_1 > 0$, a transition occurs from $F < 0$ for $x > 2K_1$ to $F > 0$ values for $x < 2K_1$. These waves are not included in the combined plots in Figs. 4-7.

In Figs.4-6, we provide schematic plots of ω versus k including several harmonics on each plot for ratios of ω_p^2/ω_b^2 ranging from 0 to 2 (Fig.4), $n(n+1)$ to $n(n+2)$ (Fig.5) and $n(n+2)$ to $(n+1)(n+2)$ (Fig.6). These include all possible combinations and can be readily adopted to topside ionospheric conditions. These plots are obtained by making use of our previous results in Fig.3.

Figure 7 shows corresponding curves for the ordinary wave, and the inserts show sample conditions around $n\omega_b$ when $\omega \gtrless \omega_p$ respectively. Equation (17) (valid for $n = 1$ also) shows that if $\omega > \omega_p$ one needs $F < 0$ for large x values, $x > (1 - \omega_p^2/\omega^2)$, and $F < 0$ for $x < (1 - \omega_p^2/\omega^2)$. If $\omega < \omega_p$, one can follow the $F < 0$ track for all k values.

IV. NONRELATIVISTIC ANALYSIS

To obtain[1] the nonrelativistic formulation, we replace everywhere above the function $\rho + \beta k_\parallel^2$ or F by $-v_t \omega Z / k_\parallel c^2 \sqrt{2}$. If we then apply the Z-plasma dispersion function, we get a completely different picture. This formulation can be done improperly by assuming that the ad-hoc approximation $Z \approx -\zeta^{-1}$ where $\zeta = (\omega - n\omega_b)/k_\parallel v_t \sqrt{2}$, applies even for very small $k_\parallel$ values. In Ref.1, Eq.(23), we have shown that this approximation is limited to $|\mu^2\delta^2| \gg |2\mu k_\parallel^2 c^2/\omega^2| \gg |4\mu\delta| \gg 1$ and to values of $|\omega v_t Z / c^2 k_\parallel| < 1$. However, the nonrelativistic results show that we need for $n > 2$, values of $|\mu\delta| \ll 1$ and $|\omega v_t Z / c^2 k_\parallel| > 1$ in the transition region between the Appleton-Hartree solution and the electrostatic solution as well as for very small values of $k_\perp$ less than the Appleton-Hartree values. This formulation is therefore incorrect in these regions. At the end of this section, we present the proper nonrelativistic formulation. At first, we look at the results obtained by adopting the above ad-hoc nonrelativistic limit, which in Eq.(18) includes $-\omega$ values as well:

$$F_q \rightarrow \frac{v_t \omega}{c^2 k_\parallel \sqrt{2}} \left(\frac{k_\parallel v_t \sqrt{2}}{\omega - n\omega_b} + \frac{k_\parallel v_t \sqrt{2}}{\omega + n\omega_b} \right) = \frac{2v_t^2}{c^2} \frac{\omega^2}{\omega^2 - n^2\omega_b^2} \qquad (18)$$

In Eq.(10) we again neglect higher order λ terms except for the last product $(k_\perp^{4(n-2)})$ - term. The equation for $\omega^2 - n^2\omega_b^2$ becomes

$$(\omega^2 - n^2\omega_b^{\,2})^2(K_\parallel K_r - xK_\perp) - (\omega^2 - n^2\omega_b^{\,2})(2K_\parallel - x)2\omega_p^{\,2}\,\frac{\lambda^{n-1}n^2}{2^n n!} + \frac{4\omega_p^{\,4}\lambda^{2n}n^2}{(n+1)2^{2n}(n!)^2} = 0$$

where we used the expression for P in Eq.(3d). Solving the above equation for $\omega^2 - n^2\omega_b^{\,2}$ yields with the definitions of $K_\parallel$, K_r and $K_\perp$ in Eq.(5):

$$\omega^2 - n^2\omega_b^{\,2} \approx \frac{4\omega_p^{\,2}n^2\lambda^{n-1}}{K_r n!2^n}\left[1 - \frac{k_\perp^{\,2}c^2}{2\omega^2 K_\parallel}\right]\Big/\left[1 - \frac{k_\perp^{\,2}c^2}{\omega^2}\,\frac{K_\perp}{K_\parallel K_r}\right] \tag{19a}$$

and

$$\omega^2 - n^2\omega_b^{\,2} \approx \frac{\omega_p^{\,2}\lambda^{n+1}}{K_\parallel(n+1)n!2^n}\Big/\left[1 - \frac{k_\perp^{\,2}c^2}{2\omega^2 K_\parallel}\right] \tag{19b}$$

These two solutions are decoupled provided $k_\perp^{\,2}c^2/\omega^2$ is not near $2K_\parallel$.

We note that Eq.(19a) is the equivalent of Eq.(11) as is evident upon substituting Eqs.(18) and (3d). In addition we have succeeded in deriving a third wave given by (19b). Since for this wave $\omega^2 - n^2\omega_b^{\,2} \sim \lambda^{n+1}$, the $\omega - k_\perp$ dispersion curve is very much localized around $\omega \approx n\omega_b$ and never deviates appreciably from $n\omega_b$ except near coupling points between it and the other waves. This is the localized third wave which appears in the calculation of Dnestrovskii and Kostomarov[2] using nonrelativistic analysis. We note, however, from Eqs.(19a,b) that $|\omega^2 - n^2\omega_b^{\,2}| < v_t^{\,2}/c^2$ for $(k_\perp^{\,2}c^2/\omega^2)^{n-1} < (c^2/v_t^{\,2})^{n-2}$ so that the above derivation from nonrelativistic analysis is incorrect. Furthermore, we know from Ref.1 that for F or Z to be large, we require its analytic continuation with $\mathrm{Im}\omega < 0$, and then its form differs from the large values derived from Eq.(18) as $\omega \to n\omega_b$. Actually as F becomes large, ω increases above $n\omega_b$ for $k_\parallel = 0$ (see Fig.3) rather than approaches $n\omega_b$.

As $k_\perp \to 0$, Eqs.(19a,b) yield $\omega^2 - n^2\omega_b^{\,2} = 4\omega_p^{\,2}n^2\lambda^{n-1}/n!2^nK_r$ and $\omega^2 - n^2\omega_b^{\,2} = \omega_p^{\,2}\lambda^{n+1}/(n+1)2^n n!K_\parallel$. When $k_\perp^{\,2}c^2/\omega^2 \gg 1$, the equations give

the Bernstein longitudinal wave $\omega^2 - n^2\omega_b^2 = 2\omega_p^2 n^2 \lambda^{n-1}/n!2^n K_\perp$ plus the additional wave $n^2\omega_b^2 - \omega^2 = 2\omega_p^2 \omega^2 \lambda^{n+1}/(n+1)n!2^n k^2 c^2$.

Near $x_2 = 2K_1$, the n- 1 and n+ 1 waves (viz $\omega^2 - n^2\omega_b^2 \propto \lambda^{n-1}, \lambda^{n+1}$) couple. Also the n - 1 wave couples to the em wave near $x_1 = K_1 K_r/K_\perp$. For the four cases given in Eq.(14). the dispersion curves including the wave coupling are drawn schematically in Figs. 8a to 8d up to values of x beyond x_1 and x_2. The solid curves represent the n - 1 or n + 1 waves and the checked parts refer to coupling regions. The above illustrates the major differences in Fig. 8 as compared to the relativistic equivalents in Fig.3. The above nonrelativistic approach agrees with the relativistic analysis for the Bernstein wave in the region $|(\omega - n\omega_b)/\omega| > v_t^2/c^2$. (Compare with Eq.(16).) The form of this Bernstein es mode for λ of order one is essentially nonrelativistic. As it should, the nonrelativistic theory also provides the correct variation of the Appleton-Hartree waves outside of the $|\mu\delta| < 1$ region, which is according to (19a): $x - K_1 K_r/K_\perp =$
$- (\omega^2 - n^2\omega_b^2)^{-1}(K_1/K_\perp)^2 2\omega_p^2 \lambda^{n-1} n^2/2^n n!$ (Compare this with Eq.(11) with (18) inserted in it.)

We can similarly investigate, using the above theory, the ordinary wave dispersion when $\lambda << 1$. Substituting Eq.(18) into (17) gives $\omega^2 - n^2\omega_b^2 = 2\omega_p^2 \lambda^n/n!2^n(K_\parallel - x)$ where $K_\parallel = 1 - \omega_p^2/\omega^2$.

In Figs.9 to 11, schematic dispersion curves with several harmonic frequencies together are drawn for ω_p^2/ω_b^2 values of 0 to 2 (Fig.9), n(n+1) to n(n+2) (Fig.10) and n(n+2) to (n+1)(n+2) (Fig.11). These curves include the extraordinary, Bernstein and the additional extra mode. Both ω and k are real in this theory. In Fig.12, similar curves are shown for the ordinary wave and the inserts provide sample plots near a harmonic for $K_\parallel \gtrless 0$. Figures 9 to 12 show the behaviour for large λ values as well

and include the three cases actually computed by Dnestrovskii and Kostomarov[2] both for the ordinary and extraordinary waves. These incorrectly derived curves for $\lambda << 1$ differ in many ways from the relativistic versions shown in Fig.4 to 7 and the latter must be applied for $k_{\parallel}$ values near zero. Fortunately, the non-relativistic schematics in Figs.8-12 are still usable in a different region as shown below, although the formulation is completely different.

A <u>proper</u> nonrelativistic analysis, valid for larger $k_{\parallel}$ values (see Ref.1, Eq.(19)) such that $|y^2| >> |2\delta|$, $|y| >> \mu^{-\frac{1}{2}}$ and $|y^2(y^2 - 2\delta)| >> \mu^{-2}$ where $y \equiv k_{\parallel}c/\omega$, can be formulated as follows. As before, we replace everywhere F by $-v_t\omega Z/k_{\parallel}c^2\sqrt{2}$ but we have to differentiate between cases of real ω, complex $k_{\perp}$ and real $k_{\perp}$, complex ω.

For real ω, the plots of $(\mp Z)^{-1}$ will be similar[6] to those of $(\pm F)^{-1}$ shown in Fig.2a, except that the polar plot is symmetric about the origin with the $\mu\delta = 0$ point on the imaginary axis and with both sides asymptotic at $\pm\infty$ to the real axis. The curves are also asymptotic to all sector lines in Fig.2b. As a result, the equivalent curves to Figs.1 for the extraordinary wave show a "wiggle" symmetric about $\omega = n\omega_b (n > 2)$ with noticeable damping at and on each side of $n\omega_b$ and negligible damping away from the resonance. A minimum real $k_{\perp}$ value with noticeable damping even for $\omega > n\omega_b$ occurs for the es mode when $n > 2$ and the $n = 2$ case needs special consideration, as we discussed above for the relativistic analysis.

For real $k_{\perp}$ and complex $\omega = \omega_r + i\omega_i$ values, we use the tracks of real large values of Z for complex argument, given in Ref.1, Eq.(29), viz. $Z = \pm 2\pi e^{y^2}$ and $2xy = \pm\pi/2$ where $x = (\omega_r - n\omega_b)/k_{\parallel}v_t\sqrt{2}$ and $y = \omega_i/k_{\parallel}v_t\sqrt{2}$. Thus, instead of Eq.(18), we use $F \rightarrow \mp (2\pi v_t\omega/k_{\parallel}^2 c\sqrt{2}) \exp\left\{\left[\pi k_{\parallel}v_t/2\sqrt{2}(\omega_r - n\omega_b)\right]^2\right\}$. Note that the larger the value of Z required, the closer ω_r approaches $n\omega_b$, which is opposite to the behaviour of the relativistic F-function. The fact that $-Z \rightarrow \pm\infty$

---

6. B.D. Fried and S.D. Conte, <u>The Plasma Dispersion Function</u>, Academic Press, N.Y. (1961), Figs.1 and 2.

as $\pm(\omega - n\omega_b) \to 0$ makes its behaviour like that of $(\mu\delta)^{-1}$ in Eq.(18). As a result, the schematic dispersion curves will be similar to the incorrect nonrelativistic ones in Figs. 9 to 11 except that cyclotron damping occurs near $n\omega_b$ and the predicted $(\omega - n\omega_b)/\omega$ values are of order v_t^2/c^2 rather than some higher power of v_t^2/c^2. In Fig. 8a-d, the labelling is simplified, using the sign of Z, as shown in brackets. Although the extraordinary and additional waves are coupled, we can easily connect the various coupled regions by following the tracks of $Z < 0$ if $\omega > n\omega_b$, or $Z > 0$ if $\omega < n\omega_b$. It is reasonable to suppose that even if we include the ω_i part in the K functions, we will find very large damping ($\omega_i \to \infty$) at the $\omega_r = n\omega_b$, $k_\perp = 0$ point, in contrast to the real solution obtained from the incorrect nonrelativistic analysis.

Figure 12 for the ordinary wave is, however, changed drastically. The substitution for F given in the previous paragraph does not apply here. The analysis in Section II(c) can be generalized to yield the ordinary wave dispersion equation: $K_\parallel - k_\perp^2c^2/\omega^2 + (\varepsilon_{33})_w - (\varepsilon_{13}^2)_w/(\varepsilon_\parallel)_w$. Applying the nonrelativistic warm elements (Ref. 1, Eq.31) for $n > 1$ results in a cancellation involving $\zeta Z' + (Z')^2/2Z = -Z'/Z \approx 2\zeta$ for large Z values. Thus, $(\varepsilon_{13}^2)_w/(\varepsilon_{11})_w - (\varepsilon_{33})_w = 2\omega_p^2\,\lambda^n\zeta/\omega k_\parallel v_t\sqrt{2}\;2^n n!$, which is always small for $(\omega - n\omega_b) << n\omega_b$. As a result, the solution never deviates much from $k_\perp^2c^2/\omega^2 = K_\parallel$ and in fact, no resonances occur for $n > 1$ and $\lambda << 1$.

In a nutshell, this paper shows that nonrelativistic dispersion theory in the vicinity of cyclotron resonances is incorrect for $\lambda << 1$ and for near zero $k_\parallel$ values. For larger $k_\parallel$ values, but $\lambda << 1$, nonrelativistic theory giving undamped solutions near cyclotron harmonics is not valid. A distinction between complex ω and complex $k_\perp$ values is necessary. We have also pointed out the differences in dispersion effects near $k \to 0$ and in regions where em modes and coupled em and es modes exist, based on relativistic and nonrelativistic approaches.

ACKNOWLEDGEMENTS

The author acknowledges very stimulating discussions with Dr. T.W. Johnston and his many useful leads. This work was supported by the Fields and Plasma Branch of the Goddard Space Flight Center, National Aeronautics and Space Administration, Greenbelt, Maryland under contract NASw-957.

CAPTIONS FOR FIGURES

Figure 1 Schematic dispersion curves for the extraordinary electromagnetic and plasma electrostatic waves for real ω and complex k based on relativistic analysis. Dashed parts indicate very complex k values. k_r is the real part of k_i. Here $x_1 \equiv K_l K_r / K_\perp$ is positive in (a) and (d) and negative in (b) and (c). Figures 1(a) to 1(d) correspond to the cases in Eq.(14). The interval $\Delta\omega/n\omega_b$ is typically of order $10 v_t^2/c^2$. We illustrate cases when $n > 2$. Also

$$\omega\left(\begin{matrix}L\\R\end{matrix}\right) = \mp \frac{\omega_b}{2} + \left(\frac{\omega_b^2}{4} + \omega_p^2\right)^{\frac{1}{2}} \quad \text{or } X = 1 \pm Y \quad \text{or } K\left(\begin{matrix}l\\r\end{matrix}\right) = 0$$

and

$$\omega_T = (\omega_p^2 + \omega_b^2)^{\frac{1}{2}} \quad \text{or } X = 1 - Y^2 \quad \text{or } K_\perp = 0$$

with

$$X = \omega_p^2/\omega_b^2, \quad Y = \omega_b/\omega, \quad K_{l,r} = 1 - \omega_b^2/\omega(\omega \pm \omega_b) \quad \text{and}$$

$$K_\perp = 1 - \omega_p^2/(\omega^2 - \omega_b^2)$$

Figure 2a A schematic polar plot of the complex function F^{-1} and $(-F)^{-1}$ using the analysis in Ref.2 with the correct sign for ImF. The numbers 0 and $\pm\infty$ are values of $\mu\delta$, the argument of F, marked on the polar plot.

2b Schematic polar plot of $F^{-[2(n-1)]^{-1}}$ which is required when $\omega^2 > \omega_T^2$ and of $(-F)^{-[2(n-1)]^{-1}}$ required when $\omega^2 < \omega_T^2$. The root is taken in the sector where its imaginary part is small at $\mu\delta = \pm\infty$ respectively, and is positive, giving a damped wave.

Figure 3 Schematic dispersion curves (Figs. 3(a) to 3(d)) for the coupled extraordinary and electrostatic waves, for $n \geq 2$, complex ω and real wave numbers ($\lambda \ll 1$) based on relativistic analysis. The four figures correspond to those in 1(a) and 1(d). In Fig.3(e) and 3(f) we show schematic dispersion curves for the extra wave (Eq.12) when $K_l \gtrless 0$.

The dashed parts indicate the coupling regions between $F > 0$ and $F < 0$ branches. ω_r refers to the real part of ω, $x_1 \equiv K_1 K_r / K_\perp$ and $x_2 \equiv 2K_1$.

Figure 4 Schematic complex ω-real k dispersion curves from relativistic theory including several harmonics for the coupled extraordinary and plasma waves when $2\omega_b^2 > \omega_p^2$. The two dashed lines indicate approximately the locations of the light and thermal velocity lines.

Figure 5 Same as Figure 4 when $n(n+2)\omega_b^2 > \omega_p^2 > n(n+1)\omega_b^2$ with $n \geq 1$. For $n = 1$, omit dispersion effects shown below ω_L. Also for $n = 1$, the hump near ω_T occurs much nearer to the light line and this wave based on es theory appears as backward instead of starting as the forward wave shown here.

Figure 6 Same as Figure 4 when $(n+1)(n+2)\omega_b^2 > \omega_p^2 > n(n+2)\omega_b^2$ with $n \geq 1$. For $n = 1$, omit dispersion effects shown below ω_L.

Figure 7 Schematic complex ω-real k dispersion curves from relativistic theory including several harmonics for the ordinary wave with $n \geq 1$. For $n = 1$, omit dispersion curves below ω_p. For a given $n > 1$, omit dispersion curves below ω_b. The inserts show sample dispersion effects near cyclotron harmonics when $\omega \gtrless \omega_p$.

Figure 8 Nonrelativistic version of the dispersion curves for the coupled extraordinary and plasma waves. The four cases (Figs.8a to 8d) correspond to (a) to (d) in Figs. 1 or 3. The checked portions on the curves indicate coupling regions between the waves. In incorrectly applied nonrelativistic theory, the waves vary as $\omega - n\omega_b \propto \lambda^{n-1}$ or λ^{n+1} and the designations $n-1$ and $n+1$ refer to these. The

designations $Z \gtrless 0$ refer to properly applied nonrelativistic theory as discussed towards the end of the text. In properly applied nonrelativistic theory, replace here and in Figs. 9-12, ω by ω_r and remember that very strong damping occurs at the cyclotron harmonic cutoffs. The curves shown are for $n \geq 2$.

Figure 9 Nonrelativistic schematic version of the dispersion curves including several harmonics for the coupled extraordinary and plasma waves when $2\omega_b^2 > \omega_p^2$. The dashed line is the approximate location of the light line.

Figure 10 Same as Figure 9 when $n(n+2)\omega_b^2 > \omega_p^2 > n(n+1)\omega_b^2$ with $n \geq 1$. For a given $n \geq 1$, omit all dispersion curves below the one localized just below ω_b. For $n = 1$, the hump near ω_T occurs much nearer to the light line and this wave based on es theory appears as backward instead of starting as the forward wave shown here.

Figure 11 Same as Figure 9 when $(n+1)(n+2)\omega_b^2 > \omega_p^2 > n(n+2)\omega_b^2$ with $n \geq 1$. For a given $n \geq 1$, omit all dispersion curves below the one localized just below ω_b.

Figure 12 Nonrelativistic dispersion curves for the ordinary wave with $n \geq 1$. For $n = 1$, omit dispersion curves below ω_p. For a given $n > 1$, omit dispersion curves below ω_b. The inserts show sample dispersion effects near cyclotron harmonics when $\omega \gtrless \omega_p$.

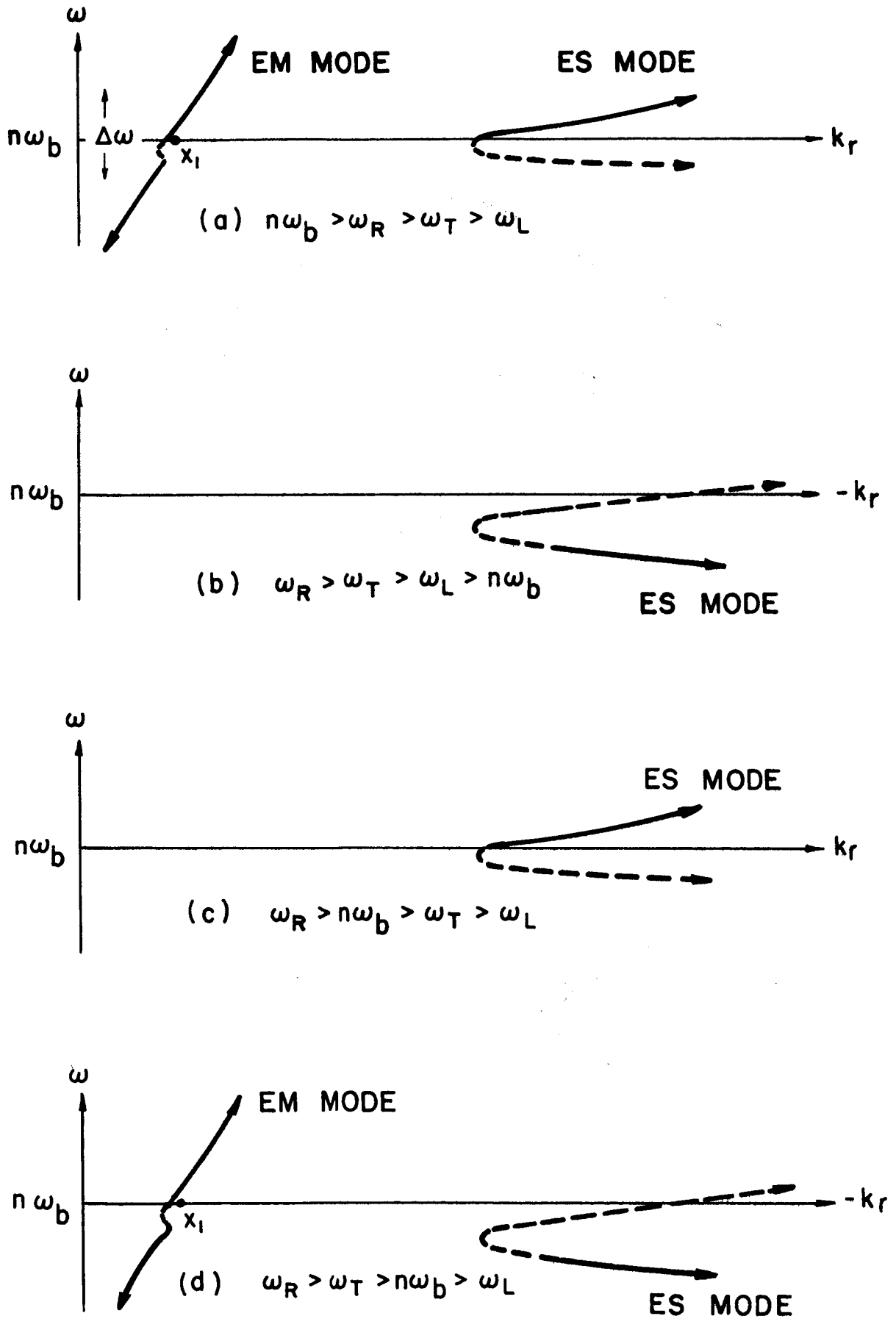
ω
EM MODE
ES MODE
nω_b
Δω
x_1
k_r
(a) nω_b > ω_R > ω_T > ω_L
ω
nω_b
-k_r
(b) ω_R > ω_T > ω_L > nω_b
ES MODE
ω
ES MODE
nω_b
k_r
(c) ω_R > nω_b > ω_T > ω_L
ω
EM MODE
nω_b
x_1
-k_r
(d) ω_R > ω_T > nω_b > ω_L
ES MODE

FIG. 1

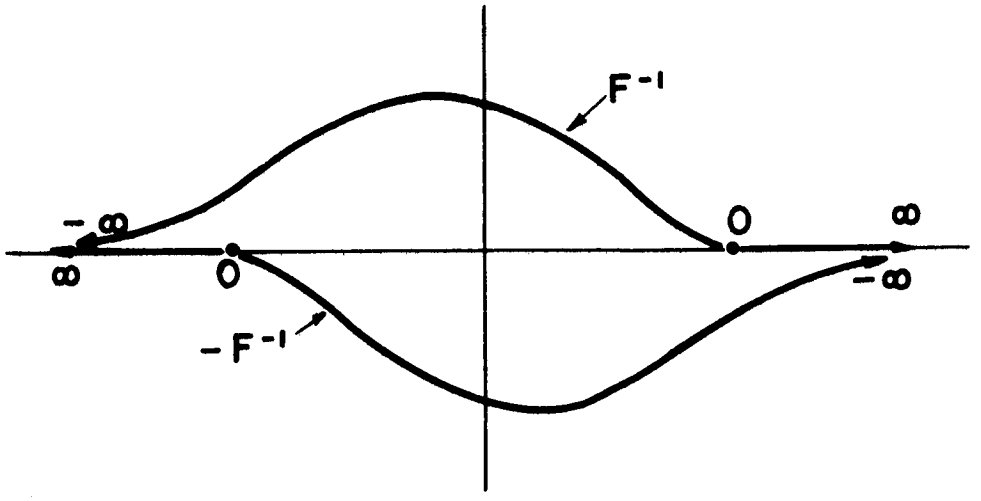
F^{-1}
$-\infty$
∞
0
0
∞
$-\infty$
$-F^{-1}$

(a)

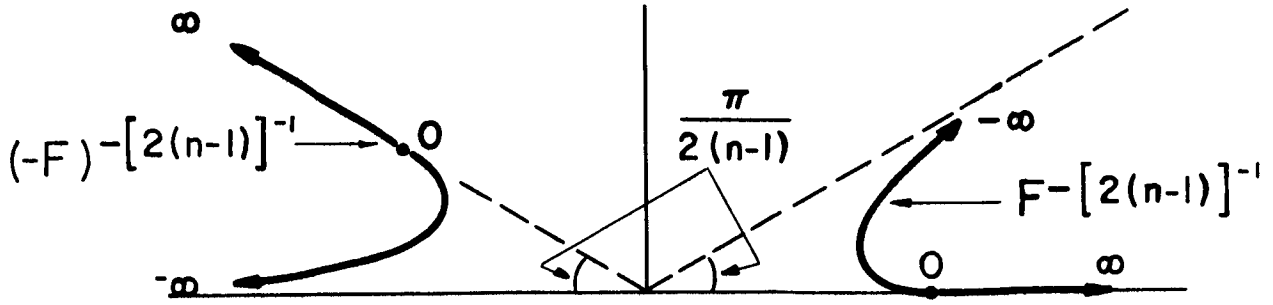
∞
$(-F)^{-}[2(n-1)]^{-1}$
0
$-\infty$
$\frac{\pi}{2(n-1)}$
$-\infty$
$F^{-}[2(n-1)]^{-1}$
0
∞

(b)

FIG. 2

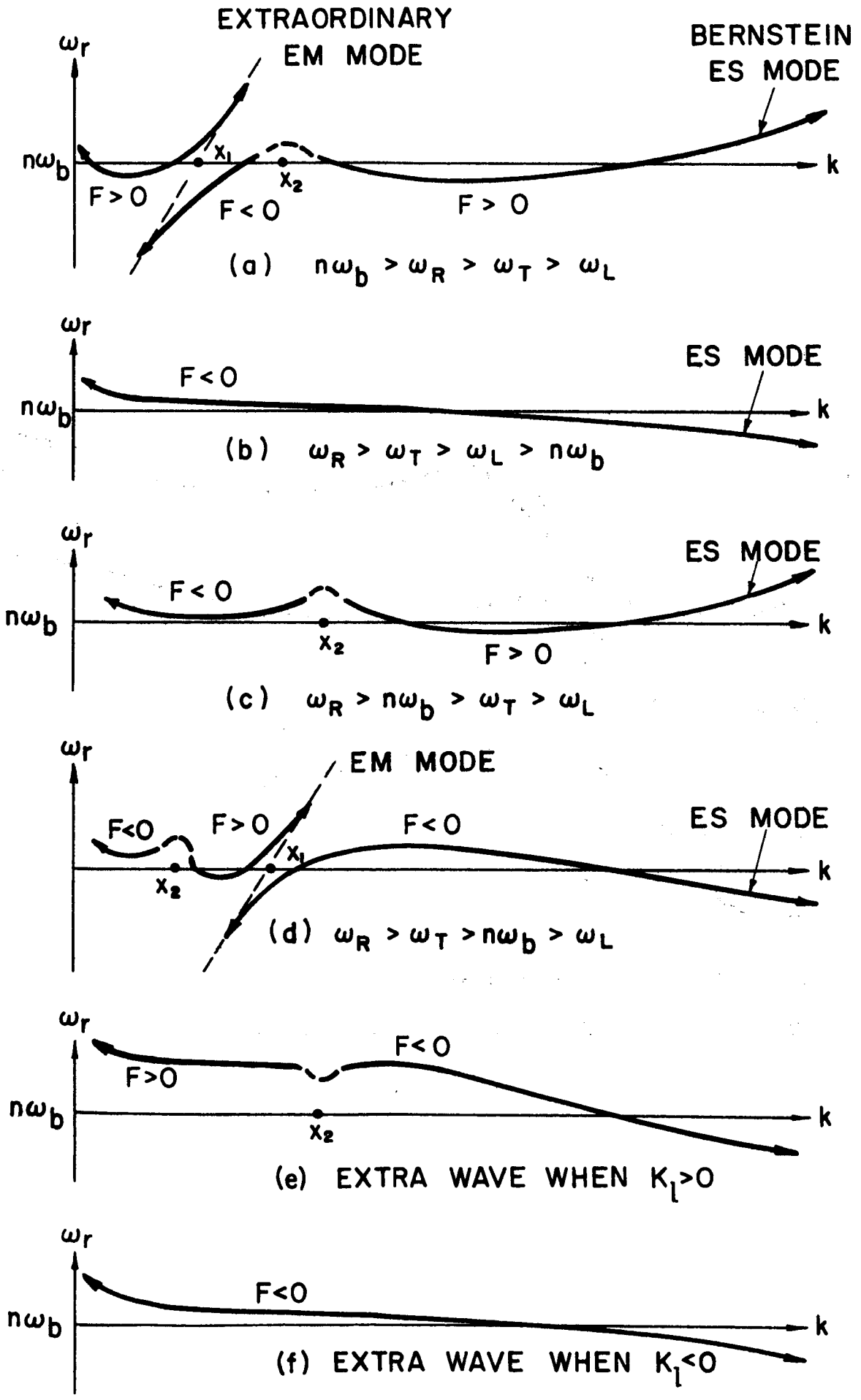
EXTRAORDINARY
EM MODE
BERNSTEIN
ES MODE
ωr
nωb
k
x1
x2
F > 0
F < 0
F > 0
(a) nωb > ωR > ωT > ωL
ωr
ES MODE
F < 0
nωb
k
(b) ωR > ωT > ωL > nωb
ωr
ES MODE
F < 0
nωb
x2
k
F > 0
(c) ωR > nωb > ωT > ωL
ωr
EM MODE
F<0
F>0
F<0
ES MODE
x2
x1
k
(d) ωR > ωT > nωb > ωL
ωr
F<0
F>0
nωb
x2
k
(e) EXTRA WAVE WHEN K1>0
ωr
F<0
nωb
k
(f) EXTRA WAVE WHEN K1<0

FIG. 3

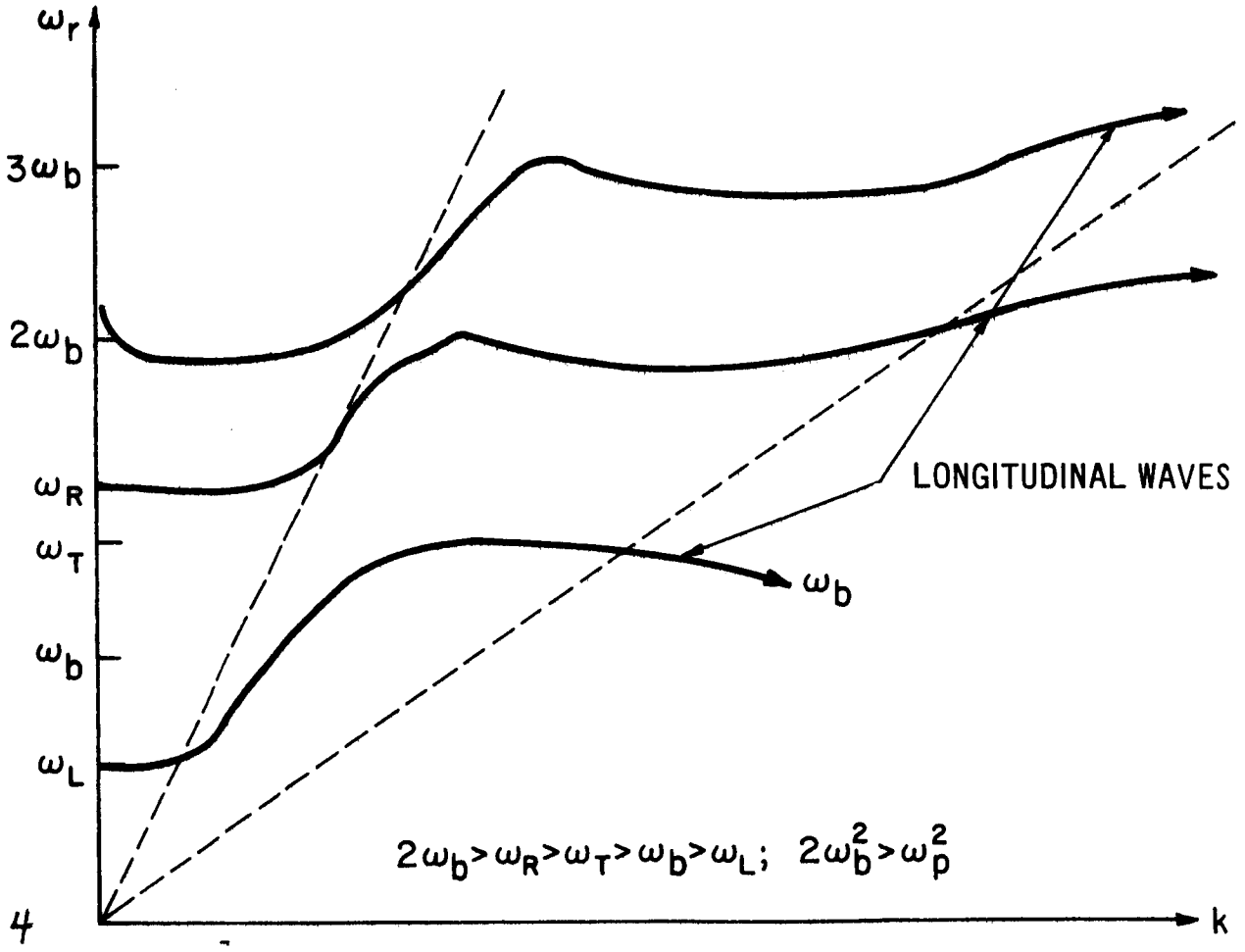
ω_r
$3\omega_b$
$2\omega_b$
ω_R
ω_T
ω_b
ω_L
LONGITUDINAL WAVES
ω_b
$2\omega_b > \omega_R > \omega_T > \omega_b > \omega_L$; $2\omega_b^2 > \omega_p^2$
k

FIG. 4

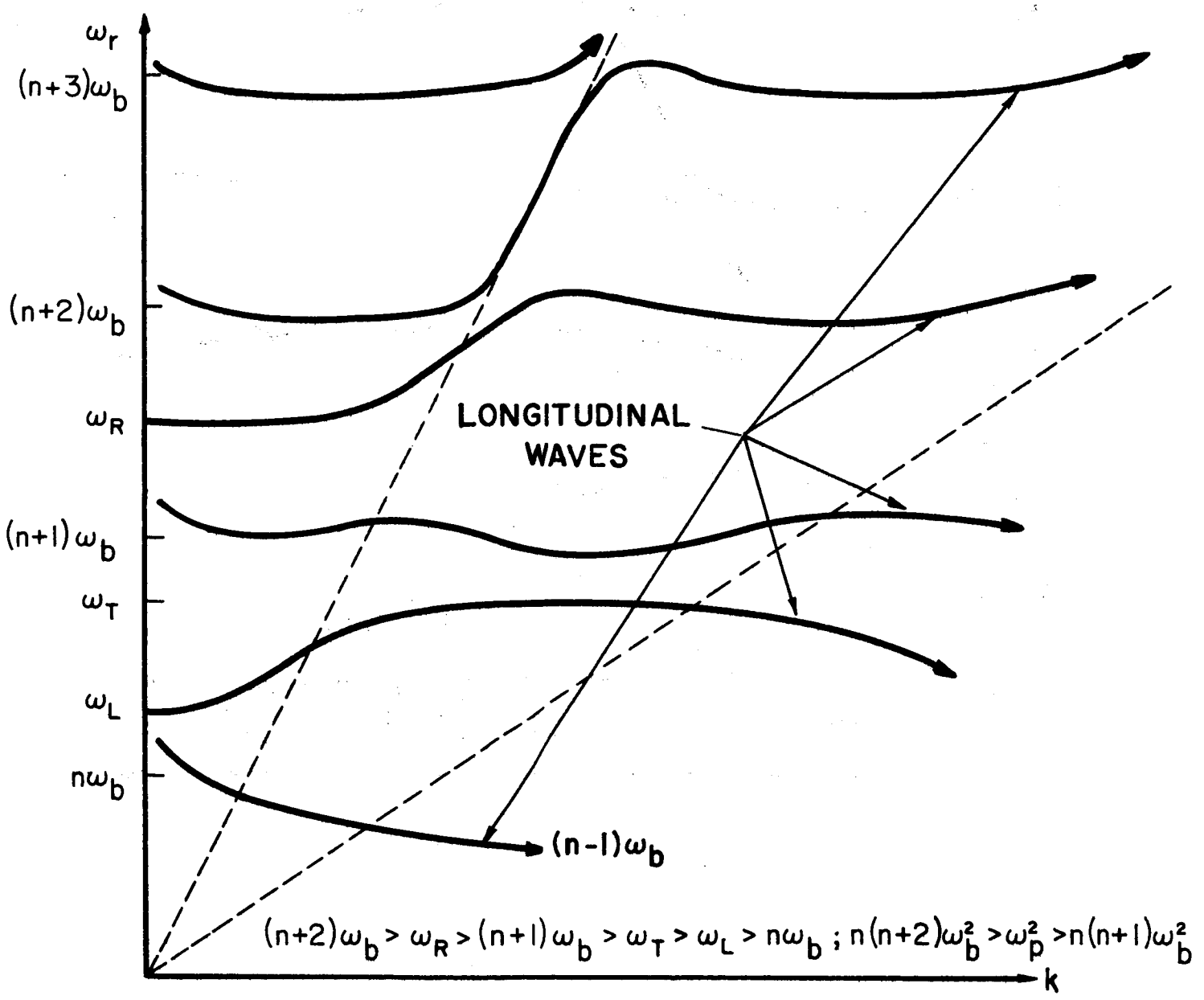
ω_r
$(n+3)\omega_b$
$(n+2)\omega_b$
ω_R
$(n+1)\omega_b$
ω_T
ω_L
$n\omega_b$
LONGITUDINAL WAVES
$(n-1)\omega_b$
$(n+2)\omega_b > \omega_R > (n+1)\omega_b > \omega_T > \omega_L > n\omega_b$; $n(n+2)\omega_b^2 > \omega_p^2 > n(n+1)\omega_b^2$
k

FIG. 5

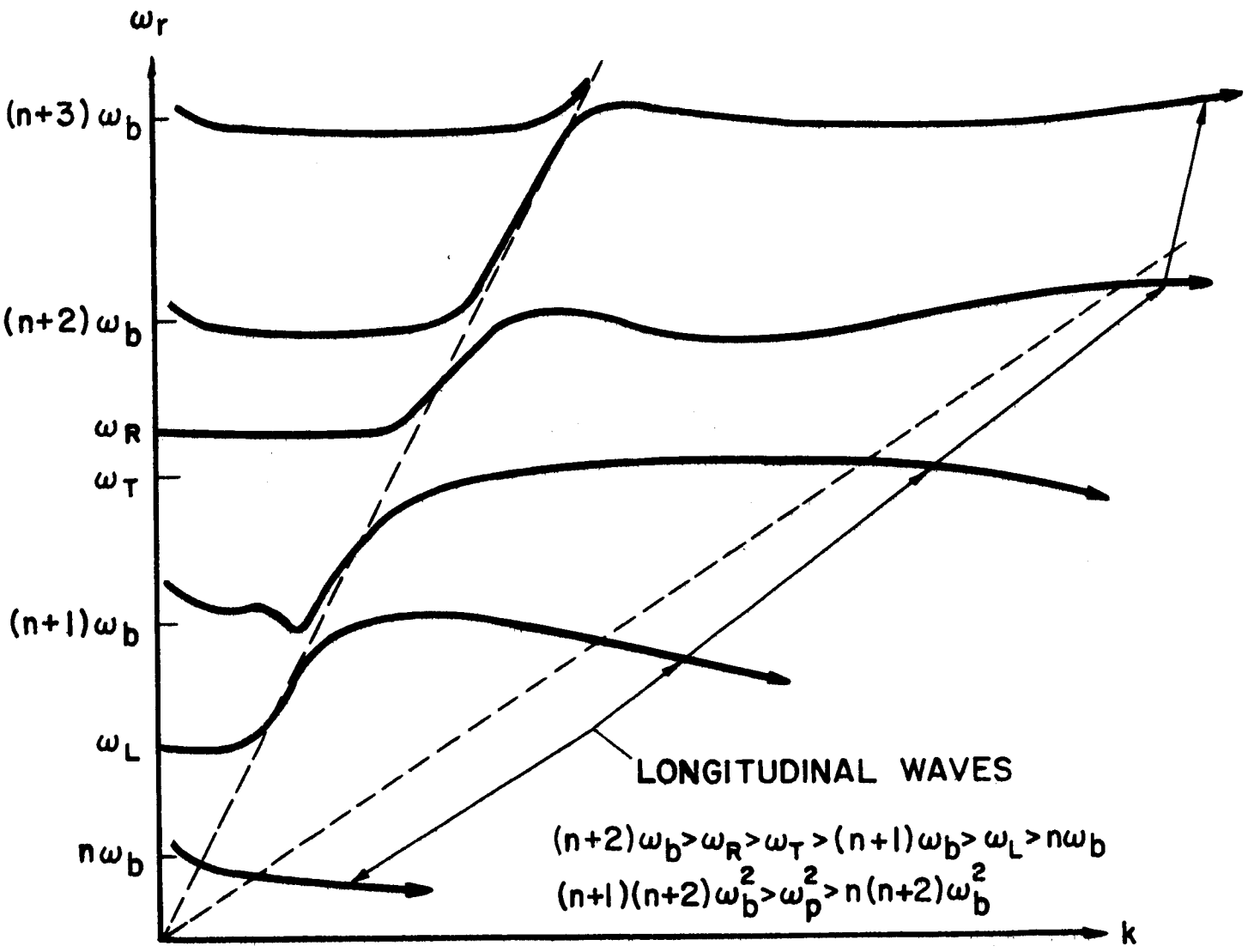
ω_r
$(n+3)\,\omega_b$
$(n+2)\,\omega_b$
ω_R
ω_T
$(n+1)\,\omega_b$
ω_L
$n\omega_b$
LONGITUDINAL WAVES
$(n+2)\omega_b > \omega_R > \omega_T > (n+1)\omega_b > \omega_L > n\omega_b$
$(n+1)(n+2)\omega_b^2 > \omega_p^2 > n(n+2)\omega_b^2$
k

FIG. 6

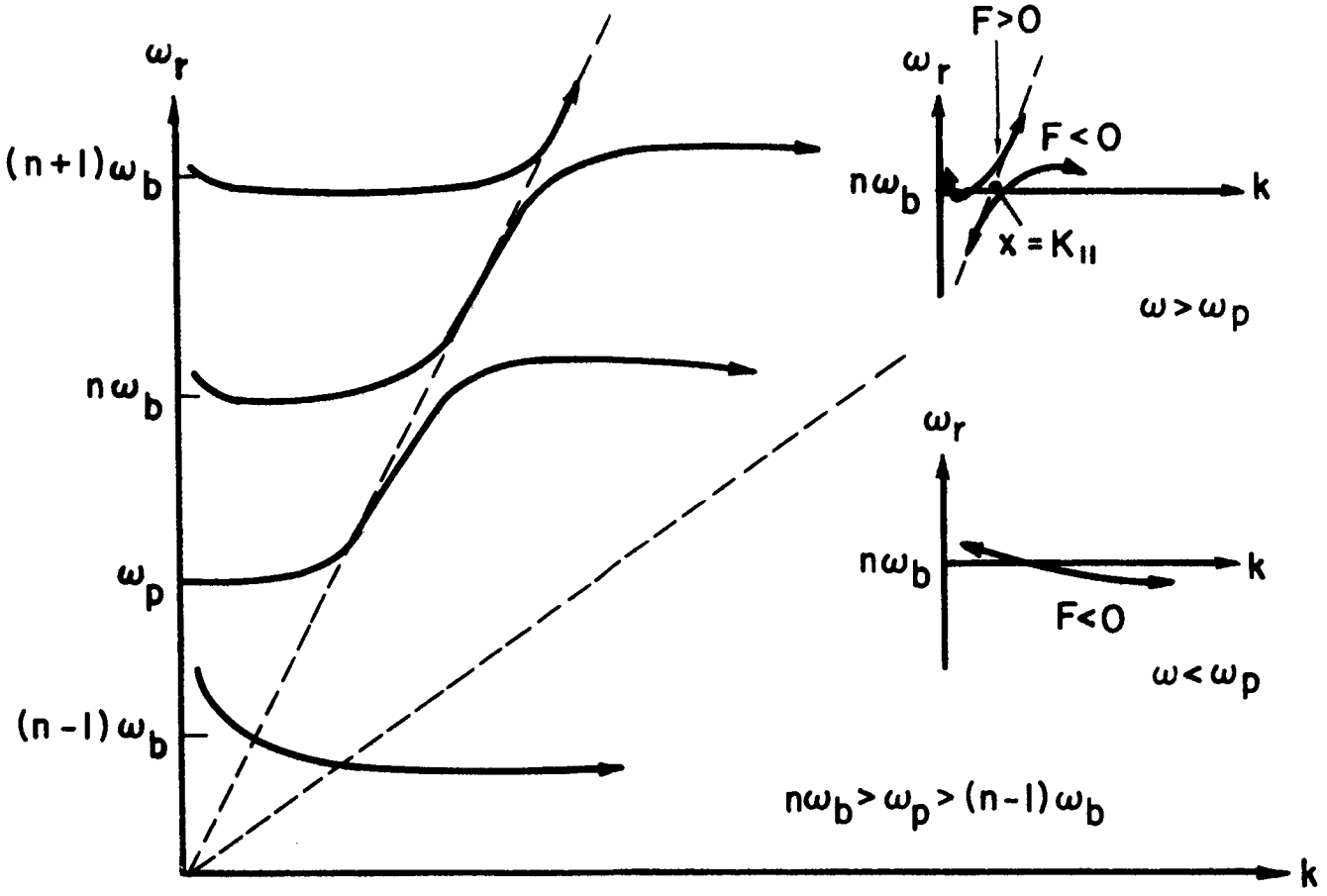
ω_r
$(n+1)\omega_b$
$n\omega_b$
ω_p
$(n-1)\omega_b$
k
F>0
F<0
$x = K_{\parallel}$
$\omega > \omega_p$
$\omega < \omega_p$
$n\omega_b > \omega_p > (n-1)\omega_b$

FIG 7

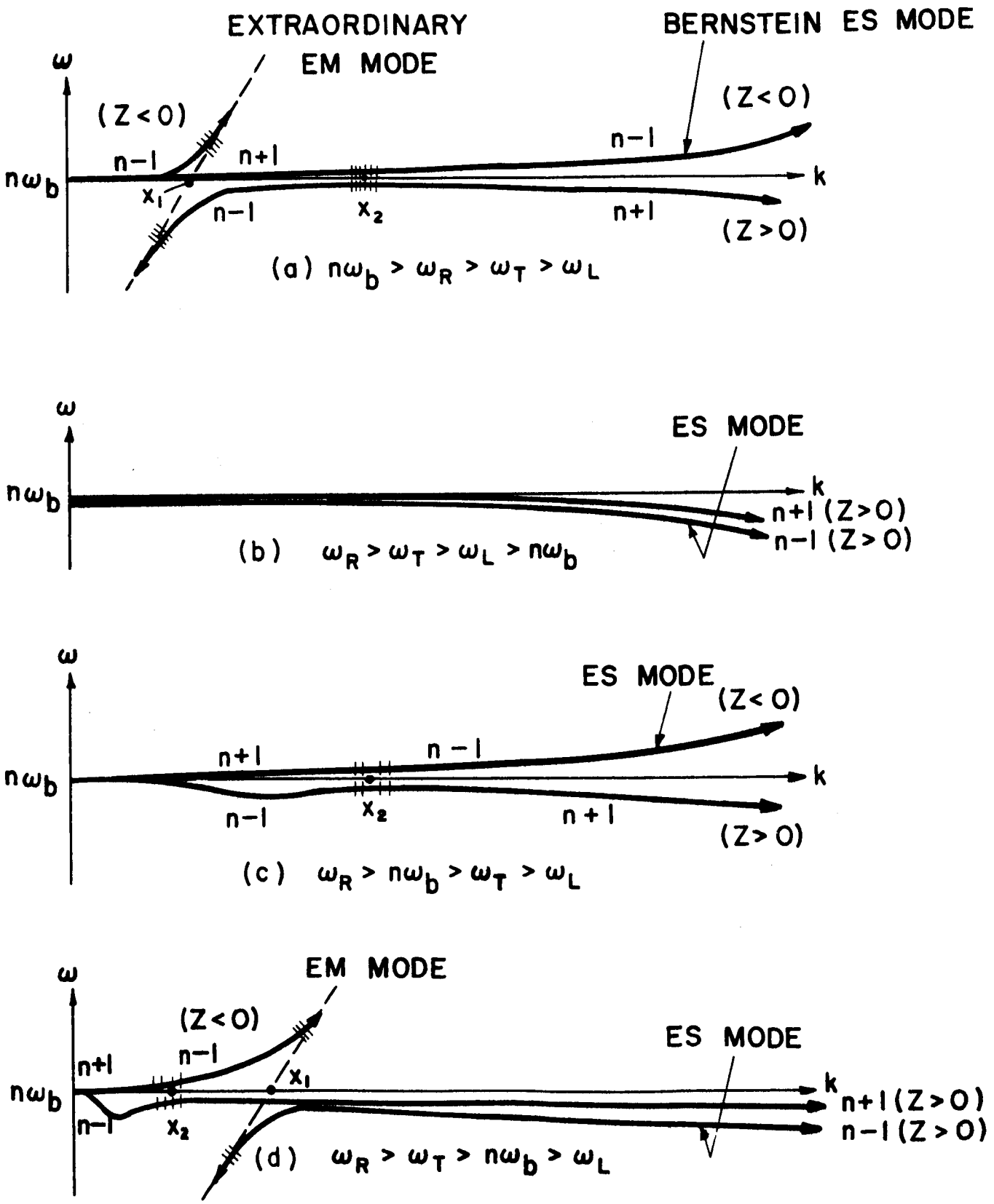
EXTRAORDINARY
EM MODE
BERNSTEIN ES MODE
ω
(Z<0)
(Z<0)
n−1
n+1
n−1
nω_b
k
x_1
n−1
x_2
n+1
(Z>0)
(a) nω_b > ω_R > ω_T > ω_L
ω
ES MODE
nω_b
k
n+1 (Z>0)
n−1 (Z>0)
(b) ω_R > ω_T > ω_L > nω_b
ω
ES MODE
(Z<0)
n+1
n−1
nω_b
k
n−1
x_2
n+1
(Z>0)
(c) ω_R > nω_b > ω_T > ω_L
ω
EM MODE
(Z<0)
ES MODE
n+1
n−1
x_1
nω_b
k
n+1 (Z>0)
n−1
x_2
n−1 (Z>0)
(d) ω_R > ω_T > nω_b > ω_L

FIG. 8

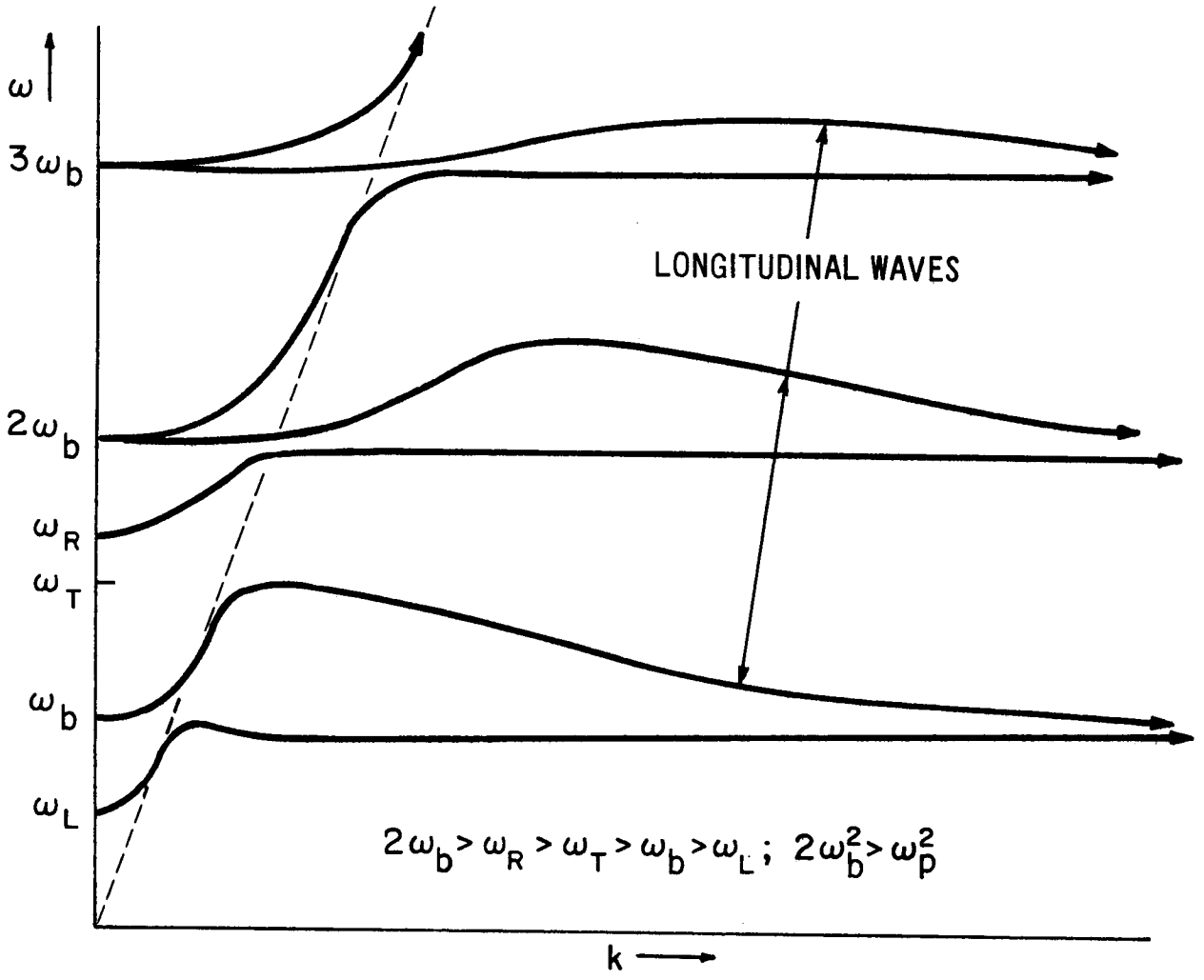
ω
3ω_b
2ω_b
ω_R
ω_T
ω_b
ω_L
LONGITUDINAL WAVES
2ω_b > ω_R > ω_T > ω_b > ω_L ; 2ω_b^2 > ω_p^2
k

FIG. 9

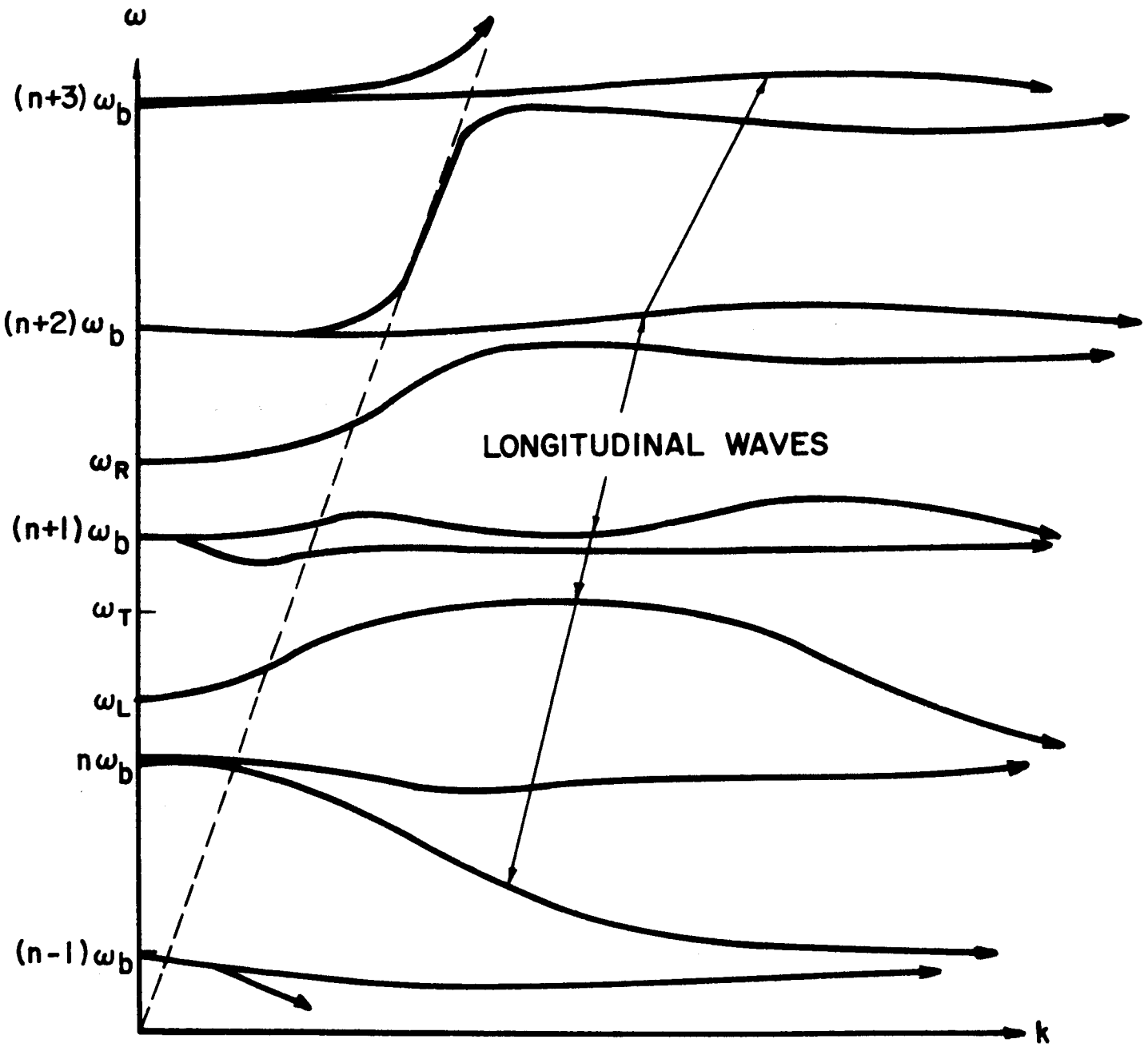

$$(n+2)\omega_b > \omega_R > (n+1)\omega_b > \omega_T > \omega_L > n\omega_b \; ; \quad n(n+2)\omega_b^2 > \omega_b^2 > n(n+1)\omega_b^2$$

FIG 10

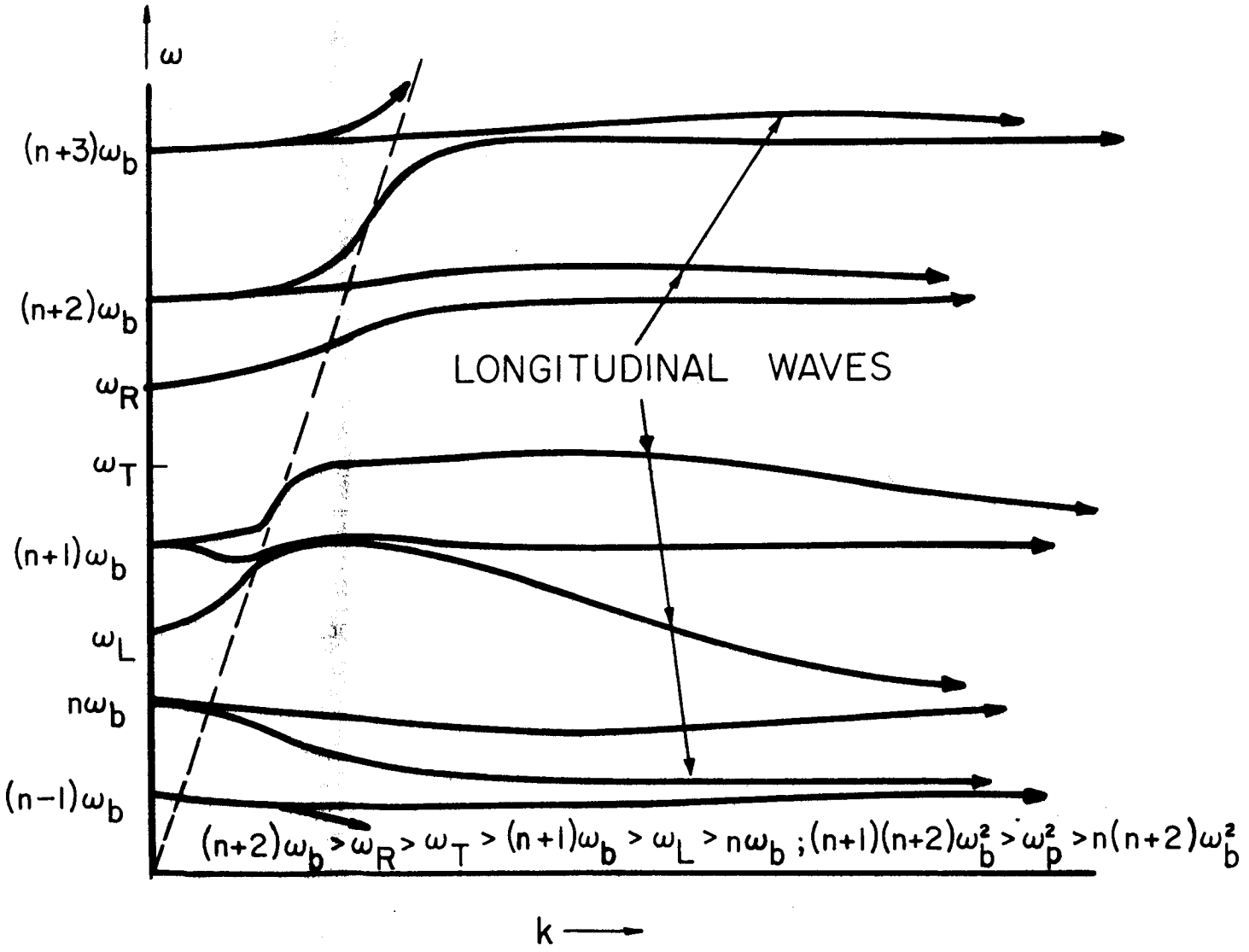
ω
(n+3)ω_b
(n+2)ω_b
ω_R
ω_T
(n+1)ω_b
ω_L
nω_b
(n-1)ω_b
LONGITUDINAL WAVES
(n+2)ω_b > ω_R > ω_T > (n+1)ω_b > ω_L > nω_b ; (n+1)(n+2)ω_b^2 > ω_p^2 > n(n+2)ω_b^2
k

FIG 11

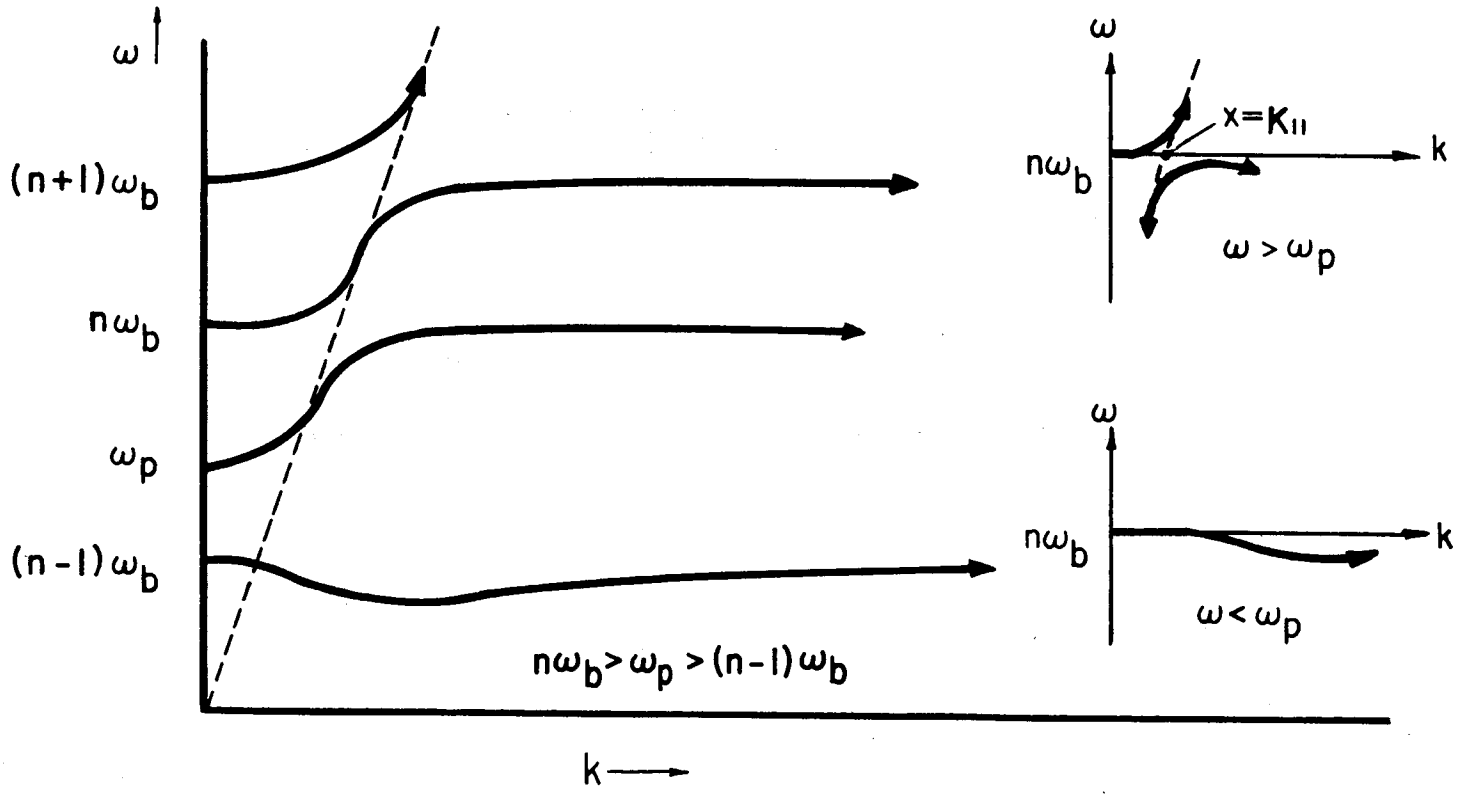

FIG. 12

- APPENDIX III -

I. LIST OF PUBLICATIONS

Related Work Prior to Contract

T.W. Johnston and J. Nuttall, "Cyclotron Harmonic Signals Received by the Alouette Top-side Sounder", J. Geophys. Res. 69, 2305-2314, June 1 (1964); RCA Victor Res. Report 7-801-28 (Revised)Jan. (1964).

J. Nuttall, "Theory of Collective Spikes Observed by the Alouette Top-side Sounder", J. Geophys. Res. 70, 1119-1125, March 1, (1965); RCA Victor Res. Report 7-801-29c, April (1964).

J. Nuttall, "Singularities of the Green's Function for a Collisionless Magnetoplasma", Physics of Fluids 8, 286-296, February (1965); RCA Victor Res. Report 7-801-29a, February (1964).

J. Nuttall, "Plasma Frequency Singularity of the Green's Function for a Magnetoplasma", RCA Victor Res. Report 7-801-29b, May (1964).

Publications Under Contract

I.P. Shkarofsky and T.W. Johnston, "Cyclotron Harmonic Resonances Observed by Satellites", Phys. Rev. Letters 15, 51-3, July 12 (1965).

T.W. Johnston and I.P. Shkarofsky, "Resonances in Ionospheric Magnetoplasma", RCA Engineer 11, No.4, December (1965)/January (1966), p52-55; also Proc. of Second AAS Symp. on the Interactions of Space Vehicles with an Ionized Atmosphere (to be published).

I.P. Shkarofsky, "Dielectric Tensor in Vlasov Plasmas Near Cyclotron Harmonics", Physics of Fluids 9, No.2, February (1966).

I.P. Shkarofsky, "Dispersion of Waves in Cyclotron Harmonic Resonance Regions in Plasmas", Physics of Fluids 9, No.2, February (1966).

T.W. Johnston and I.P. Shkarofsky, "Excitation of Cyclotron Harmonics in a Warm Plasma", (Abstract only), Bull. Am. Phys. Soc. Series II, 10, No.2, p.231 (1965).

T.W. Johnston and I.P. Shkarofsky, "Time Decay of Cyclotron Harmonics", (Abstract only), Bull. Am. Phys. Soc., Series II, 10, No.5, p.611 (1965).

I.P. Shkarofsky, "Dispersion of Waves in Cyclotron Harmonic Regions" (Abstract only), Bull Am. Phys. Soc., Series II, 10, No.5, p.597 (1965).

I.P. Shkarofsky and T.W. Johnston, "Applicability of Cyclotron Harmonic Dispersion Functions", (Abstract only), Bull. Am. Phys. Soc. (1966). (To be published.)

Reports Under Contract

I.P. Shkarofsky and T.W. Johnston, "Satellite Cyclotron Harmonic Resonances", RCA Victor Res. Report 7-801-35, March (1965).

I.P. Shkarofsky, "Duration of Cyclotron Harmonic Resonances Observed by Satellites", RCA Victor Res. Report 7-801-44, January (1966).

Talks Under Contract Given by

T.W. Johnston, "Applicability of Cyclotron Harmonic Dispersion Functions" Plasma Phys. Div., Am. Phys. Soc., San Francisco Meeting, Nov. 11 (1965).

I.P. Shkarofsky, "Cyclotron Harmonic Waves and Dispersion Functions", given at Massachusetts Inst. of Technology, Research Lab. of Electronics, Cambridge, Mass. November 2 (1965).

T.W. Johnston, "Resonances in the Ionosphere Magnetoplasma", Second AAS Symp. on the Interactions of Space Vehicles with an Ionized Atmosphere, Miami, Florida, November 27 (1965); also Can. Symp. on Plasma Physics, NRC (Ottawa), October 13 (1965).

T.W. Johnston, "Time Decay of Cyclotron Harmonics", Am. Phys. Soc., New York Meeting, June 25 (1965).

I.P. Shkarofsky, "Dispersion of Waves in Cyclotron Harmonic Regions" Am. Phys. Soc., New York Meeting, June 25 (1965).

T.W. Johnston, "Excitation of Cyclotron Harmonics in a Warm Plasma", Plasma Phys. Div., Am. Phys. Soc., New York Meeting, November 7 (1964).

II. CORRECTIONS TO PREVIOUS WORK

Report 7-801-35 (Part 1)

	Original	Corrected
Page 8, Eq.(10a)	$\left(1-\frac{\omega_b}{\omega}\right)$	$\left(1-\frac{n\omega_b}{\omega}\right)$
Page 8, Eq.(10b)	$\frac{k_n^2 c^2 t^2}{\sqrt{2}\, v_t \omega}$	$\frac{k_n c^2 t}{\sqrt{2}\, v_t \omega}$
Page 10, Eq.(16b)	$\frac{3c^4 k_n^2}{v_t^2 \omega^2}$	$\frac{3c^4 k_n^2}{2v_t^2 \omega^2}$
Page 21, Eq.(31d)	z^n	z^p
Page 25, 2nd Eq.	$\frac{i\pi}{\mu\delta\sqrt{-2\delta+\gamma^2}}$	$\frac{-i\pi}{\mu\gamma\sqrt{-2\delta+\gamma^2}}$
Figure 1b	$\mathrm{Im}F_q(\mu\delta)$	$-\mathrm{Im}F_q(\mu\delta)$

Report 7-801-35 (Part 2)

Page 1	Omit "Furthermore, ... three", since a more careful analysis shows the existence of a third wave. See Appendix II of this report.
Pages 10-11	The ϕ integration is incorrect since D is a function of $\underset{\sim}{k}.\underset{\sim}{V}$ or of ϕ as well.

Report 7-801-35 (Part 2) cont'd.

Page 13 $3F_{n+1/2}-6F_{n+3/2}+3F_{n+5/2}$ should be $3F_{n+3/2}-6F_{n+5/2}+3F_{n+7/2}$

" $7F_{n+5/2}-8F_{n+3/2}+3F_{n+1/2}$ " " $3F_{n+1/2}-2F_{n+5/2}+F_{n+3/2}$

Page 15 See Appendix II of this report.

Page 17, Eq.(22e) $\omega = \omega_b$ should be $\omega = 2\omega_b$

Page 19, 2nd line, 2nd par. After "value" insert "for $n > 2$"; (see also corrections below for Figs. 3a and b).

Page 28, Eq.(29b) Same corrections as for p.13.

Page 33, Table 3 The word "Exact" refers to $\omega >> \omega_T$ since only then is the wave sufficiently localized that one I_n term in the expansion is sufficient.

Figs. 2a-f These figures are incorrect since they are based on ImF being positive whereas it is actually negative. For corrected versions, see Appendix II.

Fig. 4b $\tan \frac{\pi}{(n-1)}$ should be $\tan \frac{\pi}{2(n-1)}$

Report 7-801-35 (Part 3) (see main part of this report)

Paper in Physics of Fluids 15, 51-3 (1965)

Page 51, 1st par. "equal to one" should be "usually equal to 3/2"

Page 51, end of last par. — After "small" insert "that is usually less than $100\ v_t^2/c^2$".

Page 53, beginning of 2nd par. — After "$n \leq 3$" insert "for forward waves, but it can nearly always be accomplished for backward waves $(\omega^2 << \omega_b^2 + \omega_p^2)$".

Figure 1 — The word "spurious" refers only to the $\lambda<<1$ part of the curves, since for larger $\lambda \sim 1$, relativistic theory also shows that the same extra wave exists below the harmonic. (See Appendix II here.)

Page 52, 2nd last par. — Change "less than 3 by a factor $v_t^2/cV_\perp$" to "about the same order of magnitude as 3" (see this report). Also change "$(v_t^2/cV_\perp)^2$" to "$(v_t^3/cV_\perp^2)(V_\perp/c)^{1/2}$"

Pages 52-53 — The equations for $E_{r,l}$ and E_n have to be modified as given in this report. As an order of magnitude correction, the right hand sides can be divided by

$$(2\pi V_\perp k_\perp' t)^{\frac{1}{2}} \sim (2\pi V_\perp \omega t/c)^{\frac{1}{2}}$$

which for the times of interest is of order one. Hence the results in the calculation given in the comparison with experiment are numerically unchanged.

The changes on pages 52 and 53 are due to the incorrect ϕ integration used previously in the satellite frame of reference. Although the dispersion (D) relation at a pinch point does not depend on $\underset{\sim}{k}\cdot\underset{\sim}{V}$ or ϕ, nonetheless, its expanded form around the pinch point depends on ϕ. This is the same as saying in Section II, that

$$\partial^2 D/\partial(k_y')^2 \text{ and } \partial^2 D/\partial(k_x')^2$$

involve not only

$$\partial^2 D/\partial(k_\perp')^2 \text{ but also } \partial^2 D/\partial\phi^2$$

As mentioned above, the corrections do not affect the results for the time decay.